SLENDER REINFORCED CONCRETE COLUMNS

by

NARIMAN JABER KHALIL

(B.Sc.)

Submitted in accordance with the requirements for the degree of

DOCTOR OF PHILOSOPHY

The University of Leeds

Department of Civil Engineering

September 1991

The candidate confirms that the work submitted is her own and that appropriate credit has been given where reference has been made to the work of others.

ABSTRACT

The analysis of slender reinforced concrete columns is complicated because the non-linearities of the materials (caused by the cracking of concrete and time-dependent effects) are combined with the geometric non-linearity which characterises the behaviour of such columns.

A simple analytical method based on a graphical technique, originally proposed by *Beal,* is developed. The method takes account of the material and geometric non-linearities and allows rapid and accurate analysis of slender pin-ended reinforced concrete columns, concentrically or eccentrically loaded, without the need for iterative procedures or simplification of section behaviour. The method allows for sustained load effects and enables the reduction in the short-term ultimate capacity to be predicted.

The theoretical analysis is backed by nineteen short and long-term full-scale tests on pinned reinforced concrete columns having slenderness ratios between 18 and 63, loaded eccentrically. The experimental results substantiated the fact that instability is the primary failure criterion for slender columns; and it occurs at relatively low compressive concrete strains of the order of 0.001-0.002. Material failure eventually follows, but for slenderness ratios of 33 and above this requires considerable bending to occur.

Creep was found to strongly influence the buckling load; with a sustained load of 60% of short-term capacity, creep causes a considerable reduction in the load capacity of a slender column and can be as much as 40%. Initial imperfections are inevitable during column construction. This was accounted for in the theoretical approach and the results obtained demonstrated the sensitivity of slender columns to such imperfections.

The accuracy of the proposed method is further established when comprehensive comparisons are made with the experimental work of other investigators. Significant improvement is noted over the existing design methods in BS8110 and ACI318. The design procedures adopted in the two Codes are based on strength calculations which are proved to be almost irrelevant for slender columns. The BS8110 approach was found to be unsafe in predicting the long-term buckling loads of the columns tested because it does not make allowance for creep effects. This is in contrast to ACI318 recommendations which were found to be conservative in predicting the failure loads.

To my Mother

To the Memory of my Father

To the Source of Love and Endless Giving ...

my Family

ACKNOWLEDGEMENTS

I wish to express my sincere gratitude to *Professor A.R. Cusens,* Dean of the Faculty of Engineering, for his unfailing advice, encouragements and interest in the work. His understanding, patience and readiness to help, particularly at times of difficulty are highly appreciated. My deepest thanks are also due to *Mr. M.D. Parker* for his constructive criticism and detailed discussions throughout the course of the research. His indispensable help and continuous attentions are much acknowledged.

Financial support was provided by Al-Baath University (Syria), to whom I am indebted.

The experimental programme required novel testing frames and techniques. Thanks are due to the technical staff of the George Earle Laboratory of the Department of Civil Engineering for their skill and efficiency in handling it. I am particularly indebted to *Mr. V. Lawton,* chief technician, not only for his expertise and practical advice but also for his moral support and invaluable help during the two years of experimental work. *Dr J. Uren* and his students, and *Mr. R. Duxbury* gave their assistance with the theodolite measurements.

I am grateful to *Mr. A.N. Beal* from R.H. Thomason and Partners for the valuable discussions of the graphical method.

I thank *Dr. B. El-Haddadeh* and *Miss B. Wright* for their assistance with the computer work and the entire staff of the Civil Engineering Department for the friendly atmosphere they provided.

The interest and encouragement of *Dr. A.M. Shiekh Hussien,* President of Al-Baath University, *Dr. M.F. Riffai* and *Dr. N.N. Anis,* of the Department of Civil Engineering of Aleppo University, are appreciated.

My gratitude goes to all my friends in Leeds for the homely environment they created and to those in Syria for keeping in touch despite the distance.

Finally, to my dearest friends ever, Amal Hassan, May Al-Labbad and Jacques Le BOT for keeping up my faith in the essential goodness of human nature.

TABLE OF CONTENTS

LIST OF TABLES

LIST OF FIGURES

CHAPTER 5

CHAPTER 6

CHAPTER 7

APPENDIX B

NOTATION

The following notation is used in this thesis unless otherwise stated

A	area
A_c	gross cross-sectional area of concrete (Note that A_c is used for net area in BS8110-Eq.2.5)
A_s, A_{sc}	area of vertical reinforcement
$\%A_s$	percentage of reinforcement = A_s/bh
a_u	deflection at ultimate limit state
a_1	constant (see Eq.B.1 in Appendix B)
b	width of column cross-section
b'	smaller dimension of the column
b_1	constant (see Eq.B.1 in Appendix B)
C_m	factor relating actual moment diagram to an equivalent uniform moment diagram
c_1	constant (see Eq.B.1 in Appendix B)
d	effective depth to tension steel
d'	distance from extreme compression fibre to centroid of compression steel
E_c	modulus of elasticity of concrete
E_e	effective modulus of elasticity of concrete
E_s	modulus of elasticity of steel
e	eccentricity
e_i	initial load eccentricity

e_{min}	design minimum eccentricity (= 0.05h≤20 mm in BS8110)
e_{tot}	total eccentricity at the critical section (= e_1+e_2, see Eq.2.19)
e_1	= e_f +e_a
e_f	first order eccentricity
e_a	additional eccentricity to account for any uncertainty concerning the location of the point of incidence of external forces
e_2	second order eccentricity
e_e	equivalent eccentricity
e_{os}, e_{oi}	first order eccentricities at the ends of the column, e_{os} being positive and larger than e_{oi}
e_c	additional deflection due to creep strain
e_t	total eccentricity at the mid-height of the column (= e_0+e_i+e_u, see Eq.7.2)
e_0	initial imperfection
e_u	= a_u
e_m	magnified eccentricity
e_{test}	mid-height eccentricity at the point of instability measured experimentally
e_{theory}	predicted mid-height eccentricity at the point of instability
f_{cu}	concrete cube strength
f'_c	concrete cylinder compressive strength
f_{co}	maximum concrete compressive stress
f_{cn}	concrete stress corresponding to the neutral axis at the (n-1) position (Eq.3.1, Eq.3.2 and Fig.3.3)
f_y	tensile yield stress of steel
f_{s1} (f_{s2})	stress in top (bottom) steel of column cross-section (Eq.3.3, Eq.3.4 and Fig.3.4)

f_{st} = f_{s2} (Figs.7.1 to 7.5)

h overall depth of column section

I second moment of area

I_g second moment of area of gross concrete section about centroidal axis, neglecting reinforcement

I_{se} second moment of area of reinforcement about centroidal axis of member cross-section

K reduction factor (Eq.2.4)

k effective length factor (Eq.2.14)

k_1, k_2 parameters of concrete stress block (see Fig.B.2 and Eqs.B.11 and B.12 in Appendix B)

L column length

l_e effective column length

$\frac{l_e}{h}$ slenderness ratio

M moment

M_{add} additional design ultimate moment induced by deflection of column

M_1 smaller initial end moment due to design ultimate loads

M_2 larger initial end moment due to design ultimate loads

M_i initial design ultimate moment in a column before allowance for additional design moments arising out of slenderness

M_c magnified factored moment

M_{1b} value of smaller factored end moment on a compression member due to the loads that result in no appreciable sidesway, calculated by conventional elastic frame analysis, positive if member is bent in single curvature, negative if bent in double curvature (Eq.2.15)

M_{2b} value of larger factored end moment on compression member due to loads that result in no appreciable sidesway, calculated by conventional frame analysis (Eq.2.11 and Eq.2.15)

M_{2s} value of larger factored end moment on compression member due to loads that result in appreciable sidesway, calculated by conventional frame analysis (Eq.2.11)

M_{sd} first order applied moment (Eq.2.20)

M'_c resultant concrete moment

M_s resultant steel moment

M_{RC} resultant moment of reinforced concrete section ($= M'_c+M_s$)

N design ultimate axial load on the column

N_{uz} design ultimate capacity of a section when subjected to axial load only

N_{bal} design axial load capacity of a balanced section

N_{sd} applied longitudinal force (Eq.2.20)

P compressive load or buckling load

P_c critical load (Eqs.2.14 and 3.10)

P_u factored axial load at given eccentricity ($\leq \phi_1 P_n$)

P_n nominal axial load strength at given eccentricity

P'_c resultant concrete force

P_s resultant steel force

P_{RC} resultant force of reinforced concrete section ($= P'_c+P_s$)

P_0 axial compression capacity (squash load)

P_{bal} axial load capacity of a balanced section

P_{BS} failure load according to BS8110

P_{ACI} failure load according to ACI318-89

r	radius of gyration of cross-section of column
$\frac{1}{r}$	curvature
t	time
t_0	age at first loading (Table 7.8)
w_c	density of concrete
$\overline{x}$	centroid of concrete stress block (Fig.B.1 in Appendix B)
x	neutral axis depth
x_1, x_2	length along x-axis
y_1	length along y-axis
β_a	slender column coefficient (Eq.2.3)
β_d	ratio (Eq.2.16 and Eq.2.17)
γ_m	partial safety factor for strength of materials
δ_i	lateral displacement of column
$\Delta\delta$	increase in the lateral displacement δ_i due to sustained load
δ_b	moment magnification factor for braced frames
δs	moment magnification factor for unbraced frames
ε	strain
ε_o	strain at which maximum compressive stress of concrete is first attained
ε_{cu}	ultimate concrete strain in compression (= 0.0035 in BS8110)
ε_t	total strain of plain concrete cylinders
ε_i	instantaneous strain of plain concrete cylinders
ε_{sh}	shrinkage strain of plain concrete cylinders
ε_{cr}	creep strain of plain concrete cylinders (= ε_t - (ε_i+ε_{sh}))
ε_n	strain at nth interval (see Eq.3.9 and Fig.3.3)

ε_s	strain in steel
ε_y	tensile yield strain in steel
η	ratio ($= \varepsilon_o/\varepsilon_{cu}$)
λ	slenderness ratio (Eq.2.18)
λ_{lim}	limiting slenderness ratio (Eq.2.25)
$\mu\varepsilon$	microstrain
ρ	reinforcement ratio ($= \%A_s$)
ϕ	creep coefficient ($= \varepsilon_{cr}/\varepsilon_i$)
ϕ_1	strength reduction factor

CHAPTER ONE

INTRODUCTION

1.1 General

In most structural members, deflection under loading may not affect the strength and can generally be ignored. In some situations, however, particularly in the case of reinforced concrete columns, deflection may be such as to add significant additional moment (the P-Delta effect). The possibility of this occurring increases as the slenderness ratio of the column increases. This **geometric non-linearity** is further complicated by **material non-linearity**, caused by the use of concrete which has a non-linear stress-strain curve, a tendency to crack and is known to exhibit time-dependent deformation when subject to continuous loading. Under sustained load, creep and shrinkage of concrete cause increase of deformation and redistribution of stresses, which in the case of a slender column may eventually lead to **buckling failure**. It is now well-known that **material failure** is the controlling factor for stocky columns, while for slender columns, failure essentially occurs due to **instability**.

The analysis and design of slender reinforced concrete columns were hampered in the early days by the lack of experimental and theoretical data about their behaviour. However, the knowledge of slender column behaviour has been greatly enhanced during the past 15 to 20 years and analytical procedures have become available to accurately model their strength and stiffness [1]. Because of the nature of the problem (combined **geometric** and **material non-linearities**), such procedures are generally too complex to be efficiently employed in everyday design-office use [2,3,4].

Codes of practice simplify the problem and recommend alternative design methods for slender columns based on modifying the axial loads and moments obtained from elastic analysis of the structure to account for the **secondary moments** induced by lateral deflection. Generally, these methods are approximate and largely empirical.

In response to the increasingly stringent architectural and cost requirements in modern buildings, the use of slender buildings and slender building components have become more common, making it necessary to provide a comprehensive evaluation of their behaviour. The advancement of computerized solution techniques combined with the

production of high quality concrete and high steel strength have encouraged the design and construction of such structures. Examples of reinforced concrete compression members with high slenderness ratios constructed successfully are quoted by *Dracos* [5], confirming demand for and desirability of such elements.

A simplified acceptable design method which provides a reliable, accurate, economic and safe solution is therefore necessary. Because of the great number and range of variables involved, a fairly extensive experimental programme, particularly under long-term loading conditions, would best provide the results for the evaluation and verification of the analytical method.

1.2 Outline of the problem

Consider the simple case of a pin-ended column, subject to a compressive force P applied at an initial eccentricity e_i. When the load is first applied, the column deflects laterally by amount δ_i. The total moment at any section away from the column ends, thus consists of two components; the first Pe_i is referred to as the **primary moment** and the second $P\delta_i$ caused by the lateral displacement is the **secondary moment.** The value of δ_i depends on the curvature at that section, which in its turn depends on the applied moment. If the load P increases, the lateral displacement δ_i increases too but at a faster rate than the rate of increase of P, until the column becomes unstable and unable to support load.

For **slender columns,** the secondary moments may amount to several times the initial moments, causing reduction in the column-carrying capacity, so that such a column would fail by **instability** at relatively small compressive load, much less than that of a corresponding **short column,** i.e well before the ultimate strength of the material is exhausted. This problem is brought about by the change in geometry of the column and is referred to as **geometric non-linearity.**

The primary moments in real structures represent the end moments due to continuity, or they may be caused by transverse loads or application of loads at initial eccentricities. The initial imperfections present contribute to the problem and add to the lateral deflection.

If load P is sustained on the column, a further increase in the lateral deflection ($\Delta\delta$) at mid-height will develop with time. Time-dependent deformation, mainly creep of concrete, will lead to an increase in the concrete compressive strains, consequently the curvature will increase causing the column to deflect even further. The gradual increase in the secondary moment with time $P(\delta_i+\Delta\delta)$ reduces the carrying capacity and **creep buckling** may occur.

1.3 Objective and scope of the present investigation

The principal concern of the current research was to study the behaviour of slender pin-ended reinforced concrete columns subject to eccentric loading under short and long-term conditions, both experimentally and analytically. The following objectives were set:

1- A method of analysis was to be developed which would accurately predict the short-term buckling load and the reduction in column capacity due to sustained load, without the need for complicated numerical calculations or iteration procedures.

2- Verification of the method by carrying out a programme of experiments, which would provide further data particularly on long-term loading.

3- Assessment of the design recommendations available in current codes of practice.

The analytical approach enables the short-term buckling load to be obtained directly. It takes account of creep properties of concrete and allows the reduction in column capacity under sustained load to be predicted. Initial imperfection at mid-height is accounted for and the total mid-height eccentricity at the point of instability is simply determined.

Eleven reinforced concrete columns having slenderness ratios between 18 and 63 are tested under short-term load and eight similar columns tested under sustained load. The slenderness ratio was the main variable examined; other parameters, such as percentage of reinforcement, concrete strength and initial eccentricity are kept relatively constant.

The applicability of the method proposed is checked against 118 tests, reported in the recent literature. These tests were performed on slender reinforced concrete columns under short and long-term loading.

The adequacy of design methods in the British and American Codes of Practice is examined and evaluated.

1.4 Layout of the thesis

The work completed in pursuit of the objectives set out above, is organized and outlined here, in the following manner:

In an attempt to clarify the existing gap in the analysis and design of slender reinforced concrete columns, a summary of the various design methods available in the literature and in different codes of practice is made, examining their advantages and limitations; this is given in Chapter 2. In the same Chapter, full coverage of reported experimental work in the field, range of variables considered and type of loading is also provided.

The main concern in Chapter 3, is to describe the development of the analytical method and the computer programs required to produce and plot the theoretical data; finally examples illustrating its application are shown.

An experimental programme was established for short and long-term periods. The range of variables considered, design of the testing frames and instrumentation required, materials used and method of column construction are specified in detail in Chapter 4.

Various aspects of the experimental investigation carried out, descriptions of test columns, concrete properties and test procedures are fully covered in Chapters 5 and 6. Discussion of the observations made and comparisons between theoretical and experimental results are to be found in the same Chapters.

Assessment of the design methods recommended in two current Codes of Practice BS8110: 1985 [6] and ACI318-89 [7] is made against the experimental buckling loads obtained. The general validity of the proposed approach is checked by extensive comparisons with test data reported by other investigators. The results of this stage are evaluated and presented in Chapter 7.

Finally Chapter 8 contains a summary of the conclusions drawn, further possible developments and extensions to the analytical approach and suggestions for future work.

CHAPTER TWO

REVIEW OF DESIGN METHODS FOR SLENDER COLUMNS

2.1 Introduction

The development of column buckling theory is perhaps the oldest among structural theories. It has a continuity over nearly 300 years. A tremendous volume of work, theoretically and experimentally, has been carried out on this topic. Adequate coverage for that is available in standard literature and many researchers have well documented the story; therefore a detailed review will not be repeated here, particularly for the periods up to the 1970's. However, the major steps will be indicated and for more information the reader will be referred to the appropriate references. Reasonable coverage of the important researches in the field and of recent work is given here.

In **1678** *Robert Hooke* was the first to provide the necessary preliminary to the development of elastic buckling theory, followed by *Bernoulli's* contribution. *Leonard Euler* (1707-1783), in the Appendix to his **1744** book, presented his famous formula for the elastic critical buckling load of a slender column (Equation 2.14) which still bears his name and continues to be in use today. Extending *Euler's* theory to predict column strength in the inelastic range was due to *Considére* and *Engesser* in **1889**. Explicit expressions for the reduced modulus were derived by *Von Kármán* in **1910**. These basic initial steps were followed by substantial developments and modifications. Complete accounts of the early history of column investigations can be found in references [8,9,10,11,12,13,14,15].

In **1934**, *Baumann* [16] applied the *Von Kármán* theory to reinforced concrete columns having slenderness ratios up to 41 (the slenderness ratio is referred to in terms of l_e/h unless noted otherwise). Further contributions experimentally and analytically were made by *Thomas* in **1939** [17], *Hognestad* **1951** [18], *Ernst et al* in **1953** [19] and by *Broms and Viest* in **1958** [20].

The **1960**'s were marked by the advent of computers, which helped the investigators in handling the lengthy calculations and performing analytical solutions to the buckling problem which were based on iterative procedures. The high storage capacity of the computer was used to store the large numbers of data required to establish

the relationship between the load-moment and curvature. Among those who utilized computers were *Pfrang and Siess* in **1964** [21], *Pfrang et al* in **1964** [22], *Breen* in **1964** [23] and *Cranston* in **1967** [24].

Increasing attention was given to the study of the behaviour of slender reinforced concrete columns experimentally; tests were carried out by *Chang and Ferguson* [25] in **1963**, *Sàenz and Martin* [26] in **1963**, *Breen and Ferguson* [27] in **1964** and *Pannell and Robinson* [28] in **1968**.

Comprehensive review of some of the previous work can also be found in references [5,29,30].

The effect of sustained load on the ultimate strength of a slender column was realized by many investigators to have importance in design. However, the number of long-term tests remained limited due to the fact that such tests require considerable care and time to complete.

Green and Breen [31] in **1969** tested ten eccentrically loaded reinforced concrete columns for periods up to 1.5 years. The columns had a slenderness ratio of 19. The load was maintained by means of springs. Two specimens failed after two months of loading; these members were loaded up to 37% of the ultimate section capacity for concentric load. The deformations of the other columns did not reach a limiting value after 1.5 years.

In the same year, *Ramu et al* [32] carried out a research programme on the behaviour of reinforced concrete columns under sustained loads. The results of thirty seven tests on unrestrained columns were reported. A few columns were loaded to failure in short-term tests. All the others were tested under constant sustained loads. A description of the *Ramu* long-term tests follows in Chapter 7.

In **1970** *Goyal* [33] studied the behaviour of pin-ended eccentrically reinforced concrete columns under short and sustained loads, both experimentally and theoretically. He concluded that, if the sustained load on the column is within the working range, i.e 30 to 40 percent of the short-term ultimate load, its effect on the column-carrying capacity will be negligible. However, substantial reductions in strength occur for sustained loads equal to 60 percent of the short-term ultimate load. *Goyal* adopted the Newton-Raphson method for the solution of non-linear simultaneous equations relating axial load, bending moment and edge strains. Concrete was assumed to have the stress-strain relationship suggested by *Hognestad,* for long-term analysis he used a reduced concrete modulus. Although *Goyal's* analytical procedure does not require large storage capacity within the computer, it still clearly involves a lot of iteration.

Hellesland and Green [34] in **1971** studied the effect of sustained and cyclic loading on concrete columns having slenderness ratio of 15. At the same time, *Drysdale and Huggins* [35] carried out tests exploring the behaviour of slender concrete columns under sustained biaxial load.

In **1971** *Cranston and Sturrock* [36] examined the lateral instability of pin-ended slender reinforced concrete columns subject to axial load and moment applied about either major or minor axis. In all cases, failure was by buckling about the minor axis. They also emphasised the importance of the tensile resistance of the concrete on deflection at low loads. In **1972** *Cranston* [37] presented the results of an extensive computer analysis which covered a wide range of different column cross-sections and different end and loading conditions for braced and unbraced columns. In the computer model the column was divided into a number of segments and the cross-sections were idealized into a number of elements. The method of analysis is iterative and consist of finding successive solutions as the load on (or deflection of) the column is increased in steps. The method developed by *Cranston* formed the basis for the design of slender columns in CP110 [38]. Extensive comparisons with the test data available at that time were made to validate the method which appeared to work reasonably well for columns with slenderness ratio up to 20, tested under short-term loading conditions.

Further experimental and theoretical research was performed in **1975, 1976** and **1977** particularly oriented towards the behaviour of slender columns as parts of frames (which is a more realistic case) and under sustained loads. Such investigations were undertaken by *Green and Hellesland* [39], *Bolmeier and Breen* [40], *MacGregor and Hage* [41], *Behan* [42] and finally by *Wu and Huggins* [43]. Theoretical contributions to the development of second-order analysis of tall steel structures were made by *Wood et al* [44,45] in **1977**.

All columns which are reported to have been tested, had a slenderness ratios up to 40 and very few exceeded this limit (eg. *Cranston and Sturrock* [36]). In **1977** a research programme was established by *Pancholi* at the University of Bradford to study the behaviour of very slender reinforced concrete columns. *Pancholi* [29] looked at the design of very slender concentrically loaded reinforced concrete columns having aspect ratios between 30 and 80. A fourth order polynomial was used for the theoretical deflected shape. The buckling load was determined using the fundamental *Euler* approach to the problem. From his long-term experimental work, he derived two expressions for reduction factors which when multiplied by the short-term buckling failure load would give recommended safe design loads.

In **1982**, in a continuation of the Bradford research programme, *Dracos* [5] took over and investigated the problem both analytically and experimentally. The stress-strain

relationships of concrete and steel were represented by continuous mathematical functions which enabled expressing the applied load and imposed moment on a column in terms of the edge strains in two relationships spanning over the entire range of curvature variation. This procedure was reported to have computational advantages over previous analyses; however, an iterative process was still required to produce the solution. A total of forty eccentrically loaded slender columns,reinforced with mild steel, were tested by *Dracos* under short-term and sustained loads. He concluded that creep effects have a considerable influence on the load-carrying capacity of slender reinforced concrete columns and must be accounted for in their design. His analytical studies indicated that the reduction in strength due to sustained loading can be as high as 59% of the short-term load-carrying capacity. He recommended that the serviceability load does not exceed the load that would cause a maximum lateral deflection of 5 mm when sustained for a period of 25 years. A proposed second order analysis enabled the designer to check that creep deformations do not exceed such a value.

In the same year **1982**, *Behan and O'Connor* [46] investigated the behaviour of reinforced concrete columns with induced initial imperfections. Fifty one columns were tested under short-term conditions and sixteen under long-term conditions. All columns were pin-ended with a range of slenderness ratios from 8-48, the column sizes varied from 76×38×1830 mm to 127×64×500 mm, welding wire was chosen for the main reinforcement. The maximum reduction in short-term capacity due to creep was found to be 60%, recorded for slenderness ratio l_e/h=48. No other definite conclusions could be drawn.

In **1983** *Schofield* [30] approached the problem from a rather different angle. In a continuation to the research programme at Bradford University, *Schofield* tested fifty five concrete column specimens, reinforced with mild steel, having slenderness ratios between 29 and 59. Fifty columns were tested to destruction under short-term loading conditions and five specimens under sustained loads for periods up to 2 years. A concentric axial load was applied with independent primary end moments. A non-linear second-order computer analysis was developed for the prediction of deflections of hinged columns throughout the loading range, from zero load to buckling failure. The analysis proposed used a fundamental approach based on the derivation of load-moment-curvature relationships which were then used in an iterative solution of the deflected shape of the column at each load. *Schofield* emphasized the importance of considering the effect of sustained load in design which substantially increases the deflection of very slender columns. The maximum observed reduction was 46% of the short-term buckling load.

Sakai et al [47] in **1983** reviewed the basic concepts in dealing with the slender column buckling problem. They adopted what is known as the additional eccentricity method in their study, which is based on an iterative procedure consisting of two parts; a

second-order elastic analysis based on the finite element method to consider geometric non-linearity and a cross-sectional analysis to consider material non-linearity. The proposed formula for additional eccentricity took account of slenderness ratio, location of reinforcement, compressive strength of concrete, yield strength of steel bar and the ratio of sustained loads to their associated short-term ultimate loads. The numerical analysis carried out showed that the slenderness ratio has the most significant effect on the additional eccentricity; this effect was expressed by a cubic equation.

The treatment of the instability problem in *Sakai's* work is quite rational and the derived formula for the additional eccentricity is based on logical proposals covering all important factors which affect the behaviour of slender columns. However, the application of the design method does not give a direct solution and a repetitive procedure still has to be carried out. This work was republished in **1984** [48] with more details.

In later investigations, there was increased attention towards the behaviour of reinforced concrete columns subjected to axial compressive force and biaxial bending, such as the work by *Kwan and Liauw* [49], *Davister* [50] and *Iwai et al* [51].

In **1986** *Beal* [52] proposed a graphical method for the analysis of axially and eccentrically loaded slender reinforced concrete columns. The method has several advantages over the previously reported methods. Details of it are given in section 2.3 below.

Kong et al in **1986** [53] presented a graphical method for predicting the buckling loads of slender concrete columns. The method compares moment with deflection for a given column slenderness. Curves relating these parameters can be drawn for various axial loads and the method provides a rapid solution to the load capacity with a variety of eccentricities for that column. In **1987** *Kong and Wong* in improving the method, developed a computer program illustrated in ref.[54] to generate moment-deflection curves without the need for human intervention. However, a separate set of moment-deflection lines must be drawn for each column slenderness considered. The method becomes tedious when different combinations of slenderness ratios are considered for analysis with different combinations of concrete strength, reinforcement and load duration as the number of graphs required becomes quite large.

A new definition for the slenderness of reinforced concrete columns was proposed in **1987** by *Cauvin and Macchi* [55]. The modified definition takes into account the influence of axial load, percentage of steel reinforcement and concrete strength. The definition was justified by parametric numerical tests as well as by theoretical considerations.

In October **1987**, *Dinku* [56] completed his M.Sc. dissertation in which he investigated *Beal's* proposals. Coverage of his development is to be found in section 2.3 below.

Towfighi [57] in **1988** developed a computer program to obtain design tables for reinforced columns subjected to axial load and biaxial bending.

El-Metwally et al [58] in **1989** presented a three dimensional non-linear analysis of reinforced concrete slender columns under biaxial bending combined with axial compression. The method was based on the numerical integration technique originally developed by *Cranston* [59]. Both material and geometric non-linearities are accounted for in the analysis. The finite element method is used for the discretization of the column into a sufficient number of segments, as well as the division of the cross-section into a number of finite areas. Comparisons with test data showed advantages in using this extended method.

A study by *Mirza and MacGregor* in **1989** [60] was undertaken to determine the variability of short-time ultimate strength of slender tied reinforced concrete columns. Results indicated that the slenderness ratio, the longitudinal steel ratio and the end eccentricity ratio significantly influenced the probability distribution properties of the column strength. The variability of concrete strength was shown to be a major contributing factor to the slender column strength variability in a region of low eccentricity ratios, whereas the variability in steel strength made a major contribution to the slender column strength variability when the end eccentricity ratios were high.

In **1989**, an iterative computer based procedure for the analysis of slender reinforced and prestressed concrete columns under sustained eccentric loading was developed by *Gilbert* [61]. Time-dependent behaviour, cracking of the concrete and geometric non-linearity were taken into account. Individual cross-sections were analysed using an age-adjusted effective modulus method to include the time-dependent effects of creep and shrinkage. By dividing the time scale into several increments, the gradual development of time-dependent cracking was traced as the lateral deflection of the column and the internal secondary moments increased with time due to creep. Predictions were compared with a few laboratory tests and the agreement obtained was considered to be good.

Recently in **1989** [62] *Rangan* developed a simple expression for estimating the lateral deflection under sustained load for the standard case of a pin-ended slender column with equal end eccentricity and bent in single curvature. The expression compared reasonably well with 28 selected test data. The author suggested that the proposed

expression could be treated as an additional eccentricity in the strength calculation of slender columns.

In more recent work [2] *Rangan* proposed a stability analysis method for a standard pin-ended column, in which the moment-thrust-curvature relations were converted to moment-deflection curves for a chosen value of the axial thrust. The moment-deflection diagrams required in the analysis were idealized as either elastic-plastic or elastic-brittle. The formula for creep deflection developed in the previous work [62] was utilized. Based on the proposed method, proposals for design have been made. Despite the gross simplifications of section behaviour adopted by the author (pure elastic-plastic or pure elastic-brittle), his analysis still involved much iteration and the design method proposed is still quite laborious for real designs. Moreover, *Rangan* assumed a value of 0.003 for concrete failure strain in his calculations. Although this is a reasonable assumption for short-term loads, this failure strain under sustained loads can reach a magnitude of 0.008 or 0.009. This argument will be fully covered in later Chapters.

As a summary of the above cited literature, the problem of buckling instability in slender reinforced concrete columns has been well defined and recognised over the past years. Many investigators have tackled the problem both analytically and experimentally. The theoretical procedures adopted were either quite laborious to use in routine design calculations, (despite the simplifications in their assumptions, tedious cycles of numerical calculations are required to produce the answer), or were so rigorous in their approach that they were limited in their application.

The numerical and experimental results obtained, indicated that the time-dependent secondary moments in slender columns may be significantly greater than the instantaneous values and all researchers agreed that in the design of such columns, the effects of creep must be adequately quantified.

An accumulation of test data, shown in Table 2.1 which is adapted from reference [48], has been made to examine the validity of various design formulas proposed for slender columns. A total of 909 tests has been gathered, of which 381 tests were assembled by *Cranston* [37], 245 by *Sakai et al* [48] and the remainder, totalling 283, has been added.

It can be seen from Table 2.1 that most of the experimental work has been focussed on the behaviour of slender columns under short-term loads, until 1969 when increased attention was given to sustained load effects. Nevertheless, the number of tests performed is still insufficient.

Full-scale tests can undoubtedly provide the most reliable information. However, the number of parameters involved, the effort and technique required to cast and test very

slender reinforced concrete columns having a slenderness ratio greater than about 40 and the time necessary to complete long-term experiments, have restricted previous investigators and almost prohibited such tests.

A proper theoretical analysis using conventional techniques is iterative and expensive in computing time. A simplified rational approach for the analysis and design of slender reinforced concrete columns, which removes the need for iteration procedures, backed by extensive full-scale long-term tests, seems to be highly preferable.

2.2 Slender column design by Codes of Practice

The analysis of slender reinforced concrete columns is complicated because the non-linearities of the materials (caused by the cracking of concrete and time-dependent effects) are combined with the geometric non-linearity which characterises the behaviour of such columns.

Fundamentally, the design of a slender reinforced concrete column should be based on a rational second-order analysis of the structure. Such an analysis takes account of the secondary moments produced by the vertical loads acting on the laterally deformed structure. Ignoring these additional moments in the analysis will overestimate both the stiffness and the strength of the structural members. As discussed in section 2.1 above, this kind of calculation requires complicated procedures, thus the method will not be convenient in use. Therefore, the provisions for accounting for slenderness effects in codes of practice are based on simplified approaches which reduce the time and expense required in design.

In the approximate design methods for slender reinforced concrete columns in various codes, the basic forces and moments obtained by first order elastic analysis are empirically adjusted to reflect the reduction in strength of the column caused by stability effects.

These approximate methods fall in three major categories:

(a) *Reduction factor method*

In this method the axial load and moment computed from an ordinary analysis are divided by a reduction factor which is a function of slenderness ratio. This method is the first concept in the design of slender columns and it is recommended as an alternative design tool in the Commentary to the American Building Code ACI318-89 [7]. Design of slender columns according to CP114 [63] was also based on this principle.

(b) *Moment magnification method*

To approximate slenderness effects in this procedure, the column is designed for an axial load and a magnified moment. The moment magnifier, by which the moments based on conventional analysis are multiplied, is a function of the factored axial load and the critical buckling load of the column.

This method is adopted for design in the current American Standard ACI318-89 and the Australian Standard AS 3600-1988 [64]. It is considered to be a significant improvement over the reduction factor method prescribed earlier as it calls attention to the basic phenomenon in slender compression members. Detailed study of this method is to be found in ref.[65].

(c) *Additional eccentricity method*

According to this method, the moment at the critical section is taken as equal to the sum of the applied moment and a complementary moment equal to the applied load times an additional eccentricity.

This method seems to be rational since it closely reflect the actual behaviour of slender columns. It is widely accepted for design in Europe. The additional eccentricity is expressed as a function of the slenderness ratio in the current British Standard BS8110: 1985 [6] and in the European Standard Eurocode No.2: 1984 [66].

In the following sections coverage of the design methods adopted in the various codes of practice is given.

2.2.1 British Standard BS8110: 1985

The design of slender columns in BS8110: 1985 [6] is based, as mentioned above, on the additional moment concept. For braced columns (defined in Cl.3.8.1.5 in the Code), the procedure is as follows:

The additional moment M_{add} caused by the lateral deflection due to buckling is given by:

$$M_{add} = N\, a_u \tag{2.1}$$

$$a_u = \beta_a\, K\, h \tag{2.2}$$

$$\beta_a = \frac{1}{2000}\left(\frac{l_e}{b'}\right)^2 \tag{2.3}$$

$$K = \frac{N_{uz} - N}{N_{uz} - N_{bal}} \leq 1.0 \qquad (2.4)$$

$$N_{uz} = 0.45\, f_{cu}\, A_c + 0.87\, f_y\, A_{sc} \qquad (2.5)$$

In these equations:

N = design ultimate axial load on the column (referred to as P in later Chapters).

a_u = deflection at ultimate limit state (referred to as e_u in later Chapters).

K = reduction factor.

h = depth of the cross section measured in the plane under consideration.

b' = smaller dimension of the column.

N_{uz} = design ultimate capacity of a section when subjected to axial load only.

N_{bal} = design axial load capacity of a balanced section; for symmetrically-reinforced rectangular section, it may be taken as $0.25 f_{cu} bd$.

A_c = net cross-sectional area of concrete in a column.

A_{sc} = area of vertical reinforcement.

The initial moment M_i at the point of maximum additional moment (i.e near mid-height of the column) is assumed to be given by:

$$M_i = 0.4M_1 + 0.6M_2 \geq 0.4M_2 \qquad (2.6)$$

where M_1 and M_2 are the smaller and the larger initial end moments due to design ultimate loads, respectively. Assuming the column is bent in double curvature, M_1 should be taken as negative and M_2 positive.

The maximum design moment will be the greatest of (a) to (d):

(a) M_2 (2.7)

(b) $M_i + M_{add}$ (2.8)

(c) $M_1 + M_{add}/2$ (2.9)

(d) $N\, e_{min}$ (2.10)

e_{min} is the minimum eccentricity equal to 0.05 times the overall dimension of the column in the plane of bending considered, but not more than 20 mm.

For unbraced columns, the additional moment given in Eq.(2.1) may be assumed to occur at whichever end of the column has the stiffer joint; the additional moment at the other end may be reduced in proportion to the ratio of the joint stiffnesses at either end. At the critical section, the additional and initial moments act in the same direction and the two are additive.

The approach described above applies to columns having slenderness ratios l_e/h equal to or greater than 15 for braced columns or 10 for unbraced columns. These limits will in terms of l_e/r equal to 50 and 33.3 respectively for rectangular columns, where r is the radius of gyration of the cross-section and is taken as 0.3h. Below these limits the column is classified as short. Sixty is the upper limit permitted for the slenderness ratio l_e/h of braced columns.

No recommendations concerning long-term deformations were given.

2.2.2 American Standard ACI318-89

The ACI Building Code [7] provisions for slenderness evaluation of reinforced concrete columns encourage the use of second-order frame analysis wherever possible or practical. In lieu of such improved analysis the Code provides for an approximate design method based on a moment magnifier principle. Alternatively, the Commentary to the Code [7] permits the use of the reduction factor method in certain cases.

According to the moment magnification method, a compression member will be designed for a factored axial load P_u and a magnified factored moment M_c defined by:

$$M_c = \delta_b M_{2b} + \delta_s M_{2s} \tag{2.11}$$

$$\delta_b = \frac{C_m}{1 - \dfrac{P_u}{\phi_1 P_c}} \geq 1.0 \tag{2.12}$$

$$\delta_s = \frac{1}{1 - \dfrac{\Sigma P_u}{\phi_1 \Sigma P_c}} \geq 1.0 \tag{2.13}$$

$$P_c = \frac{\pi^2 EI}{(kL)^2} \tag{2.14}$$

$$C_m = 0.6 + 0.4 \frac{M_{1b}}{M_{2b}} \geq 0.4 \tag{2.15}$$

$$EI = \frac{(E_c I_g / 5 + E_s I_{se})}{1 + \beta_d} \tag{2.16}$$

or conservatively $$EI = \frac{(E_c I_g / 2.5)}{1 + \beta_d} \qquad (2.17)$$

where

M_{1b} = value of smaller factored end moment on a compression member due to the loads that result in no appreciable sidesway, calculated by conventional elastic frame analysis, positive if member is bent in single curvature, negative if bent in double curvature.

M_{2b} = value of larger factored end moment on compression member due to loads that result in no appreciable sidesway, calculated by conventional elastic frame analysis.

M_{2s} = value of larger factored end moment on compression member due to loads that result in appreciable sidesway, calculated by conventional elastic frame analysis.

δ_b = moment magnification factor for frames braced against sidesway, to reflect effects of member curvature between ends of compression member.

δ_s = moment magnification factor for frames not braced against sidesway, to reflect lateral drift resulting from lateral and gravity loads.

C_m = a factor relating actual moment diagram to an equivalent uniform moment diagram.

P_u = factored axial load at given eccentricity $\leq \phi_1 P_n$ (referred to as P in later Chapters).

P_n = nominal axial load strength at given eccentricity.

P_c = critical load.

ϕ_1 = strength reduction factor (referred to as ϕ in the Code).

EI = flexural stiffness of compression member.

E_c = modulus of elasticity of concrete.

E_s = modulus of elasticity of reinforcement.

I_g = second moment of area of gross concrete section about centroidal axis, neglecting reinforcement.

I_{se} = second moment of area of reinforcement about centroidal axis of member cross-section.

β_d = ratio of maximum factored axial dead load to maximum total factored axial load, where the load is due to gravity effects only in the calculation of P_c in Eq.(2.12), or the ratio of the maximum factored sustained lateral load to the maximum total factored lateral load in that storey in the calculation of P_c in Eq.(2.13).

k = effective length factor.

L = unsupported length of the column (referred to as l_u in the Code).

ΣP_u and ΣP_c are the summation for all columns in a storey.

The slenderness effects may be neglected when the slenderness ratio kL/r is less than $(34\text{-}12\ \frac{M_{1b}}{M_{2b}})$ for braced members, or 22 for unbraced members. When the slenderness ratio kL/r is greater than 100, second order analysis shall be made.

The ACI Code recognizes the effect of stiffness upon the strength of a slender column, which decreases due to long-term loads, hence the introduction of the factor β_d in the EI expression ($\beta_d = 0$ in the case of no sustained load).

For the past ten years, research has been done in North America to introduce reliability-based load and resistance factors for use in computing the moment magnification of slender reinforced concrete columns [67,68,69].

2.2.3 Eurocode No.2: 1984

Eurocode No.2: 1984 [66] classifies structures into sway frames, rigid frames and individual columns. The method of accounting for second-order effects in the last type depends upon the value of the slenderness ratio which is defined as:

$$\lambda = \frac{l_e}{r} \tag{2.18}$$

where l_e = effective length.

r = radius of gyration.

A check for buckling must be made if $\lambda > 25$, for $25<\lambda<140$ the practical design methods given below apply. For higher slenderness ratios the considerations set out for

large compression structures apply. The use of slenderness ratios higher than 200 is not advised.

The practical design methods basically depend on the additional moment approach. In the critical section, the total eccentricity attributed to columns of constant section comprises:

a - First order eccentricities equal at both ends

$$e_{tot} = e_1 + e_2 = e_f + e_a + e_2 \tag{2.19}$$

$$e_f = \frac{M_{sd}}{N_{sd}} \tag{2.20}$$

$$e_a = \frac{l_e}{300} \geq 20 \text{ mm} \tag{2.21}$$

$$e_2 = \frac{l_e^2}{10} \frac{1}{r} \tag{2.22}$$

where e_f = first order eccentricity (referred to as e_o in the Code).

e_a = additional eccentricity intended to account for any uncertainty concerning the location of the point of incidence of external forces.

e_2 = second order eccentricity.

M_{sd} = first order applied moment.

N_{sd} = applied longitudinal force.

$\frac{1}{r}$ = curvature.

b - Different eccentricities at the ends

In this case an equivalent eccentricity e_e is introduced to replace e_f in Eq.(2.19). The equivalent eccentricity is taken as the larger of the following two values:

$$e_e = 0.6\, e_{os} + 0.4\, e_{oi} \tag{2.23}$$

$$e_e = 0.4\, e_{os} \tag{2.24}$$

where e_{oi} and e_{os} denote the first order eccentricities at the two ends, e_{os} being positive and larger than e_{oi}.

The check for stability can be ignored if λ does not exceed:

$$\lambda_{lim} = 50 - 25 \frac{e_{oi}}{e_{os}} \qquad (2.25)$$

The second order eccentricity e_2 is determined using the "model column method" which is an approximation found to be applicable to a large number of cases. According to that model, equation (2.22) can be applied by means of tables or by using equilibrium method or an alternatively simplified procedure giving two equations for the curvature $\frac{1}{r}$ can be used.

The effects of creep deformations are recommended to be considered in either of the following approximate methods:

- The additional deflection e_c due to creep strain is added in Eq.(2.19). Where e_c is calculated using linear creep theory for the uncracked section.

- The stress-strain diagram for concrete is modified by multiplying the strain by coefficients which take account of the relationship between the action effects giving rise to creep and the total design action effects.

Revisions to Eurocode No.2: 1984 are now underway and the final draft is produced as preliminary and not for publication. In the recent revised draft [70], a more simplified approach regarding slender columns is recommended, similar to the BS8110 design method. The major changes cover the following points:

- The limit beyond which slenderness effects should be considered is expressed in terms of the axial force, cross-sectional area and the concrete cylinder compressive strength.

- Equation (2.21) for the additional eccentricity.

- Equation (2.22) for the second order eccentricity.

- The application of equation (2.22) is much simplified and one expression is given to calculate the curvature.

- The treatment of the effects of long-term deformations is different and is almost ignored.

2.2.4 Other National Codes

2.2.4.1 Japanese Standard: 1986

According to the Japanese Standard [71], a reinforced concrete column is classified as slender when its slenderness ratio l_e/r is greater than 35. In this case the effect of lateral displacements of the columns shall be considered in the structural analysis. The Code stipulates that in the determination of the secondary moments due to lateral displacements, the following factors should be taken into account: slenderness ratio, geometry of the cross section, types of load, conditions of confinement at the ends of the column, properties of materials, quantity and arrangement of reinforcement, effect of shrinkage and creep and so forth. Since such analysis is complicated the Code permits the use of an approximate method in which the secondary moment is calculated separately. However, the Code does not specify any approach for approximating the secondary moments, though *Sakai et al* [48] mention that the reduction factor method has been adopted in the JSCE Concrete Code: 1980.

2.2.4.2 Australian Standard: 1988

The Australian Standard AS 3600-1988 [64] allows two procedures for the design of slender columns. In the first, the axial forces and bending moments shall be determined from a rigorous structural analysis which takes into account the relevant material properties and geometric effects; in this case no approximation of secondary moments is required in design. The second procedure is based on the moment magnification concept, where the axial forces and bending moments are determined by elastic analysis of the structure. The equation provided for the critical load varies from that given in ACI318-89 and tends to be more complicated. The effect of long-term loads is considered by introducing the factor β_d directly in the buckling load expression.

2.2.5 Direct comparison

The development of new Codes of Practice is influenced by other national codes and world-wide research. Similarities between Codes are therefore inevitable due to their historic development (e.g. BS8110 and Eurocode, ACI and AS).

Due to the numerous variables involved in the stability problem of slender columns, the formulation of an exact design method may not readily be possible and it appears that only a rigorous structural analysis which takes into consideration all the factors affecting column strength will provide the desirable accuracy. Accordingly each of

the three basic methods adopted by different Codes of Practice has its own advantages and limitations. A rigorous analysis was permitted in some Codes (ACI, JSCE and AS).

In terms of accuracy, a comparison with test results [65], showed that the additional eccentricity method gives a slightly better estimation of failure loads than the moment magnification method and much better than the reduction factor method, which in certain cases of unbraced frames was very unsafe. The moment magnification method adopted in the ACI Code, produces conservative results for slender columns subjected to low end eccentricities and unconservative results for slender columns with high end eccentricities [2,60,62].

In respect of simplicity in use, the moment magnification method is classified as difficult in application because of the complexity of determining the EI value required to calculate the buckling load. The reduction factor method and additional eccentricity method are considered easier methods for design [65].

The expressions provided for EI in the ACI Code (Eq.2.16 and 2.17) were re-examined by *MacGregor et al* in 1975 [3] and more recently by *Mirza* in 1990 [72]. Based on statistical evaluation of the parameters that affect the flexural stiffness of slender reinforced concrete columns subjected to short-time loads, *Mirza* suggested alternative EI expressions to those quoted for design in the ACI Code, claiming that Eqs.2.16 and 2.17 are quite approximate when compared with the values of EI derived from thrust-moment-curvature relationships. Furthermore, he pointed out that ACI318-89 Eq.(10-11) (Eq.2.17 here) is in most cases less conservative than ACI318-89 Eq.(10-10) (Eq.2.16), contradicting what is stated in the ACI Building Code.

Previous research work confirms the reduction in the capacity of slender column when it is subjected to continuous loading. Some Codes have shown their awareness of this fact by including allowance for long-term deformations in their provisions (ACI and Eurocode), while others omitted any recommendations on this issue (BS8110).

All Codes agree on ignoring the slenderness effects up to a certain limit, which has a fixed value in BS8110 and the Japanese Code, whereas it varies according to the ratio of end eccentricities acting on the column in ACI and Eurocode 2. In the Australian Standard, beside the ratio of end eccentricities, the ratio of the axial force to the axial compression capacity is also included in defining the limit.

The criteria used for the design of slender columns in various Codes reviewed, is based on a material failure mode i.e when the cross-section of the column develops its ultimate strength capacity.

2.3 *Beal's* method of analysis and *Dinku's* development

A recent paper by *Beal* [52] proposing a graphical method for the design of pin-ended slender columns, created some doubts about the accuracy of design methods adopted in current Codes of Practice outlined above.

The method allows rapid determination of column capacity under any combination of slenderness and initial eccentricity, simply and directly, once section moment-curvature relationships are known. Instead of plotting moment against curvature in the conventional fashion, *Beal* plotted load eccentricity against curvature. He based his calculation on the stress-strain diagrams for concrete and steel as suggested by CP110: part 1 "The structural use of concrete" [38]. Another set of graphs were prepared relating mid-height eccentricity and curvature geometrically assuming a sine curve for the deflected shape of the column. By overlaying the two graphs the section capacity could be established.

To investigate the method, *Beal* carried out sample analyses of pin-ended reinforced concrete columns with two values of reinforcement ratio and concrete grade under specified load eccentricity and initial imperfection. He arrived at proposed reduction coefficients for the design of the columns considered under different slenderness ratios. In verifying the method he compared it with the test results reported by *Cranston* [37], quoting encouraging figures for the standard deviation and coefficient of variation of the ratio maximum load/predicted load obtained and recording substantial improvement over the corresponding figures for CP110 and CP114. Based on these findings, *Beal* questioned the adequacy of the CP110 Code Provisions for the instability problem, bringing the safety margins allowed for in the design formulae in the Code into doubt and open to criticism, claiming that the theoretical superiority of CP110 over CP114 is not particularly certain. Considering that the Code of Practice BS8110 would give only slightly different answers to CP110, this is a substantial criticism of current design practice.

Dinku [56] conducted an investigation of the proposals set by *Beal* in the light of existing experimental data provided in *Cranston's* report [37] and in comparative examples with some design calculations [6,53,73]. The results obtained verified that the graphical method could predict concentrically or eccentrically loaded pin-ended slender column capacity, in short and long-term loading conditions, faster and more safely than the existing alternative methods once the graphs are prepared.

Dinku developed computer programs to generate load eccentricity-curvature graphs in terms of capacity ratio (P/P_0), based on stress-strain relationships for concrete and steel specified in CP110. In producing load eccentricity-curvature curves for long-term loading conditions, *Dinku* made allowance for sustained load effects by taking

the long-term strains as 2.5 times short-term values. Different material strengths and reinforcement percentages with three conditions of initial imperfection were considered in the investigation. Based on the reduction coefficients obtained, he concluded that eccentrically loaded pin-ended slender columns have lower capacity than respective concentrically loaded columns under the same material and sectional properties, when subjected to similar loading. The effect of slenderness was found to be more significant than material strength and reinforcement percentage in terms of strength reduction.

The results obtained by *Beal* and *Dinku* were promising and encouraged the carrying out of further research to investigate the graphical method proposed and verify it by a programme of tests under short and long-term loading conditions. In particular it was recommended that more accurate prediction of column capacity could be achieved if the treatment of creep and concrete failure strain in the long-term were better represented.

Table 2.1 : Test data.

Researcher	Date	No.of tests	Type of column*			Method of loading**					
			H	F	B	S	L	L-S	L-C	L-C-S	C-S
Baumann [16]	1934	43	30	13	-	43	-	-	-	-	-
Thomas [17]	1939	14	14	-	-	14	-	-	-	-	-
Rambøll [74]	1951	38	38	-	-	38	-	-	-	-	-
Ernst et al [19]	1952	8	8	-	-	8	-	-	-	-	-
Gehler&Hütter [75]	1954	50	50	-	-	50	-	-	-	-	-
Gaede [76]	1958	16	16	-	-	8	8	-	-	-	-
Kordina [77]	1960	4	4	-	-	4	-	-	-	-	-
Aas-Jakobsen [78]	1960	20	20	-	-	20	-	-	-	-	-
Chang&Ferguson [25]	1963	6	6	-	-	6	-	-	-	-	-
Sàenz&Martin [26]	1963	52	-	52	-	52	-	-	-	-	-
Breen&Ferguson [27]	1964	6	-	6	-	5	-	1	-	-	-
Ramamurthy [79]	1965	55	-	-	55	55	-	-	-	-	-
Martin&Olivieri [80]	1966	8	8	-	-	8	-	-	-	-	-
MacGregor& Barter [81]	1966	8	4	4	-	8	-	-	-	-	-
Furlong& Ferguson [82]	1966	7	-	7	-	6	-	1	-	-	-
Ferguson&Breen [83]	1966	8	-	8	-	7	1	-	-	-	-
Green [84]	1966	5	5	-	-	-	5	-	-	-	-
Pannell& Robinson [28]	1968	17	9	-	8	17	-	-	-	-	-
Green&Breen [31]	1969	10	10	-	-	-	10	-	-	-	-
Mehmel et al [85]	1969	16	14	2	-	16	-	-	-	-	-
Breen&Ferguson [86]	1969	10	10	-	-	10	-	-	-	-	-
Ramu et al [32]	1969	37	37	-	-	6	19	12	-	-	-
Goyal [33]	1970	46	46	-	-	26	-	20	-	-	-

Continued

Researcher	Date	No.of tests	Type of column*			Method of loading**					
			H	F	B	S	L	L-S	L-C	L-C-S	C-S
Hellesland& Green [34]	1971	7	7	-	-	-	-	-	-	7	-
Drysdale& Huggins [35]	1971	57	8	-	49	26	16	15	-	-	-
Cranston& Sturrock [36]	1971	8	3	-	5	8	-	-	-	-	-
Hirasawa [87]	1974	55	11	-	44	35	-	10	2	3	5
Kordina [88]	1975	12	12	-	-	-	-	12	-	-	-
Green& Hellesland [39]	1975	8	8	-	-	2	-	-	2	-	4
Blomeier&Breen [40]	1975	3	-	3	-	3	-	-	-	-	-
Wu&Huggins [43]	1977	34	-	-	34	8	26	-	-	-	-
Pancholi [29]	1977	39	39	-	-	33	6	-	-	-	-
Gruber&Menn [89]	1978	4	4	-	-	4	-	-	-	-	-
Dracos [5]	1982	40	40	-	-	36	2	2	-	-	-
Behan&O'Connor [46]	1982	67	67	-	-	51	16	-	-	-	-
Schofield [30]	1983	55	55	-	-	50	5	-	-	-	-
Iwai et al [51]	1986	36	-	-	36	36	-	-	-	-	-
Total		909	583	95	231	699	114	73	4	10	9

* H = Hinged column.
F = Fixed end column.
B = Biaxially loaded column.

** S = Short-term loading.
L = Sustained loading.
C = Cyclic loading.
L-S = Long-term load followed by short-term test.

CHAPTER THREE

ANALYSIS OF SLENDER REINFORCED CONCRETE COLUMNS

3.1 Introduction

The theoretical analysis described here is fundamentally similar to that followed by *Beal* [52] and more recently by *Dinku* [56]. The computer programs initially developed by *Dinku* to generate graphs for eccentricity against curvature for different capacity ratios (P/P_0), were limited in their application due to the fixed values used for some of the variables (position of reinforcement d/h and creep coefficient ϕ). Factors of safety for concrete and steel were totally omitted in the programs. *Dinku's* programs were based on CP110 stress-strain relationships for concrete and steel, as the main aim of his work was to investigate *Beal's* proposals.

It was therefore necessary at the early stages of the current research to generalize the programs to deal with different locations of reinforcement and to take account of possible long-term deformations. Also they needed to be updated using BS8110 stress-strain diagrams for concrete and steel and making allowance for using different values for the partial safety factor for strength of materials.

This Chapter is concerned in summarizing the steps followed in the analysis and describing the modifications and developments made to the existing programs. It also covers other programs written to complete the analysis and plot the graphs required. Some of the factors which affect the theoretical results are also discussed.

3.2 Basic assumptions of analysis

Basically most of the assumptions adopted by *Beal* in his proposal for the graphical analysis and by *Dinku* in his investigation of the method are valid here.

The following principles apply throughout the theoretical analysis in the present work:

1- The analysis is restricted to columns hinged at both ends, either concentrically or eccentrically loaded with equal end eccentricities.

2- Full bond exists between steel and concrete and a linear strain distribution profile exists before and after the application of bending.

3- For short-term analysis, concrete is assumed to have the stress-strain curve shown in Fig.3.1, which is reproduced from BS8110: part 1: 1985. For long-term analysis, Fig.3.1 was modified to allow for creep effects, by multiplying the strains by $(1+\phi)$ and consequently reducing the initial tangent modulus of elasticity by the same factor.

4- The tensile strength of concrete is ignored.

5- The reinforcement steel has a bilinear stress-strain diagram as shown in Fig.3.2 (reproduced from BS8110: part 1: 1985).

6- The deflected shape of the pin-ended column follows a sine-curve.

In the overall investigation, a symmetrically doubly reinforced rectangular cross-section is considered. The gross area of concrete has been used throughout the calculations, no reduction has been made for the area occupied by the steel.

3.3 Analysis carried out

The analysis was performed in two main procedures; the first was developed to establish the relationship between load eccentricity and curvature in terms of capacity ratio (P/P_0), and the second procedure undertaken to produce the second set of graphs between buckling deflection and curvature in terms of the slenderness ratio (l_e/h).

3.3.1 Load eccentricity-curvature relationship

The procedure can be summarised in the following steps:

Step 1 The materials' properties are specified at this stage i.e. f_{cu}, f_y and $\%A_s$. Specific values are assumed for the variables: d/h and ϕ (ϕ is used in the case of long-term analysis). Factors of safety are taken as unity, for the purpose of comparing the results with the experimental work.

Step 2 The depth of the column cross-section was subdivided into forty equal intervals at 0.025h, as shown in Fig.3.3(a) (which is adapted from ref. [56]). The neutral axis was then varied from -40 outside the section to 39 inside the section.

Step 3 For each neutral axis position, within or outside the section (see Fig.3.4 adapted from ref. [56]), the concrete strain at the extreme compression fibre at the top of

the section, was varied from 0.0001 to 0.0035 for short-term loading as shown in Fig.3.3(b) and from $0.0001(1+\phi)$ to $0.0035(1+\phi)$ for long-term cases.

Step 4 For each value of the extreme compression fibre strain, the respective compressive strains in concrete throughout the section at the specified intervals were calculated and the corresponding stresses were obtained from Fig.3.1 for short-term analysis (as mentioned above the diagram was modified by $(1+\phi)$ for the long-term analysis). Integrating these stresses, using the trapezoidal rule, gave the resultant load and moment due to concrete alone. The equations used are given below:

$$P'_c = \frac{1}{80}\left[f_{c1} + 2\left(f_{c2} + f_{c3} + f_{c4} + \quad \ldots\ldots \quad + f_{c39} + f_{c40} \right) + f_{c41} \right] bh \qquad (3.1)$$

$$M'_c = \frac{1}{40}\left[4.17\times10^{-3} f_{c1} + 0.025f_{c2} + 0.05f_{c3} + 0.075f_{c4} + 0.1f_{c5} + 0.125f_{c6} + 0.15f_{c7} + 0.175f_{c8} + 0.2f_{c9} + 0.225f_{c10} + 0.25f_{c11} + 0.275f_{c12} + 0.3f_{c13} + 0.325f_{c14} + 0.35f_{c15} + 0.375f_{c16} + 0.14f_{c17} + 0.425f_{c18} + 0.45f_{c19} + 0.475f_{c20} + 0.5f_{c21} + 0.525f_{c22} + 0.55f_{c23} + 0.575f_{c24} + 0.6f_{c25} + 0.625f_{c26} + 0.65f_{c27} + 0.675f_{c28} + 0.7f_{c29} + 0.725f_{c30} + 0.75f_{c31} + 0.775f_{c32} + 0.8f_{c33} + 0.825f_{c34} + 0.85f_{c35} + 0.875f_{c36} + 0.9f_{c37} + 0.925f_{c38} + 0.95f_{c39} + 0.975f_{c40} + 0.496f_{c41} \right] bh^2 \qquad (3.2)$$

where P'_c = resultant concrete force.

M'_c = resultant concrete moment calculated about the bottom edge of the cross-section.

f_{cn} = stress corresponding to the neutral axis at the (n-1) position (Fig.3.3).

b = width of a column.

h = depth of the cross-section measured in plane of bending.

Step 5 For the same neutral axis position as in step 3 and at each specified value for the concrete strain at top of the section as in step 4, the strains in steel were evaluated and the corresponding steel stresses were determined from the stress-strain diagram shown in Fig.3.2. Multiplying these stresses by steel area, the resultant forces and moments due to steel strains can be obtained. Hence:

$$P_s = P_{s1} + P_{s2} = f_{s1}\frac{A_s}{2} + f_{s2}\frac{A_s}{2} \qquad (3.3)$$

$$M_s = f_{s1}\frac{A_s}{2}d + f_{s2}\frac{A_s}{2}(h - d) \qquad (3.4)$$

where P_s = resultant steel force.

M_s = resultant steel moment taken about the bottom edge of the section.

f_{s1}, f_{s2} = stresses in top and bottom steel respectively (see Fig.3.4).

(the term "top" here refers to steel near the highly compressed face).

A_s = area of steel.

d = effective depth of tension reinforcement.

Step 6 To obtain the total force and moment resisted by the reinforced concrete section at a particular neutral axis position and at a particular value for the concrete compressive strain at the extreme fibre, the resultant forces and moments in concrete and steel as calculated in steps 4 and 5 were added together,i.e:

$$P_{RC} = P'_c + P_s = P \tag{3.5}$$

$$M_{RC} = M'_c + M_s = M \tag{3.6}$$

Step 7 To calculate the eccentricity, the total moment M is divided by the total force P and a value of 0.5h is subtracted from the result to obtain the eccentricity about the centroidal axis since the moments were taken about the bottom edge, hence:

$$e = \frac{M}{P} - 0.5h \tag{3.7}$$

Step 8 The ratio P/P_0 can be determined now, where P is the capacity of the reinforced section as calculated in step 6 and P_0 is the squash load given by the following formula:

$$P_0 = 0.67 f_{cu} A_c + A_s f_y \tag{3.8}$$

where A_c = gross cross-sectional area = bh.

f_{cu} = concrete cube strength.

f_y = tensile yield stress of steel.

The coefficient 0.67 takes account of the relation between the cube strength and the bending strength in a flexural member.

Step 9 For the same neutral axis position specified in step 3 and the same value given for the concrete strain at the extreme compression fibre in step 4, the curvature $\frac{1}{r}$ is calculated from:

$$\frac{1}{r} = \frac{\varepsilon_n - \varepsilon_{n-1}}{0.025h} \tag{3.9}$$

where $\frac{1}{r}$ = curvature.

ε_n = strain at nth interval.

Step 10 Steps 3-9 are repeated for all strain variations at the particular position of the neutral axis specified in step 3, but for the same assumptions as step 1.

Step 11 Steps 3-10 are repeated for all neutral axis positions but again for the same assumptions as step 1.

Step 12 Using linear interpolation the values of eccentricity and curvature were determined for the following values of the ratio P/P_0: 0.02, 0.05, 0.1, 0.2, ... , 0.8, 0.9. Hence, the data for one graph is produced.

Step 13 The assumptions of step 1 are varied and steps 2-12 are repeated for different material properties i.e f_{cu}, f_y and $\%A_s$. The effective depth ratio d/h may vary and in case of long-term analysis the creep coefficient ϕ can also be varied.

To handle the above calculations efficiently, two computer programs, namely **COLUMNBS PASCAL** for short-term loads and **COLMNBSL PASCAL** for long-term loads were used and both are provided in Appendix A. The two programs were developed from the work of *Dinku* and updated according to assumptions (3) and (5) of 3.2. They are of wider application as no fixed values are used for the variables involved.

Once step 12 is completed, the relationship between curvature and eccentricity, in terms of the specified values of the ratio P/P_0, can be represented graphically in a series of curves. A simple program written in FORTRAN was used to plot the data utilizing a graphical package, the program is called **UGHOST44** and is attached in Appendix A.

The range of variables which could be considered is very large and some restriction is necessary to keep the total number of graphs to a practical level.

After carrying out initial tests, the following values were selected as appropriate for the variables involved:

1- Concrete characteristic cube strength: f_{cu} = 40, 50, 60 and 70 N/mm^2.

2- Tensile yield stress of steel: f_y = 530 N/mm^2.

3- Reinforcement ratio: $\%A_s$ = 2, 3 and 4.

4- Effective depth ratio: d/h = 0.75 and 0.8.

5- Creep coefficient: ϕ = 2.0, for long-term graphs.

6- Partial safety factor for strength of materials: γ_m = 1.0.

Different combinations of the variables were considered to illustrate the trend. Typical examples of the graphs produced are shown in Figures 3.5 to 3.13 for short-term loading and in Figures 3.14 to 3.22 for long-term loading. These graphs were utilized later to analyse the experimental results.

The broken line at the right-hand end of the curves corresponds to the failure strain of 0.0035 for short-term loading and 0.0105 for long-term cases.

3.3.2 Buckling deflection-curvature relationship

The buckling load of pin-ended elastic strut was first established by *Euler* as:

$$P_c = \frac{\pi^2 EI}{l_e^2} \tag{3.10}$$

where P_c = buckling load.

EI = flexural stiffness of the column.

l_e = effective length of the column.

Considering equation (3.10) and assuming a sine curve for the deflected shape of the column the relationship between curvature and mid-height eccentricity can be expressed as follows:

$$\frac{e}{h} = \frac{1}{\pi^2} \frac{h}{r} \left(\frac{l_e}{h}\right)^2 \tag{3.11}$$

An allowance for initial imperfection e_0 is made by including it in equation (3.11), thus:

$$\frac{e}{h} = \frac{1}{\pi^2}\,\frac{h}{r}\left(\frac{l_e}{h}\right)^2 + \frac{e_0}{h} \qquad (3.12)$$

where e_0 = initial imperfection at mid-height given in terms of l_e.

The relationship shown in equation (3.12) was plotted for a range of slenderness ratios between 18 and 63, considering two values for the initial imperfections e_0=0.0 and $e_0=5.68\times10^{-4}L$. The resultant graphs are shown in Figures 3.23 and 3.24. Equation (3.12) was programmed using PASCAL to ease production of the data. The program was named **BUCKDEF PASCAL** and the data plotted using program **UGHOST99 FORTRAN**. Both programs are attached in Appendix A. Program **UGHOST99** is applied through a graphical package.

3.3.3 Theoretical results

Having obtained the necessary graphs, the analysis can now be performed. For the greatest convenience Figures 3.23 and 3.24 were produced on transparent overlays. The reduction in column capacity under any combination of slenderness ratio and load eccentricity can be determined directly by superimposing the overlay on the relevant graph from the load eccentricity-curvature curves. The effect of initial load eccentricity e_i is taken into account simply by sliding the overlay vertically to the appropriate value of e_i/h.

To illustrate how the method works, typical superimposed graphs are shown in Figures 3.25 to 3.28 for different combinations of load eccentricity and initial imperfection. Figure 3.25 gives the solution for a column with initial imperfection, having a slenderness ratio of 28.8 and with a load eccentricity of e_i=0.1h under short-term loading conditions. The buckling load is given at the point where the straight line of l_e/h=28.8 becomes tangential to one of the curves. Therefore,for this particular example the buckling load P equals $0.3P_0$, where P_0 is the maximum axial capacity of the section. The tangential point also gives the eccentricity of axial load about the centroidal axis at column mid-height at the point of instability, which could be read off the vertical axis, hence e=0.24h. Subtracting the values of e_0 and e_i from the eccentricity e (i.e $(e-e_i-e_0)$) will give the deflection due to first and second order effects. Fig.3.26 shows another example for a column having a slenderness ratio of 18 and a load eccentricity e_i=0.1h, loaded under long-term conditions. Assuming no initial imperfection, the buckling load was found to be $0.4P_0$ and the corresponding eccentricity at this load equalled 0.245h. In Fig.3.27 a different combination was considered for the same column. The load was assumed to be axial i.e zero eccentricity and initial imperfection of $5.68\times10^{-4}L$. Consequently the load and mid-height eccentricity were found to be $0.6P_0$ and 0.08h respectively. A fourth case is shown in Fig.3.28, where load is applied at an

eccentricity e_i of 0.1h with the initial imperfection. This is the most common combination which would occur in practice; under this assumption the buckling load for a column of slenderness ratio of 26.47, under long-term loading conditions, will be $0.2P_0$ and the corresponding eccentricity 0.315h. The case of zero initial imperfection and pure axial load was not considered as it was thought to be highly unlikely in practice.

To achieve simplicity and accuracy in obtaining the theoretical results, different scales were chosen for the vertical and horizontal axes. In cases where the tangential curve does not appear on the graph, linear interpolation may be employed to plot it.

3.4 Influences on the theoretical results

3.4.1 Stress-strain diagrams

The proposed method of analysis outlined in 3.3 is not confined to reinforced concrete columns; it can be applied to columns of any other materials, once the stress-strain relationship is determined.

The stress-strain diagrams shown in Figures 3.1 and 3.2 for concrete and steel are reproduced from BS8110: part 1: 1985. These curves have been derived from the available data to be representative for design purposes. Since the main aim of the analysis carried out is to help establish a design method, these curves were adopted here.

Tensile force taken by concrete is ignored throughout the investigation because it has a negligible effect. *Schofield* [30] made some comparisons between the results obtained with and without allowing for the effect of concrete tensile strength and concluded that "It is advisable to include an allowance for tensile concrete strength for deflection analysis but it may be safely neglected for the determination of buckling loads". *Cranston* [37] in his computer studies to develop a design method, which formed the basis of CP110 Code provisions, ignored the influence of the tensile strength of the concrete which in his opinion should increase the ultimate load in an actual test.

Strains in concrete are known to increase with time under constant stress, even at very low stresses and under normal environmental conditions, causing a decrease in the stiffness of the structural member. To cater for sustained load effects, an allowance for creep has been made by modifying the stress-strain diagram shown in Fig.3.1. The strains are multiplied by $(1+\phi)$ where ϕ is the creep coefficient and the initial modulus of elasticity is reduced by the same factor i.e using the effective modulus of elasticity. The creep coefficient was produced as a variable in COLMNBSL PASCAL, making the program capable of accepting any value. This could be measured experimentally or assessed using different methods available for estimating creep under various conditions.

A value of 2.0 was used for ϕ in producing the long-term graphs (Figs.3.14-3.22). *Beal* [52] in his long-term analysis assumed the reduced modulus of elasticity to be 40% of the short-term value. He based his assumption on figures in the handbook on the unified Code CP110 for structural concrete [90]. *Dinku* [56] adopted the same value in his investigation of *Beal's* method.

The effect of adopting BS8110: part 1 figure for the initial tangent modulus of elasticity:

$$E_c = 5.5\sqrt{\frac{f_{cu}}{\gamma_m}} \qquad (kN/mm^2) \qquad (3.13)$$

results in overestimation of column capacity if the actual figures are lower than that given by the above equation, or underestimation of the capacity if the actual figures are higher. Considering the purpose of this work and the fact that the value of E_c is likely to vary throughout the height of the column, using the BS8110 figure for E_c stands as a reasonable assumption.

Equation (3.10) was used in the moment magnification procedure adopted for design of slender columns in ACI318-89 [7]. The main problem in that formula, as stated in the Commentary-ACI318R-89 [7], is the choice of the stiffness parameter EI. Based on detailed study, *MacGregor et al* [3] concluded that it is difficult analytically to derive a unique expression for EI due to the complexity of the problem because this parameter is affected by many variables such as the magnitude of moment, degree of cracking, creep, the non-linearity of the concrete stress-strain curve and the location and amount of reinforcement.

3.4.2 Trapezoidal rule

The trapezoidal rule adopted in the program to obtain the resultant concrete force and moment was originally suggested by *Beal* in his proposal for the graphical analysis. *Beal* divided the depth of the column cross-section into 5 parts at 0.2h intervals and *Dinku* divided the section at intervals of 0.1h. A close look at *Dinku's* load eccentricity-curvature graphs in terms of P/P_0, showed that some of the curves clearly do not follow the general trend, in particular the curves for P/P_0 of 0.05 and 0.1. Examining the data for these curves revealed that there were not enough points for the eccentricity and curvature to plot the curves correctly, particularly at their final parts.

The best way to increase the number of data points was by dividing the section at smaller intervals of 0.05h i.e dividing the depth into 20 sections. Quite significant improvement was achieved in the smoothing and the trends of these two curves as the number of data points increased, thus confirming that the problem is with the trapezoidal

rule rather than any inherent defect in the proposed analysis. However, when plotting the curves at full scale (i.e up to the end points which correspond to the failure strain in concrete), it was found that in some of the graphs, the end points of two curves for P/P_0 of 0.05 (or 0.02) and 0.1 were still incorrect. The reason was that, when the neutral axis is within about 0.2h or less from the top of the section, the force due to concrete is very small compared with the moment and any small error resulting from the approximation implied by the trapezoidal rule, is considerably magnified when dividing the moment by the load to obtain the eccentricity.

In an attempt to minimise the problem, the section was further subdivided into 40 parts of 0.025h intervals. A slight improvement was achieved this time and the error was confined to the end points of the two curves for P/P_0=0.05 (or 0.02) and 0.1, and in most graphs to the curve of P/P_0=0.05 (or 0.02). This problem is considered minor as it does not affect the theoretical results in any way because it occurs outside the practical design range of the curves (instability, as will be covered in later Chapters, occurs at relatively low concrete compressive strains); accordingly the problem was considered too negligible to merit further consideration. However, for the purist the exact solution can be determined by using direct integration to calculate the area of the stress-strain block for concrete and its centroid. Alternatively, to calculate the end points precisely, the area of the simplified stress block for concrete given for design in BS8110: part 1: 1985, may be used. Details of these two methods are given in Appendix B.

The only limitation in the program due to employing the trapezoidal rule, is that the value of the effective depth ratio d/h is entered as a number of 0.025 increments, which is sufficient for design purposes.

3.4.3 Initial imperfections

The question of initial imperfections must be considered in any design method for slender reinforced concrete columns, due to the fact that the carrying capacity of such columns is greatly affected by lateral deformations. In practice, columns are never straight; inevitably there is always a bow occurring due to construction misalignment and casting errors. Therefore columns cannot be guaranteed to be truly axially loaded [91]; the possibility of accidental eccentricities always exists, hence the recommendations for minimum eccentricity adopted in codes of practice.

Assessing the amount of initial imperfection present is difficult; published data on this matter is rare and accordingly the figures adopted for the minimum eccentricity in codes of practice are arbitrary. Based on practical considerations, *Beal* [52] used a value of 0.0015L in his analysis. To investigate the effect of including the initial imperfections on the theoretical results, *Dinku* [56] considered three values: 0.0, 0.0015L and 0.003L

in his comparisons with the test data tabulated in *Cranston's* report [37]. The value of 0.0015L was found to give results which agreed reasonably with the experiments; while ignoring the initial imperfections in the analysis generally overestimated the section capacity. This, suggested that however small the initial imperfections in the laboratory test specimens, they should be considered in the theoretical approach.

Cranston [37] when applying the design method he developed to the test data, did not include any allowance for minimum eccentricity.

To clarify any doubt about this point two values were used in the present analysis for the initial imperfection: 0.0 and 5.68×10^{-4}L. Detailed discussion on this issue follows in Chapter 5.

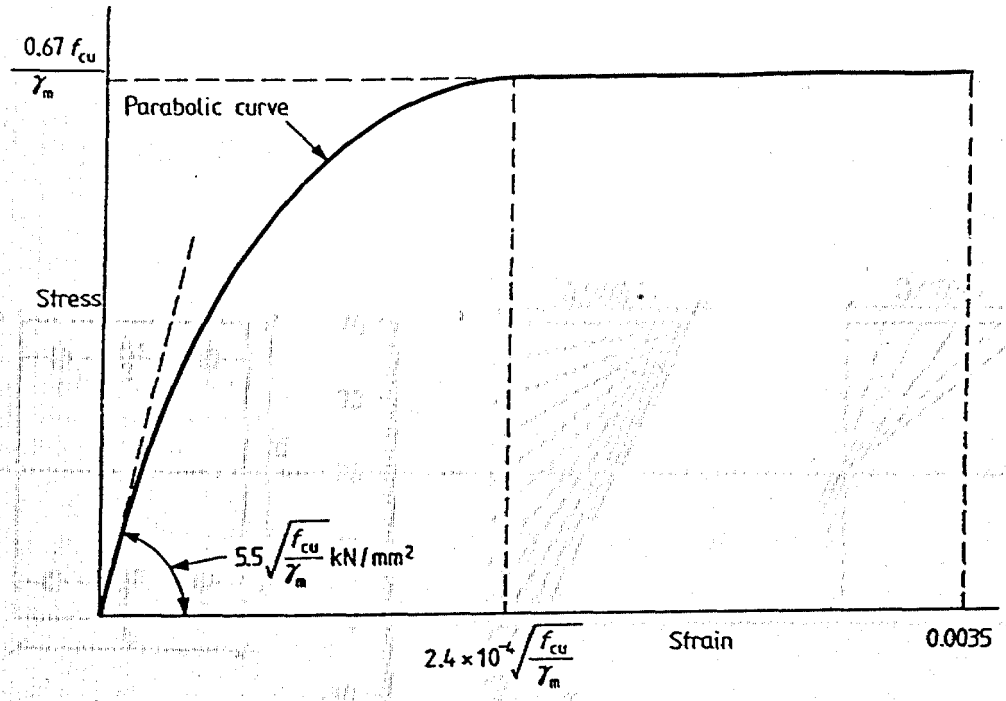

Note. f_{cu} is in N/mm^2.

Fig.3.1 Short-term design stress-strain curve for normal weight concrete according to BS8110: part 1.

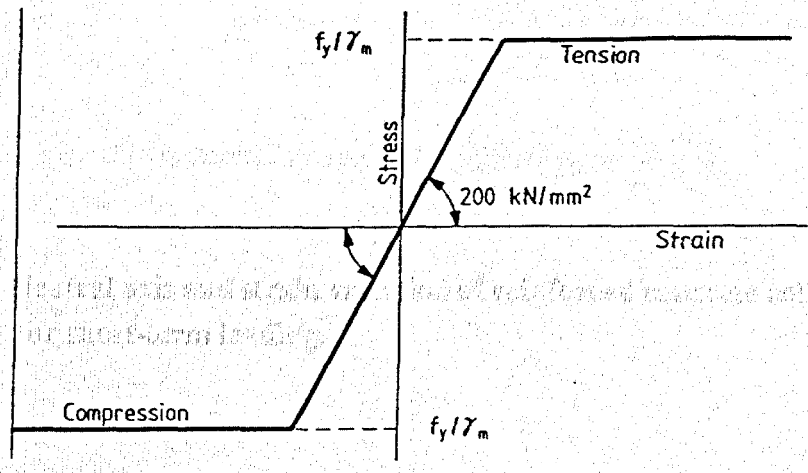

Note. f_y is in N/mm^2.

Fig.3.2 Short-term design stress-strain curve for reinforcement according to BS8110: part 1.

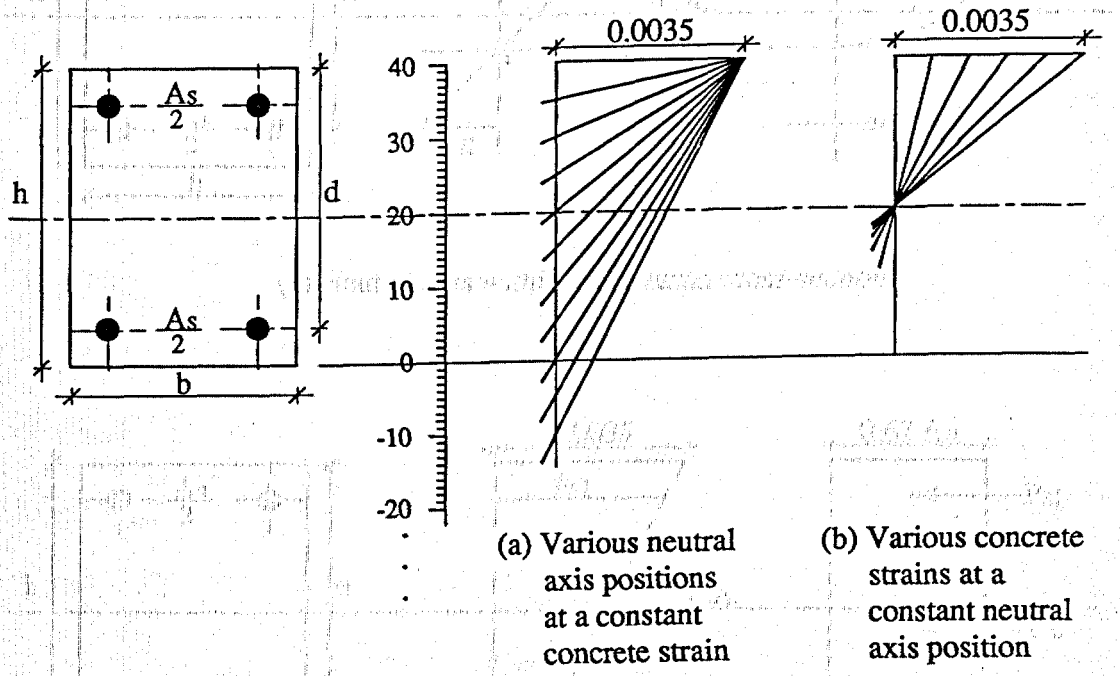

Fig.3.3 Neutral axis and strain variation of reinforced concrete columns for short-term loading.

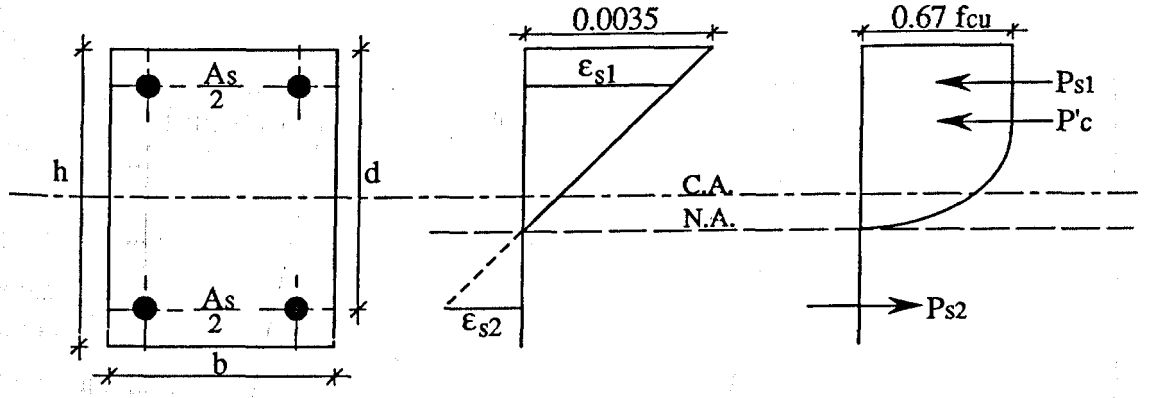

(a) Neutral axis within the column cross-section.

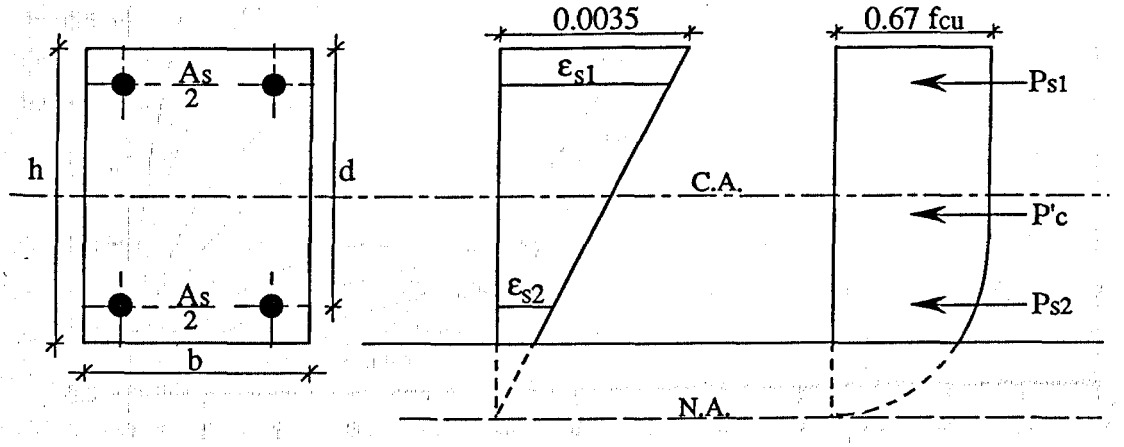

(b) Neutral axis outside the column cross-section.

C.A. Centroidal axis
N.A. Neutral axis

Fig.3.4 Strain and stress distribution for symmetrically reinforced concrete sections.

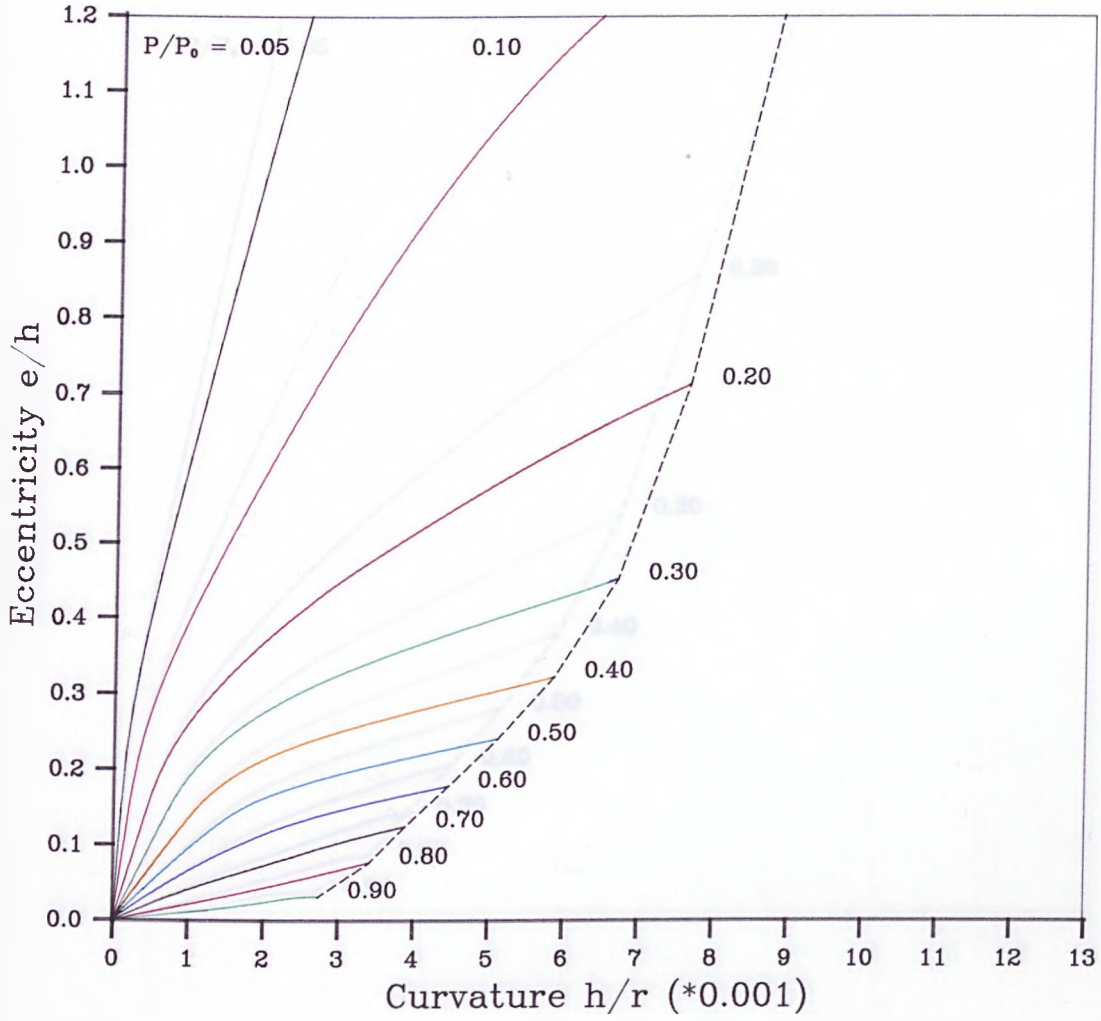

f_{cu} = 40 N/mm²
f_y = 530 N/mm²
$\%A_s$ = 3.0
d/h = 0.75

Fig.3.5 Eccentricity vs Curvature relationship for Short-Term loading.

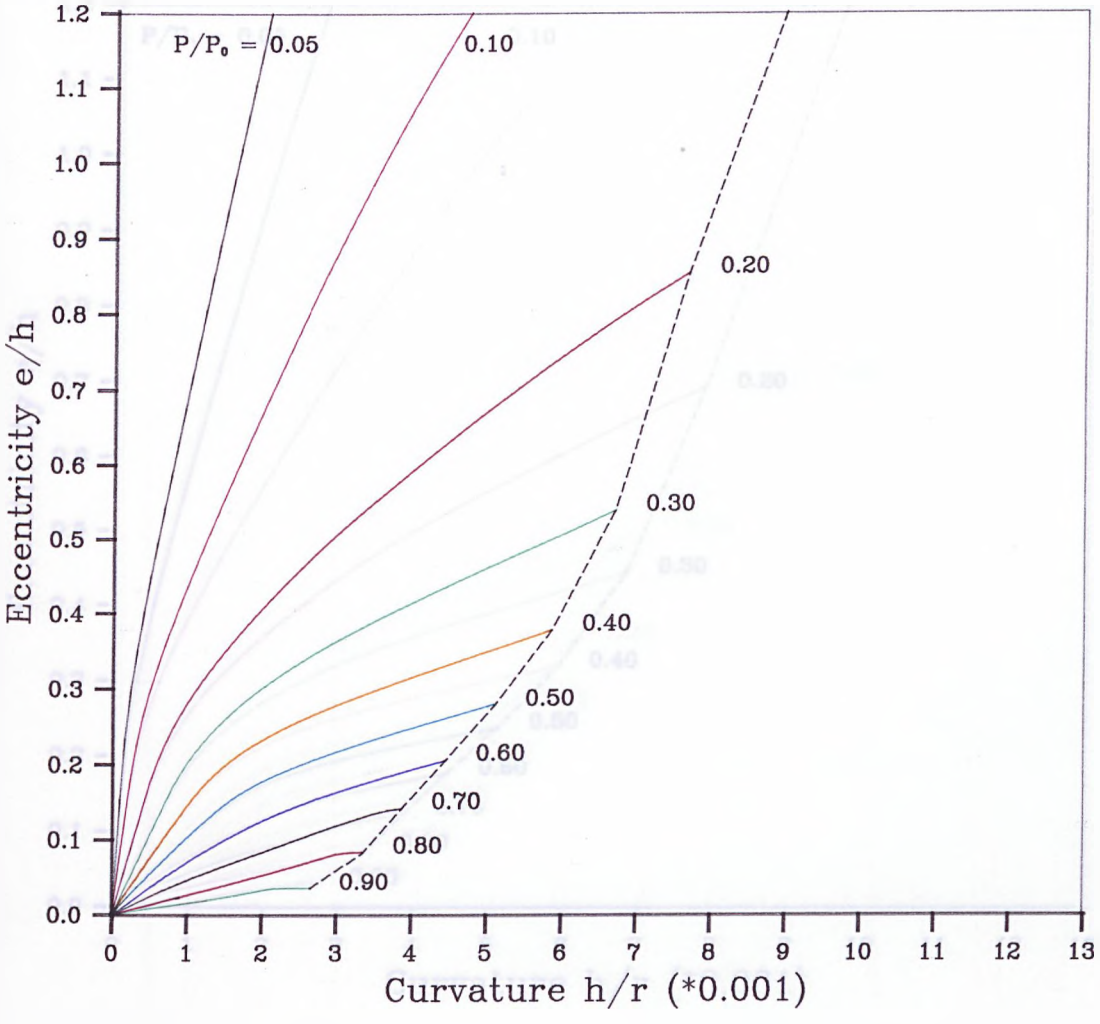

f_{cu} = 40 N/mm²
f_Y = 530 N/mm²
$\%A_s$ = 3.0
d/h = 0.80

Fig.3.6 Eccentricity vs Curvature relationship for Short-Term loading.

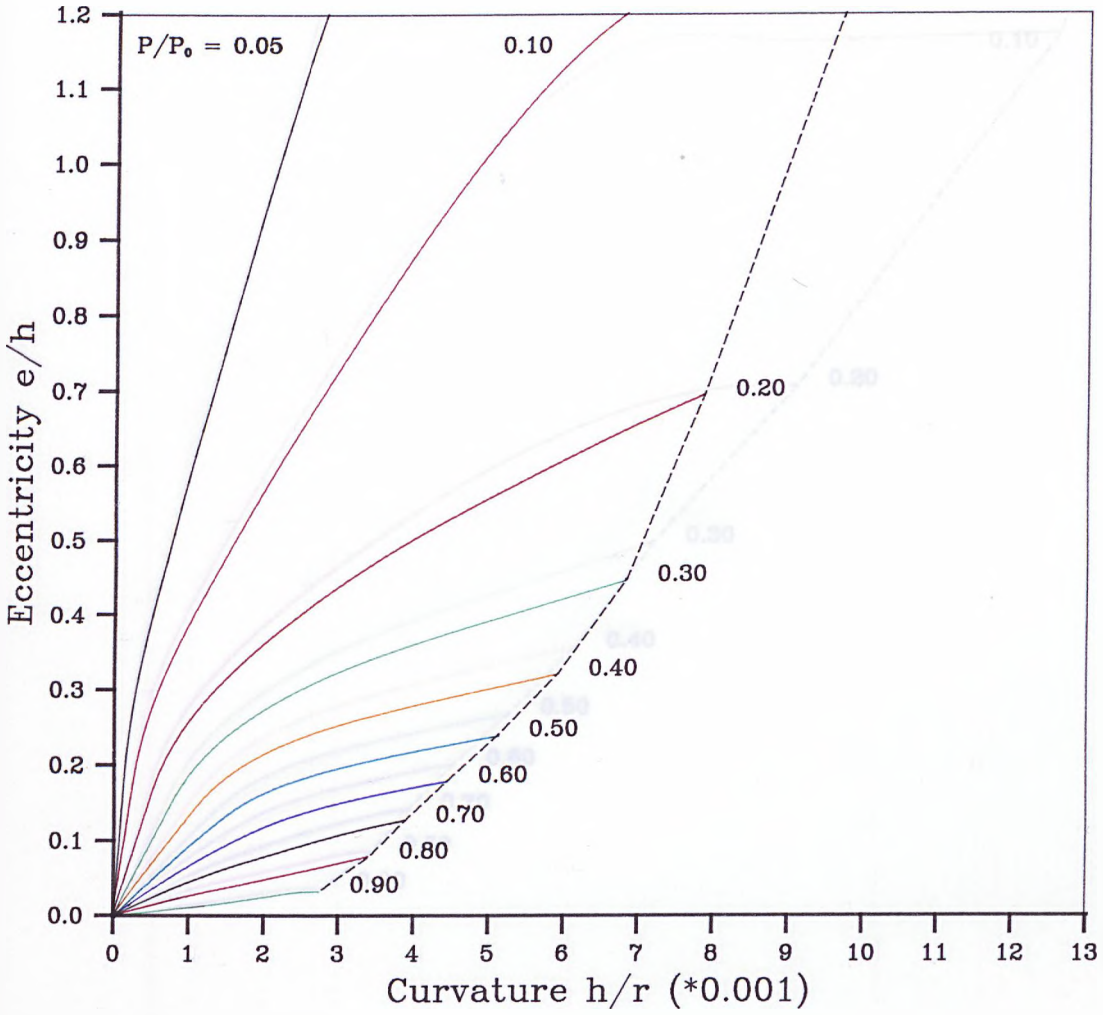

f_{cu} = 50 N/mm²
f_y = 530 N/mm²
$\%A_s$ = 3.0
d/h = 0.75

Fig.3.7 Eccentricity vs Curvature relationship for Short–Term loading.

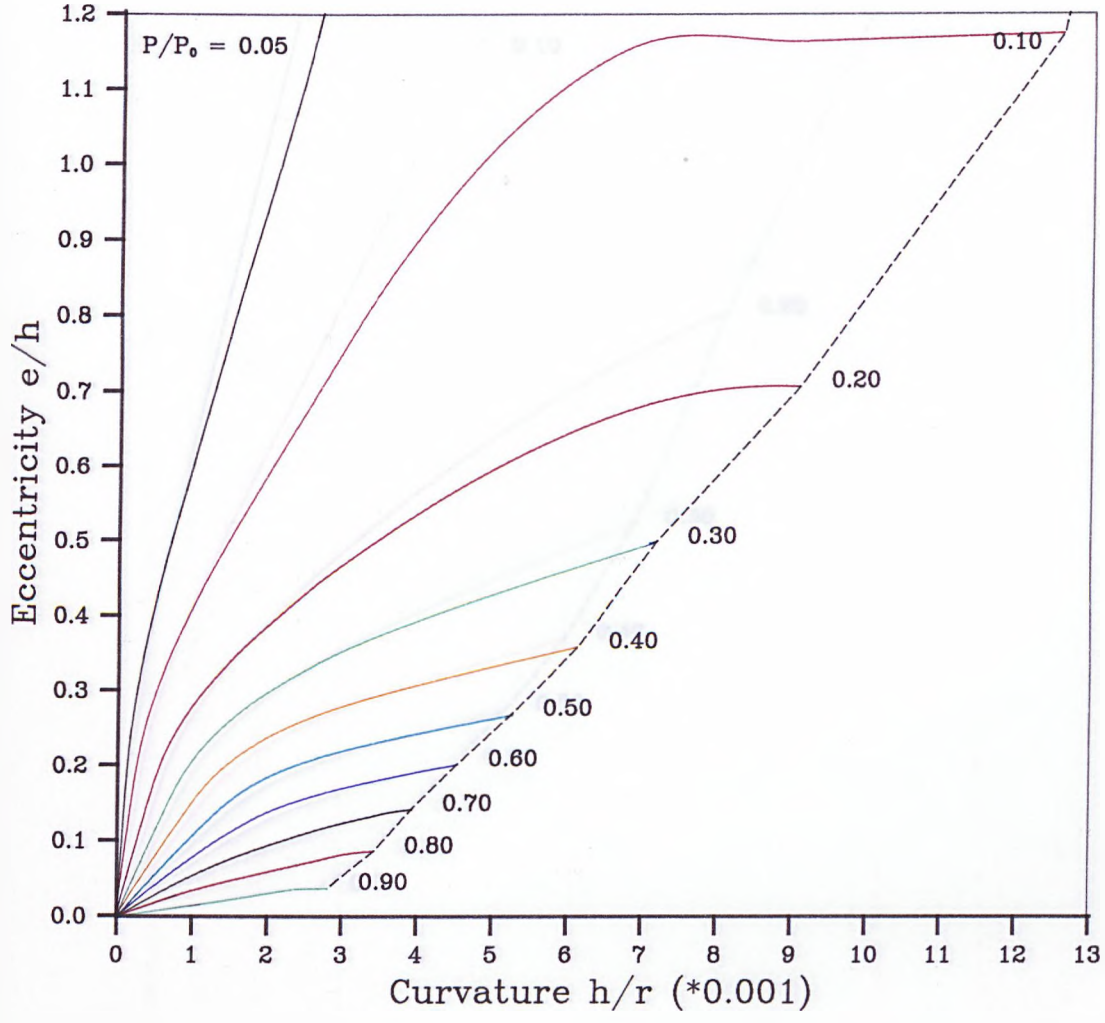

f_{cu} = 50 N/mm^2
f_Y = 530 N/mm^2
$\%A_S$ = 2.0
d/h = 0.80

Fig.3.8 Eccentricity vs Curvature relationship for Short-Term loading.

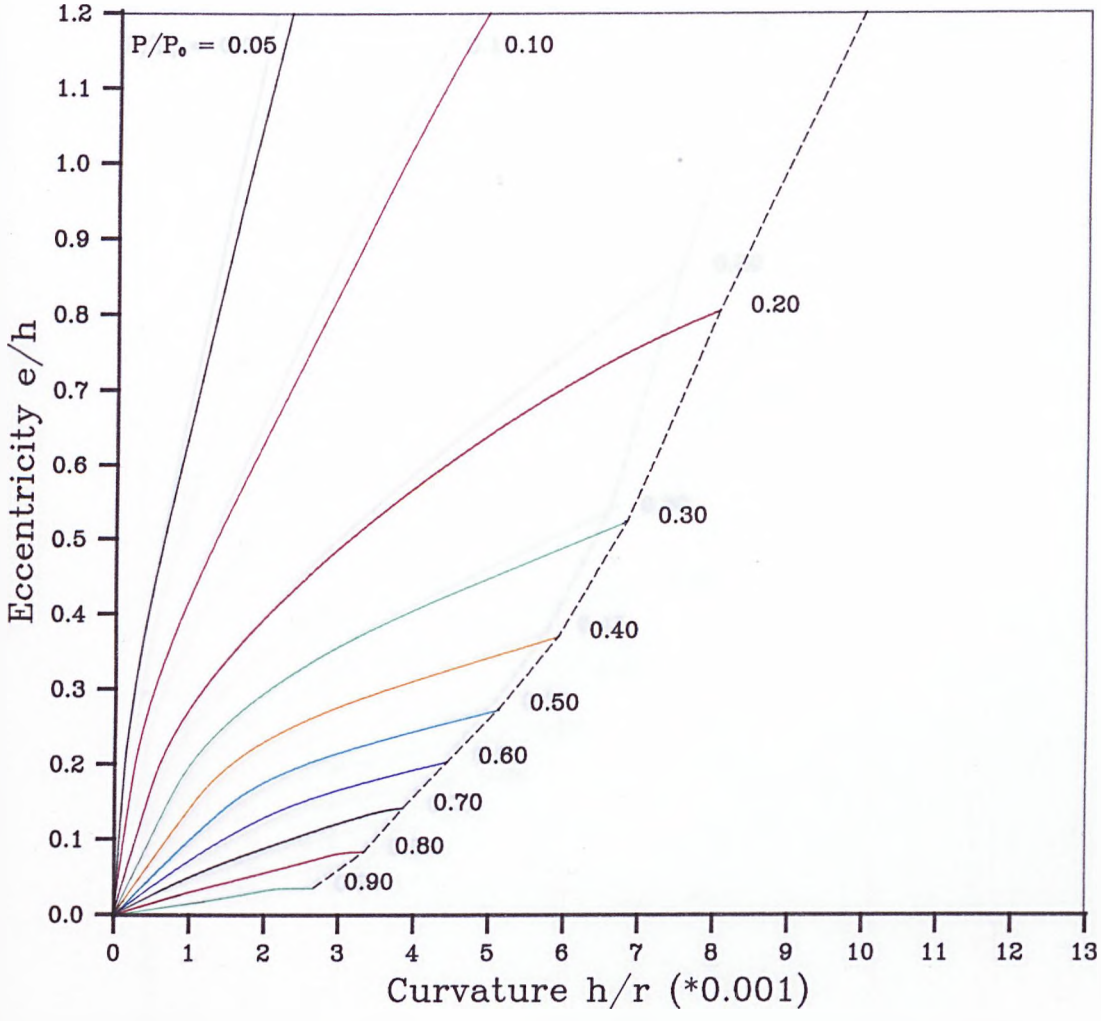

f_{cu} = 50 N/mm^2
f_y = 530 N/mm^2
$\%A_s$ = 3.0
d/h = 0.80

Fig.3.9 Eccentricity vs Curvature relationship for Short-Term loading.

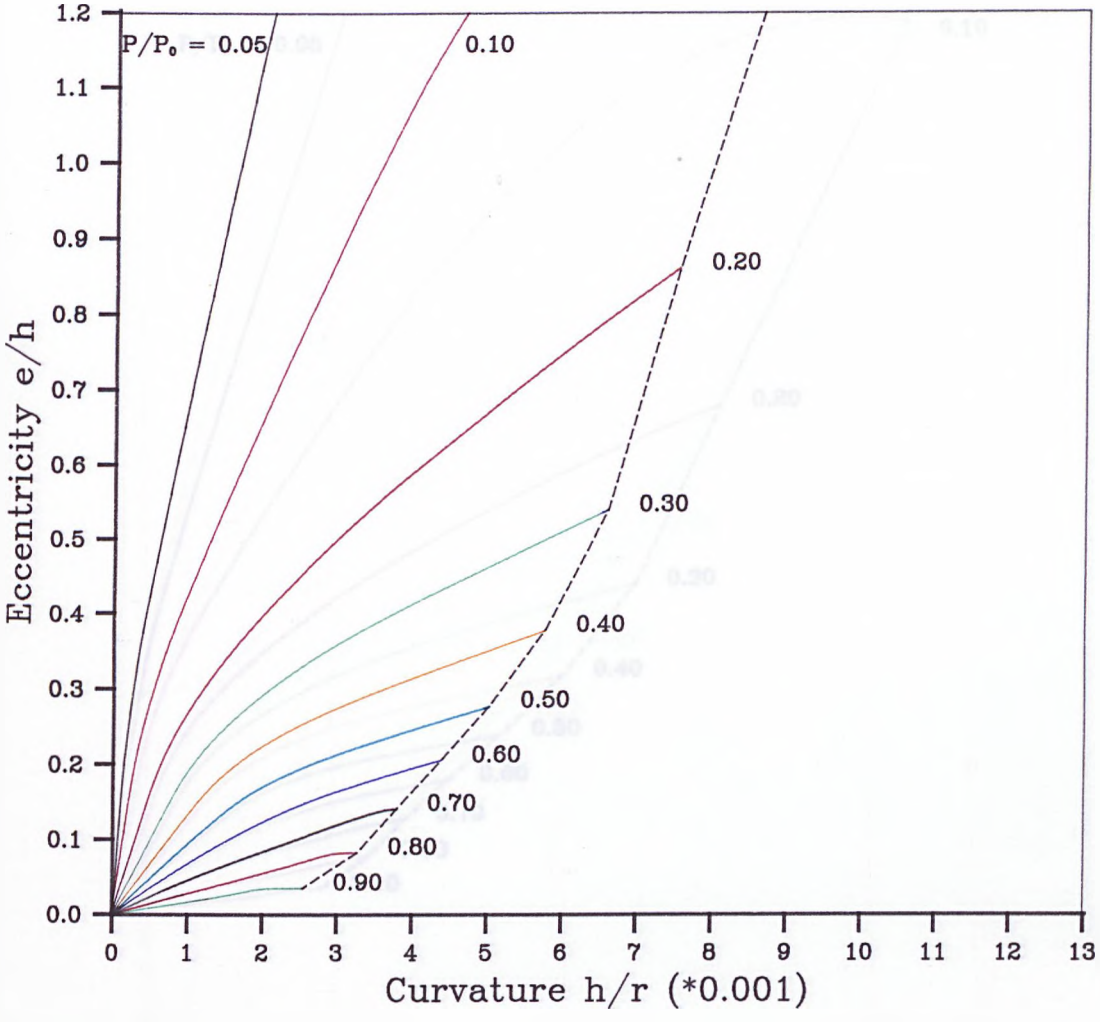

f_{cu} = 50 N/mm²
f_y = 530 N/mm²
$\%A_s$ = 4.0
d/h = 0.80

Fig.3.10 Eccentricity vs Curvature relationship for Short–Term loading.

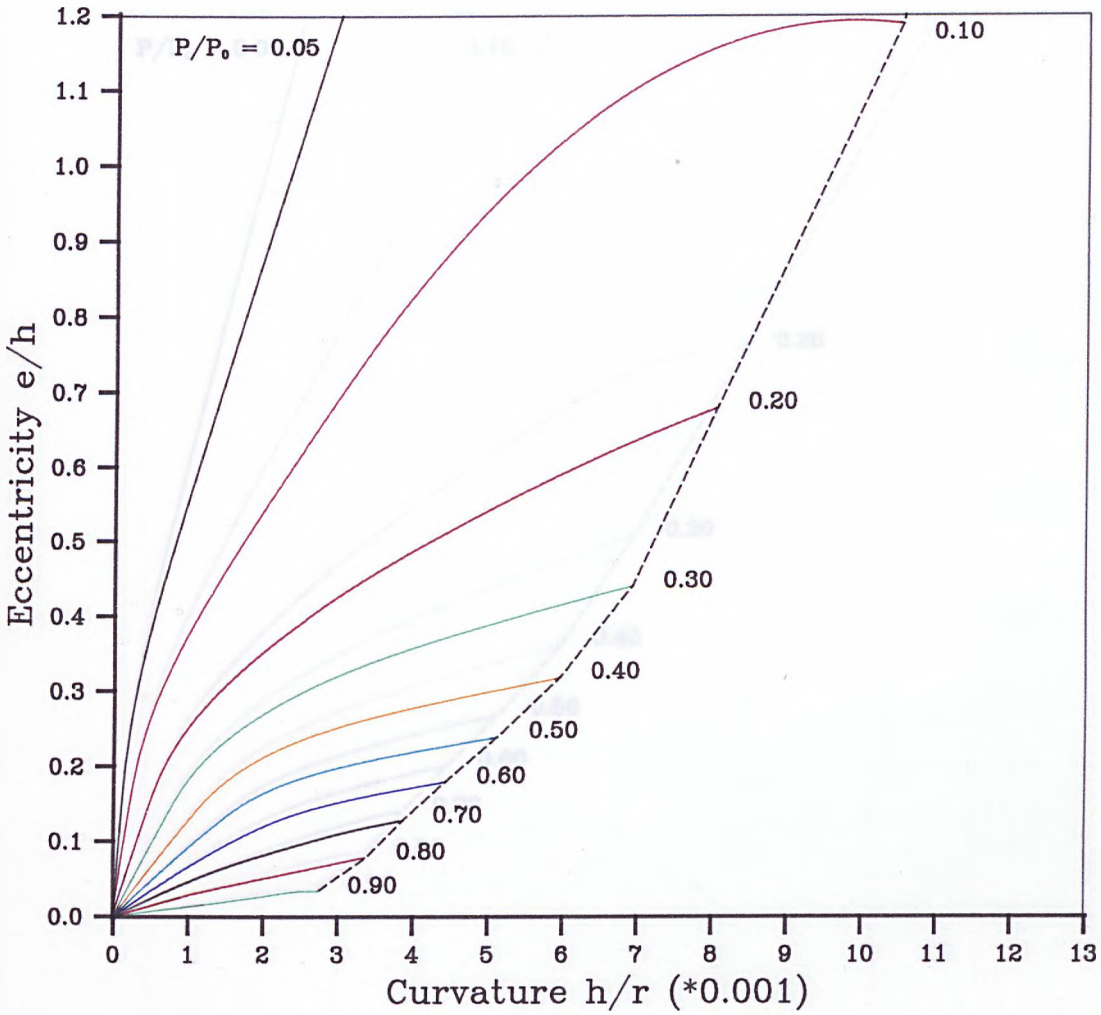

f_{cu} = 60 N/mm²
f_Y = 530 N/mm²
$\%A_S$ = 3.0
d/h = 0.75

Fig.3.11 Eccentricity vs Curvature relationship for Short-Term loading.

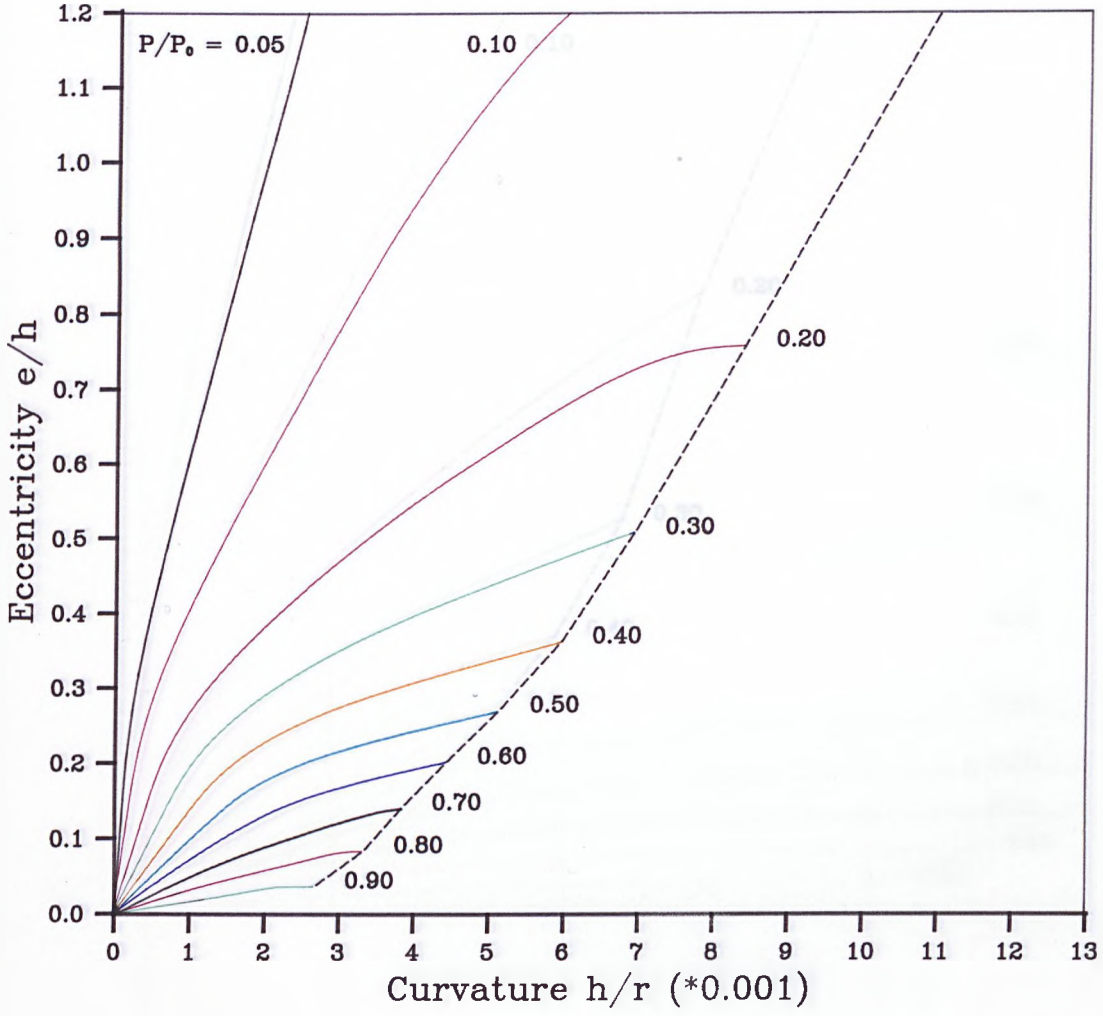

f_{cu} = 60 N/mm²
f_y = 530 N/mm²
$\%A_s$ = 3.0
d/h = 0.80

Fig.3.12 Eccentricity vs Curvature relationship for Short-Term loading.

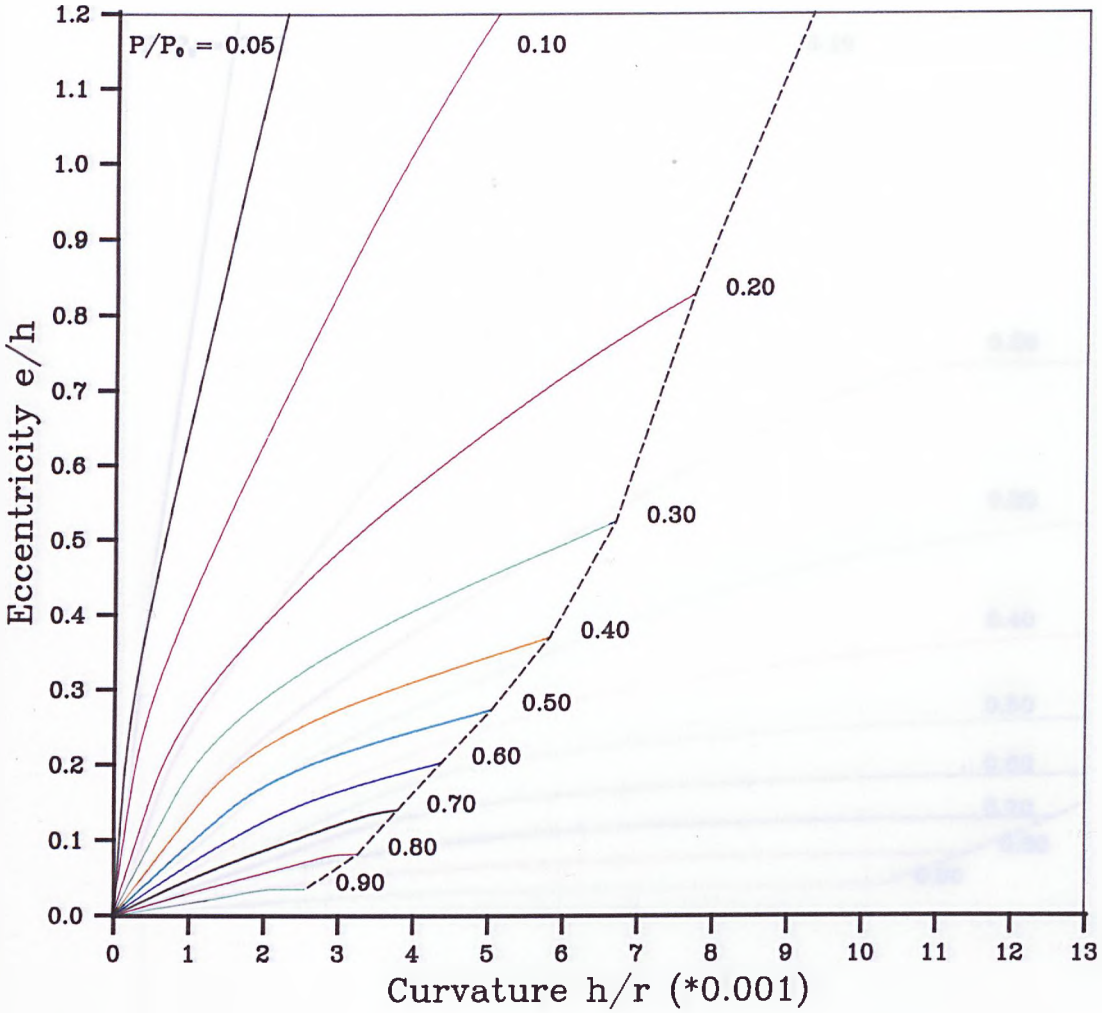

f_{cu} = 60 N/mm²
f_y = 530 N/mm²
$\%A_s$ = 4.0
d/h = 0.80

Fig.3.13 Eccentricity vs Curvature relationship for Short-Term loading.

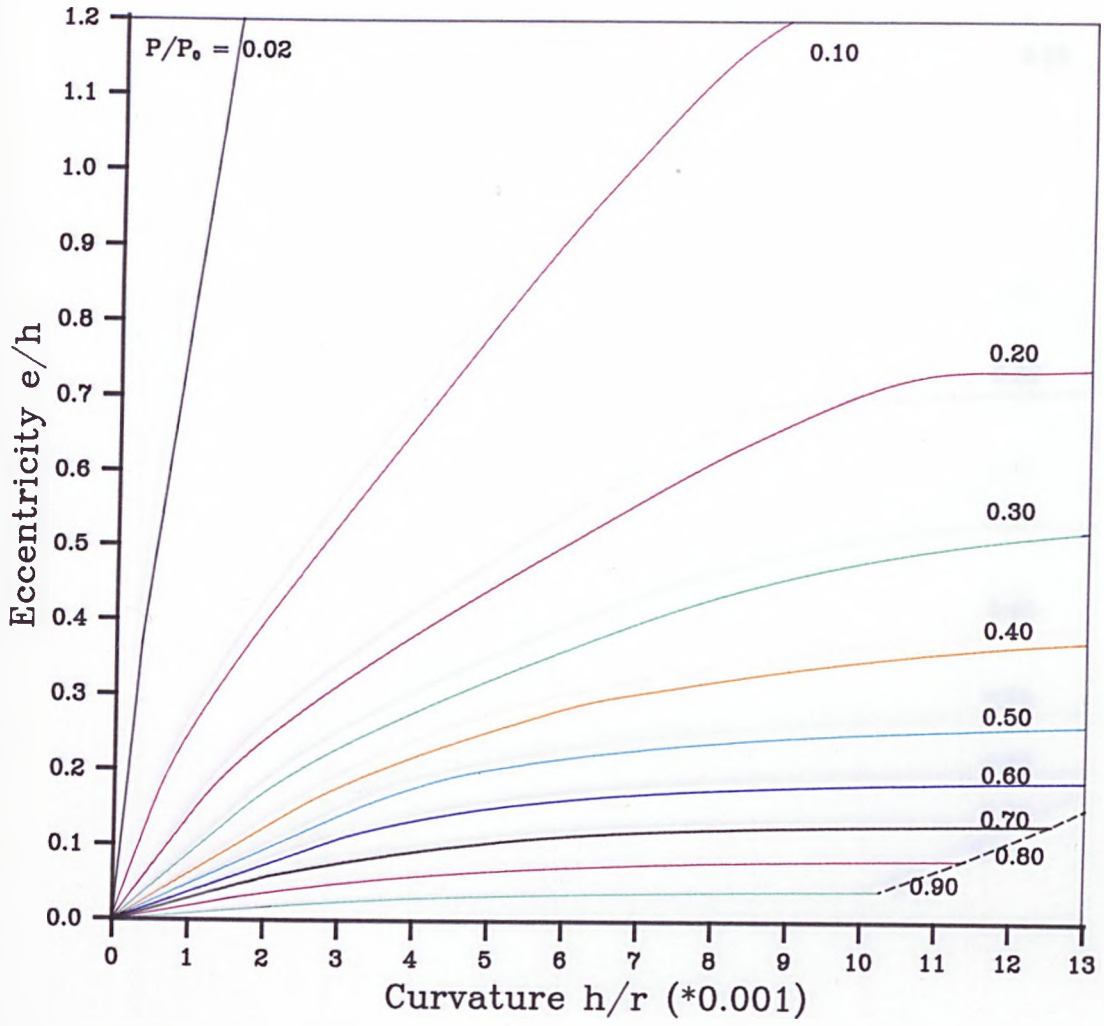

f_{cu} = 50 N/mm²
f_y = 530 N/mm²
$\%A_s$ = 3.0
d/h = 0.75

Fig.3.14 Eccentricity vs Curvature relationship for Long–Term loading.

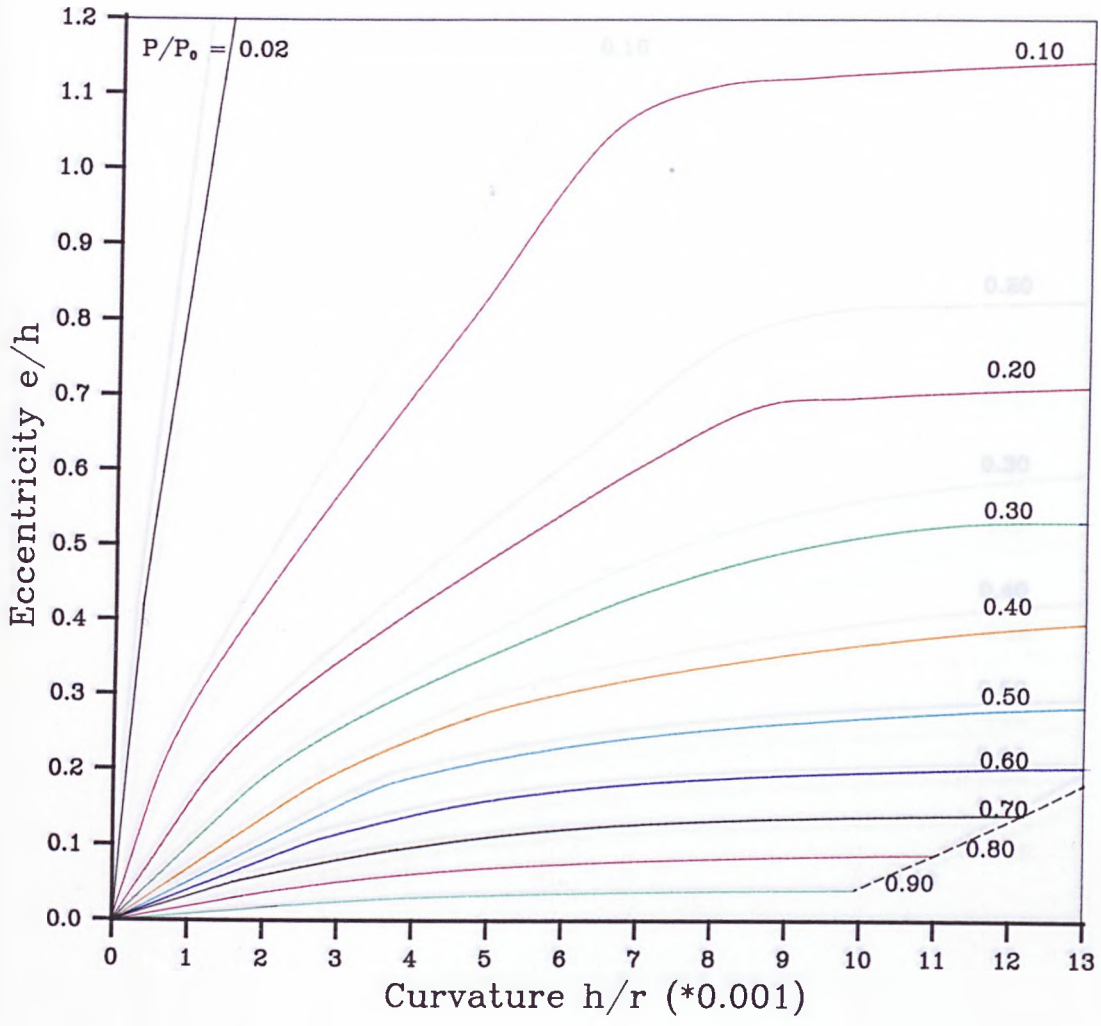

f_{cu} = 50 N/mm²
f_y = 530 N/mm²
$\%A_s$ = 2.0
d/h = 0.80

Fig.3.15 Eccentricity vs Curvature relationship for Long–Term loading.

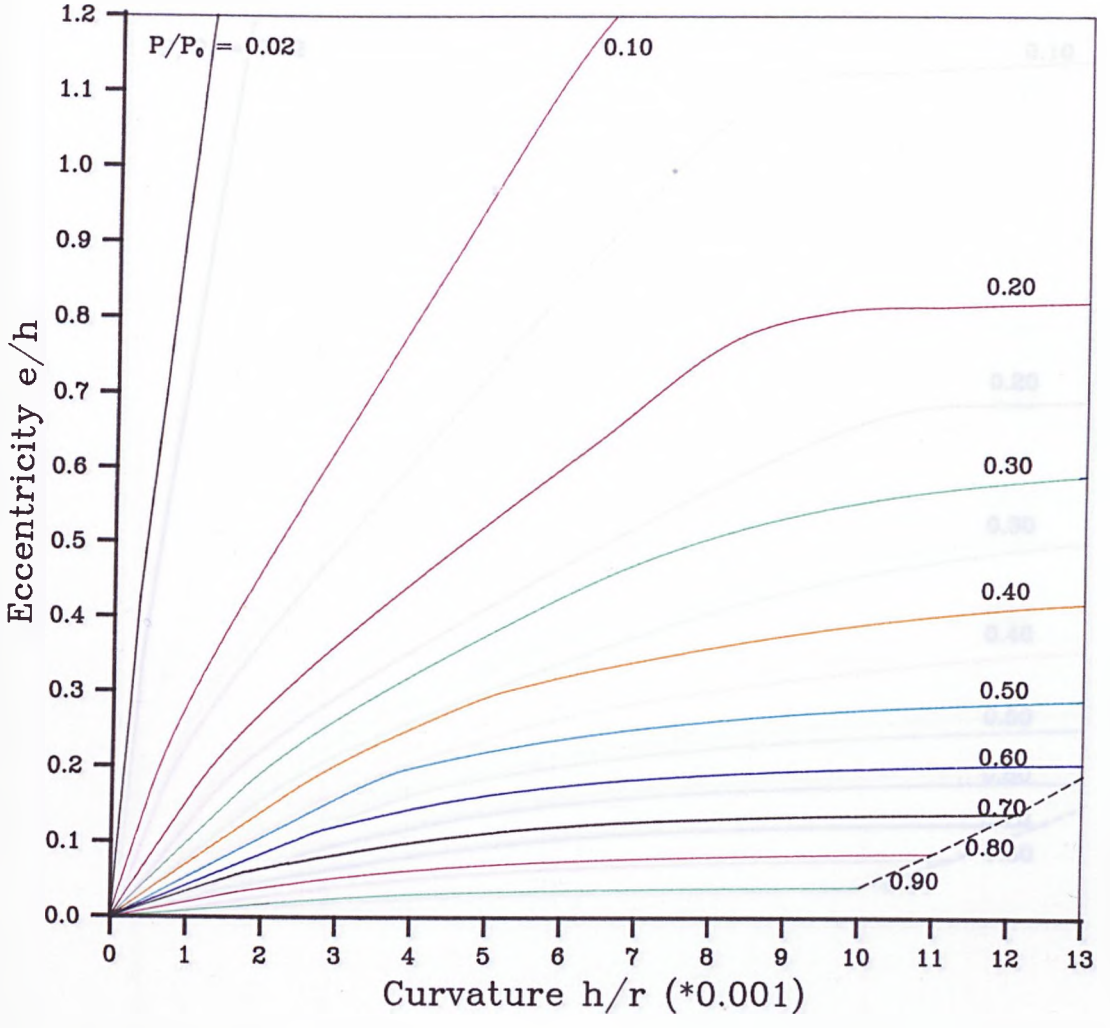

f_{cu} = 50 N/mm²
f_y = 530 N/mm²
$\%A_s$ = 3.0
d/h = 0.80

Fig.3.16 Eccentricity vs Curvature relationship for Long–Term loading.

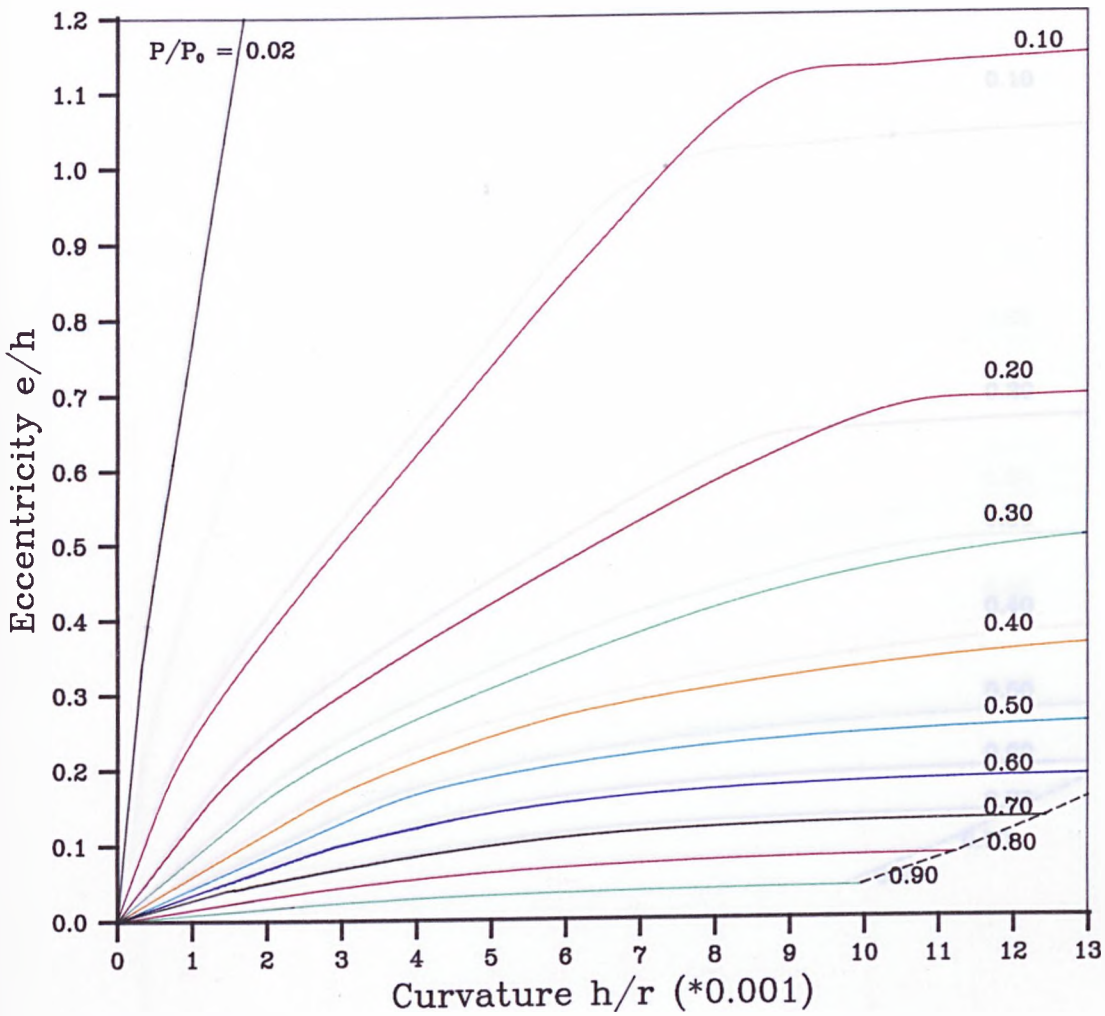

f_{cu} = 60 N/mm²
f_y = 530 N/mm²
$\%A_s$ = 3.0
d/h = 0.75

Fig.3.17 Eccentricity vs Curvature relationship for Long-Term loading.

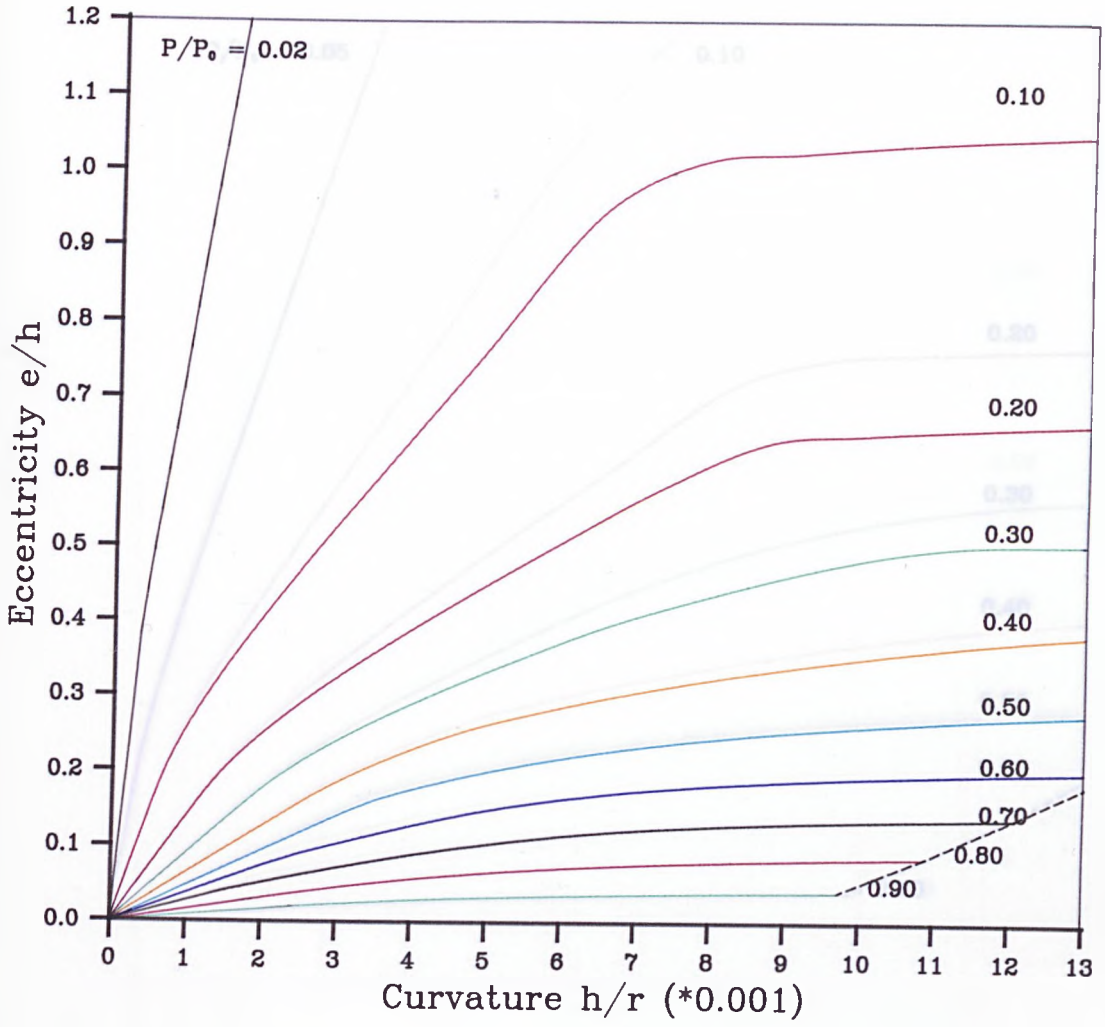

f_{cu} = 60 N/mm²
f_y = 530 N/mm²
$\%A_s$ = 2.0
d/h = 0.80

Fig.3.18 Eccentricity vs Curvature relationship for Long-Term loading.

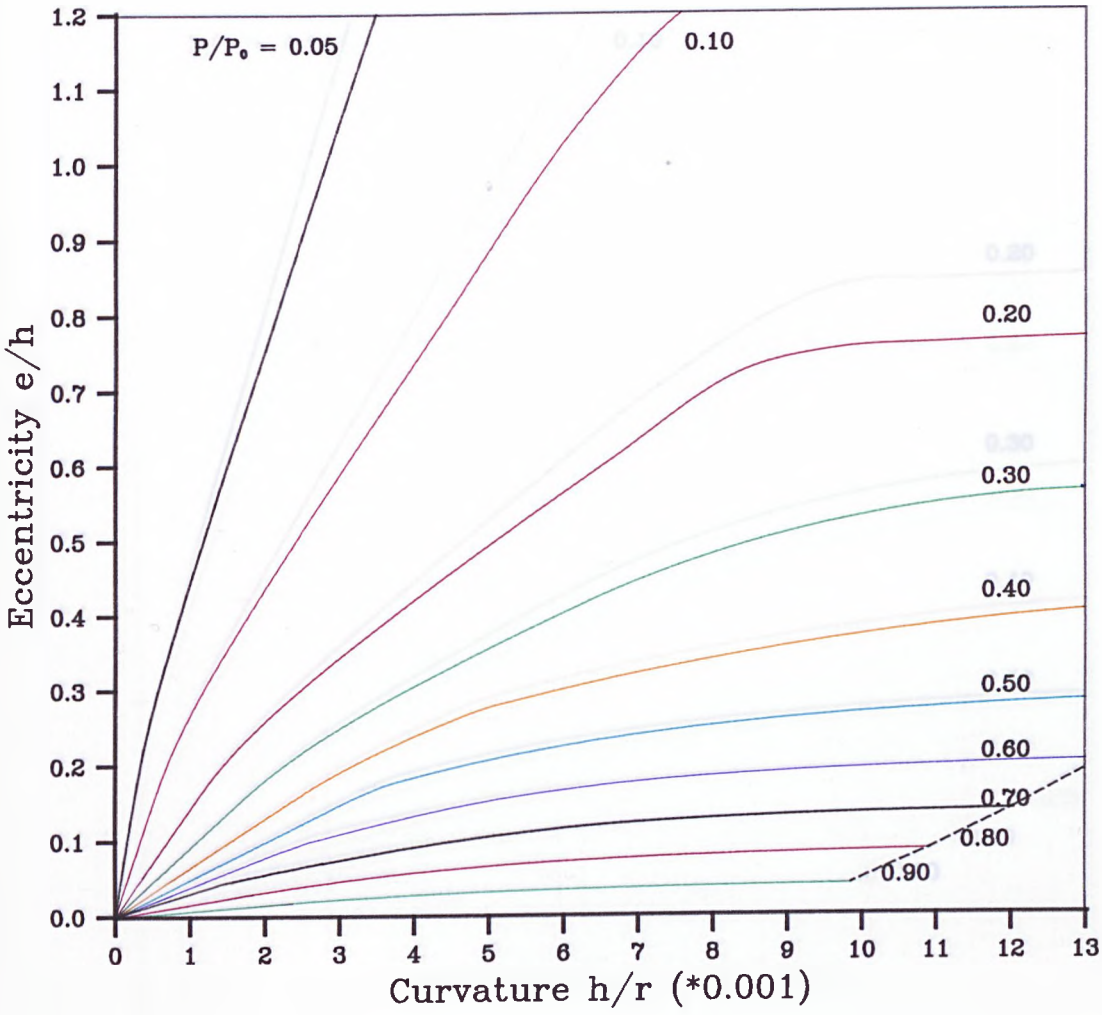

f_{cu} = 60 N/mm²
f_y = 530 N/mm²
$\%A_s$ = 3.0
d/h = 0.80

Fig.3.19 Eccentricity vs Curvature relationship for Long–Term loading.

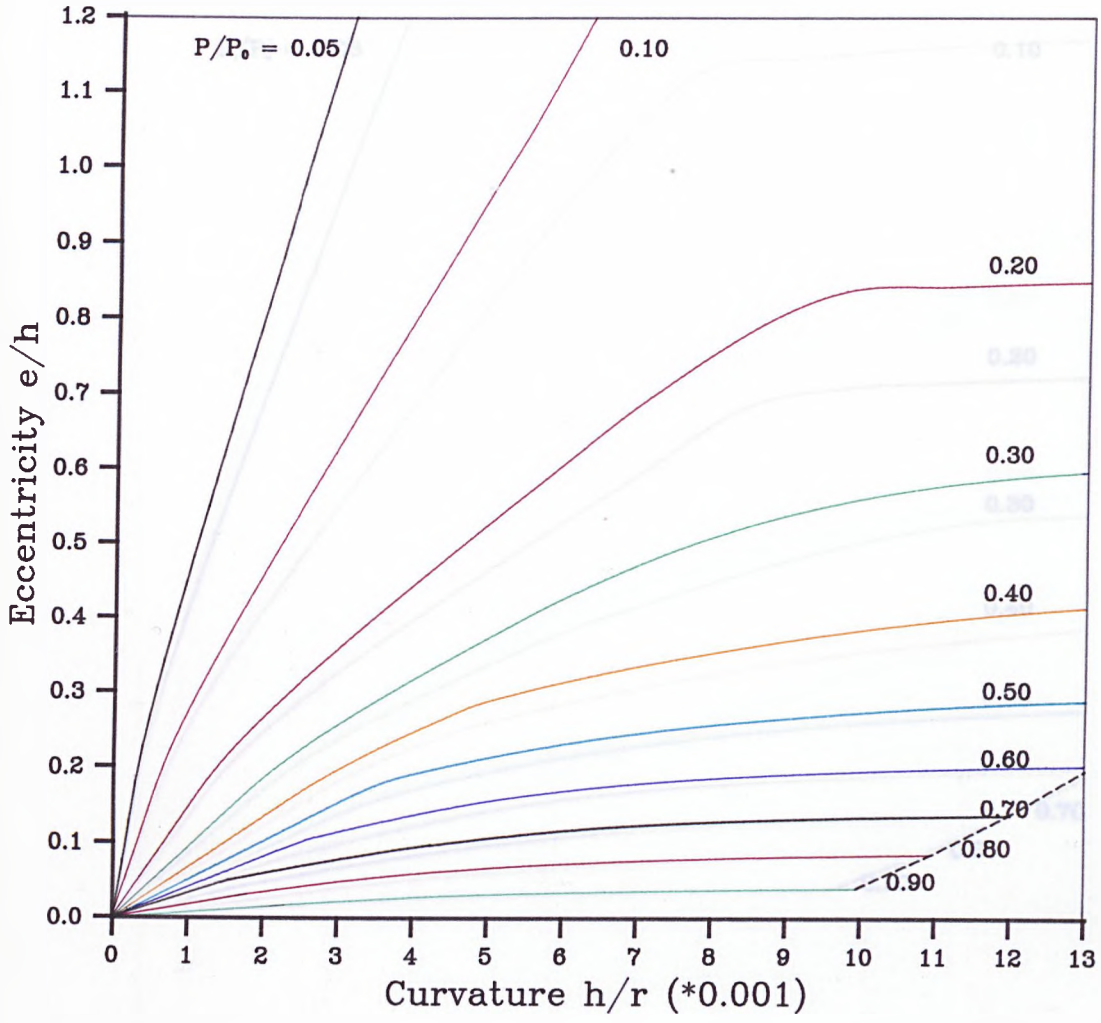

f_{cu} = 60 N/mm²
f_y = 530 N/mm²
$\%A_s$ = 4.0
d/h = 0.80

Fig.3.20 Eccentricity vs Curvature relationship for Long-Term loading.

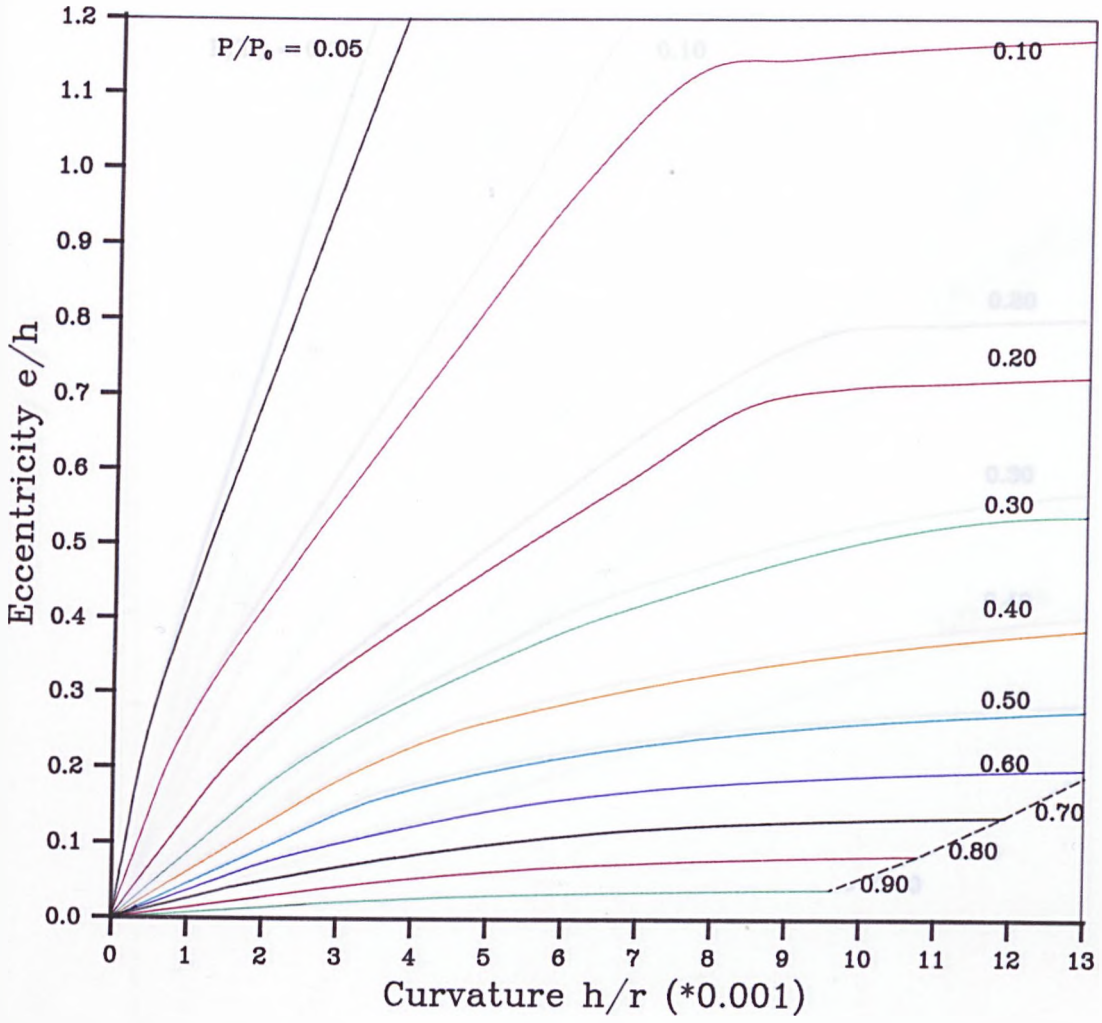

f_{cu} = 70 N/mm²
f_y = 530 N/mm²
$\%A_s$ = 3.0
d/h = 0.80

Fig.3.21 Eccentricity vs Curvature relationship for Long-Term loading.

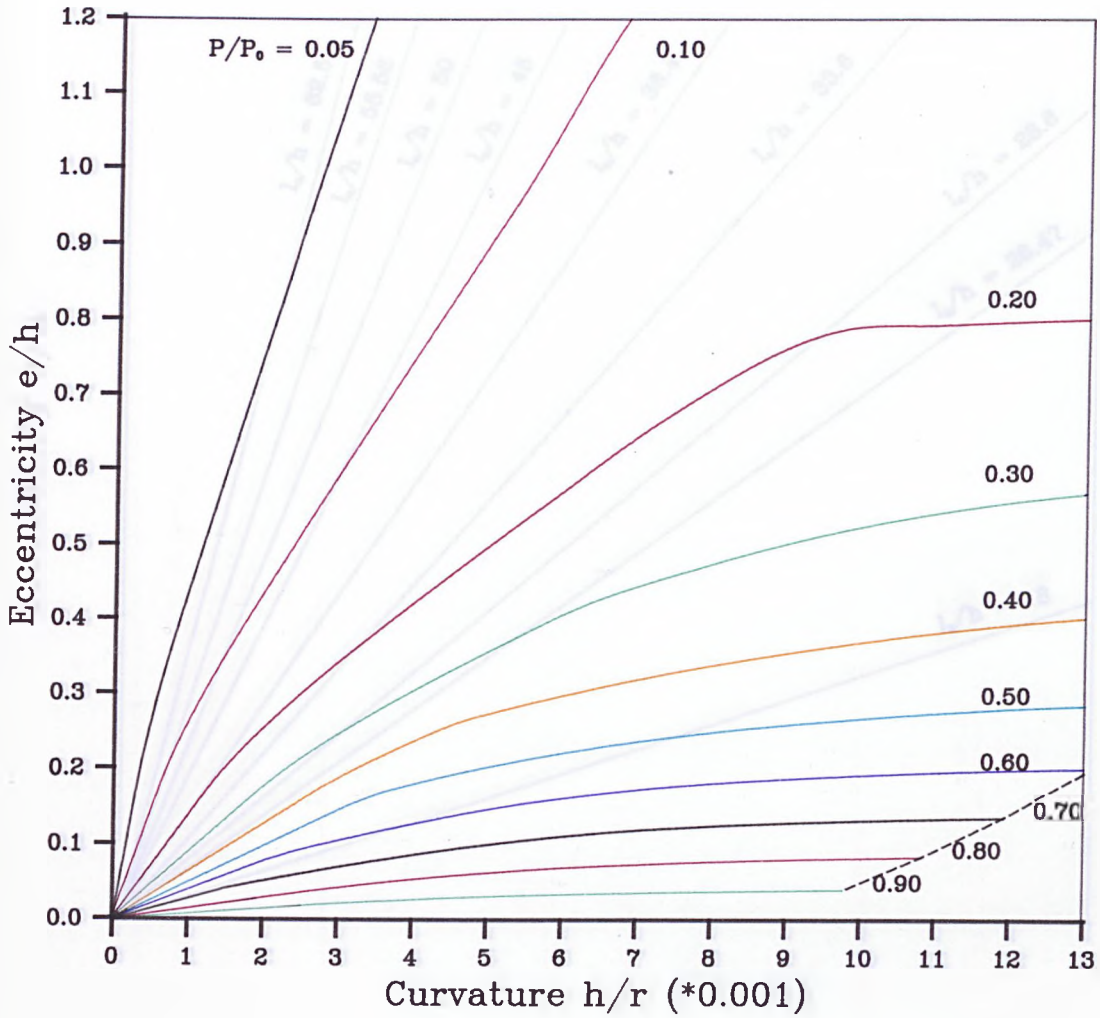

f_{cu} = 70 N/mm²
f_y = 530 N/mm²
$\%A_s$ = 4.0
d/h = 0.80

Fig.3.22 Eccentricity vs Curvature relationship for Long–Term loading.

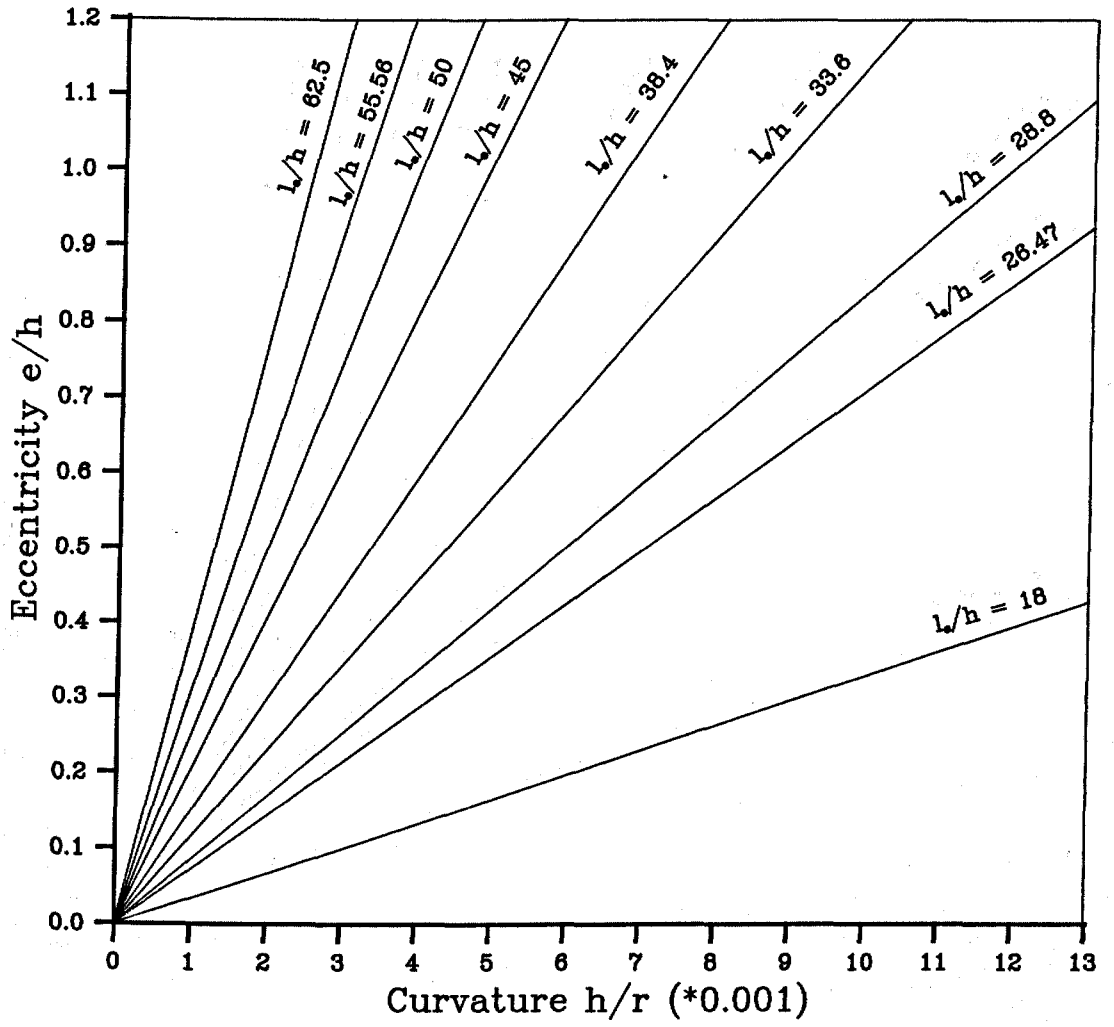

Fig.3.23 Buckling deflection vs Curvature relationship with no initial imperfection.

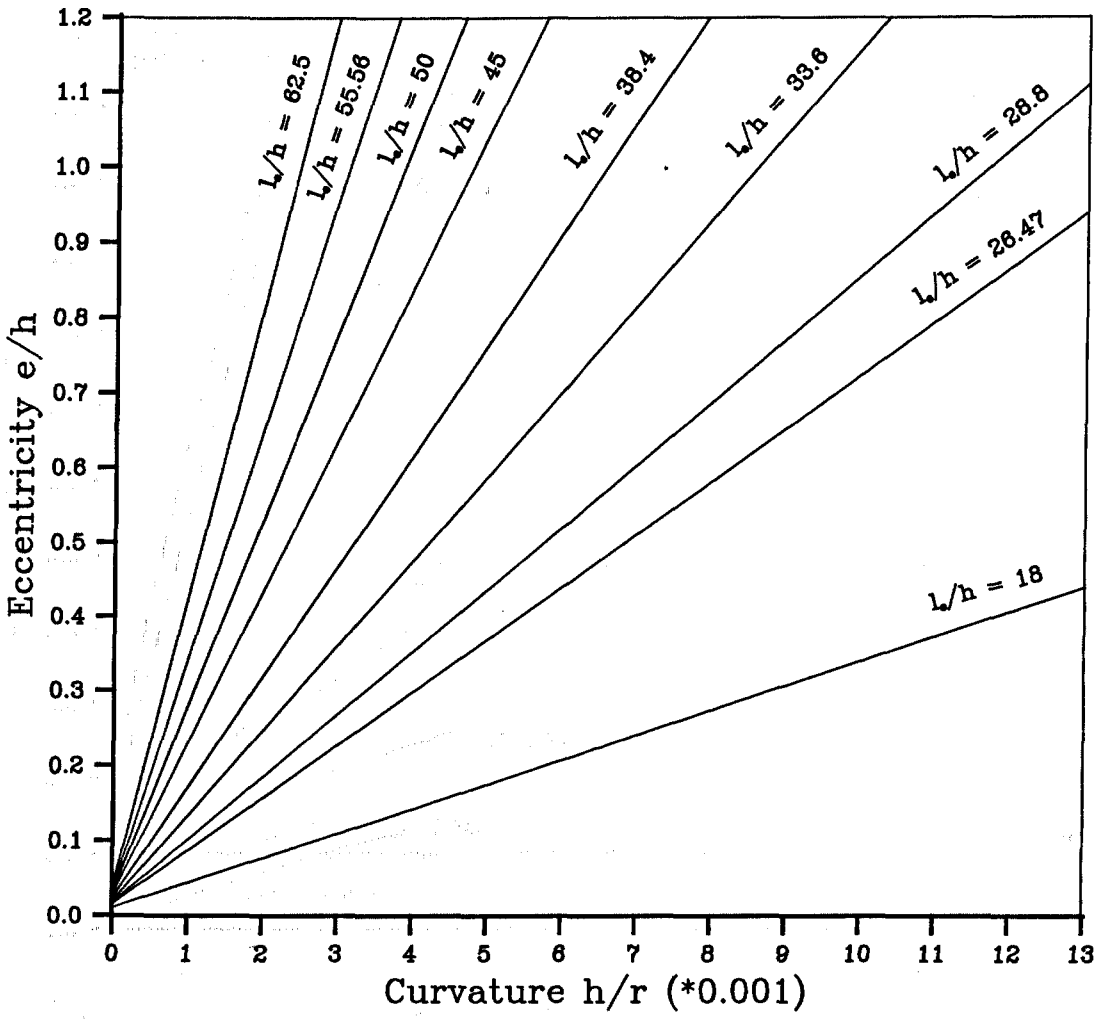

Fig.3.24 Buckling deflection vs Curvature relationship with initial imperfection of 5.68×10^{-4}L.

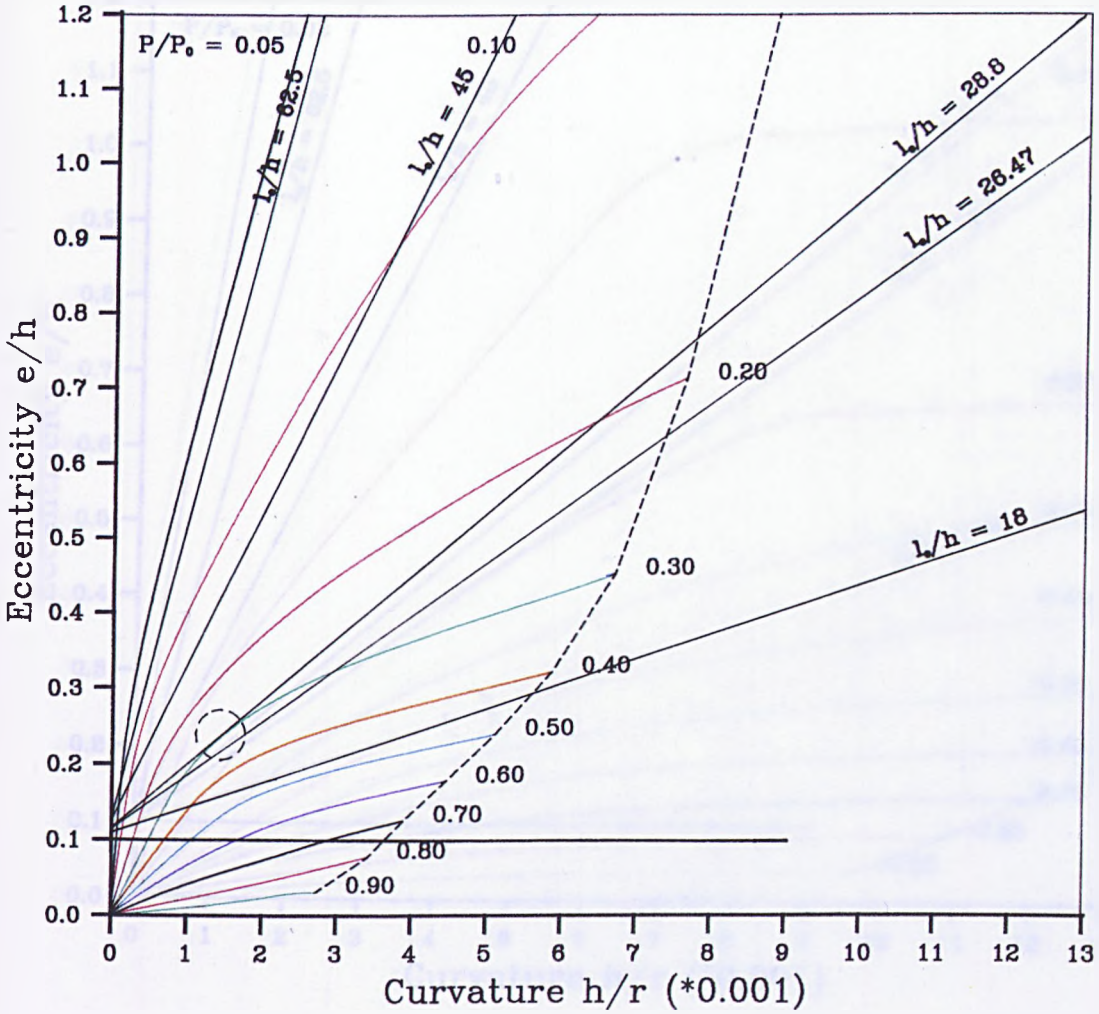

f_{cu} = 40 N/mm²
f_y = 530 N/mm²
$\%A_s$ = 3.0
d/h = 0.75

Fig.3.25 Graphical analysis of column with l_e/h=28.8, e_i=0.1h and with initial imperfection (Short–Term).

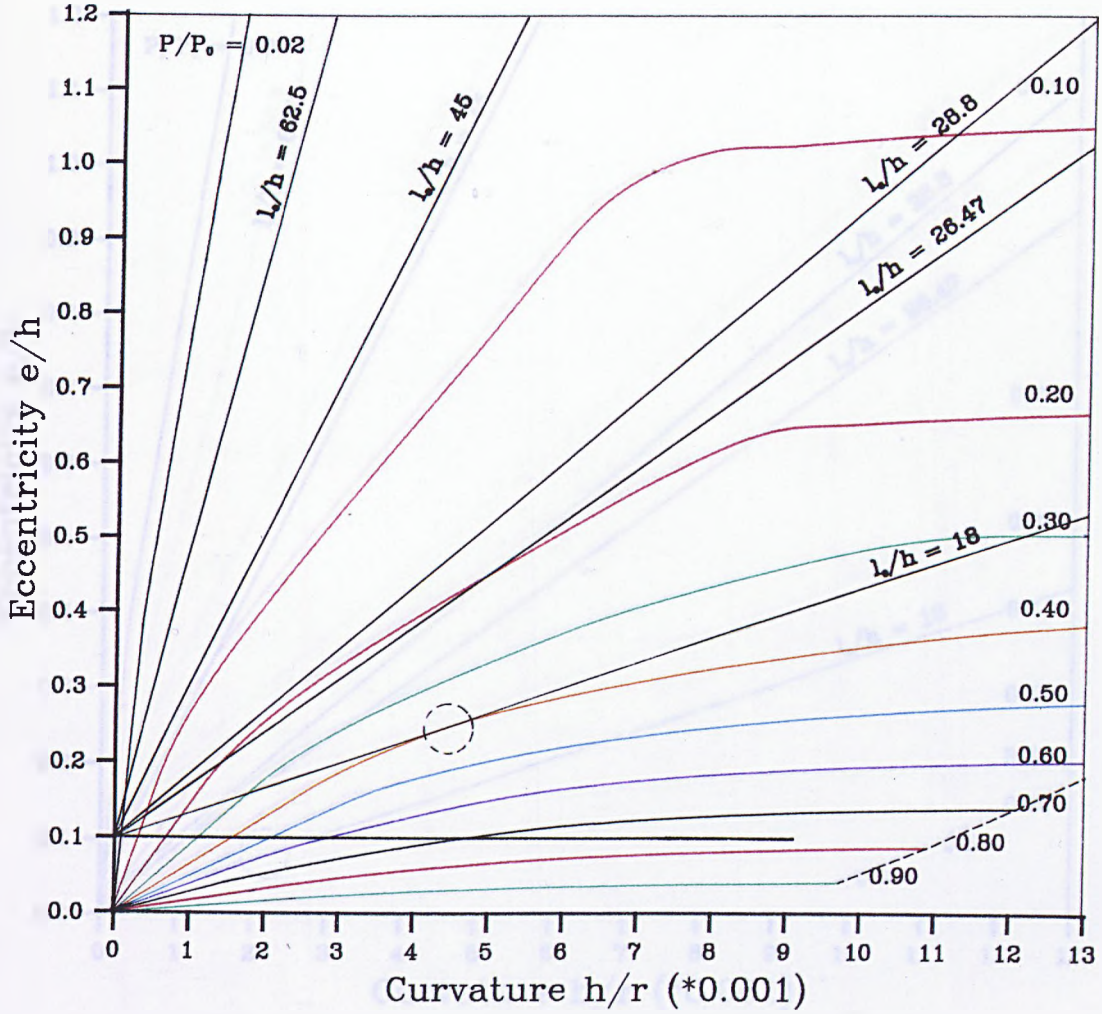

f_{cu} = 60 N/mm²
f_Y = 530 N/mm²
$\%A_s$ = 2.0
d/h = 0.80

Fig.3.26 Graphical analysis of column with $l_e/h=18$, $e_i=0.1h$ and with no initial imperfection (Long–Term).

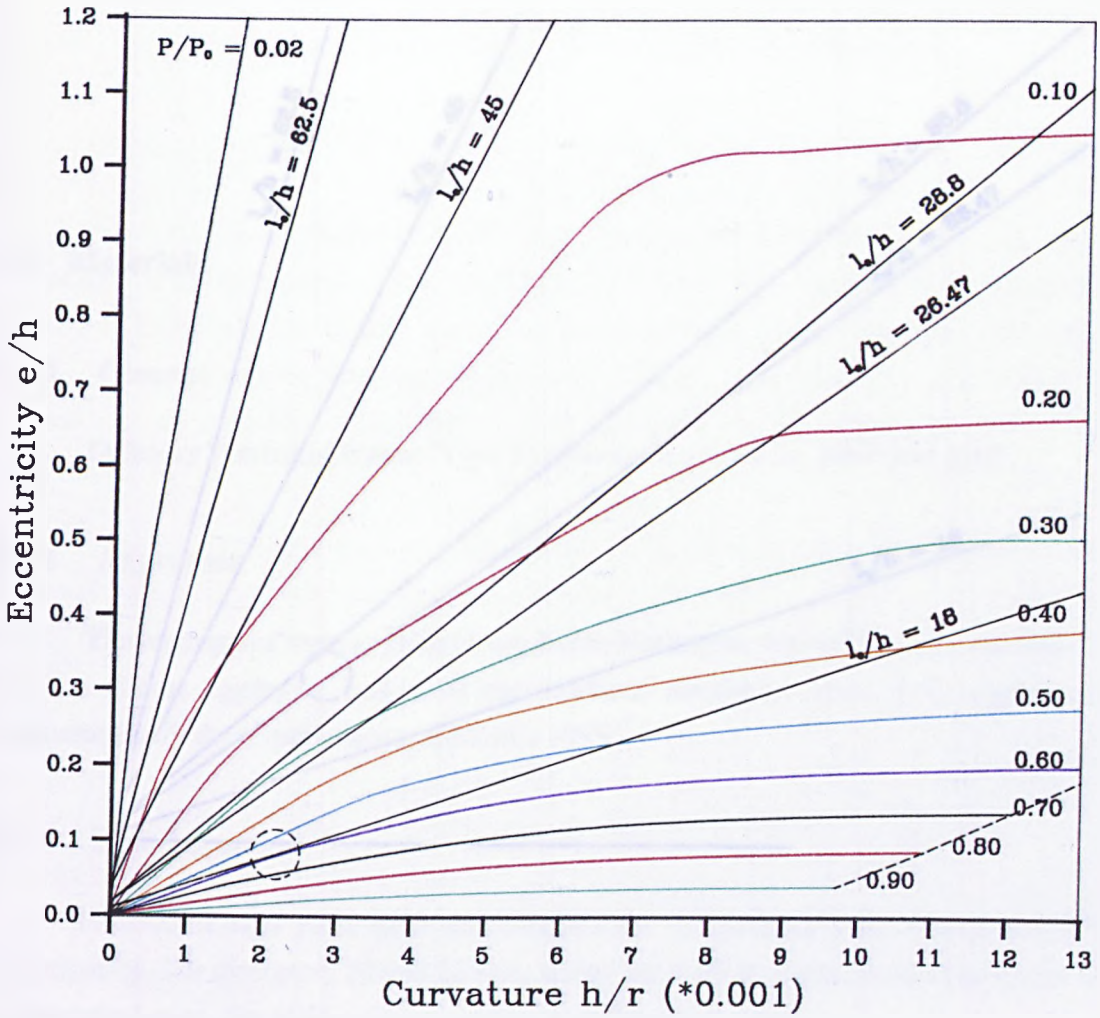

f_{cu} = 60 N/mm²
f_Y = 530 N/mm²
$\%A_s$ = 2.0
d/h = 0.80

Fig.3.27 Graphical analysis of column with l_e/h=18, e_i=0 and with initial imperfection (Long–Term).

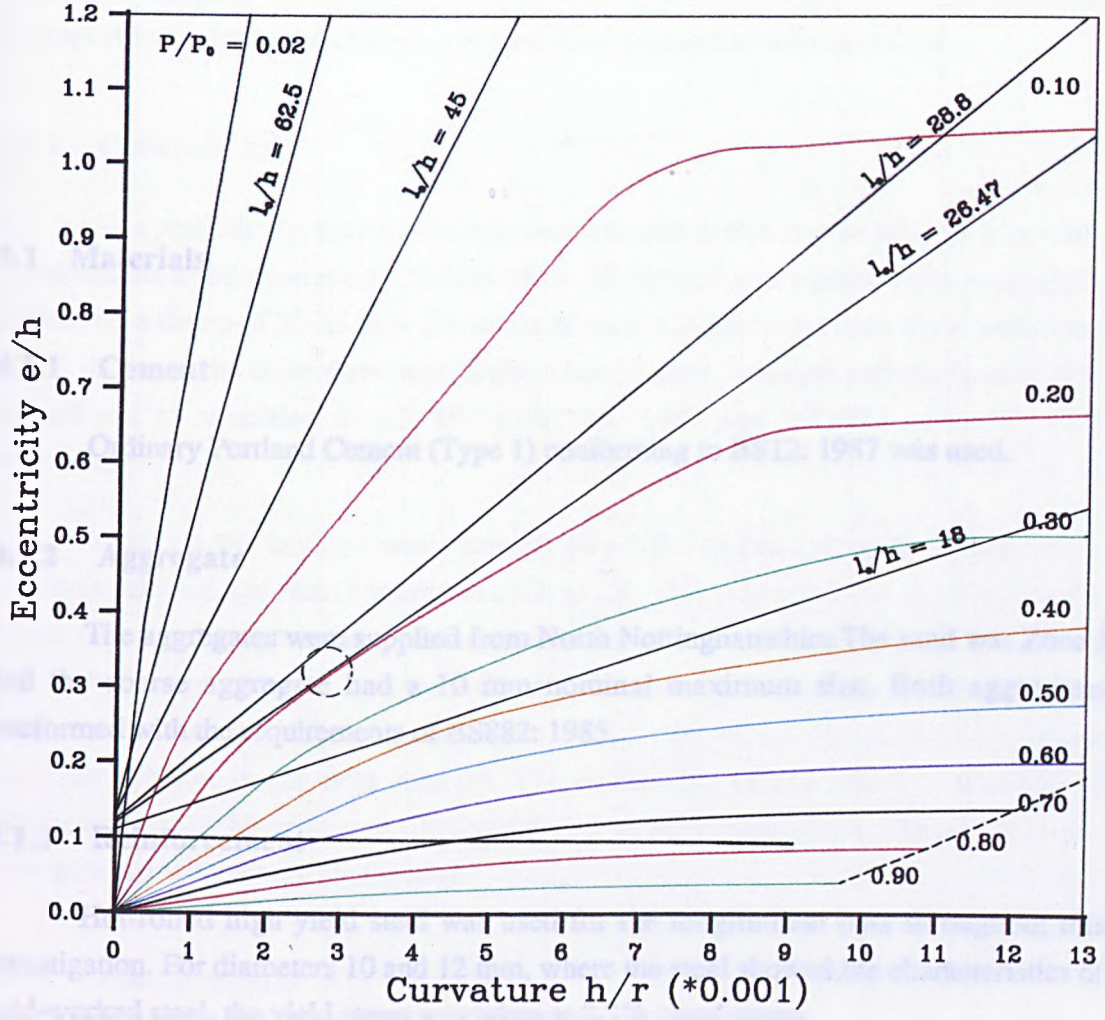

f_{cu} = 60 N/mm²
f_Y = 530 N/mm²
$\%A_S$ = 2.0
d/h = 0.80

Fig.3.28 Graphical analysis of column with l_e/h=26.47, e_i=0.1h and with initial imperfection (Long-Term).

CHAPTER FOUR

EXPERIMENTAL ARRANGEMENTS

4.1 Materials

4.1.1 Cement

Ordinary Portland Cement (Type 1) conforming to BS12: 1987 was used.

4.1.2 Aggregate

The aggregates were supplied from North Nottinghamshire.The sand was Zone 3 and the coarse aggregate had a 10 mm nominal maximum size. Both aggregates conformed with the requirements of BS882: 1985.

4.1.3 Reinforcement

Hot-rolled high yield steel was used for the longitudinal bars throughout this investigation. For diameters 10 and 12 mm, where the steel showed the characteristics of cold-worked steel, the yield stress was taken at 0.2% proof stress.

The results of tensile tests on sample bars are given in Table 4.1 and typical stress-strain curves are shown in Fig.4.1. Mild steel was used for the links.

4.2 Column construction

4.2.1 Reinforcement cage and spacers

The cage was assembled and placed in the prepared casting mould. The main bars were cut to length allowing 20 mm at each end below the design length to provide cover. Preformed mild steel stirrups complying with BS8110: 1985 requirements in terms of spacing, were fixed with steel clips. Fig.4.2 shows typical reinforcement details and the cage is shown in Fig.4.9(a).

Mortar blocks were used in the pilot-tests to maintain the position of the reinforcing cage within an accuracy of ±2 mm and to ensure the correct concrete cover. For the main tests, welded spacers (a typical one is shown in Fig.4.9(b)) were found to be more satisfactory. For each cage, four of these spacers were prewelded and distributed in proportion to the column length and then fixed in position with steel clips.

4.2.2 Concrete mix

As a preliminary, nine trial mixes were examined, to arrive at a design mix with a characteristic cube strength at 28 days of 30-45 N/mm^2 and a reasonable workability defined by a slump of 30-75 mm. Six cubes of each trial mix were cast, three were tested after 7 days and the other three were tested after 28 days. Strength and slump tests were carried out as specified in BS1881 part 116: 1983 and BS1881 part 102: 1983 respectively.

Initially a mix having a water-cement ratio of 0.6 and an aggregate cement ratio of 6.25 was selected and used for columns C1 to C4. This was modified in an attempt to reduce the cube strength using the minimum cement content allowed in BS8110: 1985 of 275 kg/m^3. Accordingly, columns C5 to C20 were cast from concrete having a water-cement ratio of 0.63 and an aggregate cement ratio of 6.8. However, there was no significant change in the cube strength. The workability of this mix was found to be satisfactory and no bleeding was observed during or after compaction. The mix was also homogeneous without any segregation.

4.2.3 Column mould

Columns C1 to C4 were cast in a 2.25 m long mould, the cross-section is shown in Fig.4.3(b). The sides of the mould consisted of two steel angles 200×125×12 mm, bolted to a steel base channel 381×102 mm in a position giving the required width (125 mm), the depth of the cross-section (85 and 125 mm) was formed using adjustable height wooden base. These relatively short columns were easy to handle, without any fear of cracking. As the columns became longer it was necessary to develop a special mould for this project to serve the casting and handling of the columns.

The mould consisted of:

(1) Two steel channels 254×89 mm, 6.5 m long, formed the two sides of the mould and were bolted to a wooden base.

(2) Steel plate 75×12 mm, 5.30 m long fixed to the base.

(3) Box section 75x50 mm, 5.30 m long.

(4) Steel plate 75x20 mm, 5.30 m long.

(5) Four, 20 mm thickness, steel plates with widths of 80, 90, 100 and 125 mm, 5.30 m long.

Components (2) to (5) were fixed using self-tapping screws to give a constant depth of 152 mm for all the columns numbered C5 to C20. Figs.4.3(a) and 4.10 show the cross-section and elevation of the mould with the position of the lifting eyes. Varnished timber stop ends were used to achieve the required length for each column.

4.2.4 Casting procedure

The mould was cleaned and coated with a thin layer of mould oil before the prefabricated reinforcement cage was fixed in position. Concrete was mixed in a 200 kg dry weight capacity, revolving blade pan mixer; for larger mixes a 350 kg capacity mixer was used. For each concrete mix, all the constituent materials were weighed in the required proportions before being fed into the mixer. The materials were turned over for about half minute before the gradual addition of the required quantity of water, which was followed by a further two minutes of mixing. A slump test on the fresh concrete was carried out before the concrete was placed.

Control specimens (see 5.2.2, 6.3.2 and 6.3.3) from each mix were also cast in steel moulds on a vibrating table, before the concrete was taken to the casting bed. The concrete was placed into the mould and compacted by means of a poker vibrator of 25 mm diameter.

All columns were cast horizontally and the concrete was placed symmetrically about the centre line of the mould i.e in respect to the lifting eyes. The exposed surface of the columns and specimens were then trowelled off after the initial set had taken place and then covered with wet hessian mats and polythene sheets. After 24 hours the control specimens were demoulded and kept alongside the column. The column mould was stripped after 3 days. Both the column and its specimens were left under cover for 7 days.

4.2.5 Accuracy of column construction

The moulds were maintained to a high degree of accuracy. Investigation showed that the overall dimensions of the cross-section were maintained to ±1.5 mm; the longitudinal reinforcement was positioned to a tolerance of ±2 mm. With regard to the

crucial point of overall straightness, the centre line of the columns, as positioned into their respective test rigs, did not deviate more than 3 mm from a line joining the two ends. The initial imperfection, as measured for all test columns, could be expressed in terms of the length as: $e_0=5.68\times10^{-4}L$. This value was used in the analytical calculations.

4.3 Curing

All columns were covered for seven days. After removing the covers, columns C1 to C4 were transferred to the curing room in which the temperature and relative humidity were maintained at 20°C±1°C and 95±5% respectively. The columns were kept there until required for testing. Columns C5 to C20 were air-cured inside the laboratory.

A seven day chart-recorder, supplied by Foster Cambridge Limited, was used to record the temperature and relative humidity in the laboratory, which were found to range between 12-29°C and 30-75% respectively, over a period of 15 months commencing in May 1989. Fig.4.8 shows typical variation curves.

In both cases, the corresponding control specimens were treated exactly in the same manner as the test columns.

4.4 Lifting procedure

Handling very slender columns at the storage position, bringing them to the test frames and mounting them ready for testing, required considerable care and organisation. The mould was especially designed for this purpose. Figs.4.11, 4.12 and 4.13 show the sequence of the operations carried out.

The column was first lifted on its bed using the crane, then it was laid on wooden blocks (Fig.4.11). Two steel boxes were fixed along the sides of the column by means of rack clamps (Fig.4.12(a)), after that it was turned over bricks to remove the bed (Fig.4.12(b)). Purpose-made clamps were then used to replace the clumsy rack clamps. This arrangement ensured that the column would not be damaged in any way during handling. Using the crane the column was transferred and positioned near the rig until the time of testing (Fig.4.12(c)). To aid lifting, a frame was designed and constructed at the top of the rig to allow the use of a block and tackle in mounting the column into the rig (Fig.4.13).

Pancholi [29] had similar difficulties in handling columns. He developed "special top and bottom clamps together with a special lifting angle inserted under the column. Lifting attachments were used as well. Column lifted clear and the angle removed ready for lifting into test rig". Columns tested by *Cranston and Sturrock* [36] were externally

prestressed to prevent cracking in transit. This prestress was maintained until the specimen was lifted into the rig.

4.5 Rig design

4.5.1 Short-term loading rig

The standard rigs available in the structural laboratory, were capable of developing a 1000 kN compressive force, but it was not possible to test reinforced concrete columns of lengths greater than 3.6 m. In addition the requirements of test programme meant that they could not be used for the long-term tests. Columns C1 to C5 were therefore tested until failure under short-term loading conditions using the rigs available, Fig.4.15 shows a typical testing frame. For the longer columns, it was necessary to design a special rig.

The arrangement and position of various items of testing equipment in the laboratory, placed restrictions on the dimensions of the required rig. The height of the rig was limited by the height of the ceiling (6.5 m) and its position was restricted by the need for access by the crane. Taking account of all these considerations the total height of the rig was set to be 6.3 m. Two rigs were designed, Figs.4.4 and 4.14 show typical rig arrangement.

Fully threaded prestressed Macalloy bars of 25 mm diameter, formed the vertical members of the rig. The characteristic failing load for each bar is 505 kN. Three bars required for each rig, giving total capacity to the rig of 1500 kN. Such capacity was in fact not required for the designed columns, however, 25 mm was the minimum diameter the manufacturers produce. *Cranston and Sturrock* [36] used 28 mm diameter "Lee-McCall" stressing rods and the required capacity of their testing rig was 1700 kN.

Grade 50 steel to BS5950, was used for the plates. For each rig, two bottom circular plates 45 mm thick and 685 mm diameter were used plus a top circular plate of 40 mm thick and 850 mm diameter, as well as three circular end plates of 40 mm thick and 310 mm diameter as can be seen in Fig.4.4.

Because the columns were to have freedom of rotation at the ends, it was necessary to use ball seatings at each end of the column in the test frame. The centre line of the ball seatings was offset from the column centre line to produce eccentric loading. Loading of the columns was carried out using a 500 kN hydraulic jack reacting against the lower plate and operated manually.

In view of the dimensions of the test set up, a stable system was desirable from the point of view of stability. A three bar system rather than two was therefore chosen. Careful attention was given to the provision of fixed and removable guards for safety reasons. The test rig was designed to make it capable of height alteration, to enable columns of different slenderness ratios to be tested.

4.5.2 Long-term loading rig

The short-term testing rigs were easily modified for the long-term tests by adding three springs to each rig as shown in Figs.4.4 and 4.14. These springs were designed to BS1726 part 1: 1987 [92] and were made to order by West Bromwich Springs Limited.

The springs were tested in an Instron servo-hydraulic testing machine; a typical load-deflection diagram is shown in Fig.4.5. Unfortunately, during the initial loading for the first long-term test, one of the springs failed in compression due to a fault in manufacture. A replacement spring was ordered which also failed during proof testing in the Instron machine. A second replacement was ordered and this performed satisfactorily. Considerable time was spent waiting for the delivery of these springs and manufacture of their replacements, causing delay in the experimental schedule.

Each spring was contained between the higher plate and the top end plate with the prestressing bar passing through both plates and spring. The working load for each spring was 150 kN, with the capability of maintaining the relatively low levels of the axial load. *Goyal* [33] adopted a similar arrangement in his experimental work, but used only two rods.

4.5.3 Creep loading frame

Details of the simplified creep frame used in the creep investigation are shown in Figs.4.7 and 4.16.

This frame was designed to hold two 76×267 mm cylindrical plain concrete specimens and 76×296 mm steel-tube load dynamometer by four tie rods, the load being applied manually by tightening the four nuts which stresses the specimens between two end plates. To enable the accurate application of axial load to the concrete specimens, plates 89 mm in diameter and 30 mm thick with 25 mm ball bearings were inserted between the load dynamometer and the concrete specimen. A similar plate was added between the two concrete specimens. The dynamometer was used to check the load and prior to loading, it was calibrated in a Denison testing machine up to 100 kN, which corresponded to 0.54 of the cylinder compressive strength. The loss of load due to creep

of concrete, was compensated for by adjusting the four nuts until the required reading on the dynamometer was within ±4 divisions of the Demec gauge (see 4.6.1 below). This represented a sensitivity of about ±5% of the applied load.

The loading frame was held horizontally in a wooden frame and rotated when readjusting the load and taking reading.

4.6 Instrumentation

4.6.1 Concrete strain measurements

Concrete strains were measured using a demountable mechanical strain gauge (Demec Gauge), which had a 200 mm (8 in.) gauge length and each division corresponded to a strain of 8×10^{-6}. The gauge length is formed by pairs of punched and drilled mild steel discs (Demec points) glued to the concrete surface, using a rapidly setting glue prepared from F88 powder and F88 solution.

Concrete strains in the column were measured on both compression and tension faces at three sections, one at the mid-height and the other two located symmetrically above and below the centre line of the column.Fig.4.6 illustrates these positions.

Strains in the creep frame specimens and dynamometer, and in the shrinkage cylinder, were measured using the same Demec Gauge. Four sets of Demec points were equally spaced on their circumferences.

4.6.2 Steel strain measurements

Strains in the reinforcement were measured using PL-5 electrical strain gauges fixed to the steel. The installation of these electrical gauges involved several stages, starting with smoothing the surface of the bar over a length of 40 mm by filing and sanding, then cleaning it with acetone which was followed by application of acidic conditioner, then alkali solution (neutraliser). The surface was treated with evaporable liquid (200 catalyst) before fixing the gauges with ultra super glue. The gauges and all exposed electrical connections were covered with a layer of M-coat D which provided insulation against possible electrical leakage caused by high humidity or damp. The M-coat D was in turn covered with Evo-stik flashband which sealed the gauge from the ingress of moisture and contaminants. The treated area was finally enclosed with a heat shrinkable tube to ensure that the coating was well protected from physical damage. This coating absorbs mechanical shocks during both fixing and concreting and it can be seen in Fig.4.9(c).

These electrical gauges had a nominal resistance of 120 ohms and were connected to a Peekel strain indicator, which had five independent input circuits. The input capacity of the Peekel was extended using an extension box which had a maximum input connection of 48 strain channels. A dummy gauge, comprised a PL-5 gauge fixed on a piece of steel identical to the column reinforcement, cast inside a 100 mm concrete cube, was also connected to the extension box.

Two sections were chosen to measure the steel strains; each had four electrical strain gauges mounted on the four reinforcing bars. Due to the labour involved in the installation of these gauges and the fact that no extra information was gained from the second section, in the later experiments, only one section was retained at the centroid of the column, as shown in Fig.4.2.

4.6.3 Deflection measurements

Dial gauges,with a travel of 50 mm and an accuracy of 0.01 mm per dial division, were used to measure the lateral displacements, at three positions as shown in Fig.4.6. These dial gauges were mounted on the compression face to avoid any damage in the event of column failure.

To measure mid-height deflections for tests to failure, the central 50 mm travel dial gauge was replaced by a bigger dial gauge, with a travel of 10 in. (250 mm) and an accuracy of 0.01 in. (0.25 mm) per dial division. This was used in all short-term tests and in the short-term tests following a period of sustained loading.

These dial gauges have two drawbacks:

1- They only recorded movement in one direction, while deflections might develop about both axes.

2- Due to the shortening of the column under load, these gauges did not necessarily bear on a constant reference point.

For these reasons, non-contact measurement techniques based on the use of electronic theodolites, in particular the Wild Heerbrugg Remote Measuring System (RMS), was used in addition to the dial gauges. The Wild RMS is a three dimensional measuring system that computes the co-ordinates of any point in space with reference to the two measuring theodolites.

A series of targets (22 targets) were placed at regular intervals down both edges of the column as illustrated in Fig.4.6. These targets took the form of inverted Demec points. The two theodolites were placed in such positions as to form a well-defined

triangle with the column. The feet of the tripods were located in specially drilled holes in the floor to prevent any inadvertent movement. The technique is accurate to within 0.1 mm in the X, Y and Z directions which was perfectly acceptable for this project.

The arrangements and positions of the dial gauges and one of the theodolites, are all shown in Fig.4.14.

4.6.4 Load monitoring

A 500 kN capacity, Defiant Strain Gauge Load Cell type C, was used in each rig to record the load. This load cell was calibrated in a Tonipact testing machine on several occasions, using a Sangamo Amplifier unit type C56, to give readings to an accuracy of ±0.5 kN.

PL-10 full bridge electrical strain gauges were mounted on steel and aluminium collars to serve as load cells for the individual Macalloy bars. Two of these load cells were used in each rig as back-up. They were calibrated in the Avery-Denison testing machine for each test and connected directly to the Peekel.

Table 4.1 : Steel properties.

Bar diameter (mm)	Cross-sectional area (mm^2)	Yield stress (N/mm^2)	Modulus of elasticity (kN/mm^2)	Yield strain
16	201	range 510 - 550	range 180 - 209	average 2.65×10^{-3}
12	113	average	average	
10	78	530	200	

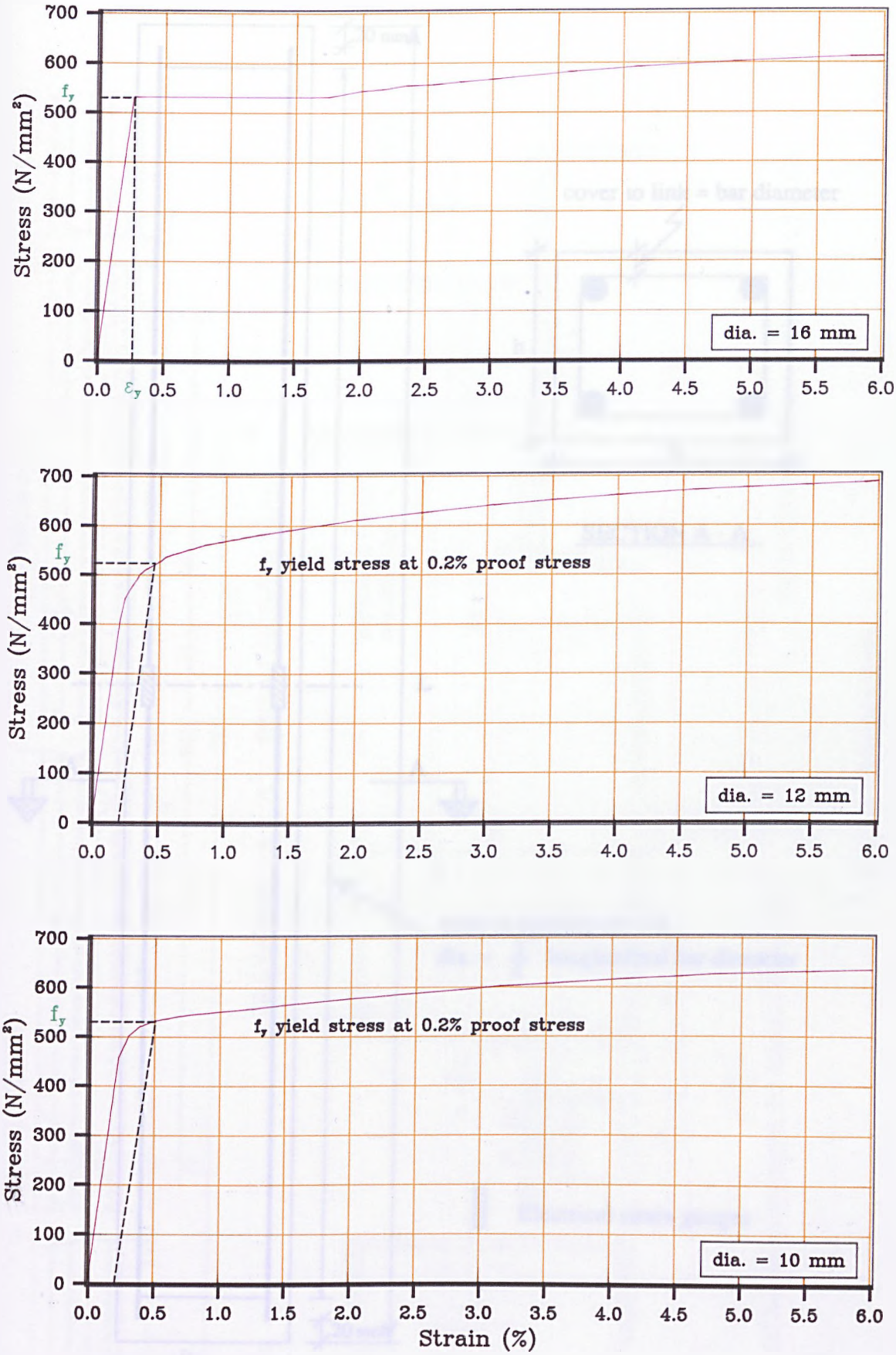

Fig.4.1 Typical stress–strain diagrams for high–yield steel.

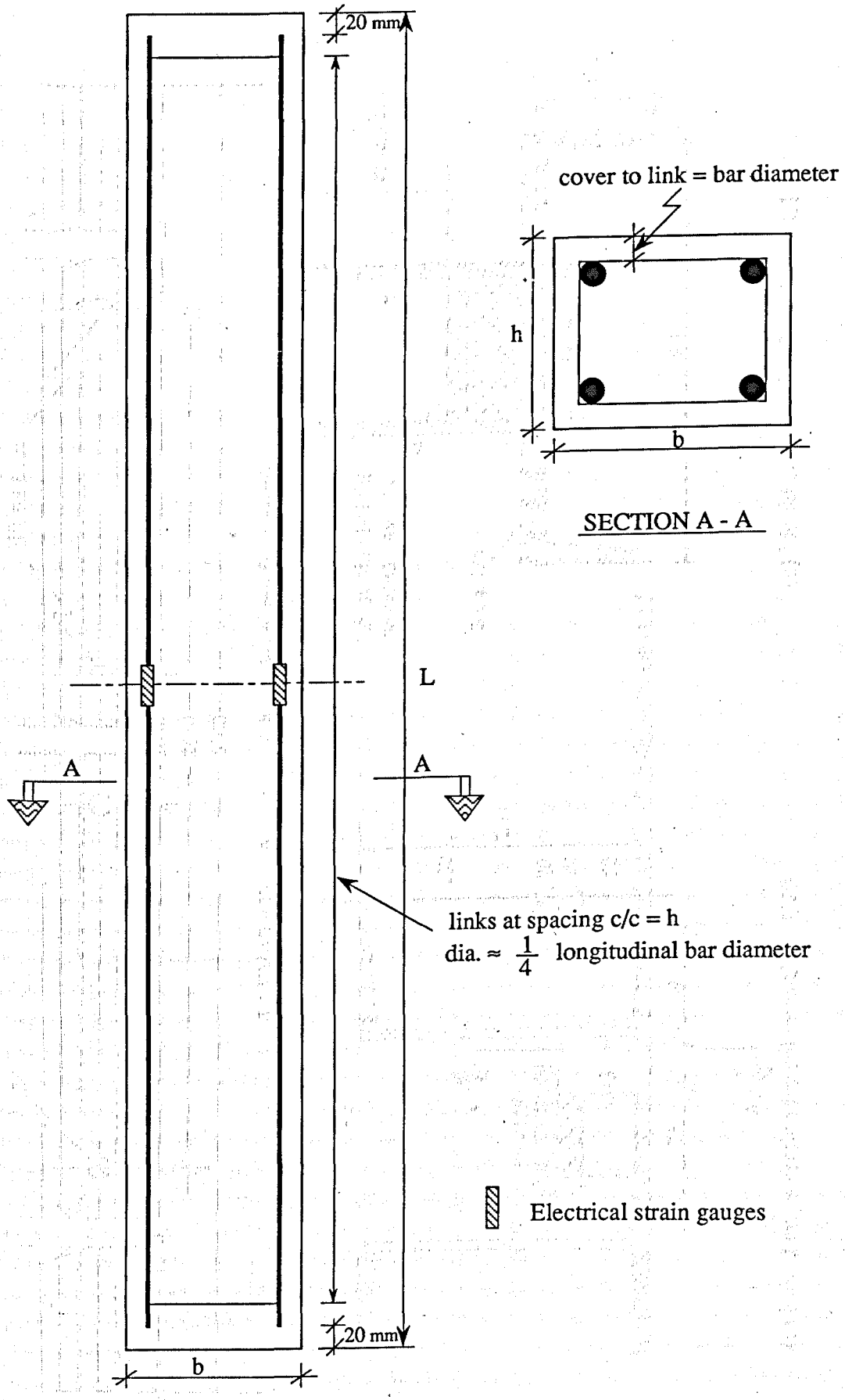

Fig. 4.2 : Typical reinforcement details.

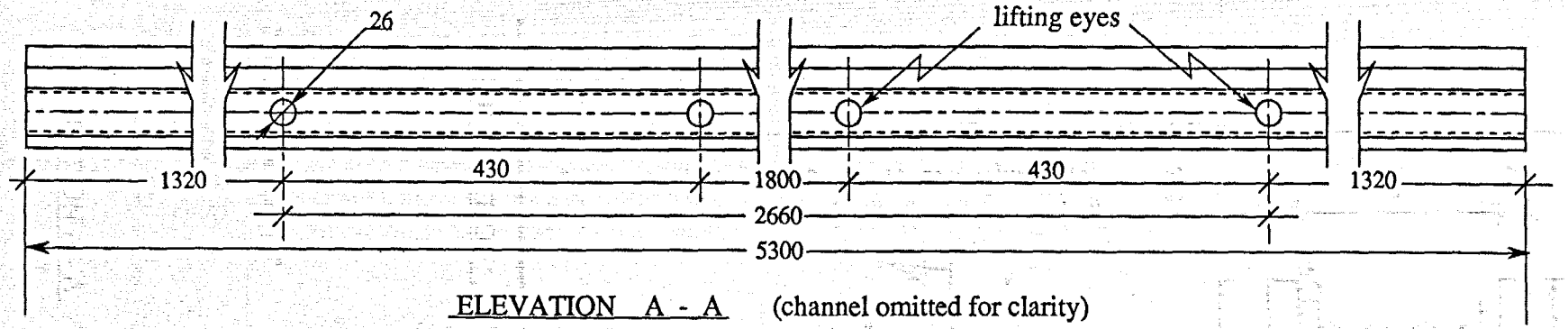

ELEVATION A - A (channel omitted for clarity)

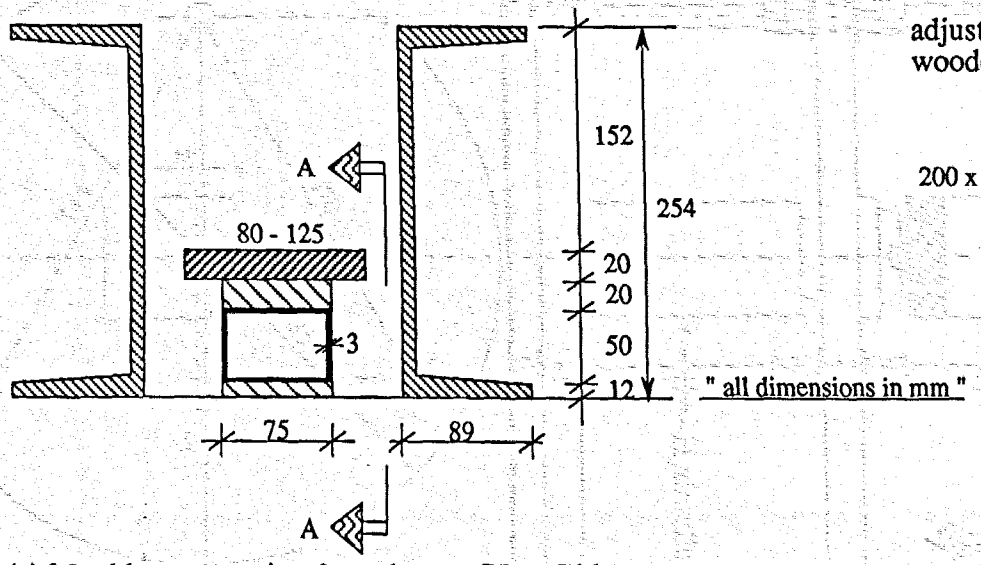

(a) Mould cross-section for columns C5 to C20

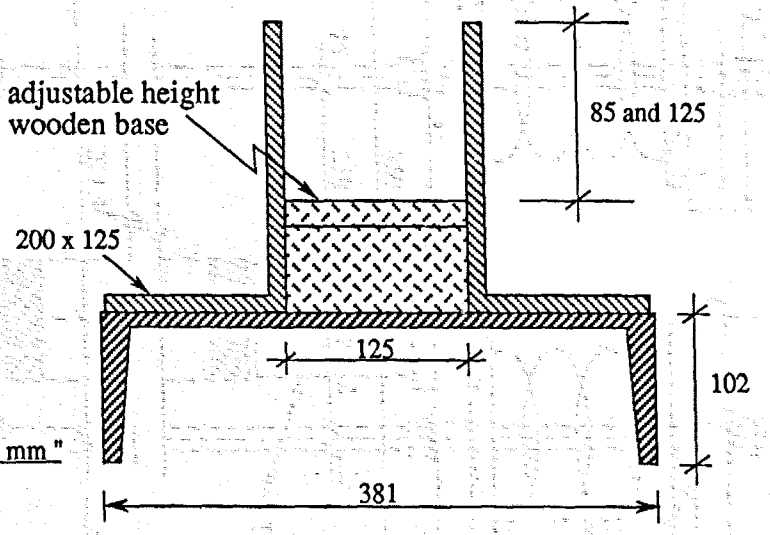

(b) Mould cross-section for columns C1 to C4

Fig. 4.3 : Mould details.

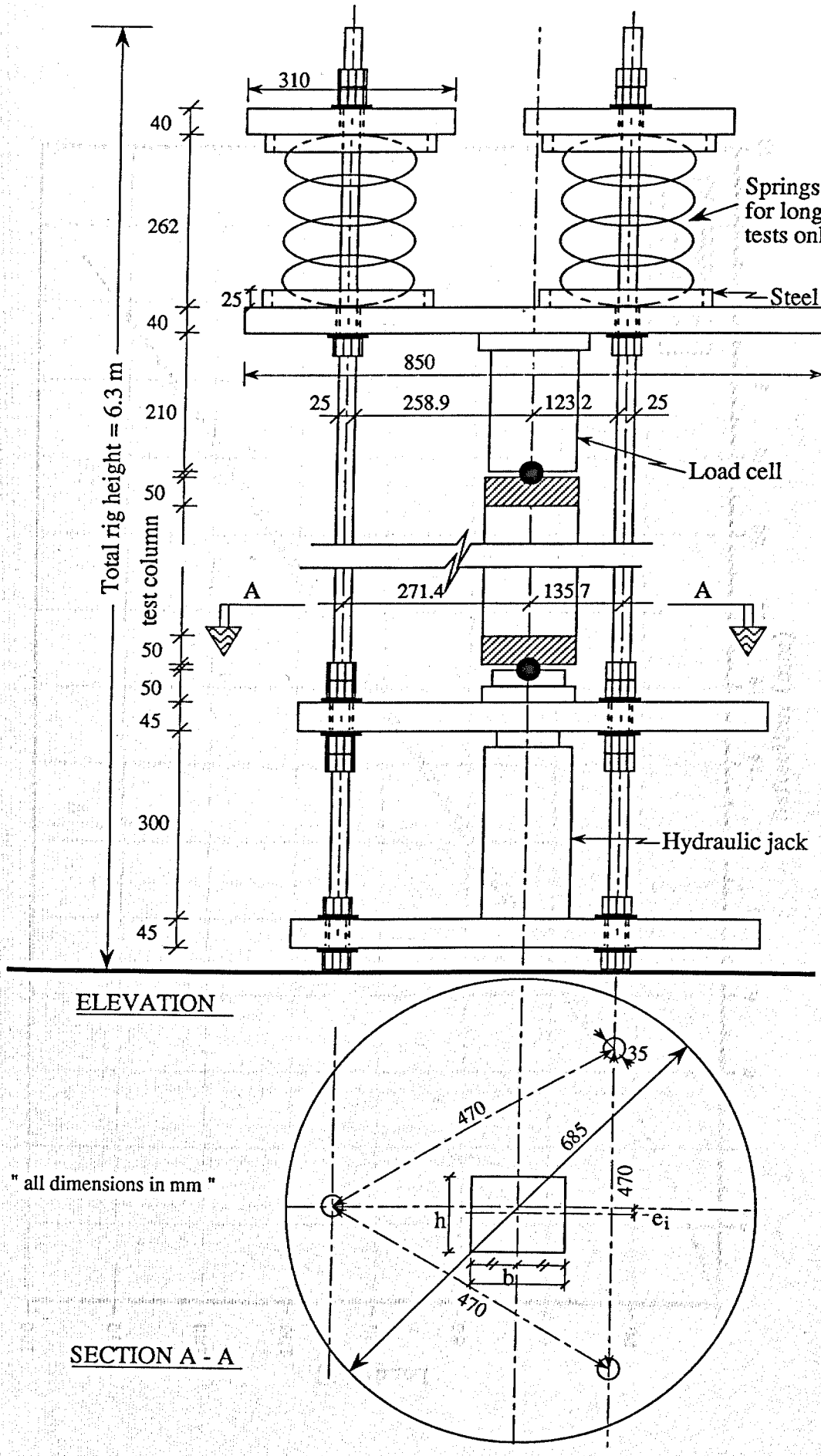

Fig. 4.4 : General arrangement of the rig.

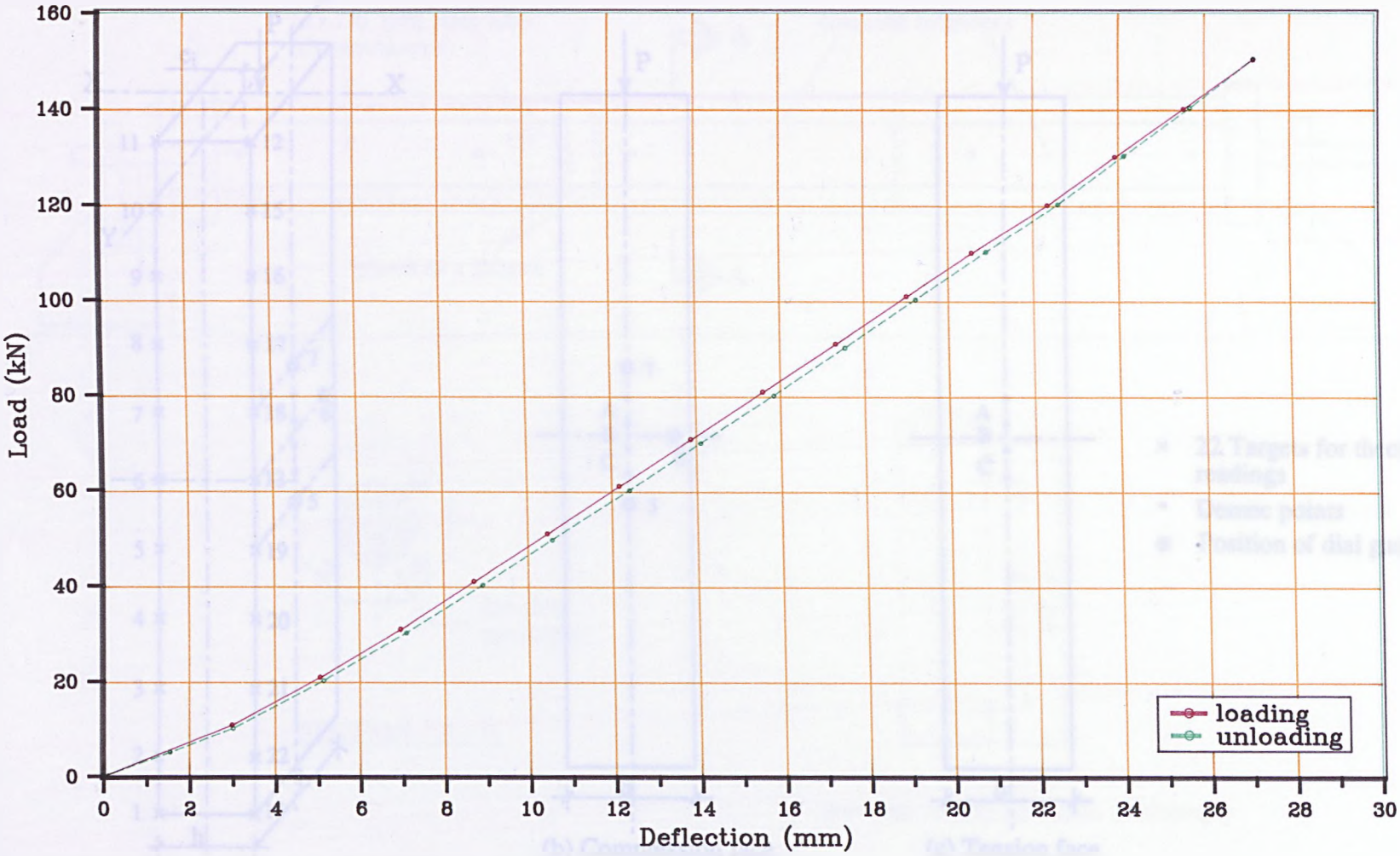

Fig.4.5 Typical load–deflection diagram for springs.

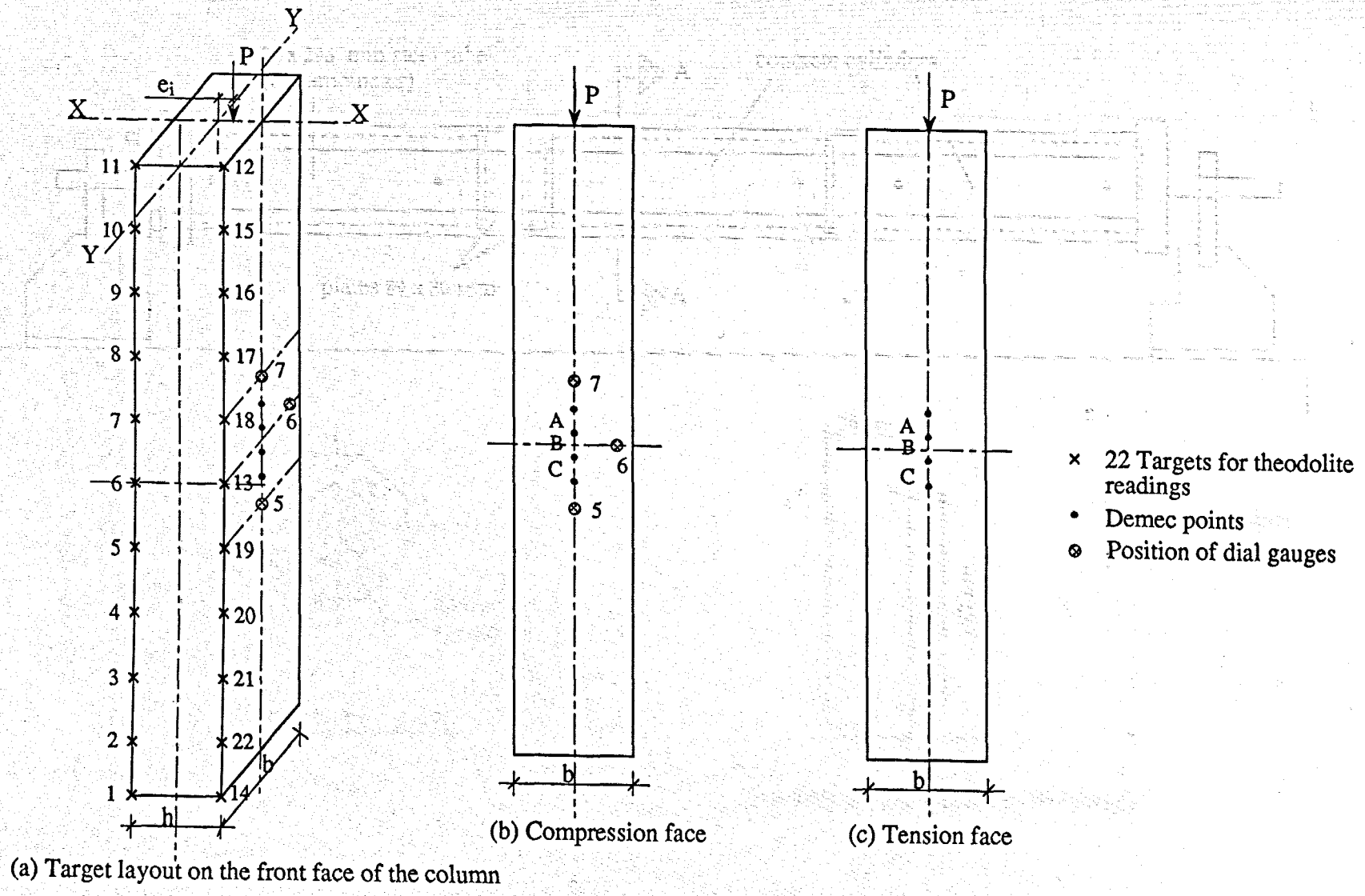

(a) Target layout on the front face of the column

(b) Compression face

(c) Tension face

Fig. 4.6 : Monitoring sections on the column.

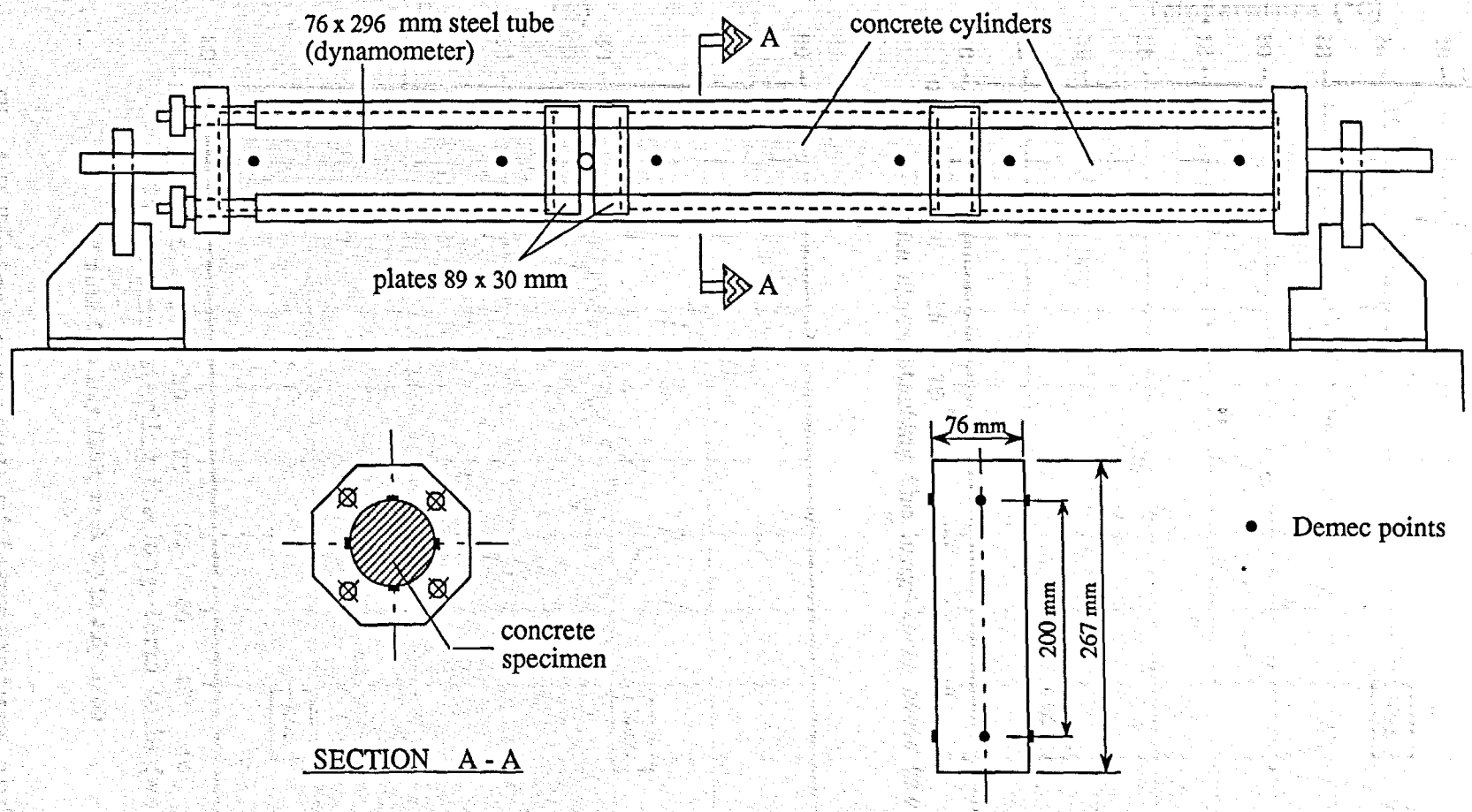

Fig. 4.7 : Diagram of simplified creep frame and shrinkage specimen.

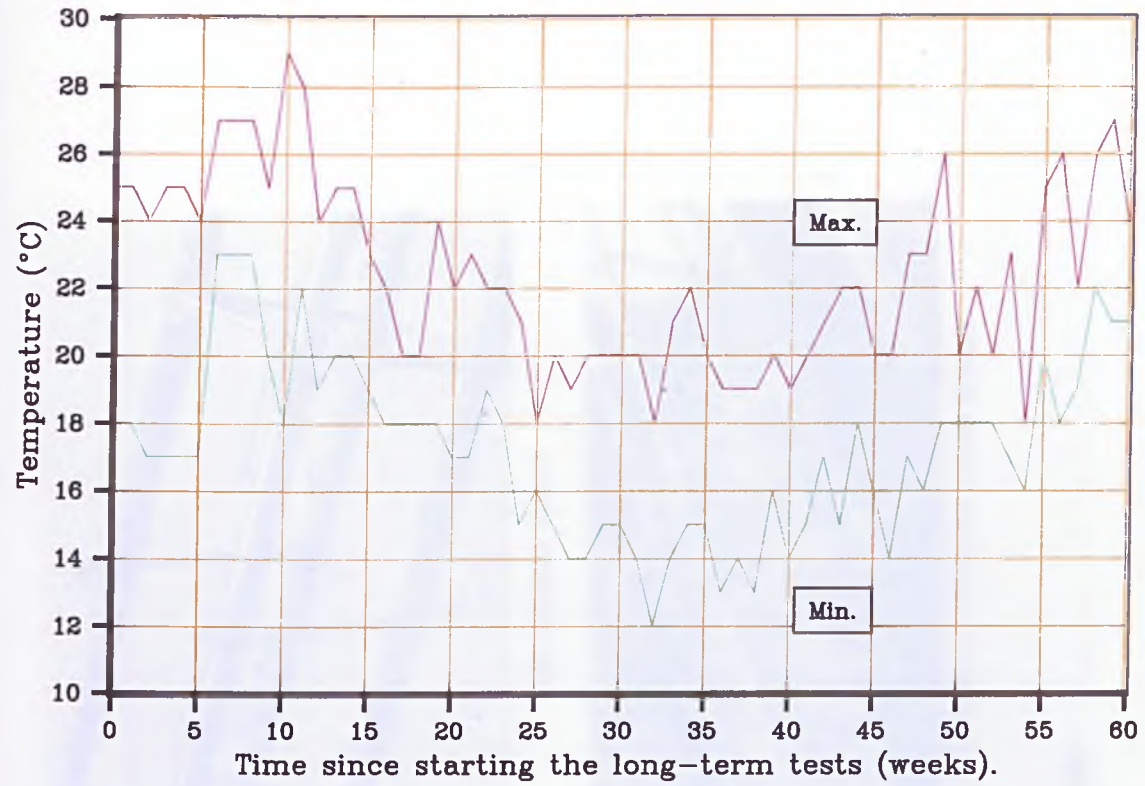

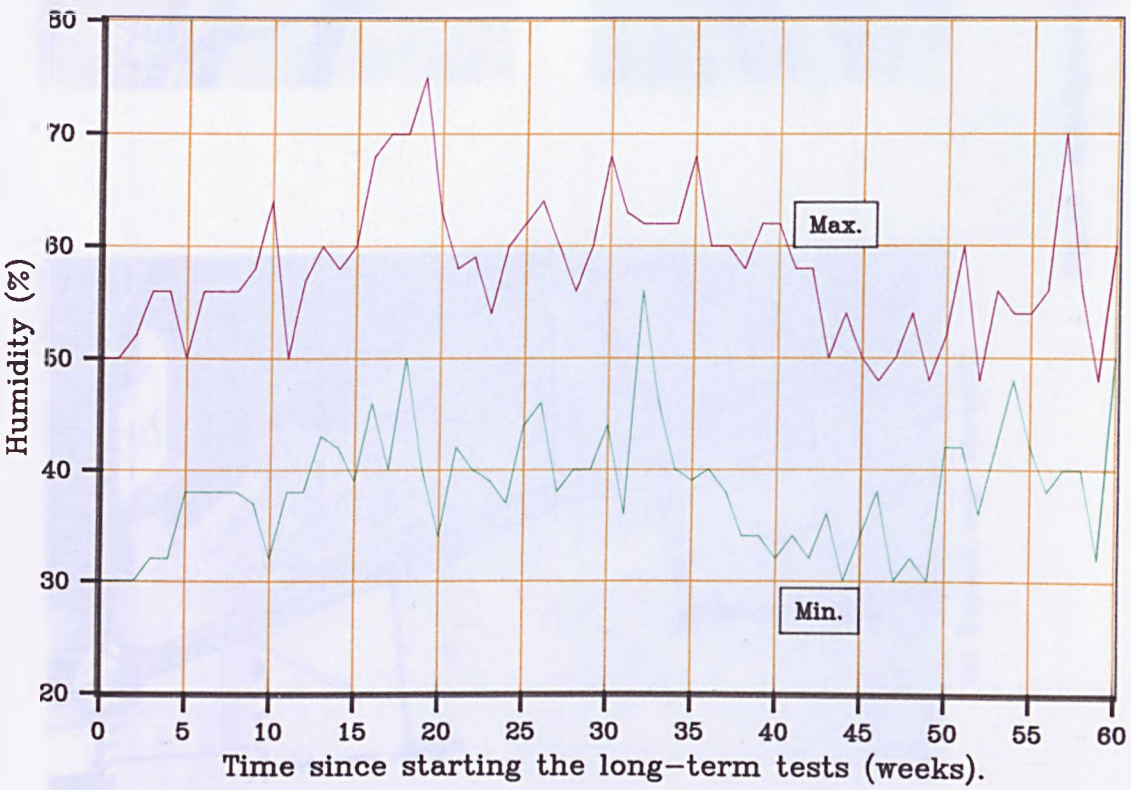

* week 0 in May 1989, week 60 in July 1990

Fig.4.8 Typical variation of temperature and relative humidity of laboratory atmosphere.

(a) Typical cage assembly

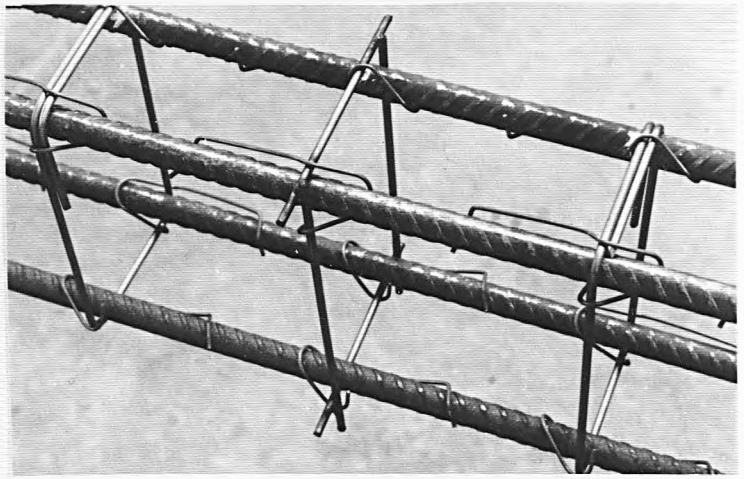

(b) Typical spacer

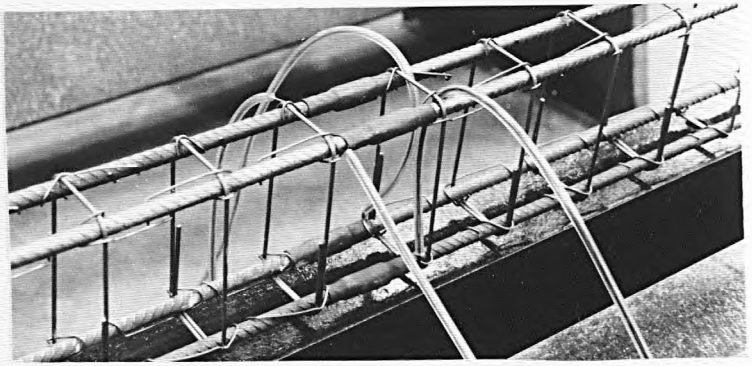

(c) Position of electrical strain gauges

Fig.4.9 Reinforcement details.

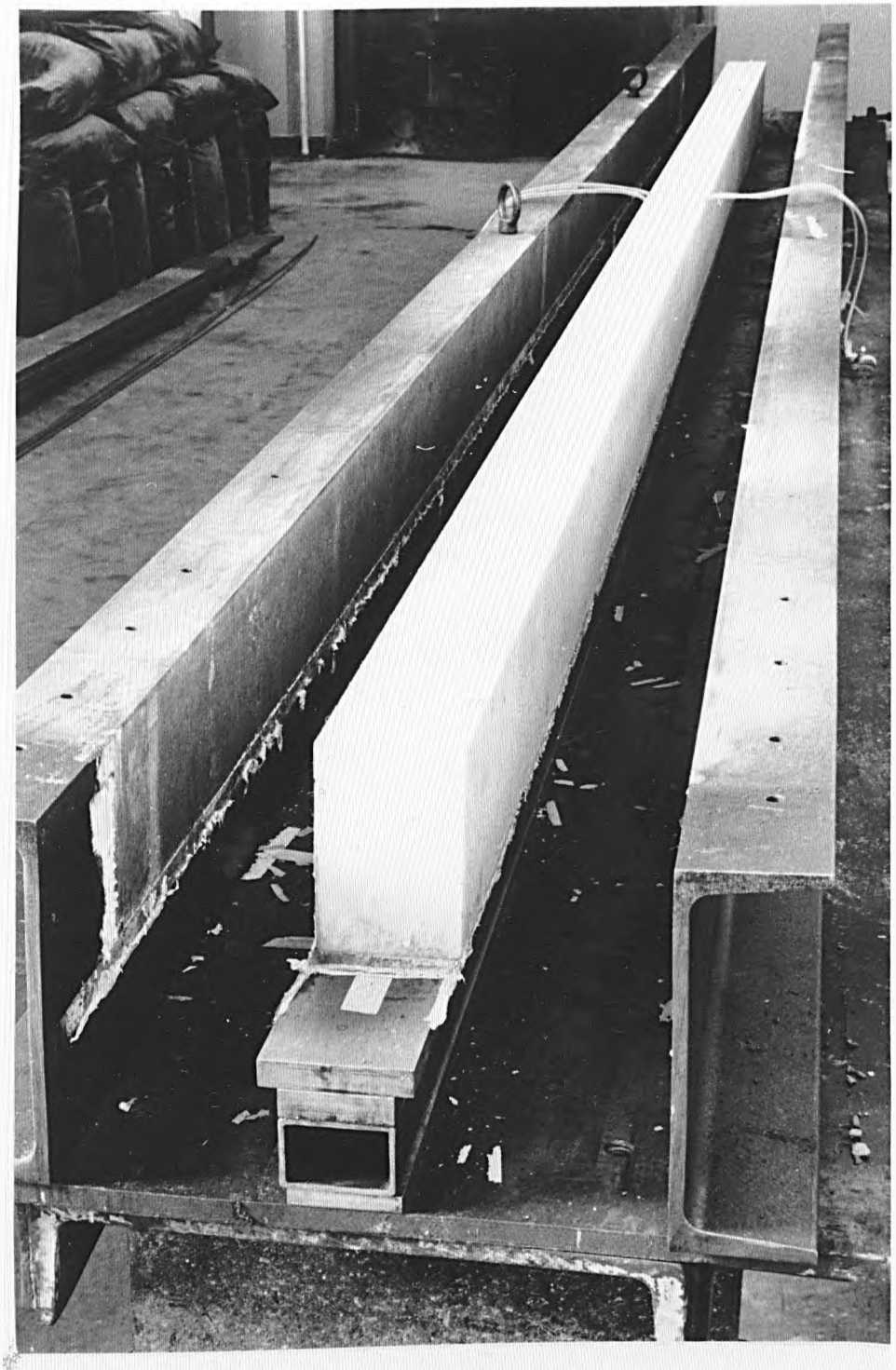

Fig.4.10 Mould used for columns C5 to C20.

Fig.4.11 Initial handling of column and mould base.

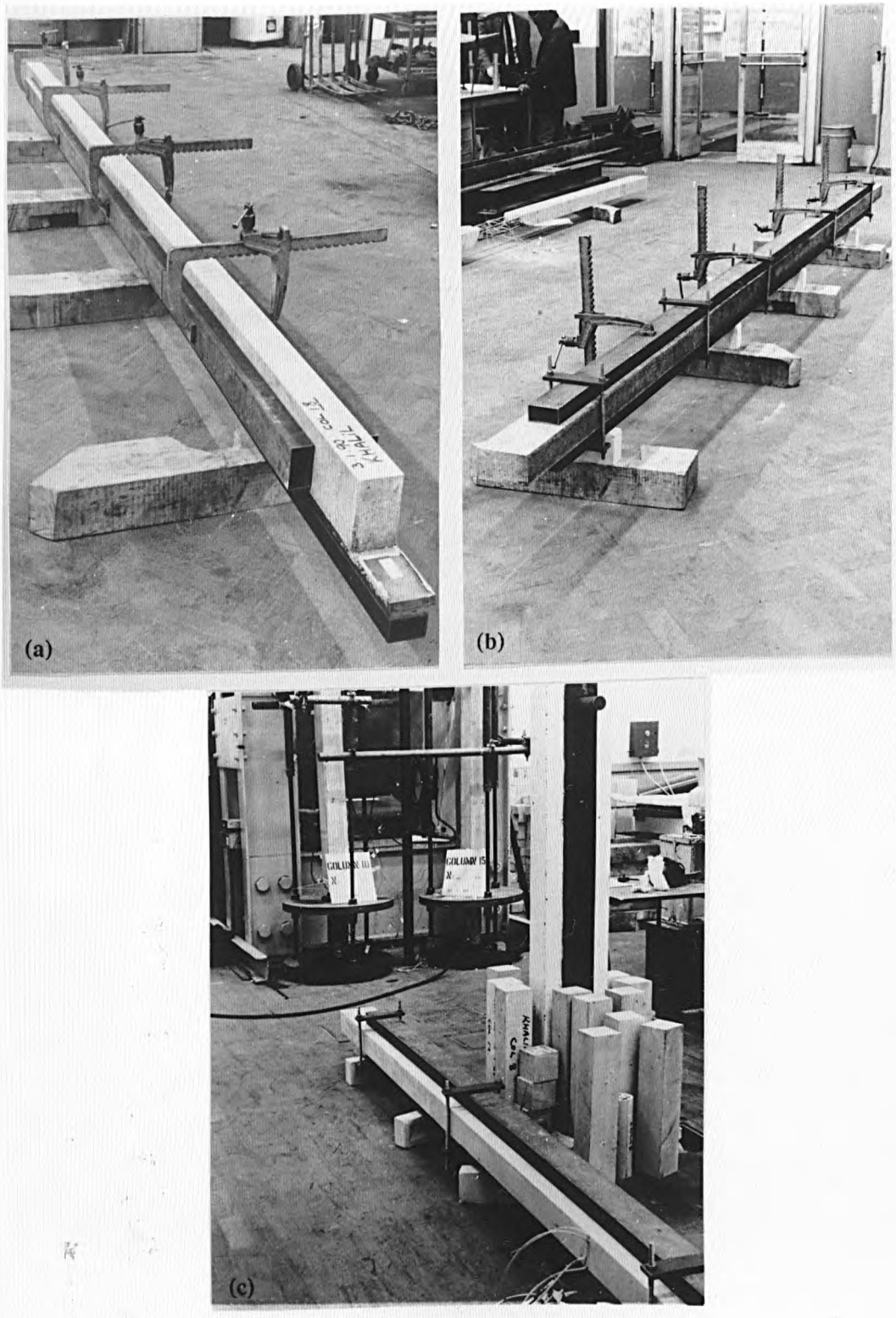

Fig.4.12 Order of handling operations.

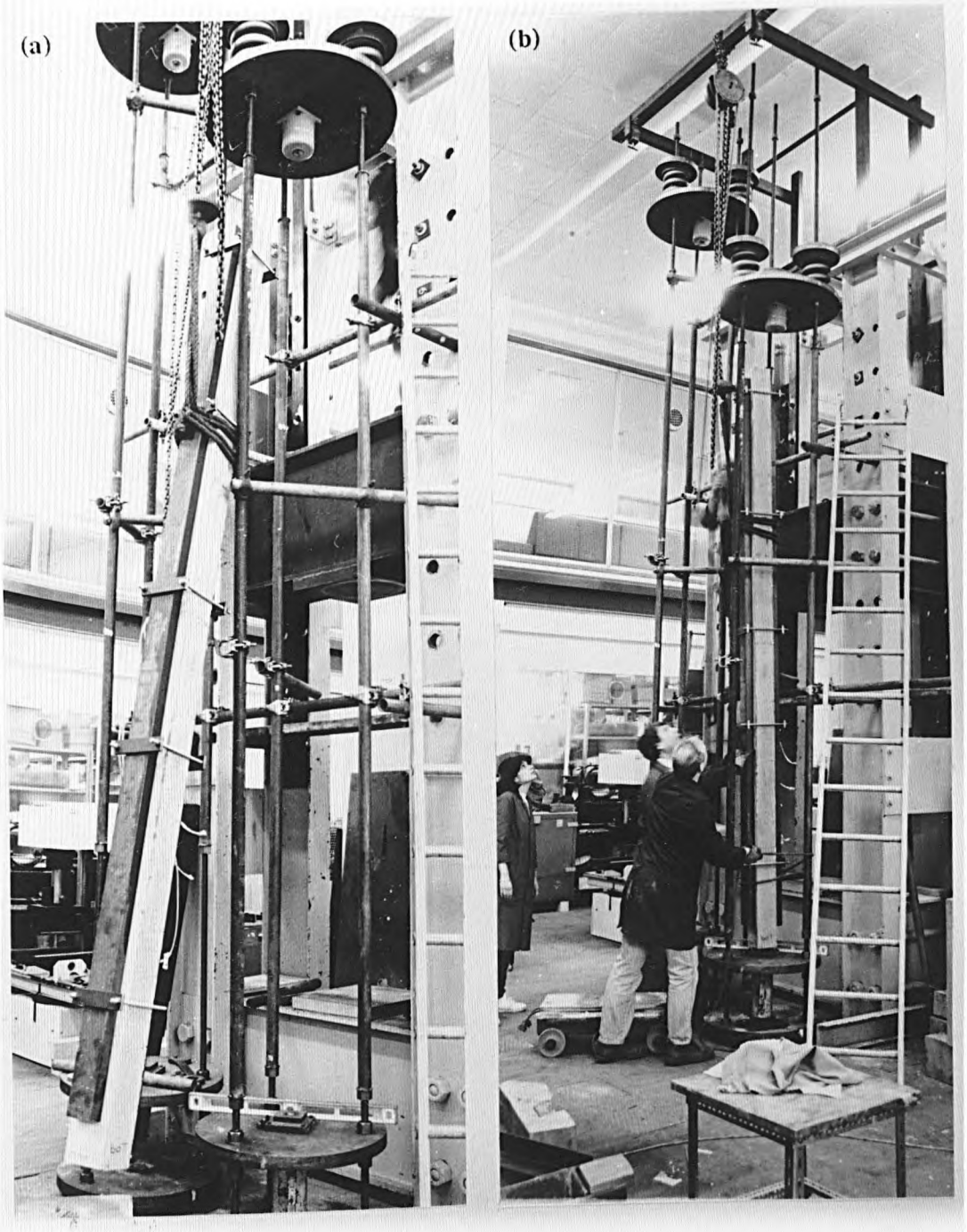

Fig.4.13 Final stage: lifting the column into the testing rig.

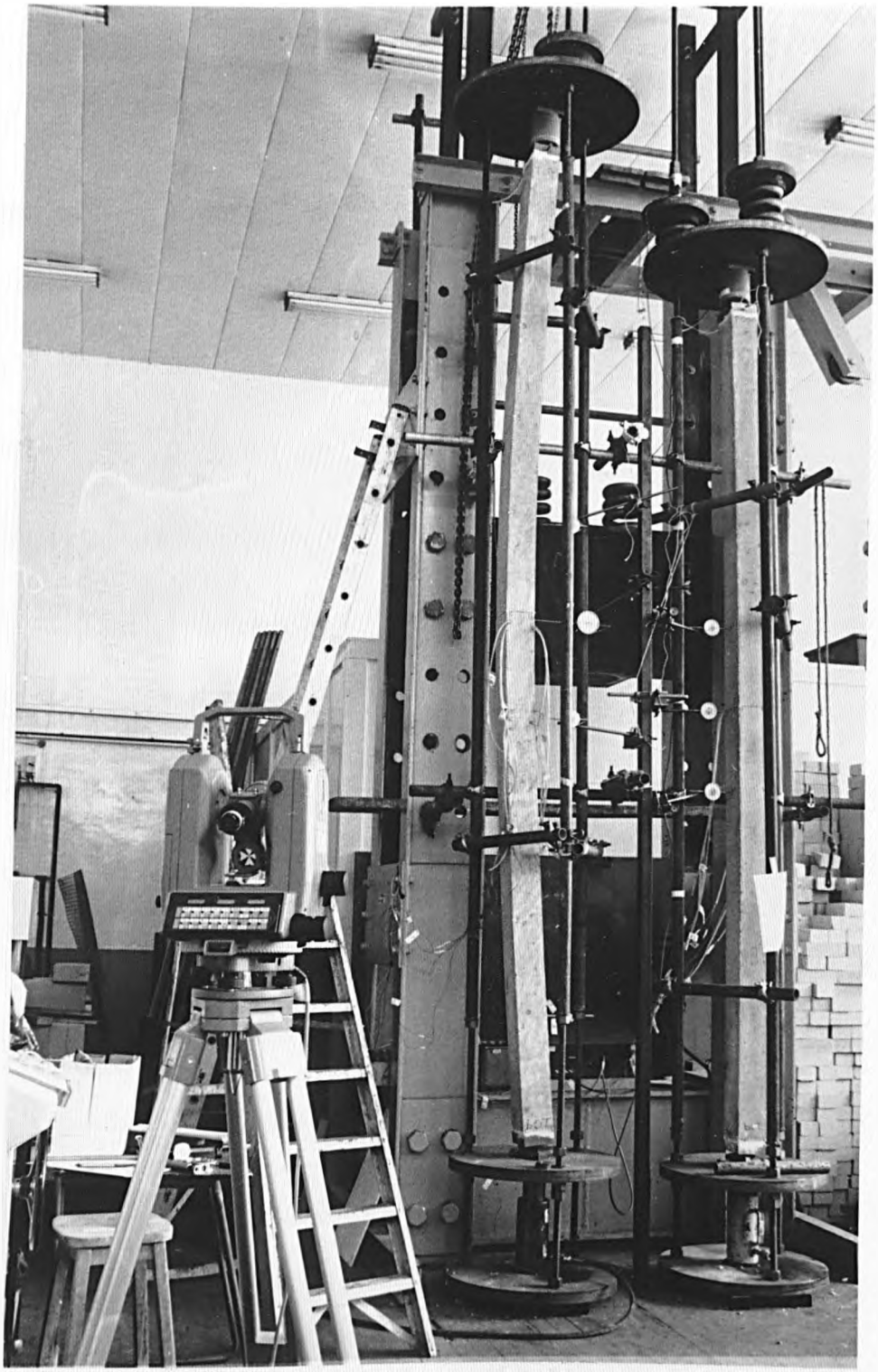

Fig.4.14 Second rig set-up.

Left: Short-Term test without springs (C7).

Right: Long-Term test in progress (C6).

Fig.4.15 First testing rig (C5 during test).

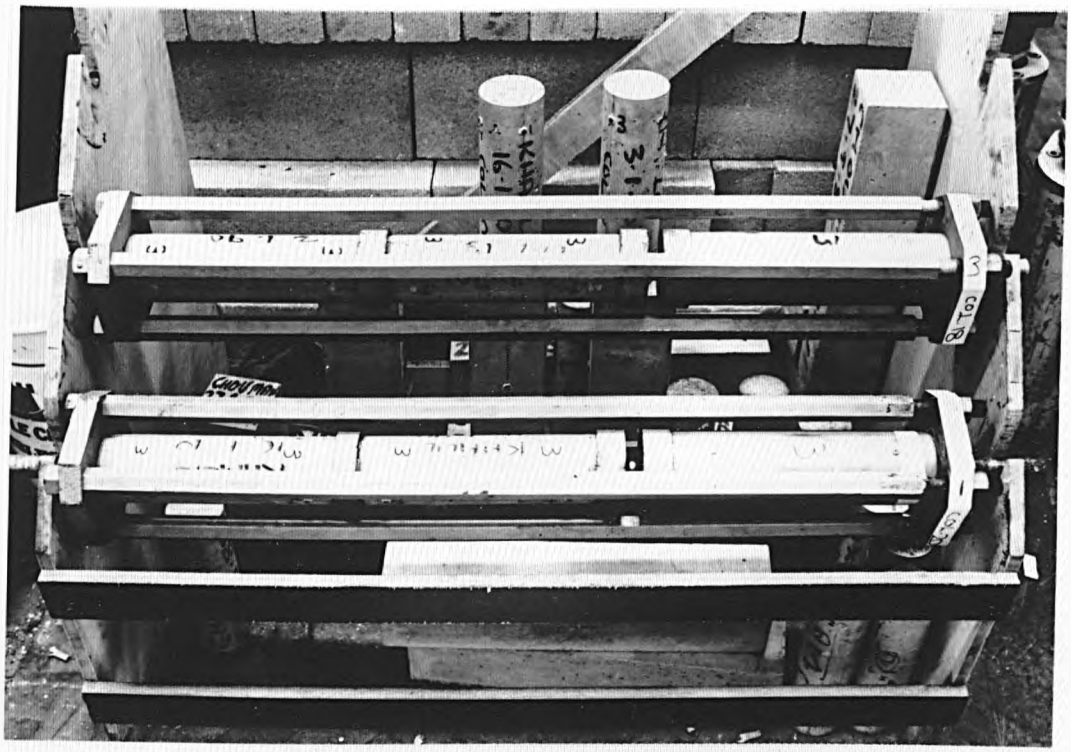

Fig.4.16 Simplified creep frames and shrinkage specimens.

CHAPTER FIVE

SHORT-TERM EXPERIMENTAL INVESTIGATION

5.1 Introduction

A total of twenty full-scale columns were designed although only nineteen were cast and tested (C16 was omitted, see 6.3.1). Eleven columns were loaded to destruction under short-term loading conditions to determine their ultimate capacity. The eight remaining columns were tested under a long-term loading condition to establish the reduction in the column capacity due to sustained load.

The main variable was the slenderness ratio; other parameters were kept relatively constant; these were:

- percentage of reinforcement
- concrete strength
- d/h ratio
- eccentricity = 10 mm for all columns.

This Chapter describes the short-term experimental programme undertaken to investigate the behaviour of hinged eccentrically loaded slender reinforced concrete columns. The experimental results are compared with the corresponding analytical values predicted by the proposed theory. The concrete properties are determined from a range of control specimen tests carried out in accordance with the recommendations of the relevant British Standards.

5.2 Description of test columns and concrete properties

5.2.1 Test columns

Tests on columns C1 to C4 were considered as pilot tests performed to establish the adequacy of the loading technique, method of erection and instrumentation. These tests helped in obtaining the experience required in testing slender reinforced concrete

columns and a clear picture was built up regarding the behaviour of such columns under short-term loading conditions. This also resulted in improvements in the instrumentation and test procedure.

The dimensions of the column cross-sections were chosen as large as possible to minimise initial imperfections and the section was made deeper in one direction to ensure uniaxial bending about the minor axis. Details of the column cross-sections are given in Fig.5.1. Table 5.1 gives a full description of the columns. To obtain the slenderness ratios, the effective length of the columns has simply been taken equal to the actual column length; theoretically for pinned columns it should be as the centre-to-centre distance between the end bearings. As can be seen from the table, columns C1 to C4 were designed so as to provide two pairs of identical columns; this was to lead to verification of individual behaviour.

Columns C5 to C20 were also designed in pairs, so that each column for short-term test is accompanied by an identical one for long-term test. These columns had a constant width of 152 mm and the slenderness ratio was varied from 28.8 to 62.5, by varying the length of the column and the depth of its cross-section.

The column end conditions were such as to allow rotational freedom in any direction. Load was applied at an eccentricity of 10 mm. A hydraulic jack activated by an electrically powered pump was used to apply the load in the pilot tests; this did not allow recording the deflections and strains beyond the peak load, because the load had to be released immediately when the deflection increased rapidly and the load decreased. Allowing further deflection, or spalling of the concrete, might damage the testing rig or injure the people engaged in the test. In later experiments a hand-operated hydraulic jack was used and the situation fully controlled.

5.2.2 Concrete properties

(a) Compressive strength

Nine 100 mm cubes were cast with each column, for the determination of compressive strength. Six cubes were cured in exactly the same environmental conditions as the corresponding column and were tested in a Tonipact testing machine, three cubes at the time of testing the column and another three at the age of 28 days. The remaining three cubes were cured in the humidity room and tested at the age of 28 days. All tests were carried out in accordance with BS1881: part 116: 1983.

(b) Density

The densities of the cubes, which were cured as the column and tested at an age of 28 days, were determined as specified in BS1881: part 114: 1983.

The results of (a) and (b) tests are given in Table 5.2, each value is the average of three tests.

(c) Slump

A slump test was carried out for each column mix as specified in BS1881: part 102: 1983.

(d) Static modulus of elasticity

This test was performed using a 100×100×500 mm prism, cast with each column. This prism was tested in the Avery-Denison testing machine in accordance with BS1881: part 121: 1983, to measure the initial modulus of elasticity at the age of 28 days and at the time of testing the column.

Table 5.2 shows the results of (c) and (d) tests.

5.3 Test procedure

5.3.1 Preparation and checks

After moving the column near to the testing rig, careful inspection was carried out for possible cracks due to shrinkage or mis-handling during transportation. Measurements for accuracy of construction and out-of-straightness at mid-height were taken and the latter was always added to the applied eccentricity.

Positions of the dial gauges were marked and targets were fixed in place (see Fig.4.6). The column was then mounted in the rig and the test set up completed by connecting the electrical strain gauges and load cells to the Peekel. Demec points were glued to the surface, loading frame plates were levelled and the column was ready for testing.

A nominal load was applied to hold the column in position. Accurate centring of the test frame was ensured by the initial design of the test frame, this was also checked by a plumb line.

5.3.2 Loading and test duration

The test started with the application of two cycles of loading, from zero up to about 10% of the expected failure load; this was necessary to establish reliable zero readings. Load increments were larger at the beginning and reduced later as failure approached. Each increment required about 10-15 minutes to make the necessary observations. An average number of 10 increments of load per test was usual. Each short-term test required over two hours, excluding the time taken to test the concrete control specimens. At the end of each test, cracks were inspected and marked.

5.4 Test results

Curves of mid-height strains in concrete against load are shown in Figures 5.2(a) to 5.2(c). In addition to mid-height concrete strains, results of the behaviour of the two symmetrical sections about the mid-height point are illustrated for columns C9 and C19 in Fig.5.3 as typical examples. In Fig.5.4 typical strain variations across the section of the column, at different load stages, are shown for columns C9 and C19.

Load-deflection curves are given in Figures 5.5(a) to 5.5(d); the deflection has been taken at the mid-height of the column using dial gauge readings. Deflection as measured by the theodolites was also plotted against the height of the column. Typical results for columns C9 and C19 are given in Fig.5.6, as representative of the general behaviour.

The theoretical and experimental buckling loads obtained for each column are compared in Table 5.3. The table also gives a comparison between the experimental and theoretical eccentricities at the mid-height of the column at the point of instability. Statistical values are provided in Table 5.4.

5.5 Observations and discussion

All columns were loaded so as to cause single curvature bending. This is the principal failure mode causing the lowest critical buckling load [93]. A nominal eccentricity of load (10 mm) was included to ensure bending about the minor axis. This value of eccentricity also satisfies BS8110 requirements regarding the minimum eccentricity to be considered.

All columns failed by reaching a critical buckling load, at which the column became unstable. This was followed by considerable bending, until material failure occurred, or in most cases, the column touched the rig without crushing but with cracks distributed over the tension face. The increase of deflection was associated with drop in

load for stable equilibrium. Attempts were then made to put more load on the column by jacking; these resulted in further increase in deflection with continuous drop in the load. For columns C1 and C5, crushing occurred suddenly almost as soon as the maximum load had been reached; a warning of instability was observed immediately before failure by a drop in the load. For all other columns, crushing did not occur because the test was stopped as soon as the column approached the rig supports. Further loading might have damaged the testing rig or affected the neighbouring long-term test in progress.

The short-term buckling loads P_{test} of the slender columns tested, are given in Table 5.3 as the maximum recorded values of experimental load. However, because of the rapid development of microcracks and creep at higher loading levels (i.e near failure), these values are dependent on the rate of loading; any delay in loading could significantly decrease the column capacity. It was attempted in the tests to repeat the same load increments and time rate as closely as possible, but inevitably there were differences between tests. This explains variations in load-deflection behaviour close to the maximum load.

Results obtained from the pilot tests (columns C1 to C4), were generally satisfactory. However, the use of the electrically operated hydraulic jack did not allow precise determination of the failure loads of these columns, nor the recording of their behaviour beyond the instability point, as mentioned earlier. Failure of column C1 was sudden and explosive with the concrete flying in all directions, fortunately without causing any injury and the load was released immediately. Figs.5.7 and 5.8 show this failure. Better estimation of the failure load was achieved in the later experiments; as a result columns C2, C3 and C4 were not allowed to crush in their testing rigs. Material failure was also seen for column C5 but was more controlled.

Columns of slenderness ratio 33.6 and above (C7 to C19) showed gradual progression towards material failure; considerable curvature was required to attain such failure which was normally not reached. Figure 5.9 shows typical bending profiles for columns C9, C11, C14, C17 and C19. It can be clearly seen in Fig.5.9 that columns C9 and C11 had touched the horizontal lateral struts at a lateral deflection of about 120 mm; these struts were later made square in plan to allow for greater deflection (by doing this the lateral deflection at the end of the test could reach a value of about 180 mm).

For all columns the failure section was at mid-height, or within 100-200 mm above or below it, depending on the location of the weakest section, which was sometimes associated with the position of the electrical strain gauges on the steel bars.

The onset of instability was indicated, as described above, by a drop of load and by the amount of lateral deformation present, but not by the crack pattern. No visible cracks appeared for loads prior to instability; this phenomenon was also observed by

Pancholi [29] who tested thirty three concentrically loaded reinforced concrete columns having slenderness ratios between 30 and 80. It was also observed by *Dracos* [5], who tested thirty six eccentrically loaded slender columns with slenderness ratios between 29 and 58.

A typical crack pattern is shown in Fig.5.10 for column C7. Generally, these cracks were initiated at the corners then extended over the full width of the column as the deflection increased and they were symmetrically distributed about the mid-height. Cracks also appeared on the compression face upon load removal. Once the load is removed, there is an immediate creep strain recovery in concrete, while the column tends to return to its original unloaded shape. The net residual deformation produces compressive stress in steel and tensile stress in concrete and the latter can sometimes be high enough to cause cracking. *Kong and Evans* [94] clearly explained this phenomenon in terms of residual stress.

Strains in concrete were recorded at three sections on both the compression and the tension faces. The results obtained show that the columns behaved symmetrically about the mid-height point. This is illustrated in the load-strain curves for columns C9 and C19 in Fig.5.3. Strains measured in the steel agree quite closely with those obtained for the concrete as shown in Fig.5.4; this validates the assumption that plane sections remain plane after bending. The variations which exist could be attributed to the difference in the location and gauge length of the Demec points and electrical strain gauges. In one case, for column C5, concrete strain measurements were rejected because they were not logical and did not follow any pattern, indicating serious errors in the readings. This was probably due to the restricted access to the column, which was tested in the first loading frame. Other measurements (strains in steel and deflection) were acceptable. With improved access and new loading arrangements the test was repeated on column C5 after a few days using a hand-operated hydraulic jack. The strains in concrete recorded during this second run were acceptable and are shown in Fig.5.2(b).

A typical maximum value for the compressive strain in concrete at the point of instability was found to be approximately 0.002 for slenderness ratios 18 and 26.4. For columns C5 to C19 with slenderness ratios 28.8 until 62.5, the value was typically 0.001, thus confirming that instability occurs well before the ultimate strain capacity (0.0035 in BS8110) of the section is reached. Similar results were found by *Schofield* [30] and others. *Schofield* tested 50 columns under short-term loads with slenderness ratios between 29 and 59. He found that the observed compressive strain at failure for these columns was typically 0.001.

The use of theodolites enabled the determination of the deflected shape of the column in the X and Y directions. Their readings were taken at alternate load stages

during the experiment. When failure approached, time spent in taking readings became crucial; only three targets were then monitored, one at mid-height and the other two at the ends of the column. The use of theodolites, however, did not eliminate the need for dial gauges, which have their own merits of giving information about the deflection directly during the test and indication about the stability of the column. Data from the theodolites had to be processed in the computer to obtain it in its final form as X, Y and Z coordinates.

For columns of 5 m length, the loading rig was somewhat flexible at the top due to lack of restraint from the tubular sections around the Macalloy bars. Horizontal movements at the ends of the column were monitored by the theodolites, reaching a typical value of 5 mm measured at the end of the test (after instability failure).

Some lateral deformation,perpendicular to the direction of bending, occurred in all tests, usually negligible up to the point of instability, but appreciable in a few experiments when approaching material failure at deflections considerably beyond the buckling failure load. This could be due to errors in placing the steel cage, or possibly the load was not perfectly axial with respect to the Y direction. The effect of the direction of casting was examined and found not to affect bending in the Y direction. *Schofield* [30] stated a similar observation in his work and attributed that to loading or casting errors.

In the case of column C2, the dial gauges indicated reverse movement (see Fig.5.5(a)) until load stage 100 kN; afterwards the column deflected in the expected direction. Because the load was applied at a small eccentricity of 10 mm, such reverse movement is probably to be expected until the column settles in the correct direction. However, the maximum value recorded for this movement in case of column C2 was high; no apparent reason was found to explain it, particularly similar movement was also recorded by the theodolites. A reverse movement was also noticed for column C11 at the first stage of loading, but it was of very small magnitude (Fig.5.5(c)).

The experimental results of buckling load and mid-height eccentricity at the point of instability are compared with the theoretical values in Table 5.3. To obtain the values of e_{test}, the initial imperfection and initial eccentricity were added to the theodolite and dial gauge readings. Values of means, standard deviations and coefficients of variation for the ratios P_{test}/P_{theory} and e_{test}/e_{theory} are given in Table 5.4. For calculating the theoretical results, Figs.3.5 to 3.13, which give the load eccentricity-curvature relationship in terms of the capacity ratio P/P_0, have been used. As discussed in Chapter 3, these graphs are based on the stress-strain diagrams for concrete and steel given in BS8110: part 1: 1985 (Figs.3.1 and 3.2). The partial safety factor for strength of materials γ_m was taken as unity, consequently the maximum concrete stress equal to $0.67f_{cu}$ and E_c equal to $5.5\sqrt{f_{cu}}$ kN/mm^2. The values of f_{cu} were chosen to cover the range of test values. Linear

interpolation between the graphs was then used for each column cube strength relevant to the time of testing.

In producing buckling deflection-curvature graph in terms of l_e/h ratio (Fig.3.24), the initial imperfections e_0 were taken as $5.68\times10^{-4}L$ as measured in the laboratory (see 4.2.5).

In general, there is very good correlation between the theoretical and experimental results. The actual failure load of column C2 is likely to be greater than the recorded value of 400 kN, as the column failed upon the application of the next increment and the load had to be released immediately, for the reasons explained earlier (see 5.2.1). Column C4 which was identical to column C3 failed at a lower load because it was tested at an earlier age than C3 and has a lower value of concrete strength.

Two values were used for the variable d/h in obtaining the theoretical results, these were 0.75 for columns C3, C4 and C17, and 0.8 for the rest of the columns. This restriction was necessary to keep the number of graphs required to a practical limit. To investigate the influence of d/h, the analysis of columns C3, C4 and C17 was repeated assuming d/h=0.8, the results obtained are shown in Table 5.5. Using a higher value than the actual one will yield a higher predicted failure load and consequently a lower P_{test}/P_{theory}; adopting a value for d/h lower than the real one will result in a higher value of P_{test}/P_{theory}. A similar influence can be seen on the ratio e_{test}/e_{theory}. Using the exact value of d/h in the analysis would improve most of the results. Comparing the actual values of d/h given in Table 5.1 with those assumed in the analysis, would explain some of the discrepancies between the theoretical and experimental results seen in Table 5.3.

Another factor affecting the theoretical results is the value of E_c. As will be shown in Chapter 7, the values of the initial modulus of elasticity calculated by the BS8110 expression are higher than those measured in the laboratory using 100×100×500 prisms. To examine the influence of E_c, the analysis of column C7 was repeated assuming three values for E_c, 30, 35 and 40 kN/mm^2. The results are given in Table 5.6. Adopting a higher value for E_c increases the apparent carrying capacity of the column and hence the ratio of P_{test}/P_{theory} will decrease, while the ratio e_{test}/e_{theory} increases. It is to be noted that the experimental value of E_c is measured after carrying out two cycles of loading on the prism (from zero up to $f_{cu}/3$ according to BS1881: part 121), while BS8110 expression gives the initial tangent modulus of elasticity, which for column C7 equal to 40 kN/mm^2.

In general, deflections have been slightly underestimated due mainly to the fact that, the theory does not account for the rate of loading or the overall testing time. Each applied load was kept on a column for about 10 minutes (or 15 minutes if a full set of reading by the theodolites was taken) to allow a complete set of measurements to be

recorded. Readings taken at high load levels, particularly for loads close to failure, would have been affected by creep. This also could explain the differences in some cases between theodolite and dial gauge readings which can be seen in Table 5.3. This is mainly due to the differences in time at which each reading was taken and the consequent variation in load which could not be kept constant as it started to drop during the taking of readings.

A back-up reading for the deflection values was taken by a plumb line at the end of each test before releasing the load. This was helpful in the case of column C14, where the battery for the theodolites ran out of charge at the end of the test.

To examine the influence of initial imperfections e_0, the analysis was repeated for all the columns taking $e_0=0$ (i.e using Fig.3.23 instead of Fig.3.24), the results are to be found in Table 5.7. It can be seen from the table, that ignoring the presence of initial imperfections could cause a discrepancy up to 10%, when comparing the mean values of P_{test}/P_{theory} obtained in both cases; while for the e_{test}/e_{theory} ratio, the discrepancy reaches 15%. These results suggest the importance of making allowance for e_0, however small its value, in the theoretical approach. The effect of the initial imperfections on the theoretical results decreases for columns with small l_e/h ratio and/or high end eccentricities.

5.6 Conclusions

1- All columns showed instability as the mode of collapse before reaching the ultimate capacity of the section. This was followed by material failure, which for slenderness ratios of 33.6 and above required considerable bending to occur.

2- Instability failure was indicated by a drop in load and by the amount of lateral deformation present, not by the crack pattern. No visible cracks appeared before reaching the maximum load.

3- Instability occurred at low compressive strains of the order of 0.001-0.002 (Figs.5.2 and 5.3), which is considerably below the ultimate strain value which in codes of practice lies in the range 0.003-0.0035. Thus it is appropriate to relate slender column design criteria to instability conditions and not to the ultimate strength of the column section.

4- Observed deflections and strains for equidistant sections above and below the mid-height point were in close agreement, thus indicating a symmetrical deflected shape.

5- In a few tests, specifically columns C17 and C19, at deflections considerably beyond the buckling failure load, bending about the Y axis was appreciable.

6- In spite of the many precautions taken, the relatively small size of the columns makes the test sensitive to the location of applied loading and steel placement; this could explain the small reverse lateral movements in the X direction which occurred during testing column C11. It also explains the lateral deflection in the Y direction which took place in all tests (normally negligible up to the point of instability).

7- The analytical procedure based on *Beal's* method, enables the actual behaviour of the eccentrically loaded reinforced concrete columns to be closely estimated. The accuracy of predicting the failure load and mid-height eccentricity at the point of instability is within acceptable limits.

8- The analysis assumes a linear strain distribution across the section and the results obtained substantiate the validity of this assumption (Fig.5.4).

9- The assumption "the curvature of pin-ended column follows a sine curve as it buckles", is verified by the results (Fig 5.6).

10- The analytical method is especially sensitive to the values of the variables: d/h and E_c (Tables 5.5 and 5.6). The values chosen for these variables and the fact that the theory takes no account of the rate of loading, could explain discrepancies between the theoretical and experimental results.

11- The comparative study made, investigating the influence of initial imperfections (Table 5.7), emphasises the importance of including it in the analysis. It also illustrates the limited stability of slender columns and their sensitivity to the presence of imperfections and initial bow.

Table 5.1 : Column details.

Column	b (mm)	h (mm)	d/h	$\%A_s$	e_i/h	L (m)	l_e/h*
C 1	125	125	0.83	2.90	0.080	2.25	18
C 2							
C 3	125	85	0.77	2.96	0.118	2.25	26.47
C 4							
C 5	152	125	0.78	4.23	0.080	3.60	28.80
C 7						4.20	33.60
C 9						4.80	38.40
C 11	152	100	0.79	2.97	0.100	4.50	45.00
C 14						5.00	50.00
C 17	152	90	0.76	3.30	0.111	5.00	55.56
C 19	152	80	0.78	2.58	0.125	5.00	62.50

* $l_e = L$.

Table 5.2 : Concrete properties.

Col.	Cube compressive strength (N/mm^2)			Cube density (kg/m^3)	Static modulus of elasticity* (kN/mm^2)		Slump (mm)
	Cubes cured with column		Standard curing		28 days	Time of testing	
	28 days	Time of testing	28 days				
C 1	52.0	$f_{cu22} = 52.2$	-	2396	31.0	30.6	65
C 2	52.8	$f_{cu21} = 53.2$	-	2416	-	35.3	-
C 3	-	$f_{cu21} = 57.3$	-	2395	-	32.8	50
C 4	-	$f_{cu18} = 48.7$	-	2413	-	-	-
C 5	59.0	$f_{cu25} = 56.4$	-	2414	36.0	34.4	55
C 7	48.0	$f_{cu33} = 51.8$	47.9	2370	-	30.0	40
C 9	50.6	$f_{cu32} = 52.0$	48.9	2362	-	32.5	50
C 11	43.8	$f_{cu29} = 47.4$	45.6	2382	-	29.7	45
C 14	52.7	$f_{cu23} = 52.8$	53.2	2395	34.6	30.8	50
C 17	56.5	$f_{cu21} = 54.8$	53.0	2420	35.8	35.9	50
C 19	49.2	$f_{cu25} = 50.1$	48.0	2394	35.3	34.6	15

* measured on prisms

Table 5.3 : Comparison between experimental and theoretical short-term results.

Col.	f_y (N/mm^2)	f_{cu} (N/mm^2)	P_{test} (kN)	P_{theory} (kN)	$\frac{P_{test}}{P_{theory}}$	e_{test} (mm)		e_{theory} (mm)	e_{test} / e_{theory}	
						Theodolites	Dial gauges		Theodolites	Dial gauges
C 1		52.2	450	439	1.03	26.3	26.3	22.5	1.17	1.17
C 2		53.2	400	445	0.90	22.3	23.8	22.5	0.99	1.06
C 3		57.3	210	172	1.22	28.3	24.3	21.8	1.30	1.11
C 4		48.7	180	154	1.17	28.3	27.3	21.8	1.30	1.25
C 5	530	56.4	360	386	0.93	35.0	32.0	31.5	1.11	1.01
C 7		51.8	250	291	0.86	29.4	37.3	31.8	0.92	1.17
C 9		52.0	205	237	0.87	39.7	40.1	33.5	1.19	1.20
C 11		47.4	102	111	0.92	35.3	35.7	29.6	1.19	1.21
C 14		52.8	85	97	0.87	37.8	37.7	29.4	1.29	1.28
C 17		54.8	65	62	1.05	29.8	30.3	27.5	1.08	1.10
C 19		50.1	45	41	1.10	37.8	37.8	27.3	1.38	1.38

e = mid-height eccentricity at the point of instability.

P = buckling load.

Table 5.4 : Statistical values for short-term tests.

Statistical parameter	$\frac{P_{test}}{P_{theory}}$	e_{test}/e_{theory}	
		Theodolites	Dial gauges
Minimum ratio	0.86	0.92	1.01
Maximum ratio	1.22	1.38	1.38
Mean	0.99	1.17	1.17
Standard deviation	0.13	0.14	0.10
Coefficient of variation	12.8%	12.0%	8.55%
Number of tests	11		

Table 5.5 : Effect of effective depth ratio.

Col.	d/h	P_{test}	e_{test} (mm)		P_{theory} (kN)		e_{theory} (mm)		P_{test}/P_{theory}		e_{test}/e_{theory}			
											d/h=0.75		d/h=0.80	
	Actual	(kN)	Theodolites	Dial gauges	d/h=0.75	d/h=0.80	d/h=0.75	d/h=0.80	d/h=0.75	d/h=0.80	Theodolites	Dial gauges	Theodolites	Dial gauges
C3	0.77	210	28.3	24.3	172	186	21.8	23.0	1.22	1.13	1.30	1.11	1.23	1.06
C4		180	28.3	27.3	154	170	21.8	23.3	1.17	1.06	1.30	1.25	1.21	1.17
C17	0.76	65	29.8	30.3	62	68	27.4	27.5	1.05	0.96	1.09	1.10	1.08	1.10

Table 5.6 : Effect of static modulus of elasticity of concrete.

Col.	P_{test}	e_{test} (mm)		$E_{c\text{-}exp}$	$E_{c\text{-}theory}$	P_{theory}	e_{theory}	$\frac{P_{test}}{P_{theory}}$	e_{test}/e_{theory}	
	(kN)	Theodolites	Dial gauges	(kN/mm^2)	(kN/mm^2)	(kN)	(mm)		Theodolites	Dial gauges
C7	250	29.4	37.3	30.0	30.0	260	34.4	0.96	0.85	1.08
					35.0	278	33.8	0.90	0.87	1.10
					40.0	293	31.3	0.85	0.94	1.19

Table 5.7 : Effect of initial imperfections.

Col.	P_{test} (kN)	$\frac{P_{test}}{P_{theory}}$ $e_0=5.68\times10^{-4}L$	$\frac{P_{test}}{P_{theory}}$ $e_0=0.0$	$\frac{e_{test}}{e_{theory}}$ $e_0=5.68\times10^{-4}L$		$\frac{e_{test}}{e_{theory}}$ $e_0=0.0$	
				Theodolites	Dial gauges	Theodolites	Dial gauges
C1	450	1.03	0.99	1.17	1.17	1.23	1.23
C2	400	0.90	0.87	0.99	1.06	1.04	1.11
C3	210	1.22	1.12	1.30	1.11	1.41	1.21
C4	180	1.17	1.07	1.30	1.25	1.39	1.34
C5	360	0.93	0.87	1.11	1.01	1.25	1.14
C7	250	0.86	0.77	0.92	1.17	1.03	1.31
C9	205	0.87	0.77	1.19	1.20	1.32	1.33
C11	102	0.92	0.79	1.19	1.21	1.42	1.44
C14	85	0.87	0.75	1.29	1.28	1.43	1.42
C17	65	1.05	0.84	1.08	1.10	1.30	1.32
C19	45	1.10	0.90	1.38	1.38	1.65	1.65
Min. ratio		0.86	0.75	0.92	1.01	1.03	1.11
Max. ratio		1.22	1.12	1.38	1.38	1.65	1.65
Mean		0.99	0.89	1.17	1.17	1.32	1.32
Standard deviation		0.13	0.13	0.14	0.10	0.18	0.15
Coefficient of variation		13.1%	14.6%	12.0%	8.55%	13.6%	11.4%
Number of tests		11					

(a) Pilot-tests

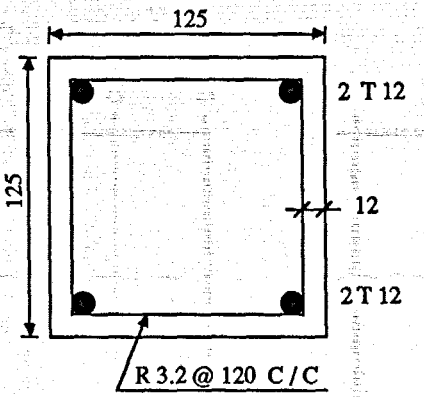

C 1 + C 2

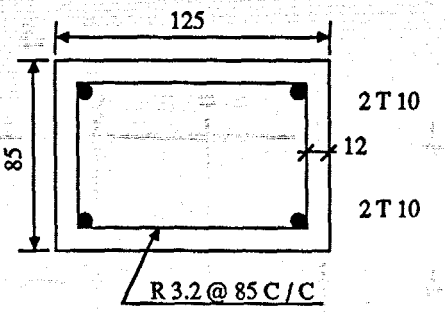

C 3 + C 4

(all dimensions in mm)

(b) Main tests

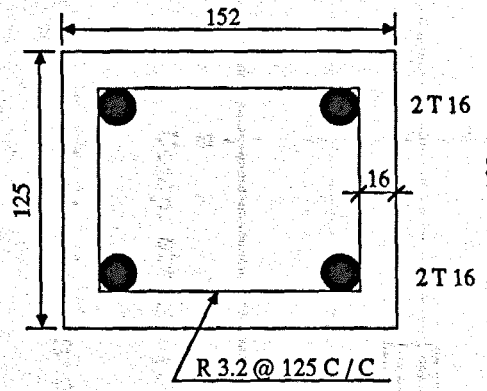

C 5 + C 6 + C 7 + C 8 + C 9 + C 10

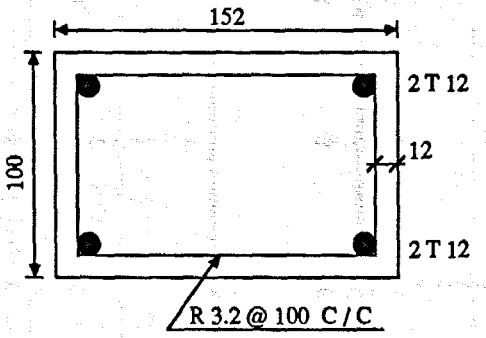

C 11 + C 12 + C 13 + C 14 + C 15 + C 16

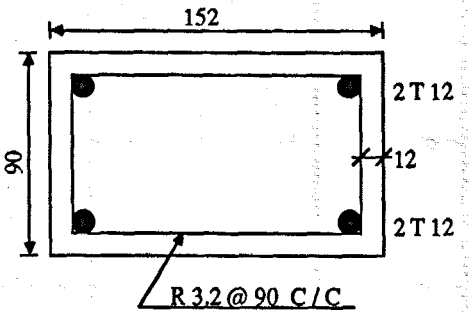

C 17 + C 18

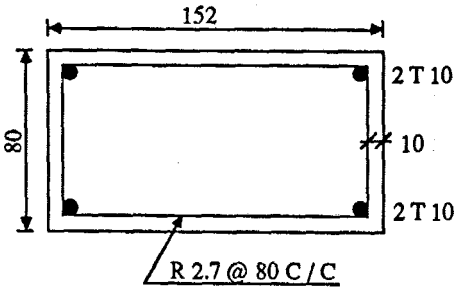

C 19 + C 20

Fig. 5.1 : Cross-section details of the columns.

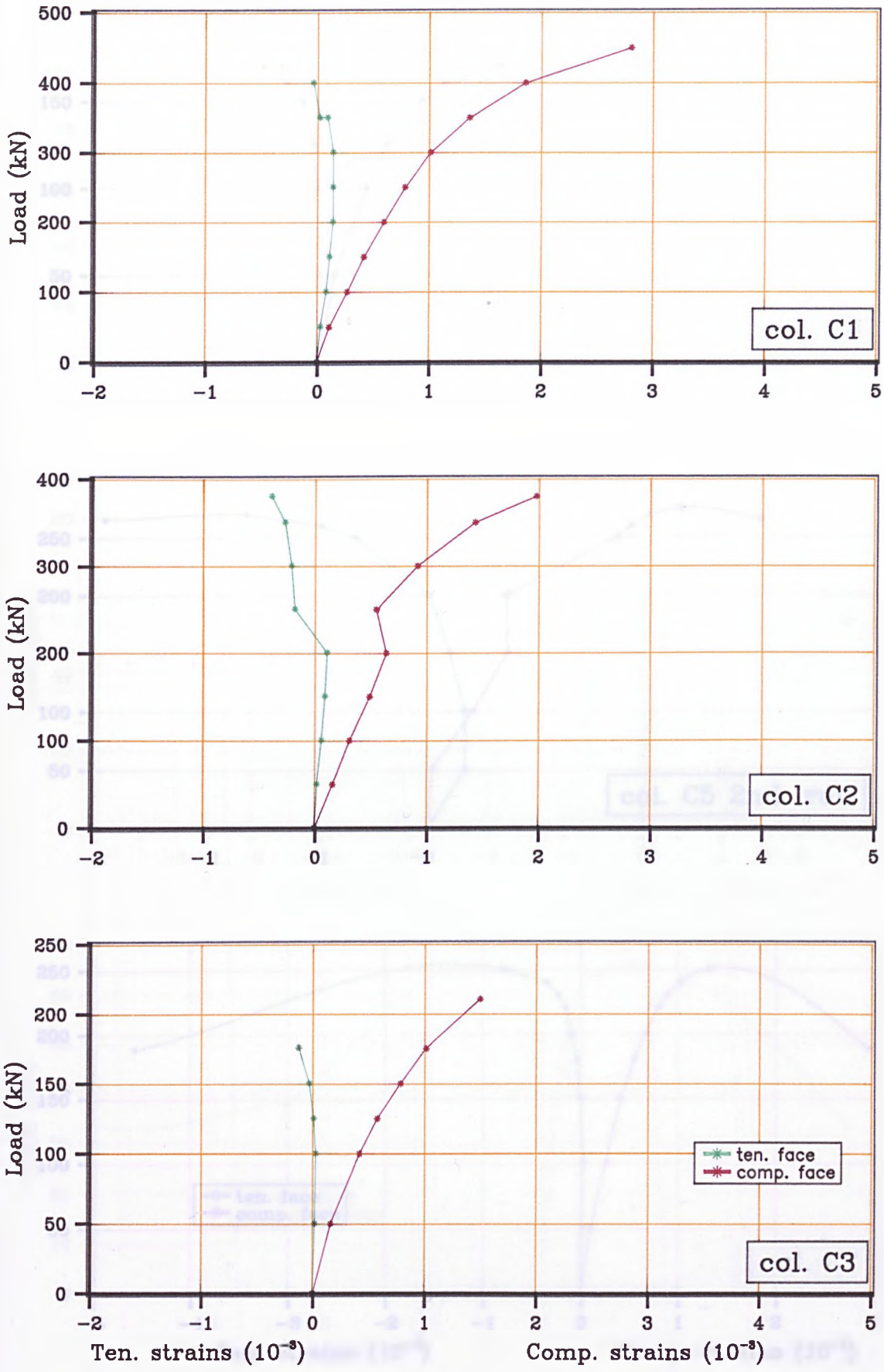

Fig.5.2(a) Curves of mid-height strains in concrete vs. Load.

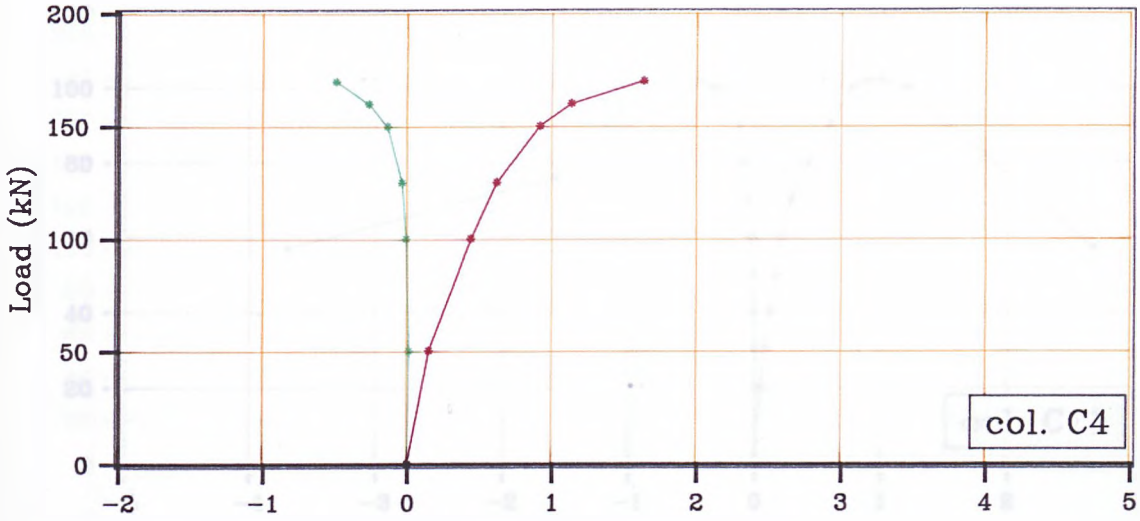

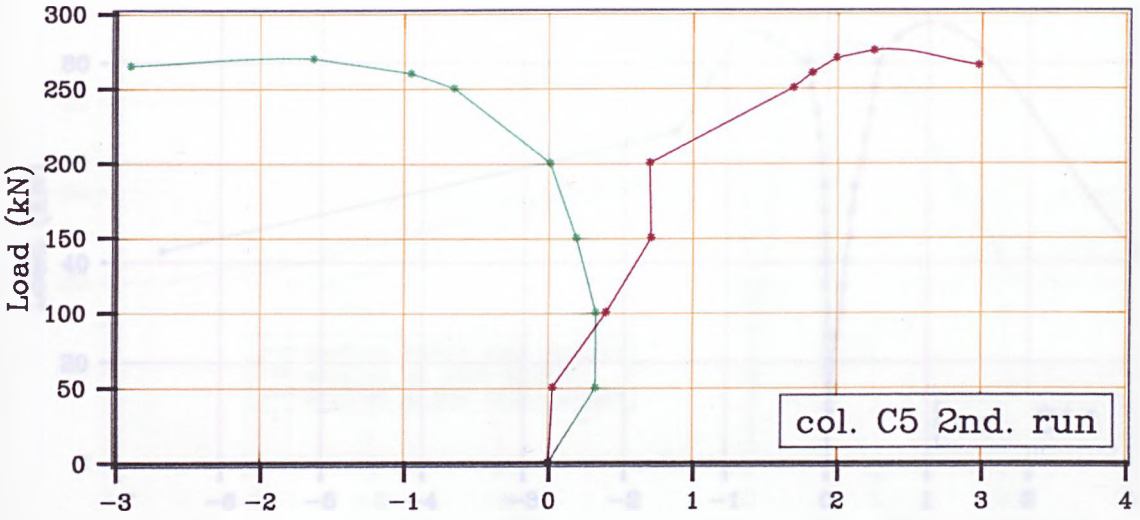

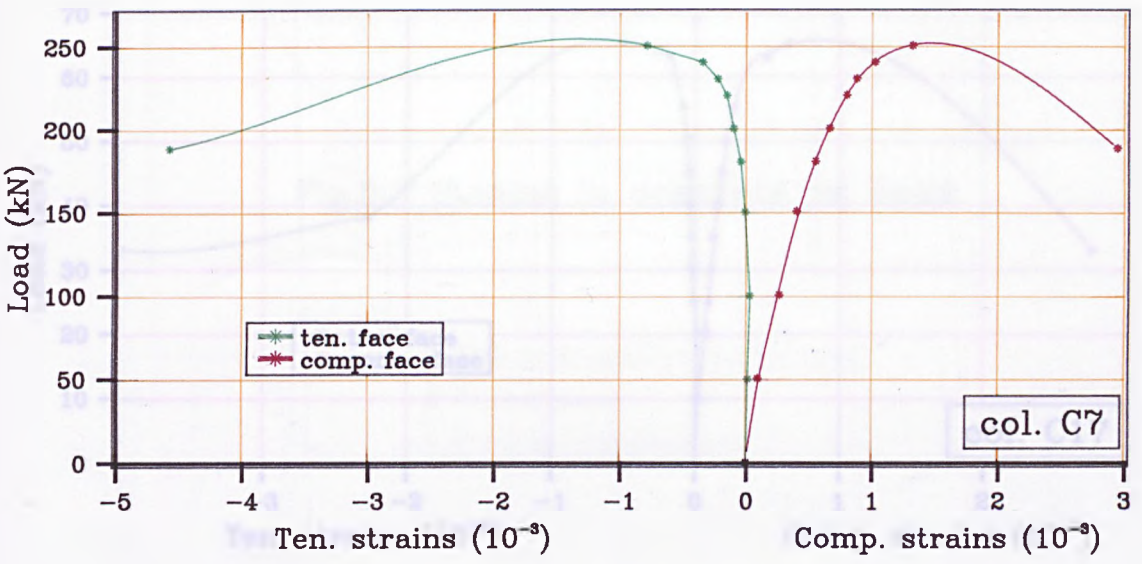

Fig.5.2(b) Curves of mid−height strains in concrete vs. Load.

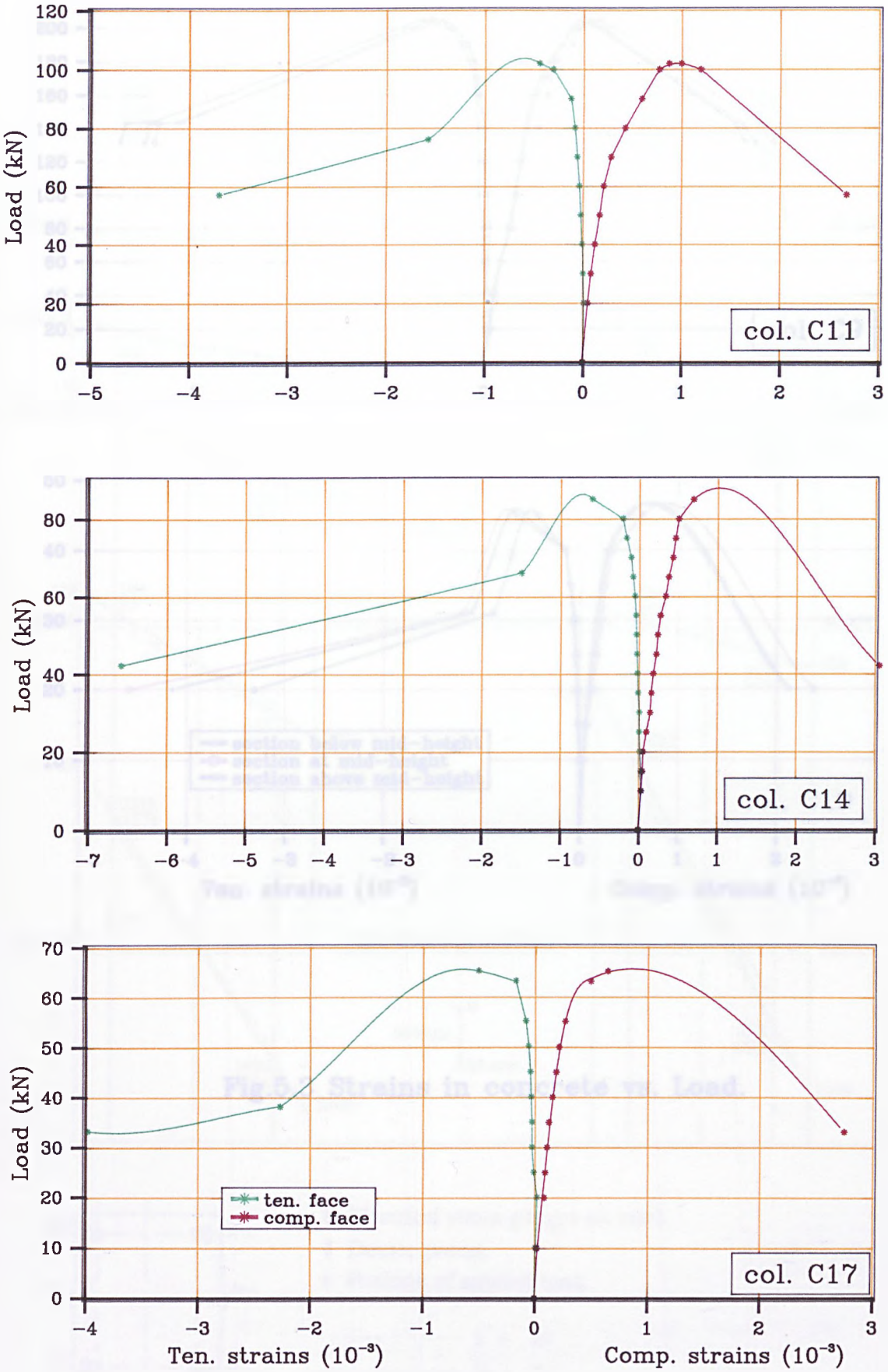

Fig.5.2(c) Curves of mid-height strains in concrete vs. Load.

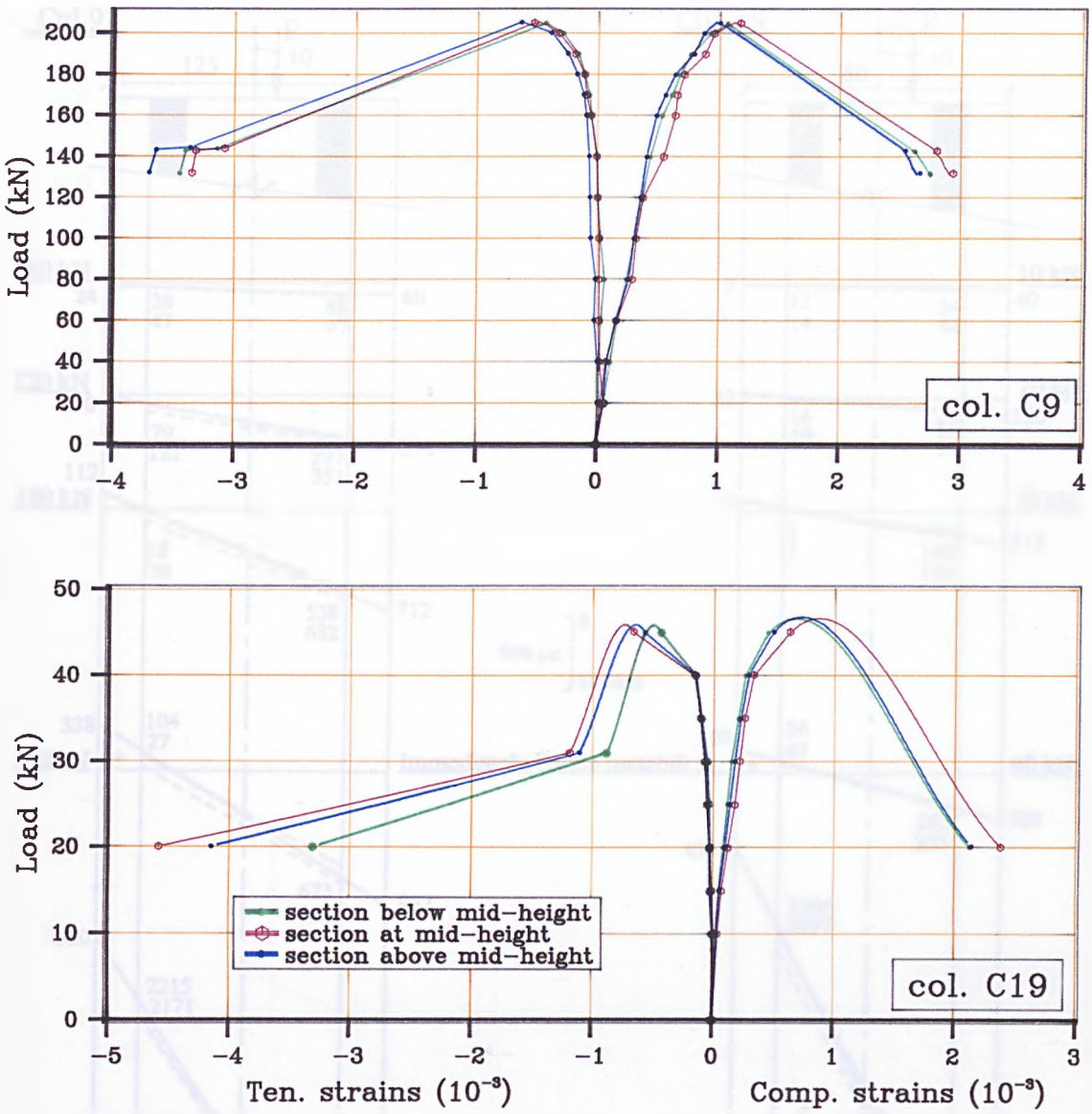

Fig.5.3 Strains in concrete vs. Load.

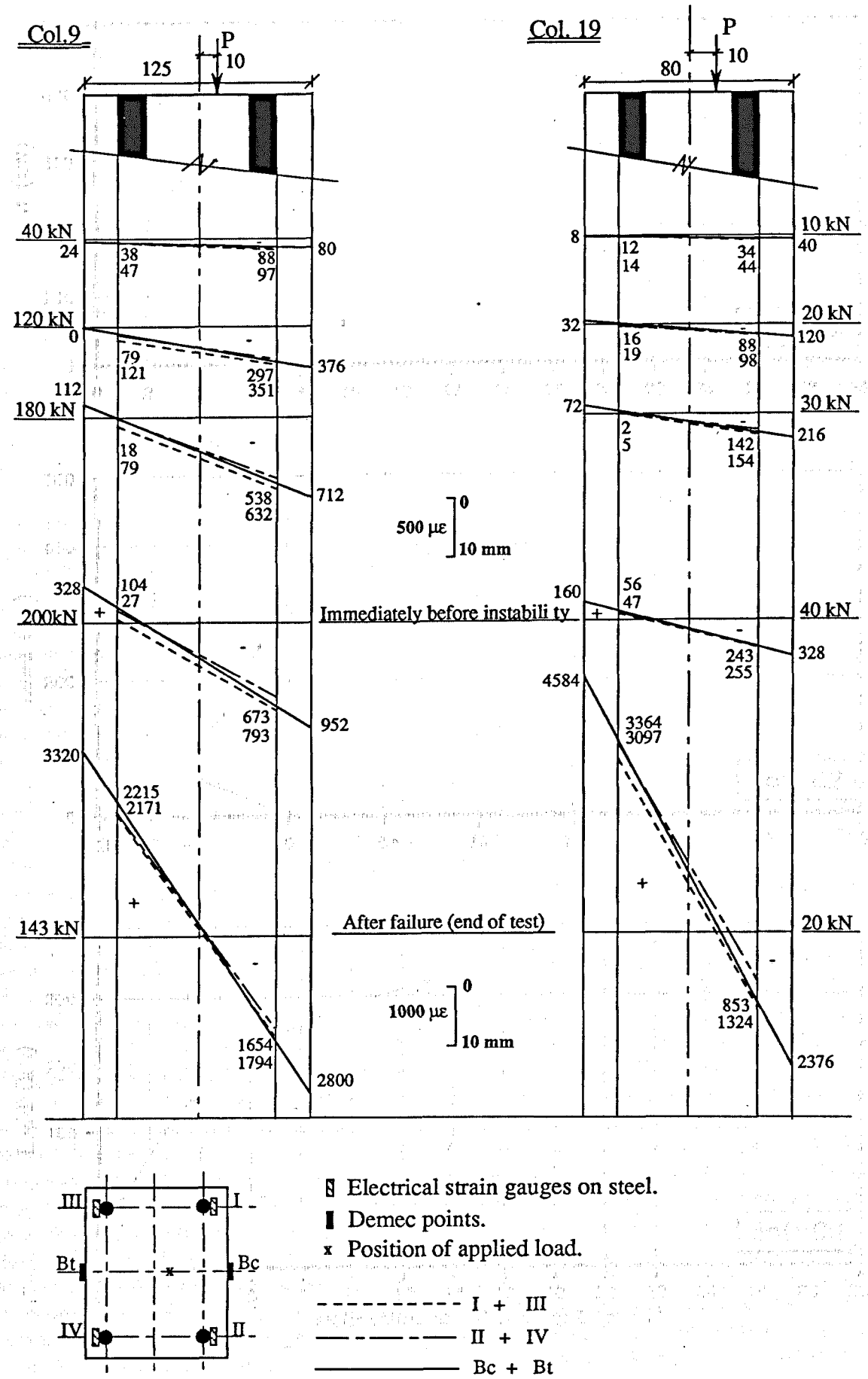

Fig. 5.4 : Typical strain variations across the section at mid-height region.

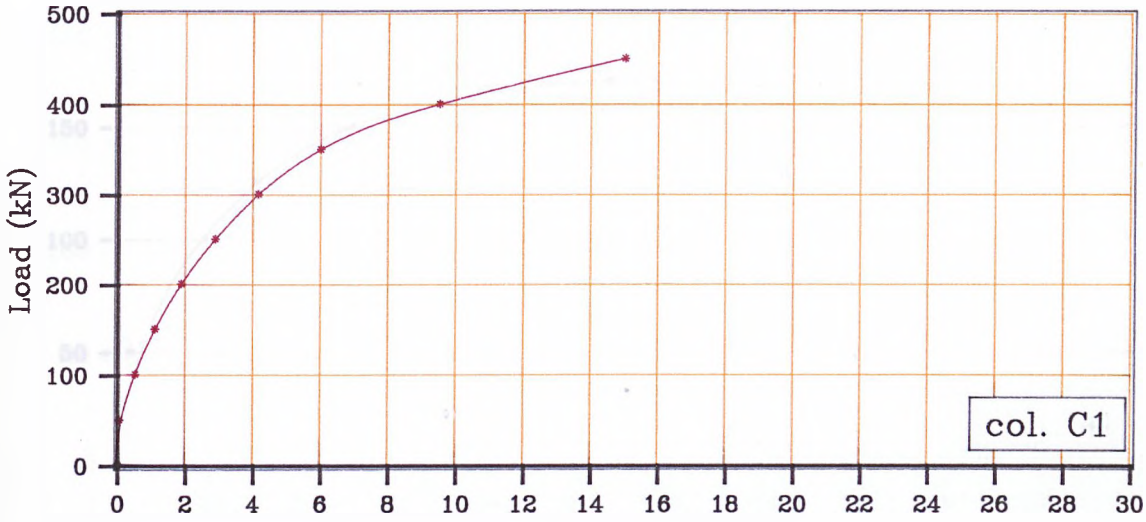

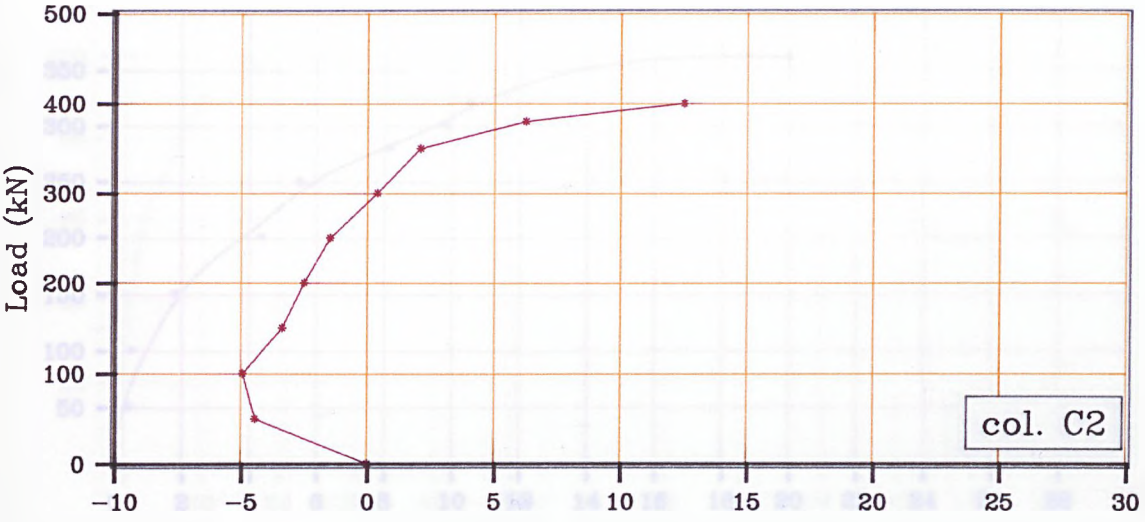

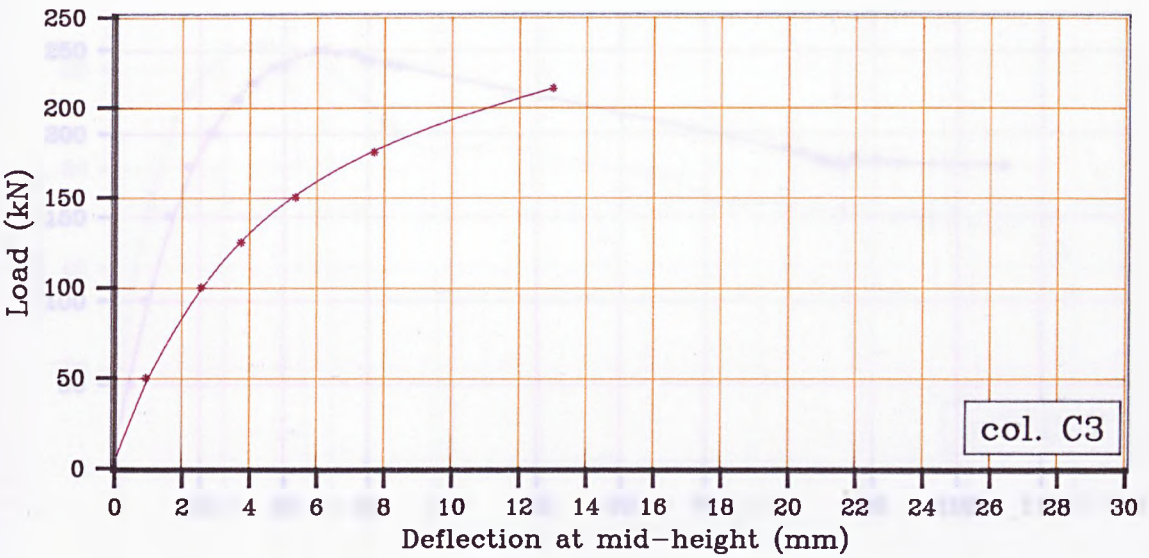

Fig.5.5(a) Load–Deflection curves (Dial gauge results).

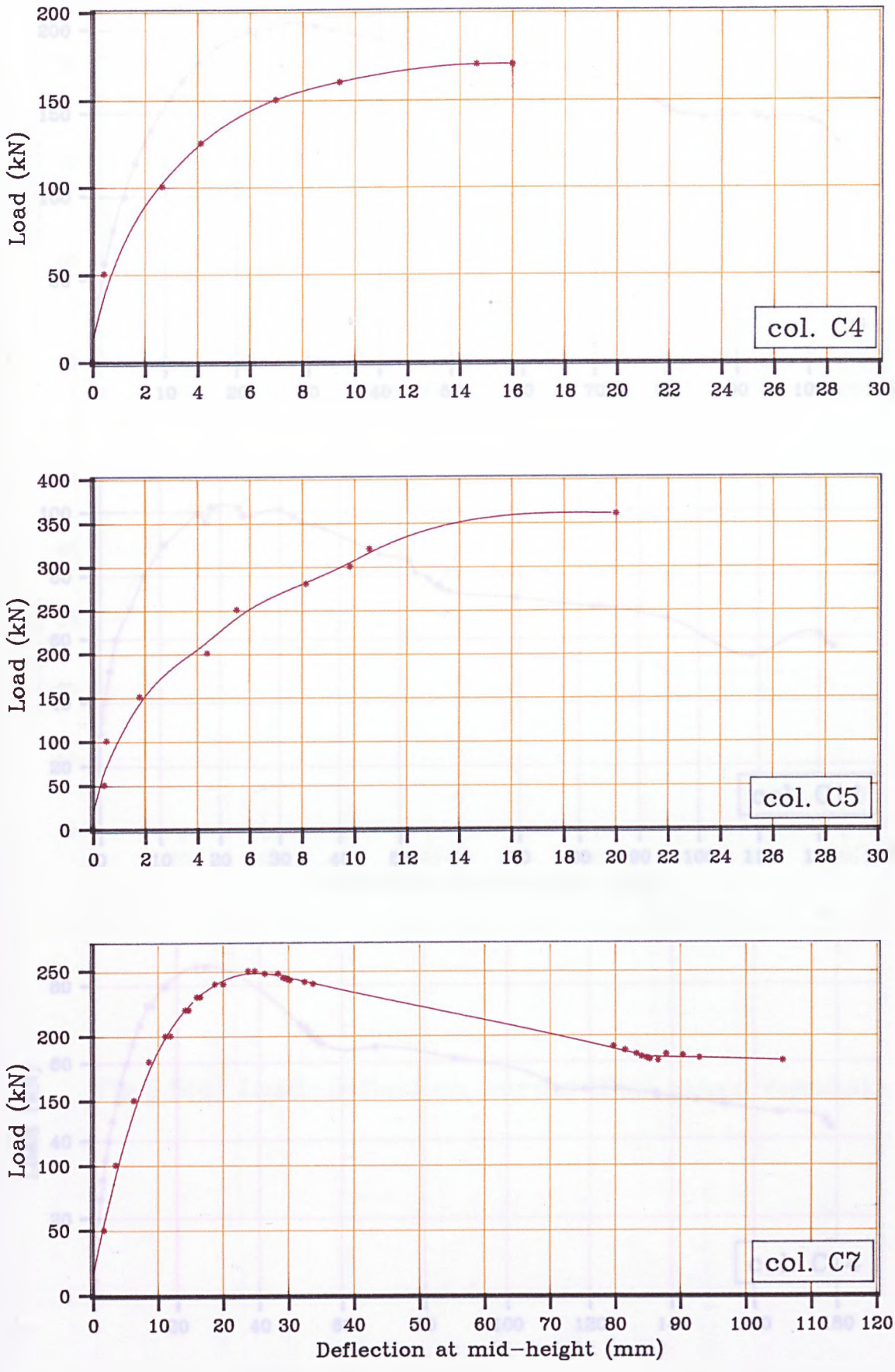

Fig.5.5(b) Load–Deflection curves (Dial gauge results).

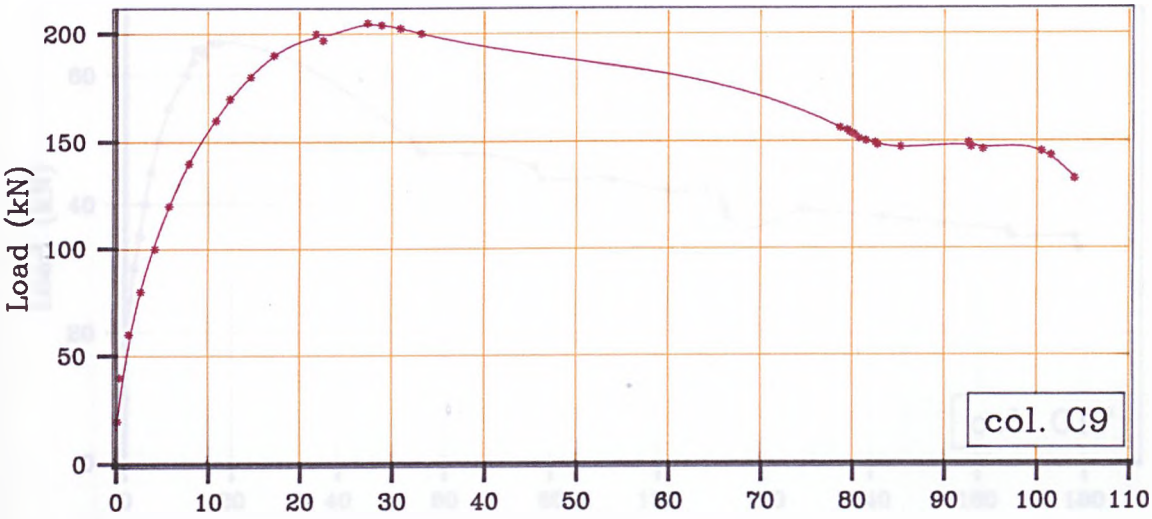

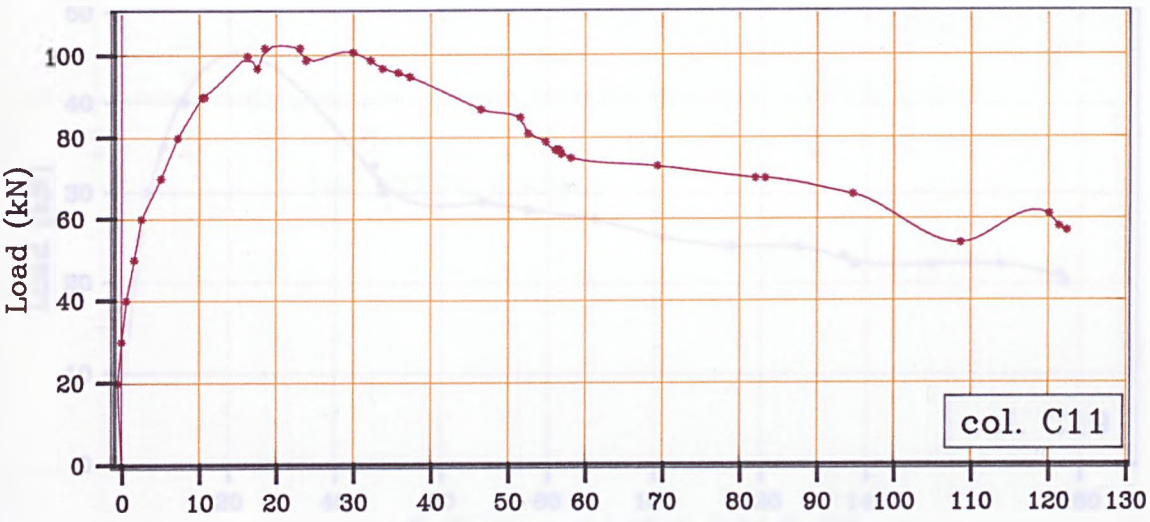

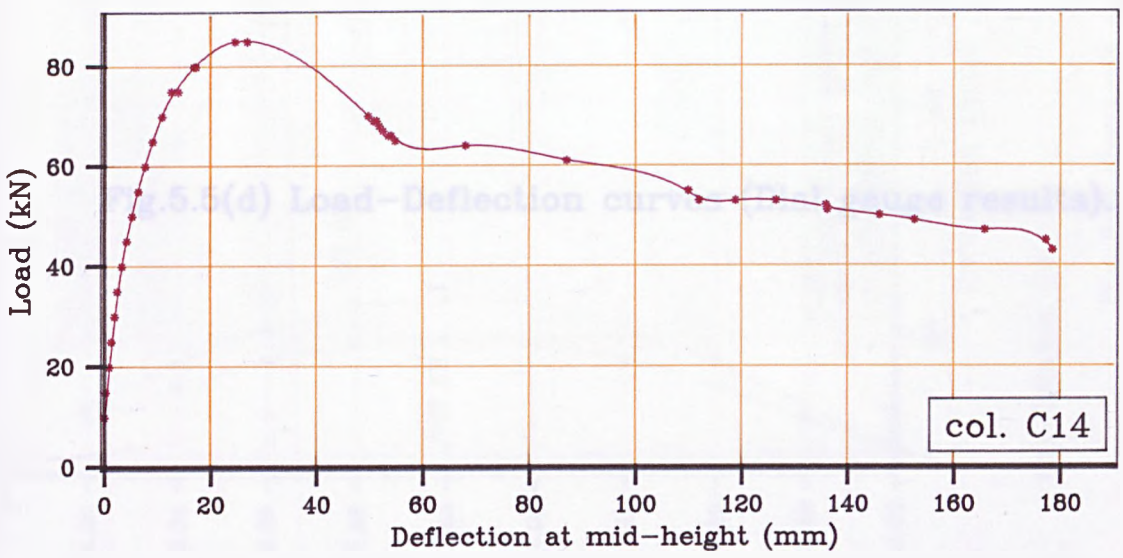

Fig.5.5(c) Load–Deflection curves (Dial gauge results).

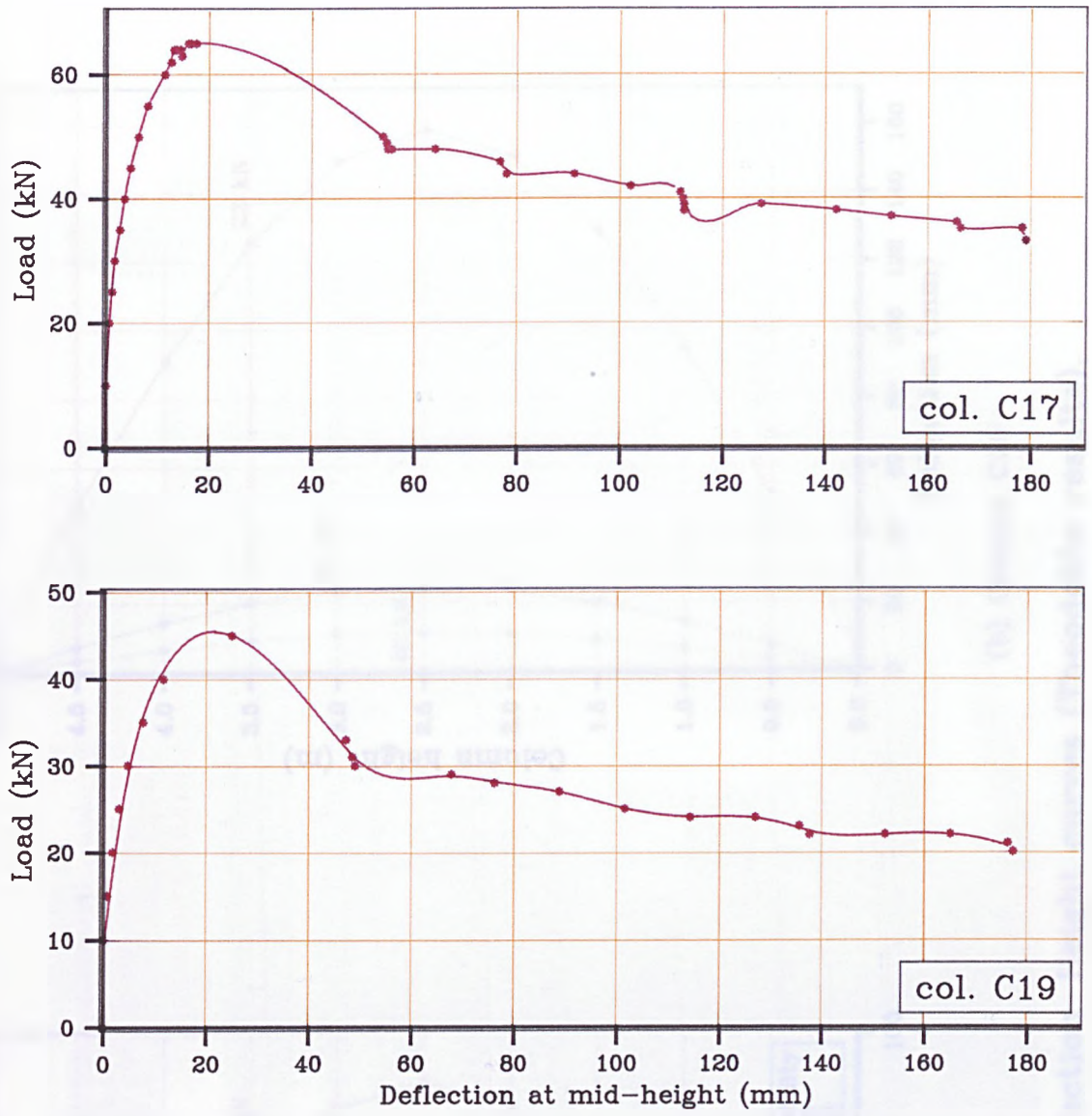

Fig.5.5(d) Load–Deflection curves (Dial gauge results).

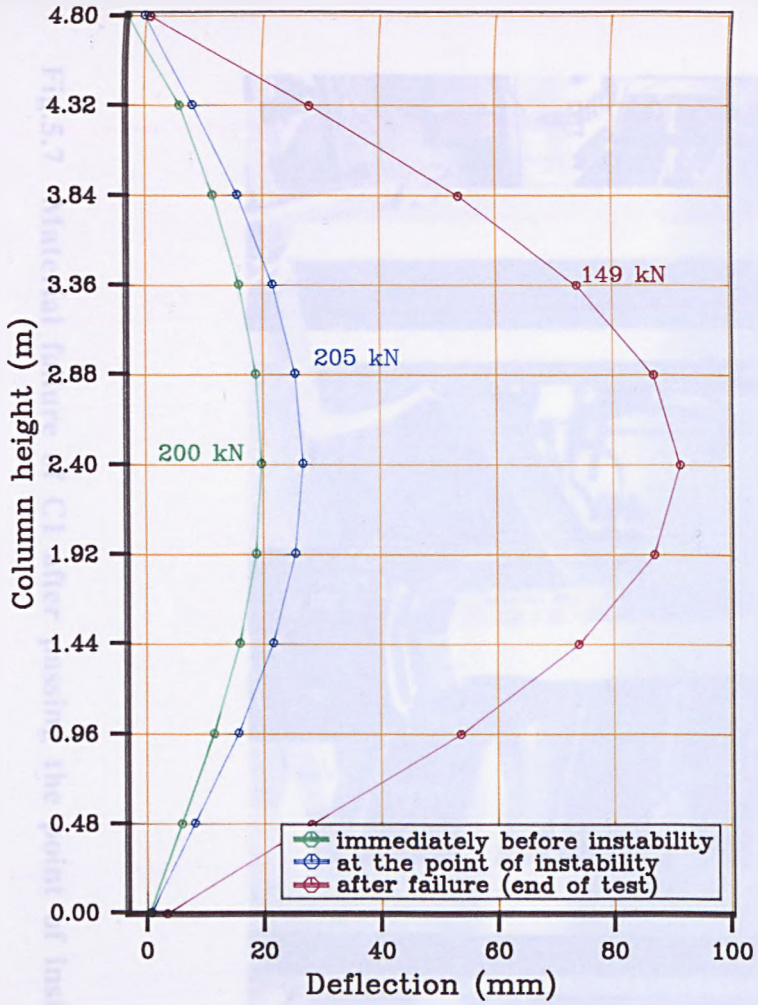

(a) Column C9

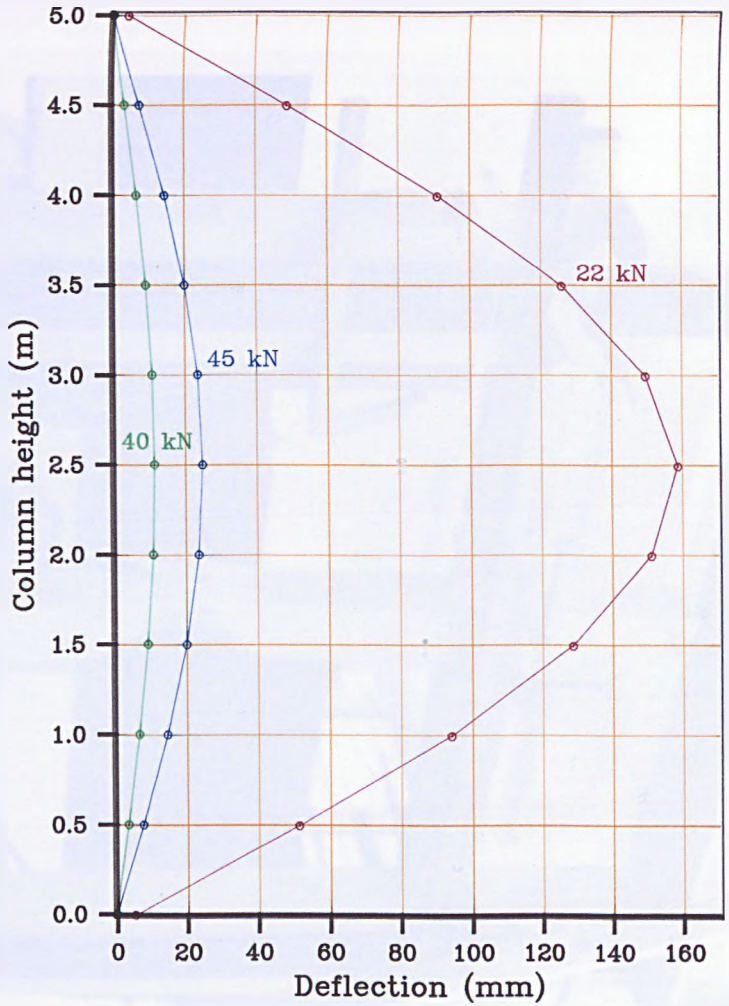

(b) Column C19

Fig.5.6 Typical deflection–Height curves (Theodolite results).

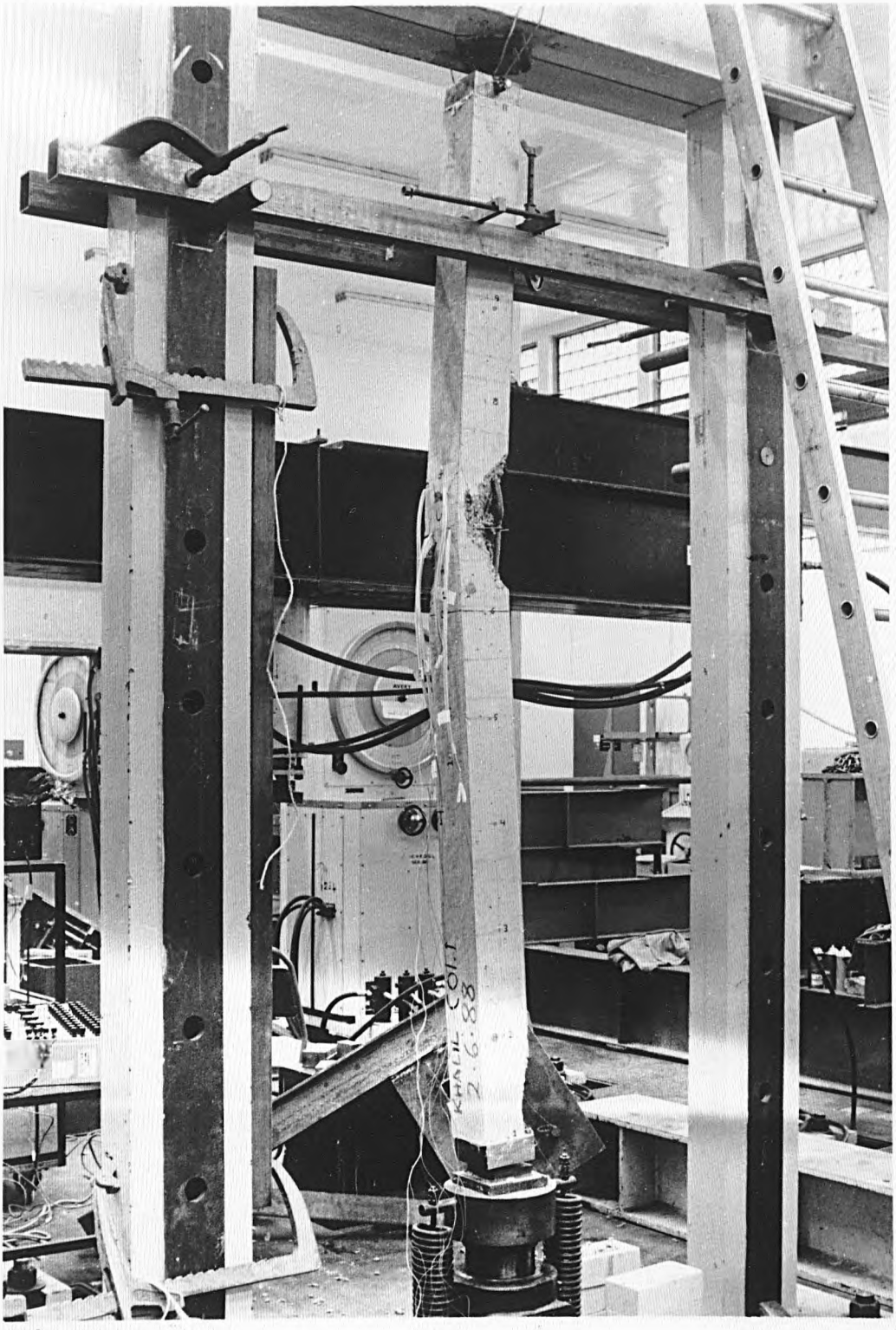

Fig.5.7 Material failure of C1 after passing the point of instability.

Fig.5.8 Close-up of the failed section of C1.

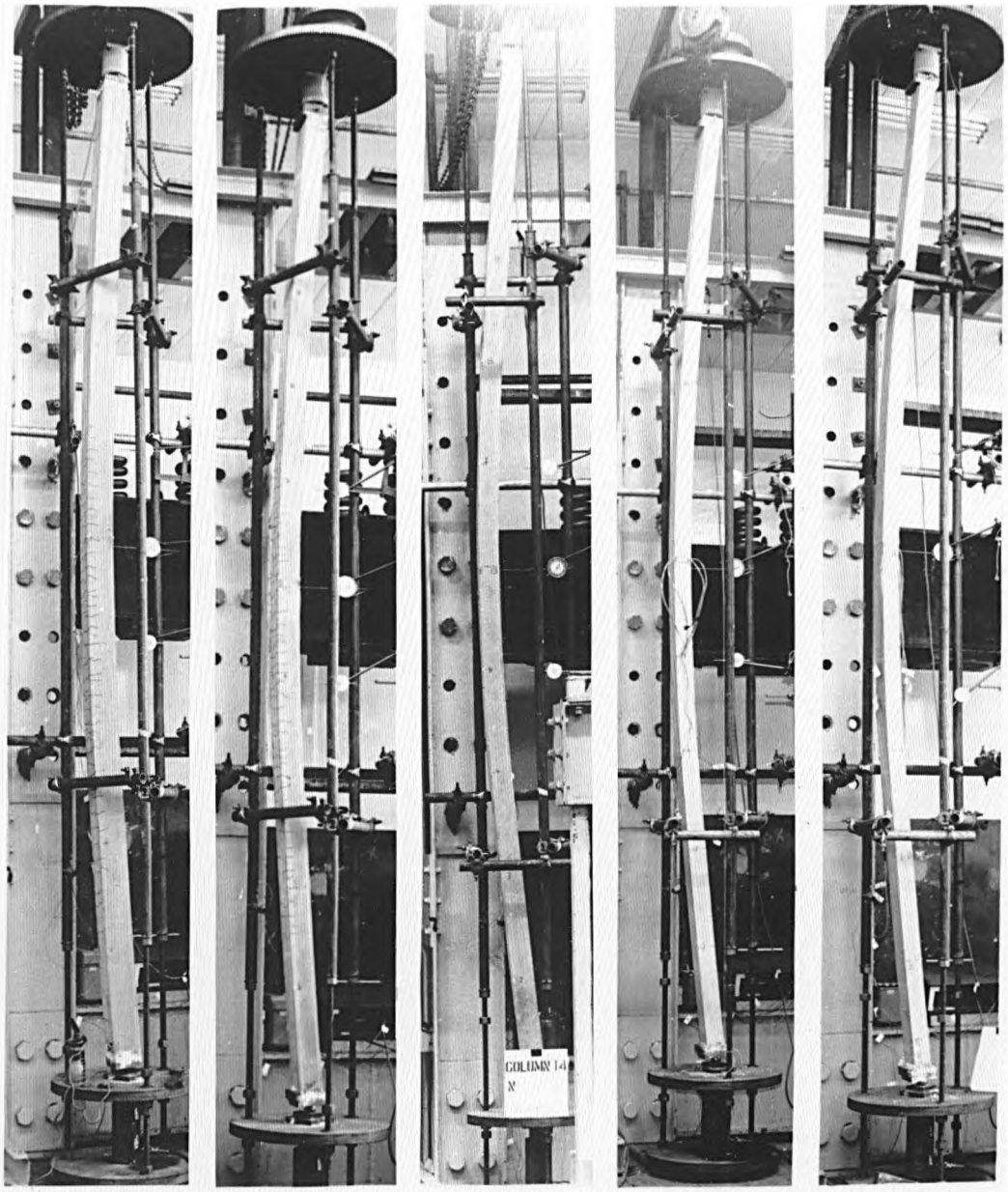

Fig.5.9 Typical bending profiles at the end of short-term tests.

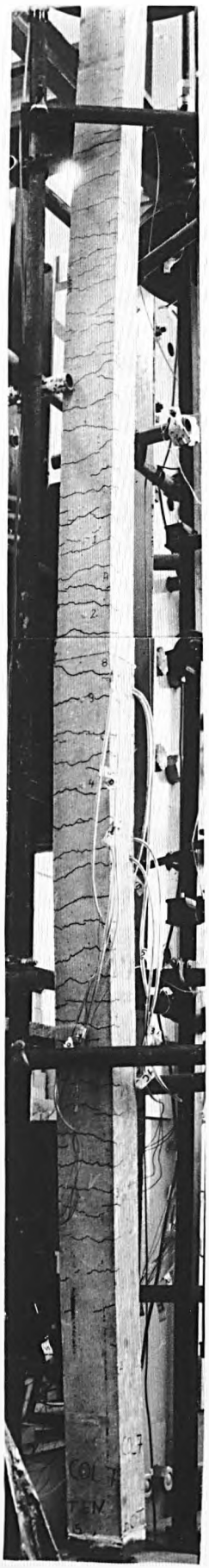

Fig.5.10 Typical crack pattern (C7).

CHAPTER SIX

LONG-TERM EXPERIMENTAL INVESTIGATION

6.1 General introduction

In practice, a proportion of the working load on a column will be sustained during the greater part of its life and the effect of this sustained load on the ultimate strength of a slender column must therefore be considered in any design approach.

Because of the time required for experimental studies of the effects of sustained load on columns, very little work of this nature has been done to date. In consequence there are few test results available to verify the applicability and use of analytical approaches.

Concrete is known to creep under load, i.e to move progressively with time causing deformations which may amount to several times the instantaneous elastic deformations. With regard to short reinforced concrete columns, where failure occurs upon the development of the full strength of the cross section (i.e ultimate strain capacities of the materials),creep does not greatly influence the failure load. However, for slender columns where instability is the normal failure criterion, creep can greatly affect the collapse load as it increases the lateral displacement and consequently reduces the carrying capacity of the column.

The objective of this Chapter is to describe the long-term tests conducted to study the behaviour of slender reinforced concrete columns under sustained load and to assess any consequent reduction in their short-term capacity. Tests on concrete cylinders were also undertaken to evaluate the amount of creep during the loading period, so that this could be accounted for in the theoretical analysis.

6.2 Introduction to creep

6.2.1 Definition

Creep of concrete is defined as the increase in strain under a sustained constant stress, after taking into account other time-dependent deformations not associated with

stress, such as shrinkage. As a matter of fact creep and shrinkage are interdependent and cannot be separated, however, it is common practice to consider them as additive.

6.2.2 Factors affecting creep

(a) Mix constituents

All the concrete mix components (aggregate content, cement content and water content) affect creep strain in some way, primarily because of their influence on the water-cement ratio and the cement-paste content.

The influence of the aggregate is to restrain the creep of the cement-paste, this effect depends upon the elastic modulus of aggregate and its volumetric proportion. Therefore, the stiffer the aggregate the lower the creep and the higher the volume of aggregate the lower the creep [95].

The type of cement affects creep mainly due to its effect on the rate of hardening of the concrete. Creep seems to be inversely proportional to the rapidity of hardening of the cement used. The effect of a decrease in water-cement ratio is to decrease creep and therefore it can be anticipated that creep varies inversely with the increase in the strength of concrete at the age of application of the load. For ages at loading greater than about 28 days the influence of the age at loading on creep is small.

(b) Reinforcement

Broadly speaking, the effect of reinforcement is to reduce total deformations. There is evidence that both creep and shrinkage are reduced by the introduction of reinforcement in the concrete section. Further research investigating the effects of different percentages of reinforcement on creep and shrinkage is necessary.

(c) Size of specimen

The general observation is that both creep and shrinkage increase with a decrease of member size. The size parameter is appropriately expressed by the volume/surface ratio of the member. *Wu and Huggins* [43] investigated the influence of size on the behaviour of slender columns under sustained loading; they concluded that the maximum sustained load/ultimate short-term capacity is reduced as the volume/surface ratio of the column is decreased and they pointed out that the effect of volume/surface ratio is not a constant factor. It varies with the age of concrete at initial loading and curing conditions.

(d) Stress

Creep is directly proportional to the applied stress up to about 40% of the short-term strength; i.e within the range of working or design stresses. Above 40 to 50% of the short-term strength, microcracking contributes to creep so that the linearity of creep-stress relationship decreases with creep increasing at an increasing rate [95].

A significant number of tests have been carried out to investigate how stress affects creep strains. *Goyal* [33] loaded concrete prisms for a period of six months under axial loads corresponding to 25%, 50% and 75% of the corresponding prism strengths. He observed a reasonably constant relation between the creep strains and the instantaneous strains at all stress levels and that creep strains are very closely proportional to the instantaneous strain up to a compressive stress of 0.75 of the ultimate stress. *Rüsch* [96] carried out creep tests on concrete cylinders and found that this approximate relationship between creep strain and elastic strain could hold up to about 80% of cylinder strength, depending upon the test duration.

In the light of the above results, it appears to be a reasonable practical approach for estimating creep strains, to accept this approximate relationship for stresses of about 50 to 60% of short-term strength. Above 70-80% of short-term strength, sustained load will eventually result in failure.

(e) Ambient conditions

Generally, for a given concrete, creep is higher the lower the relative humidity [95]. High humidity tends to reduce the rate of loss of moisture from the concrete and increases the rate of gain of strength, resulting in decrease in creep strain. The rate of creep increases with an increase in temperature up to a maximum of about 70°C, thereafter decreasing somewhat up to 100°C [94].

6.2.3 Methods of the general prediction of creep

Considerable research has been concerned with the determination of the long-term movement of concrete specimens under direct stress and has resulted in numerous theories on the prediction of these deformations.

The principal recognised methods are the following:

a- Comité Européen du Béton (CEB-FIP), 1970 [97].

b- Comité Européen du Béton (CEB-FIP), 1978 [98].

c- American Concrete Institute (ACI), 1978 [99].

d- *Bazant* and *Panula's* model II, 1978 [100].

e- Concrete Society (CS), 1978 [101] adapted by BS8110: 1985.

Details of the above methods are not given here; however, for details of application of these methods, the reader can refer to the references given for each method. Alternatively, adequate coverage is given by *Neville et al* [102].

6.2.4 Methods of creep analysis of structural members

Most of the creep tests have been performed under conditions of constant stress; however, in many practical cases stresses can vary with time. Methods for computing creep under such circumstances are available, such as:

a- Effective modulus method.

b- Rate of creep method.

c- Rate of flow method.

d- Method of superposition.

Each method is based on certain assumptions which make it capable of predicting creep reasonably well in situations where other methods fail to give good results. Full description of these methods and their application can be found in reference [102].

The effective modulus method has been adopted for the theoretical analysis. In this method, the modulus of elasticity of concrete is reduced to account for creep effects, by a factor $(1+\phi)$, where ϕ is known as the creep coefficient, thus:

$$E_e = \frac{E_c}{1 + \phi} \qquad (6.1)$$

The reduced or effective modulus E_e is then used in the analysis. The method gives reliable results in situations where stress does not vary greatly with time and where aging of the concrete is negligible because it is based on the assumption that the creep strain at any given time t, depends upon the stress acting at that time, ignoring the history of stress.

However, as discussed in section 6.2.2, the characteristics of creep depend upon many factors, some of which are themselves variable: the properties of concrete within the member itself, the ambient conditions, magnitude and nature of stress..etc. Even in

more controlled environments in laboratories, two identical concrete specimens subject to the same loading conditions will possess different rates of creep. Taking account of these practical limits, leads to a conclusion that an accurate assessment of creep is eventually unnecessary if it is not impossible. Thus the assumptions of the effective modulus method are considered acceptable.

6.3 Experimental programme

6.3.1 Test columns

Details of the nine columns which have been designed for long-term tests are given in Fig.5.1, namely: C6, C8, C10, C12, C13, C15, C16, C18 and C20. A full description of these columns is provided in Table 6.1.

To verify the overall behaviour of slender columns under sustained load, columns C13 and C16 were designed as identical to columns C12 and C15 respectively. However, due to constraints on time and because all the columns tested followed a similar pattern, column C16 was omitted.

The main aim of these experiments is to establish the reduction in the column-carrying capacity due to creep and other long-term effects. These columns were identical to the columns used for short-term tests. This implies that the major variable studied was again the slenderness ratio. The sustained load was taken as 60% of the ultimate short-term capacity for all columns. This level of sustained loading was considered to be a reasonable estimate of the long-term failure load for slender columns. All long-term tests commenced at an age of 28 days to simulate the conditions in practice where columns are normally loaded at this age. The load was to be maintained for 90 days; if at the end of the loading period the column does not fail, then it will be subjected to an increasing load, under short-term loading conditions until failure occurs.

As discussed in Chapter 4, two rigs were designed and one of them was modified for the long-term tests by adding three springs at the top. The other was meanwhile utilized to complete the short-term programme without the use of the springs. After the completion of the short-term programme both rigs were used for long-term tests. The test frame layout is shown in Fig.4.4 and the monitoring sections on the column are shown in Fig.4.6. Load was applied using a hand-operated hydraulic jack and sustained by the means of springs and Macalloy bars.

6.3.2 Concrete control specimens

Concrete control specimens were cast with each column to determine concrete properties, in the same manner described in section 5.2.2 for short-term tests. In addition, three extra cubes were cast and stored beside the corresponding column and were tested at the end of the loading period for their compressive strength. The prism used to measure the static modulus of elasticity at the age of 28 days and at the time of loading, was stored alongside the column and used to determine E_c at the end of loading.

The results of the above tests are given in Table 6.2.

6.3.3 Creep study

Six 76×267 mm cylinders were cast with each long-term test, three were used to determine the compressive strength at an age of 28 days, two were loaded in the creep frame for creep strain measurements and one cylinder remained unloaded for shrinkage strain measurements.

At the end of the loading period, creep cylinders were unloaded and tested with the shrinkage cylinder for their compressive strength. The results of compressive strength tests are given in Table 6.2.

6.4 Test procedure

6.4.1 Preparation and checks

Columns were prepared and checked in the same manner described in section 5.3.1.

6.4.2 Loading and test duration

After the column was mounted in its rig and prepared for loading, two cycles of load were applied from zero up to 10% of the expected failure load. The sustained load was applied in preselected increments similar to those used for the identical column in the short-term test. As the load is applied the springs go into compression and the Macalloy bars act in tension. On reaching the required load the nuts underneath the bottom plate were tightened using a spanner and the hydraulic jack was released.

At each load increment, deflections and strains in concrete and steel were recorded and readings of the load cells were taken. A full set of measurements was also taken

immediately after releasing the jack. The average number of increments per test was six and the overall loading time was less than two hours. After loading the column the concrete control specimens were tested and the creep frame was loaded.

Load was maintained within ±5%, any drop in load below the acceptable limit was compensated for by re-applying the jack and jacking up the column to the desired level. A complete set of readings was taken before and after every adjustment of the load. The load was checked, readings were taken and the column was visually inspected at the following intervals: after 4 hours of loading, 10 hours, every day within the first week of loading, then every two days within the second week of loading, then weekly till the end of loading period. In addition, the effect of using the second rig during the duration of the test, was also monitored by taking a full set of readings before and after using the second rig. This was found to have a small but noticeable effect only on the dial gauge readings.

6.4.3 Loading creep specimens

At an age of 14 days, the rough face of the creep specimens was wet ground in order to provide a bearing surface smooth and perpendicular to the axis. Thereafter the specimens were returned to their storage position beside the column. Before loading, all the plates of the creep frame were carefully cleaned and covered with a thin film of grease to reduce friction.

On the same day of loading the column, the creep specimens were loaded to the required level after recording the zero readings. Immediately after loading strain readings were taken to obtain the instantaneous elastic strains. An unloaded specimen was placed next to the creep frame to determine shrinkage strains. All three specimens were located close to the column to guarantee the same environmental conditions.

It was intended to keep the same loading level on both the column and its creep specimens (60% of ultimate short-term capacity). Unfortunately, the creep frames available in the laboratory were only capable of applying a maximum compressive force of 100 kN; 60% of the cylinder compressive strength for the particular concrete mix used throughout this investigation was on average 110 kN. Hence, the creep frame was used up to its maximum capacity giving an average load level of 0.54 of the cylinder compressive strength.

This load was maintained within ±5% during the loading period, creep and shrinkage strain readings were taken before and after every adjustment and at the same intervals as the readings for the corresponding column.

6.4.4 Termination of long-term tests

All tests were terminated at the end of ninety days. None of the eight long-term test columns failed during this loading period. The load was then increased under short-term loading conditions until failure occurred. The average number of increments per test was six and total testing time one hour and a half. An exception was column C20 which failed after two increments of load only.

At the end of 90 days the creep specimens were also unloaded and the immediate creep strain recovery was recorded; readings of the shrinkage strain were taken and then the three cylinders were tested for their compressive strength.

6.5 Experimental results

Comparison between experimental and theoretical buckling loads are provided in Table 6.3. The table also gives a comparison between the experimental and theoretical mid-height eccentricity at the point of instability.

To present the experimental measurements on the columns, two sets of data corresponding to columns C10 and C20 have been chosen to illustrate the trend (Figs.6.1 to 6.7). Column C10 has been chosen as a typical long-term test, while column C20 was shown as the only exception to the general behaviour.

Fig.6.1 shows the curves of mid-height strains in concrete against load. Fig.6.2 shows the development of compressive strains in concrete in the mid-height region with time elapsed since application of sustained load. Strain variations across the mid-height section during the loading period and at the end of the short-term test (after sustained load) are shown in Fig.6.3. Curves of mid-height deflection vs. load using dial gauge readings are illustrated in Fig.6.4. These readings were also plotted against time in Fig.6.5. Profiles of the column at three different stages of the test, are given in Fig.6.6 as obtained by the theodolites.

Results from the creep study are given in Table 6.6. The creep strain is obtained by subtracting shrinkage and elastic instantaneous strains from the total measured strain. The development of creep strain with time is shown in Fig.6.7.

6.6 Observations and discussion

The long-term columns were loaded similarly to the short-term tests, in respect of achieving single curvature. The sustained load was also applied at a constant eccentricity of 10 mm and the initial imperfections were added to the applied eccentricity.

All columns remained stable under the sustained load during the 90 days, except column C20 which showed a tendency to buckle towards the end of the loading period due to its high slenderness ratio of 62.5, its lower percentage of reinforcement of 2.58% and a higher e_i/h ratio as compared with other columns.

As explained in 6.4.4, the load was increased at the end of the 90 days under short-term loading conditions until the column failed. Instability was shown as the type of failure followed by considerable bending until material failure occurred (column C6 and C8) or the column approached the rig at a typical value of mid-height deflection of about 150 mm (all remaining columns). Fig.6.8 shows column C6 after failure. Typical bending profiles beyond instability for columns C10 and C20 are shown in Figs.6.9 and 6.10. While loading column C6 one of the springs failed in compression at the level of 80% of the required sustained load (see 4.5.2) and the test was discontinued. After a week the spring was replaced and column C6 was reloaded. The sustained load level was reduced to 56% of the corresponding short-term capacity to allow for the possible effects of the first run.

A few cracks were discovered on the tension faces of all columns using a magnifying glass, typically after 30-40 days under load, except column C20 where cracks appeared after only 14 days. *Dracos* [5] stated that in his tests no visible cracks were seen before failure; however, he did not inspect for microcracks. At the end of each test, cracks were marked and a typical pattern is shown for column C13 in Fig.6.11. Cracks also appeared on the compression face after removing the load for the reason explained in chapter 5 (see 5.5).

Strains in concrete were again recorded at three sections on both the tension and compression faces. The results of the two symmetrical sections on each face again confirmed the symmetrical behaviour of the column about the mid-height.

It can be seen from Fig.6.1 that the tensile strains were very low and close to zero when the column was initially loaded. During the loading period, these tensile strains increased after every adjustment of load, then with time they decreased because of loss of load and redistribution of strain across the section due to creep. The overall rate of increase at the end of the 90 days was different from that of compressive strains. The development of cracks resulted in further transfer of stresses from concrete to steel and may have contributed to this behaviour. Investigation failed to locate such observations in previous work or even any continuity of measurements of tensile strains with time. *Goyal* [33] measured the tensile strains at the beginning and at the end of the loading period; it seems that the tensile strains in many cases of *Goyal's* work, increased by about the same factor as the compressive strains.

Column C20, as can be seen in Fig.6.1(b), showed a greater increase in tensile strains during the 90 days. In fact the lateral deflection of this column during the initial loading was accidentally increased 3 mm by a technician in the process of tightening the nuts underneath the bottom plate at load stage 25 kN. This of course increased the moment acting on the column and may account, with other reasons, for the exceptional behaviour of this column. It was also noticed that on the first day of loading this column, the temperature in the laboratory had increased by 5°C; this of course increased the creep in the column at this early stage of loading.

Typical values of compressive strain at the point of instability were 0.002 for columns C6 to C12 and 0.001 for columns C13 to C20. This emphasises the fact that instability occurs at low strains. *Pancholi* [29] reported maximum buckling strains of the order 150 microstrain in his limited series of long-term tests, which appears to be very low.

The steps in the curves of Fig.6.2 are caused by the adjustment of load. It can be seen from Fig.6.2(b) that compressive strains in column C20 have increased by a factor of 7 compared with a typical value of 3.2 for all other columns.

Linear strain variations were observed during the initial loading and afterwards (Fig.6.3). The depth of the neutral axis decreased due mainly to the continuous transfer of stress from concrete to steel as long as the steel has not reached its yield point.

The effect of creep on deflection readings at loads near to instability can be clearly seen in Fig.6.4(a). The mid-height deflection of column C20 at the end of the 90 days reached a magnitude of 7 times the value on initial loading compared with a factor of 4 for all other columns. The high slenderness ratio of this column (62.5) and its low area of reinforcement made it particularly sensitive in terms of deflection as clearly reflected in the dial gauge readings; any touch to the column or the loading frame would increase the deflection, adding to that the increase due to load adjustments.

Profiles of the column at three load stages are shown in Fig.6.6. The first stage was immediately after reaching the required level of sustained load, the second stage was chosen at the end of the 90 days before the short-term test and the third stage was at the end of the test. The results obtained confirmed that the column follows a sine curve as it buckles.

There was good agreement between the theodolite and dial gauge readings, enhanced by the back-up readings taken via plumb line at the three stages defined above.

Lateral deformations perpendicular to the direction of bending occurred in a few tests, usually negligible up to the point of instability but reaching appreciable values at

deflections considerably beyond the buckling load for columns C8 and C10. This confirmed, as observed in the short-term tests, that the assumption of single curvature bending is valid in the theory and was achieved experimentally.

The experimental buckling load taken as the maximum recorded value during the test, and the corresponding mid-height eccentricity are given in Table 6.3. To obtain the values of e_{test}, the initial imperfection e_0 and initial eccentricity e_i were added to the theodolite and dial gauge readings. To calculate the theoretical results given in the same table, load eccentricity-curvature graphs given in Figs.3.14 to 3.22 were used. In producing these graphs, the creep coefficient was taken as 2.0 and the values of f_{cu} were chosen to cover the range of test values relevant to the time of failing the column at the end of the loading period. The values assumed for the effective depth ratio d/h were 0.75 for column C18 and 0.8 for the rest of the columns. Buckling deflection-curvature relationship as given in Fig.3.24 was used.

The values of the statistical parameters for the ratios P_{test}/P_{theory} and e_{test}/e_{theory} are given in Table 6.4. Generally the theory appears to be conservative in predicting the long-term failure load. The mean value of P_{test}/P_{theory} is 1.26. Good correlation was achieved in predicting mid-height deflection at the point of instability; the mean value of e_{test}/e_{theory} was 1.13 when using theodolite results and 1.15 for dial gauge results. The theory slightly underestimates deflections as previously observed for the short-term tests. The variation between theodolite and dial gauge readings, especially in the case of column C10, are again due to the difference in time, which is a crucial factor near instability, when these readings were taken. Also they are due to difference in load; although the column was usually allowed to stabilize under each increment before taking readings, when instability approaches it becomes difficult to maintain a constant load on the column and it continues to drop slowly during taking readings (see Fig.6.4(a)).

The long-term buckling load is compared with the short-term capacity in Table 6.5. The change in concrete strength due to age in a period of 7 months was shown by *Goyal* [33] to be insignificant. He arrived at this conclusion after testing 26 columns in pairs under short-term loading conditions, one was tested after 28 days and the second approximately 7 months after casting. In the present investigation, all short-term tests have been carried out on columns at ages ranging between 21-33 days while the age of columns at the conclusion of long-term tests ranged between 115-125 days, i.e the increase in concrete strength due to age during the loading period (90 days) could be ignored. This is also substantiated by the results of the compressive strength tests carried out on the concrete control specimens, cubes and cylinders (refer to Table 6.2); where the increase in concrete strength during the loading period was only up to 6%-8% on average.

The reduction in the column load capacity depends upon many factors: level of sustained load, percentage of reinforcement and load eccentricity/depth ratio. The level of sustained load was constant at 60% of short-term capacity throughout the investigation, however, for practical reasons it was difficult to keep the percentage of reinforcement and load eccentricity/depth ratio constant particularly as the column depth became smaller. For these reasons it was difficult to draw definite conclusions from Table 6.5. There is no apparent relationship between the reduction in column capacity and slenderness ratio because other factors are not identical.

The maximum reduction of 40% was recorded for column C20, while the minimum value of 10% was recorded for columns C8 and C13. Column C8 exhibited lower creep, while column C13, the identical column to C12, failed at a higher load at the end of the loading period, thus recording a lower reduction in carrying capacity as compared with column C12, which exhibited more strain and deflection during the sustained loading period. The theory predicted greater reductions for columns C12 to C20, therefore the ratios P_{test}/P_{theory} for these columns were higher.

Goyal [33] studied the behaviour of 20 columns of slenderness ratios 16, 24 and 36 under two magnitudes of sustained load: 40 and 60 percent of the ultimate short-term capacity, for a period of six months. According to the results obtained, he pointed out that if the sustained load is not more than about 40% of the short-term carrying capacity, the reduction in the load capacity is very small and becomes even smaller if the percentage of reinforcement is increased. He found that columns loaded up to 60% of the ultimate short-term loading capacity with end eccentricities of 0.167h, had a large reduction in ultimate capacity (up to 25%) after a period of six months under sustained load.

The creep coefficients given in Table 6.6 were obtained by relating creep strain to the instantaneous strain of loading, creep strain being the value of total strain minus shrinkage and elastic strains. Shrinkage strains were recorded on separate unloaded companion specimen. Negligible increases in shrinkage strains beyond the age of 28 days were reported by *Goyal* [33]. *Dracos* [5] stated also that the rate of shrinkage beyond the age of 28 days is very small. In this work shrinkage strain measurements commenced on the first day of loading. The shrinkage strain at the end of the loading period reached maximum values ranging approximately between 200-300 microstrain.

The lowest value of creep coefficient was 1.55 obtained from the specimens of column C8. There was no specific reason why these specimens exhibited such low creep in comparison with other columns' specimens. The highest value in the range was 2.68 recorded for the specimens of column C13, but that was mainly due to two loading errors in the first day where higher load than required was applied. It can be seen from the table,

that the value of 2.0 was the appropriate choice for the creep coefficient to perform the theoretical analysis.

The effects of creep coefficient on the theoretical results have been examined and shown in Table 6.7. Choosing a value of 1.0 for column C12 would give $P_{test}/P_{theory}=1.13$; increasing it to 4 gives $P_{test}/P_{theory}=1.6$. Clearly as creep increases it reduces the carrying capacity of the column and this is correctly reflected in the theory by predicting an increasing reduction in the column capacity, hence higher P_{test}/P_{theory} values.

When the creep coefficient equals 1.0 the ratio e_{test}/e_{theory} becomes 1.43, while increasing it to 4.0 yields $e_{test}/e_{theory}=0.86$. The compressive strains in the concrete increase with creep, leading to an increase in curvature with a consequent increase in deflection. The effect of the value of the creep coefficient on the ratio e_{test}/e_{theory} becomes smaller for values greater than 2.5.

6.7 Conclusions

1- Instability is the failure criterion for the columns tested, indicated by a drop in load which occurred at compressive strains in the range 0.001-0.002 (Fig.6.1).

2- A sustained load of 60% of short-term capacity causes a considerable reduction in the load capacity of a slender column and can be as much as 40% (Table 6.5).

3- Under sustained load of 60% of the short-term capacity, the mid-height deflection can typically reach a magnitude of 4 times the value on the initial loading (Figs.6.4(a), 6.5(a) and 6.6(a)).

4- While the theory appears to be conservative in predicting the long-term failure load, it closely predicts the deflection at the point of instability (Tables 6.3 and 6.4).

5- The creep coefficient was found to strongly influence the predicted buckling load (Table 6.7), emphasising the fact that creep has a major effect on the stability of slender columns and must be accounted for in the theoretical approach. For values of the creep coefficient within the range 1.5-2.5, the influence is also considerable on the predicted deflection.

6- The behaviour of tensile strains in slender columns under sustained load, merits further investigation.

Table 6.1 : Column details.

Column	b (mm)	h (mm)	d/h	%As	e_i/h	L (m)	l_e/h*
C 6	152	125	0.78	4.23	0.080	3.6	28.80
C 8						4.2	33.60
C 10						4.8	38.40
C 12	152	100	0.79	2.97	0.100	4.5	45.00
C 13						4.5	45.00
C 15						5.0	50.00
C 16†						5.0	50.00
C 18	152	90	0.76	3.30	0.111	5.0	55.56
C 20	152	80	0.78	2.58	0.125	5.0	62.50

* $l_e = L$.

† C16 was omitted.

Table 6.2 : Concrete properties.

Col.	Cube compressive strength (N/mm^2)				Cube density	Cylinder compressive strength (N/mm^2)		Static modulus of elasticity* (kN/mm^2)			Slump
	Cubes cured with column			Standard curing		Cured with column		28 days	Start of loading	End of loading	
	28 days	Start of loading	End of loading	28 days	(kg/m^3)	28 days	End of loading				(mm)
C 6	56.2	f_{cu35}= 60.8	f_{cu125} = 63.1	52.3	2378	43.6	f'_{c125} = 45.2	-	32.5	35.1	45
C 8	55.6	f_{cu32} = 57.2	f_{cu122} = 62.2	50.2	2411	40.0	f'_{c122} = 42.5	34.8	34.9	36.2	20
C 10	54.4	f_{cu32} = 56.5	f_{cu123}= 61.6	52.5	2401	37.2	f'_{c123} = 43.2	35.0	35.1	34.8	56
C 12	51.2	f_{cu28} = 51.0	f_{cu120} = 53.2	50.2	2374	39.7	f'_{c120} = 40 0	34.4	34.4	35.4	30
C 13	49.9	f_{cu28} = 50.0	f_{cu115} = 51.9	47.0	2390	38.3	f'_{c115} = 41.5	33.1	33.1	33.2	35
C 15	62.2	f_{cu29} = 62.4	f_{cu119} = 67.0	58.8	2400	45.7	f'_{c119} = 49.3	35.2	35.1	36.1	20
C 18	53.0	f_{cu29} = 52.0	f_{cu117} = 55.2	50.4	2381	39.8	f'_{c117} = 43.5	-	32.9	33.2	45
C 20	50.4	f_{cu30} = 50.4	f_{cu120} = 55.2	47.3	2389	38.5	f'_{c120} = 43.4	-	34.0	34.2	45

* measured on prisms

Table 6.3 : Comparison between experimental and theoretical long-term results.

Col.	f_{cu} (N/mm^2)	Sustained load (kN)	P_{test} (kN)	P_{theory} (kN)	P_{test} / P_{theory}	e_{test} (mm)		e_{theory} (mm)	e_{test} / e_{theory}	
						Theodolites	Dial gauges		Theodolites	Dial gauges
C 6	63.1	203	269	255	1.05	-	52.0	45.7	-	1.14
C 8	62.2	150	225	194	1.16	52.4	55.2	48.6	1.08	1.14
C 10	61.6	123	157	150	1.05	61.7	65.7	54.1	1.14	1.21
C 12	53.2	61	88	65	1.35	48.6	48.6	43.0	1.13	1.13
C 13	51.9	61	93	64	1.45	41.5	42.0	43.4	0.96	0.97
C 15	67.0	51	73	55	1.33	46.8	46.8	40.6	1.15	1.15
C 18	55.2	39	52	34	1.53	52.8	52.8	48.3	1.09	1.09
C 20	55.2	27	28	24	1.17	66.8	66.8	50.0	1.33	1.33

e = mid-height eccentricity at the point of instability.

P = buckling load after sustained loading period.

$f_y = 530\ N/mm^2$.

$\phi = 2.0$

Table 6.4 : Statistical values for long-term tests.

Statistical parameter	$\frac{P_{test}}{P_{theory}}$	e_{test}/e_{theory}	
		Theodolites	Dial gauges
Minimum ratio	1.05	0.96	0.97
Maximum ratio	1.53	1.33	1.33
Mean	1.26	1.13	1.15
Standard deviation	0.18	0.11	0.10
Coefficient of variation	14.3%	9.73%	8.70%
Number of tests	8	7*	8

* Theodolite results are not available for column C6

Table 6.5 : Reduction in column capacity.

Col.	f_{cu} (N/mm^2)	%As	e_i/h	l_e/h	P_{test} Short-term (kN)	P_{test} Long-term (kN)	Reduction in capacity (%)	Theoretical predicted reduction (%)
C 6	63.1	4.23	0.080	28.80	360	269	25	34
C 8	62.2			33.60	250	225	10	33
C 10	61.6			38.40	205	157	25	37
C 12	53.2	2.97	0.100	45.00	102	88	15	41
C 13	51.9			45.00	102	93	10	42
C 15	67.0			50.00	85	73	15	43
C 18	55.2	3.30	0.111	55.56	65	52	20	45
C 20	55.2	2.58	0.125	62.50	45	28	40	41

Table 6.6 : Results of creep study.

Test reference	$\varepsilon_i \times 10^{-6}$	Strains at the end of the sustained loading period			$\phi = \frac{\varepsilon_{cr}}{\varepsilon_i}$
		$\varepsilon_{cr} \times 10^{-6}$	$\varepsilon_{sh} \times 10^{-6}$	$\varepsilon_t \times 10^{-6}$	
C 6	892	1884	280	3056	2.11
C 8	1054	1631	216	2901	1.55
C 10	1060	2557	254	3871	2.41
C 12	1074	2310	260	3644	2.15
C 13	944	2530	212	3686	2.68
C 15	785	1733	194	2712	2.21
C 18	858	1752	290	2900	2.04
C 20	861	1944	316	3121	2.26

Table 6.7 : Effect of creep coefficient on theoretical results.

Col.	P_{test} (kN)	e_{test} (mm)	ϕ	P_{theory} (kN)	$\frac{P_{test}}{P_{theory}}$	e_{theory} (mm)	$\frac{e_{test}}{e_{theory}}$
C 12	88	48.6	1.0	78	1.13	34.0	1.43
			1.5	70	1.26	35.0	1.39
			2.0	65	1.35	43.0	1.13
			2.5	62	1.42	54.3	0.90
			3.0	58	1.52	56.0	0.87
			4.0	55	1.60	56.5	0.86

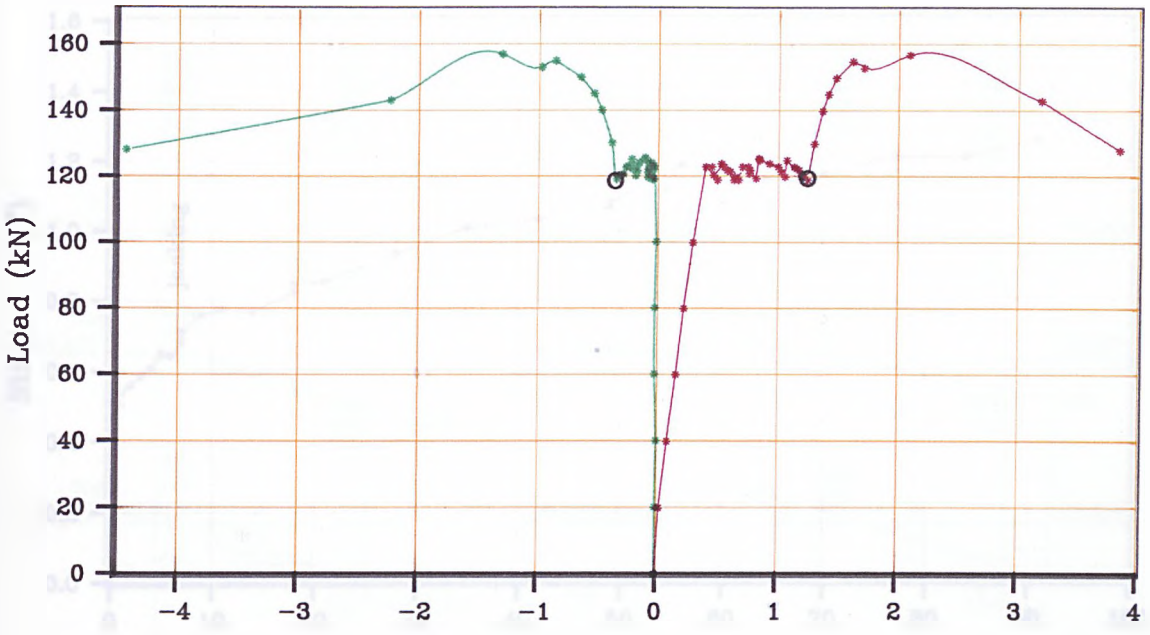

(a) Column C10

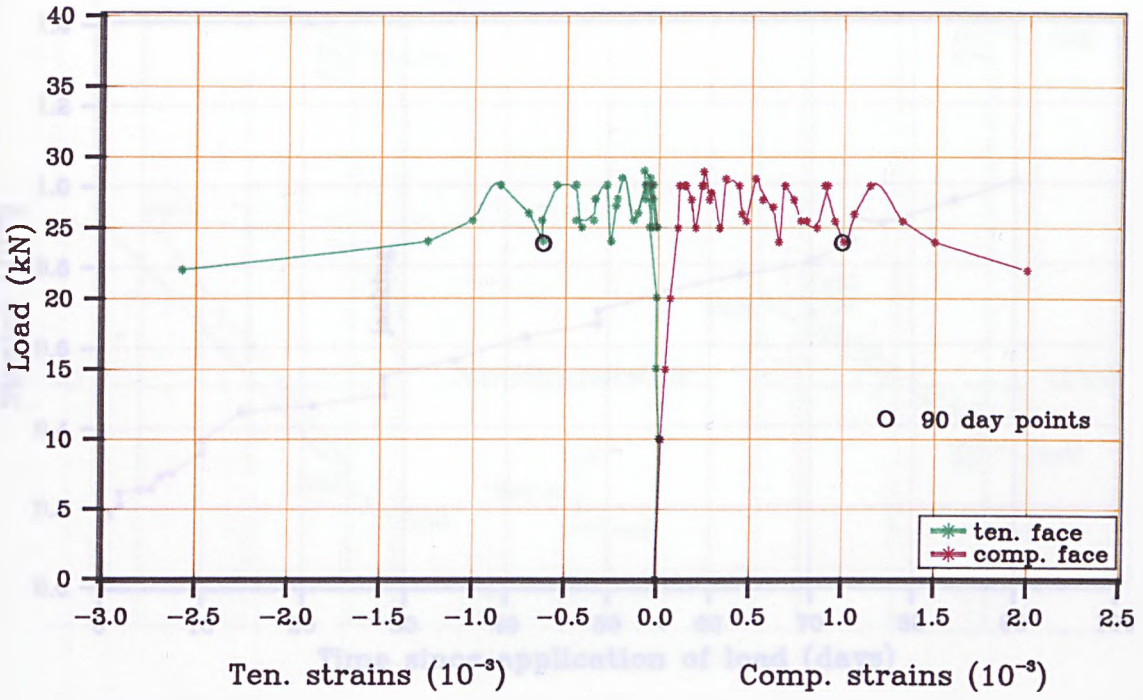

(b) Column C20

Fig.6.1 Curves of mid−height strains in concrete vs. Load.

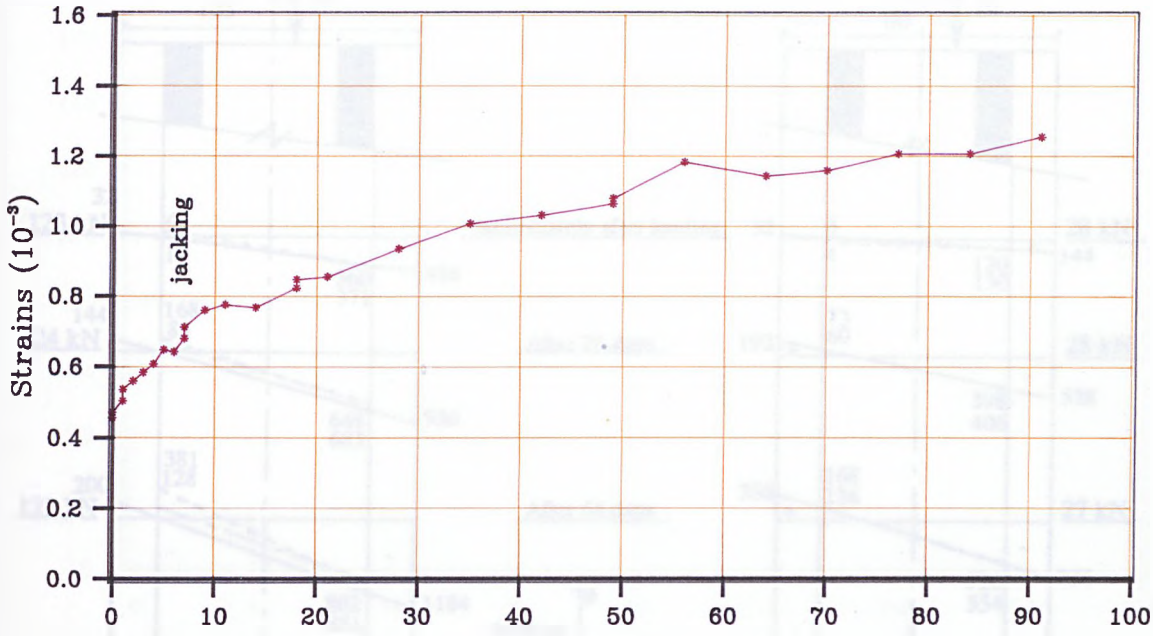

(a) Column C10

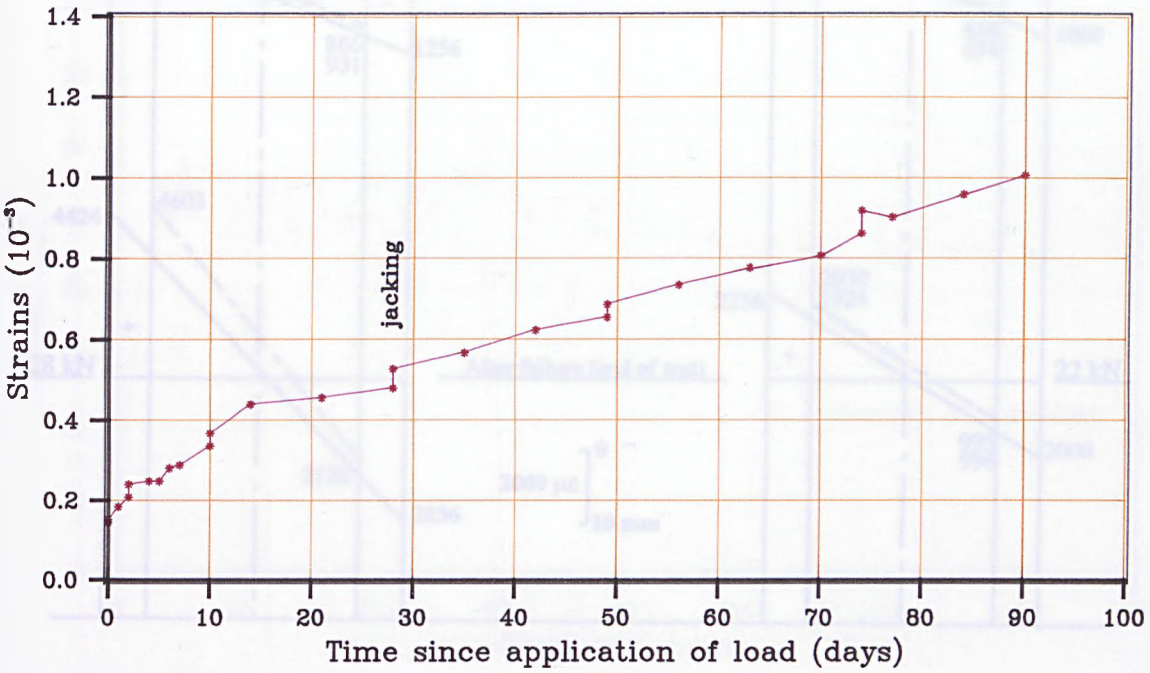

(b) Column C20

Fig.6.2 Curves of mid-height compressive strains in concrete vs. Time.

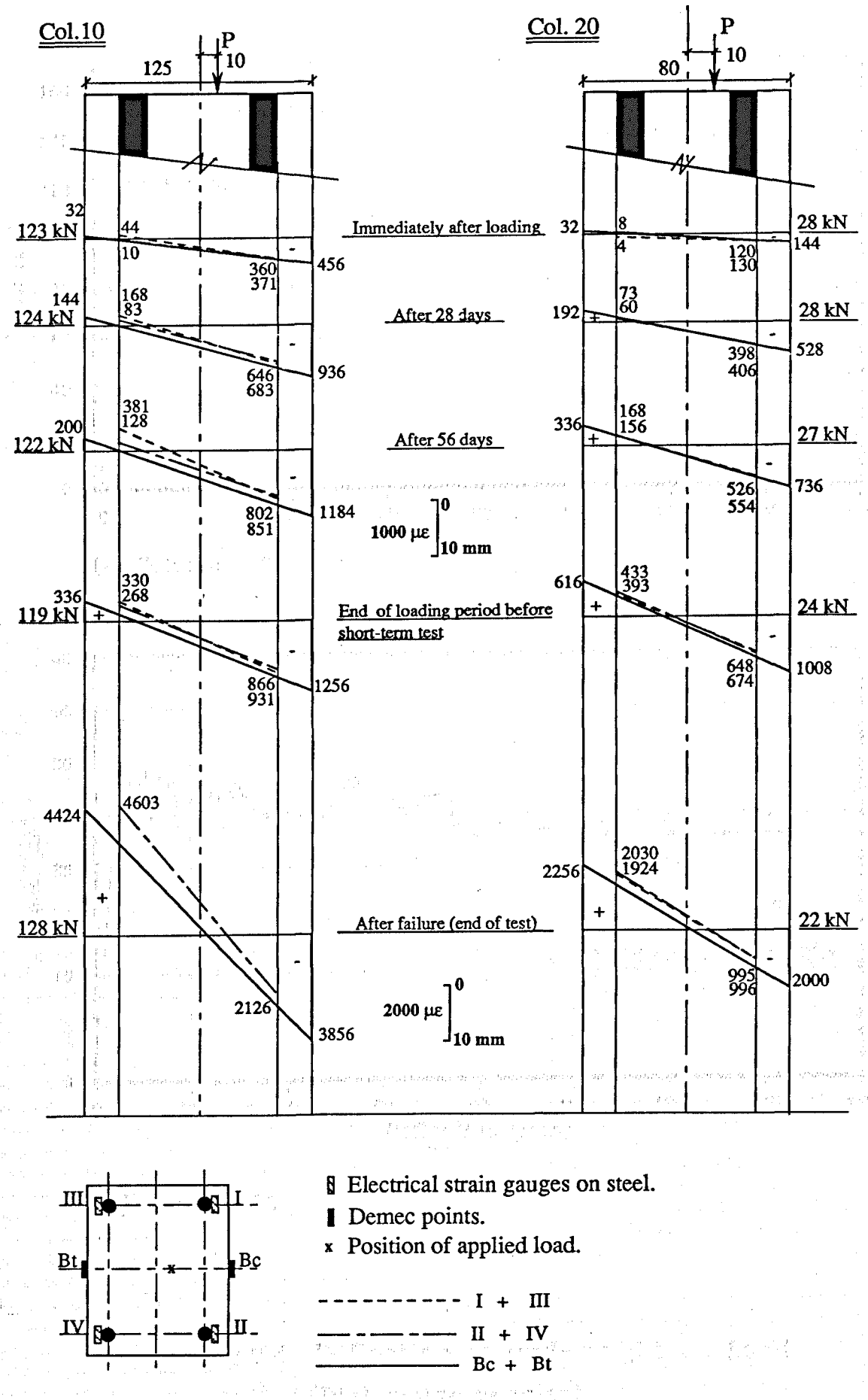

Fig. 6.3 : Strain variations across the section at mid-height region.

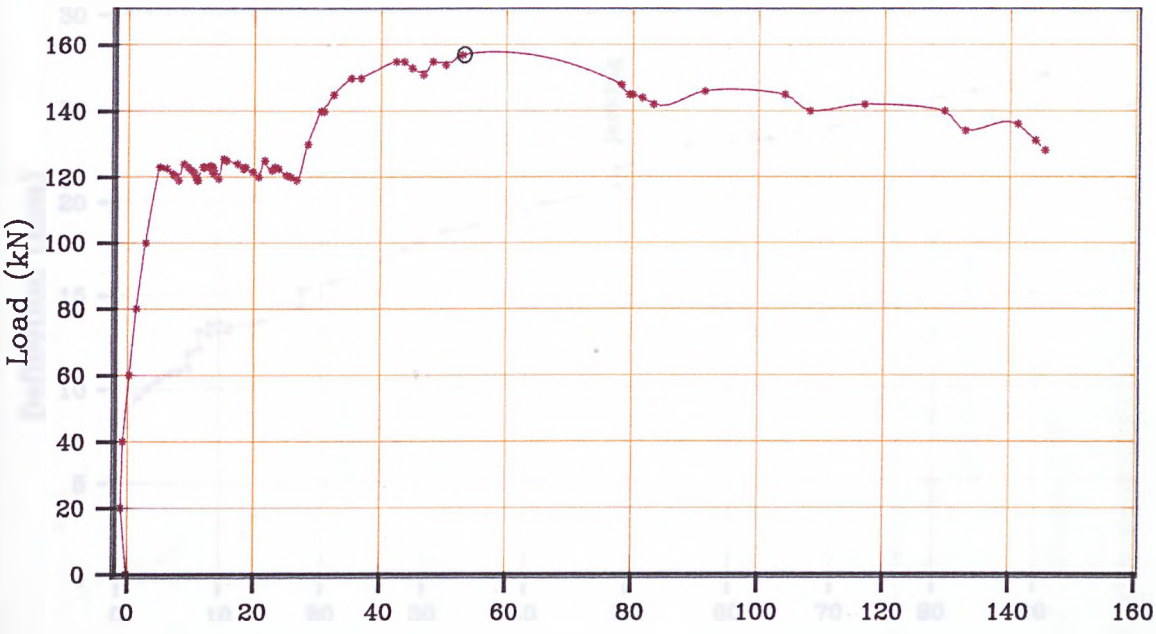

(a) Column C10

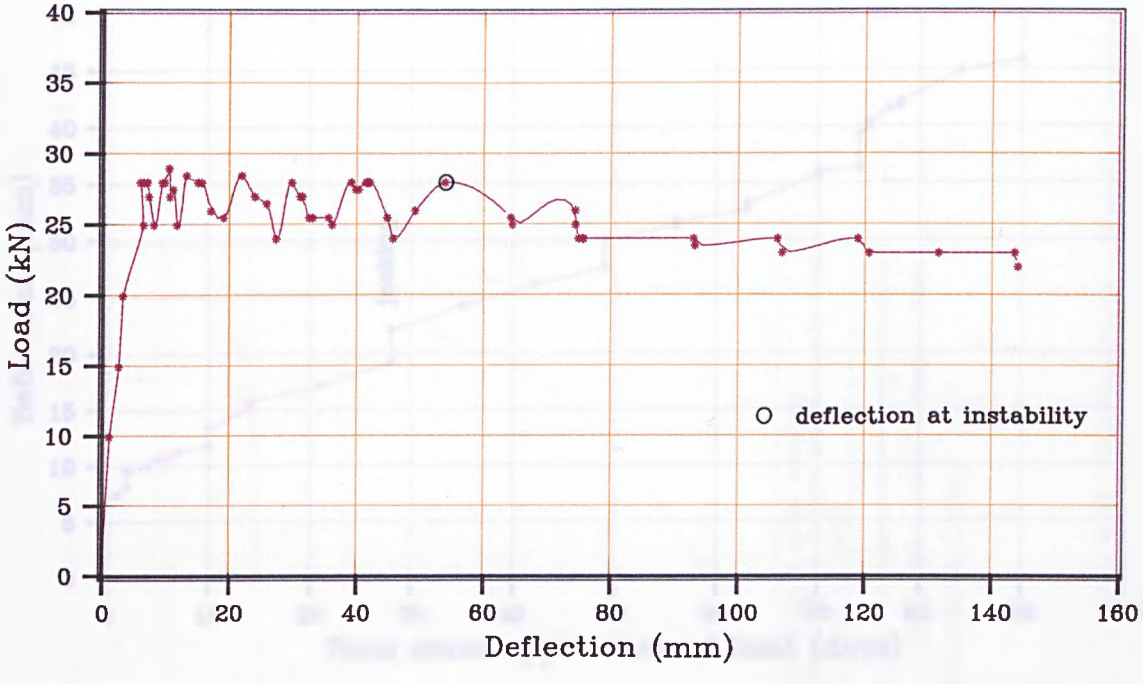

(b) Column C20

Fig.6.4 Deflection at mid-height vs. Load (Dial gauge results).

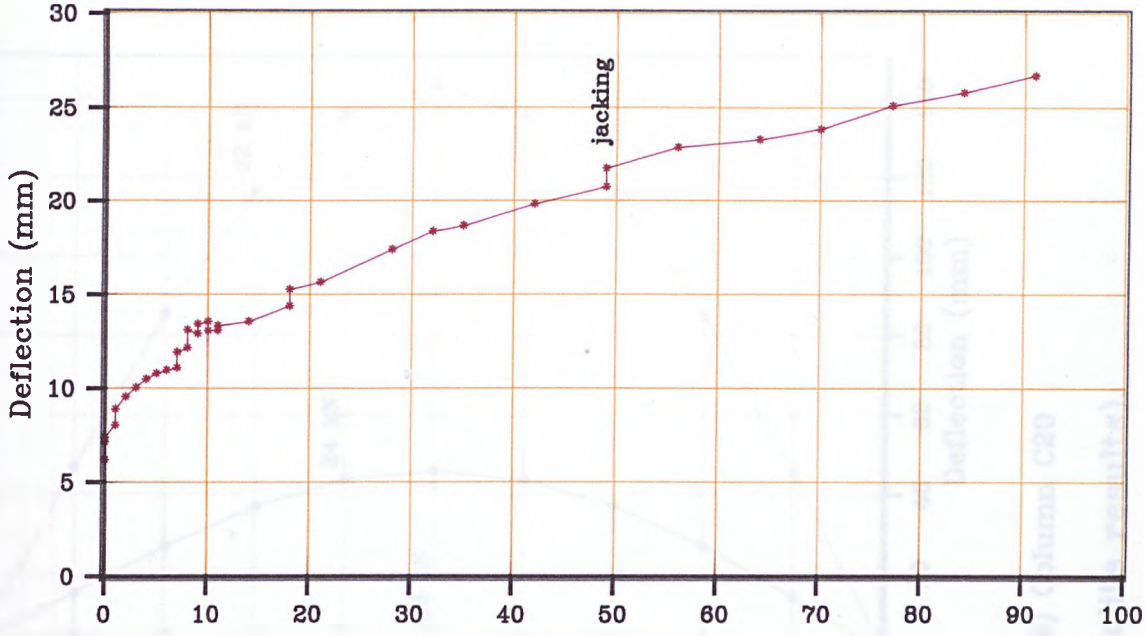

(a) Column C10

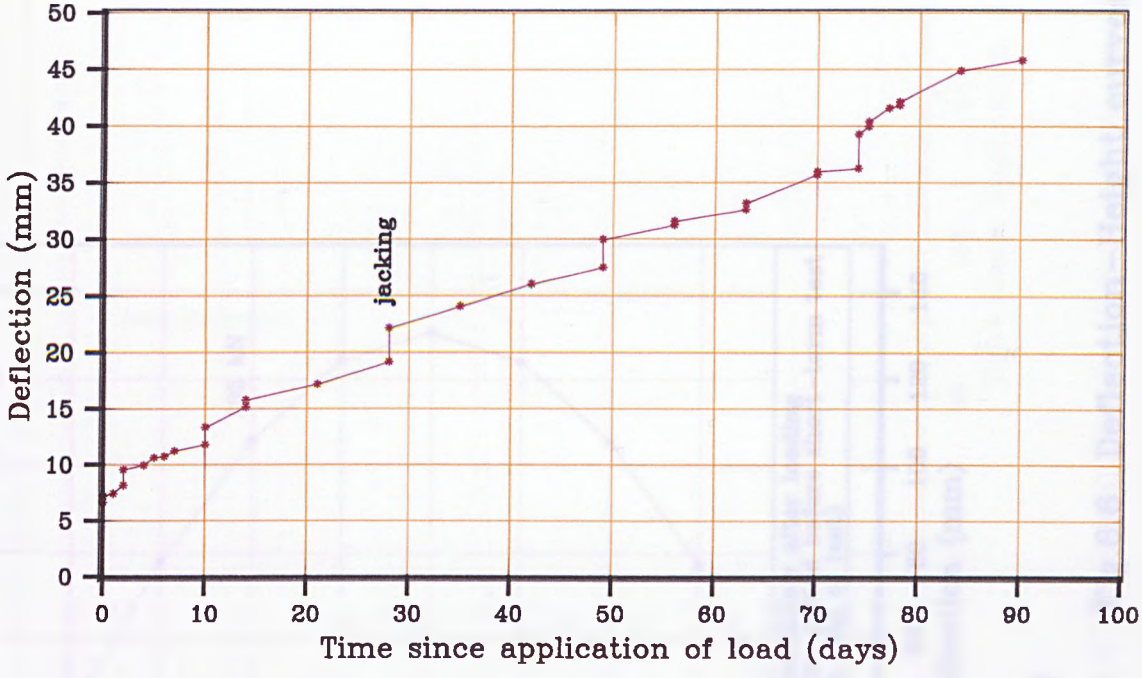

(b) Column C20

Fig.6.5 Deflection at mid-height vs. Time (Dial gauge results).

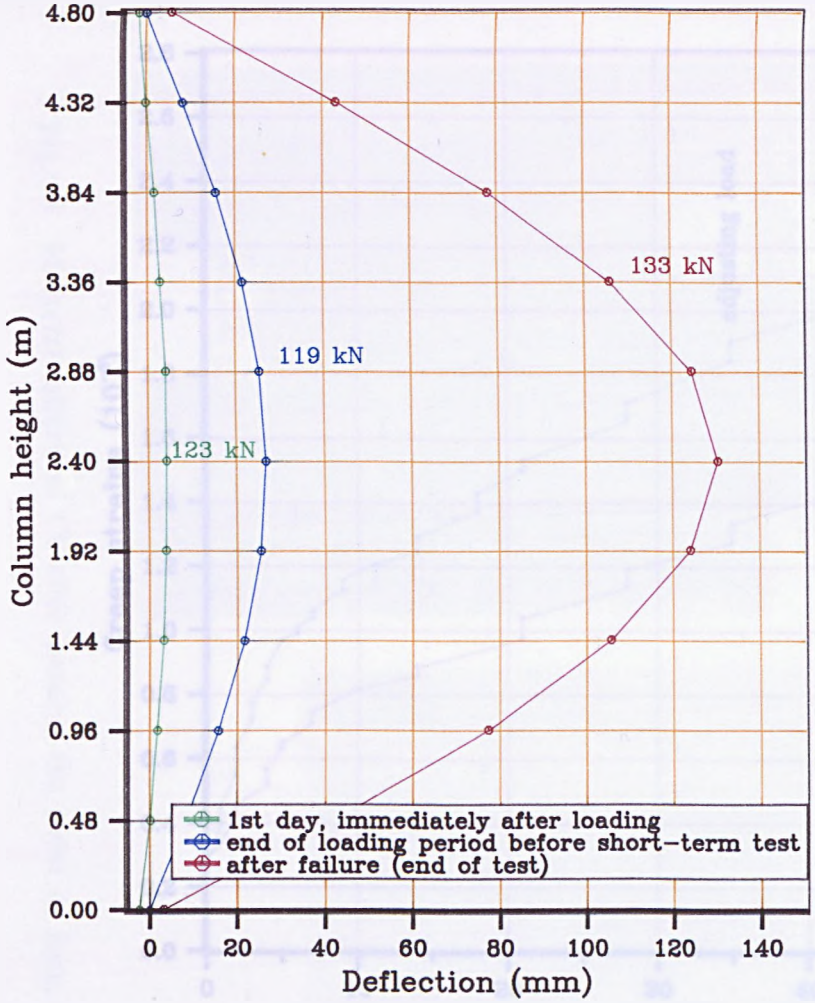

(a) Column C10

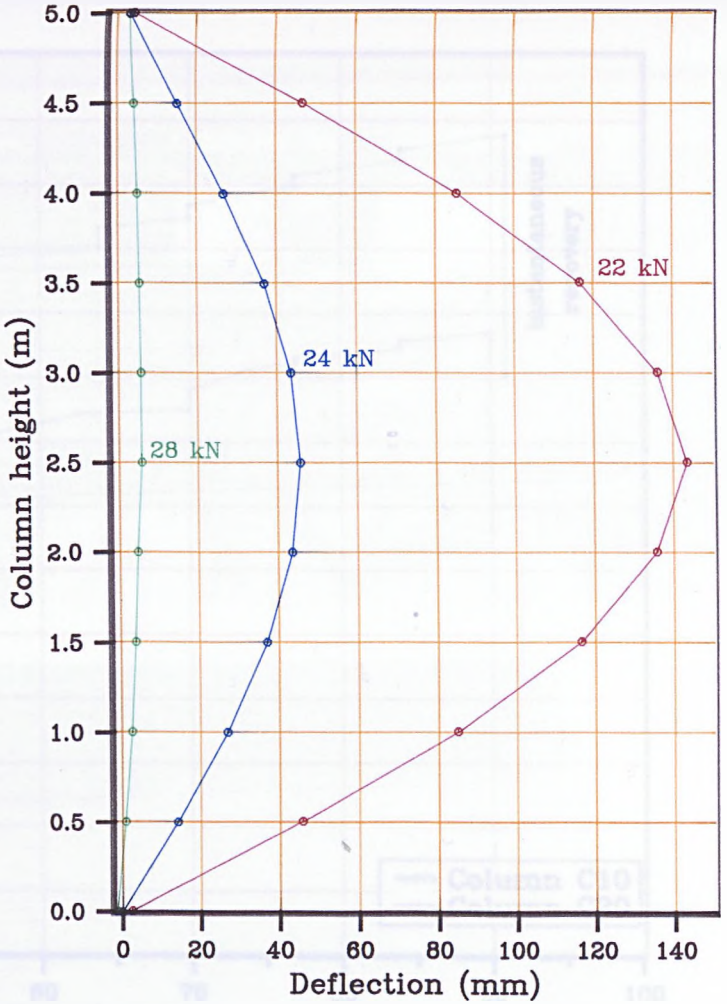

(b) Column C20

Fig.6.6 Deflection–Height curves (Theodolite results).

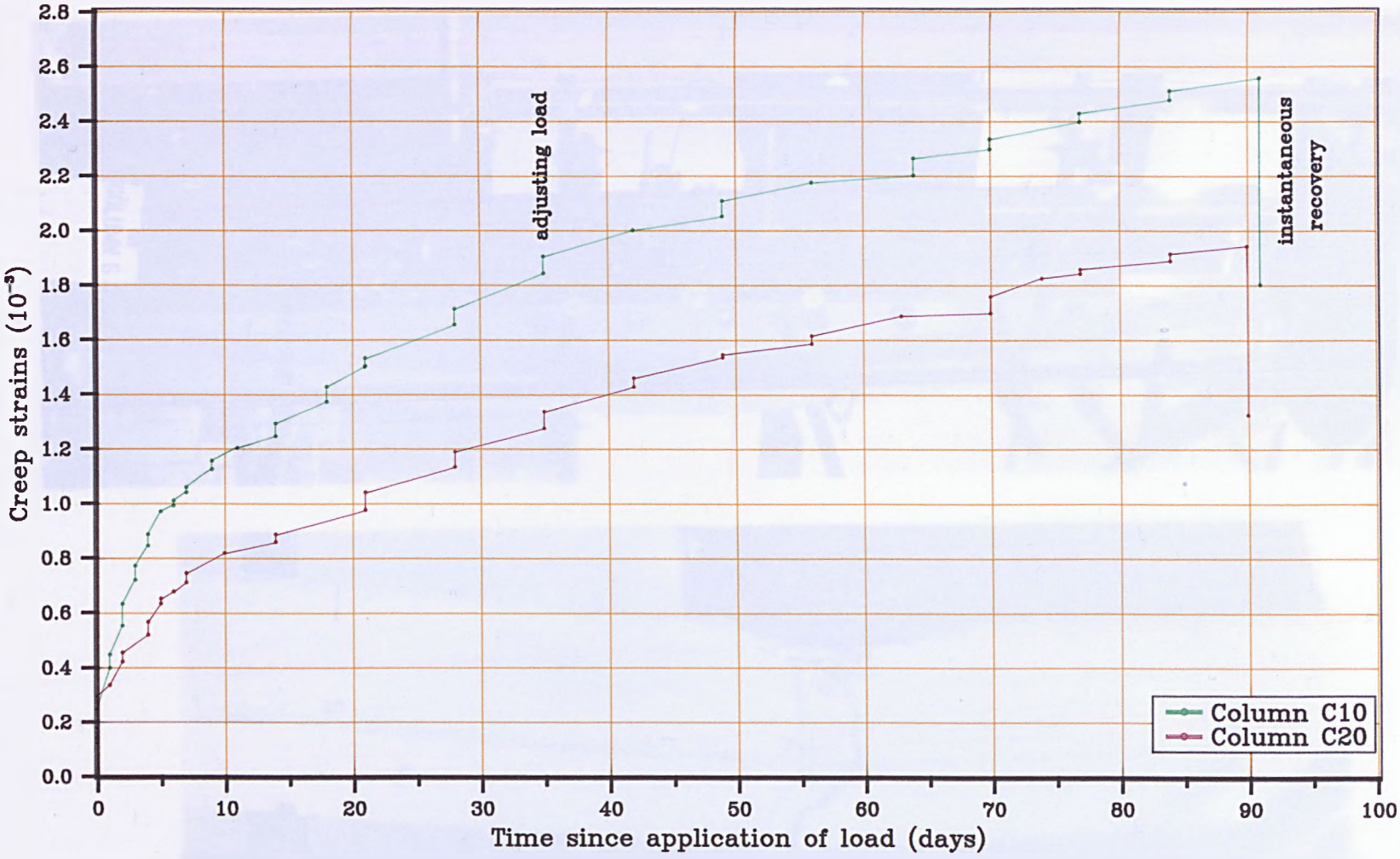

Fig.6.7 Creep strain–Time curves measured on concrete cylinders.

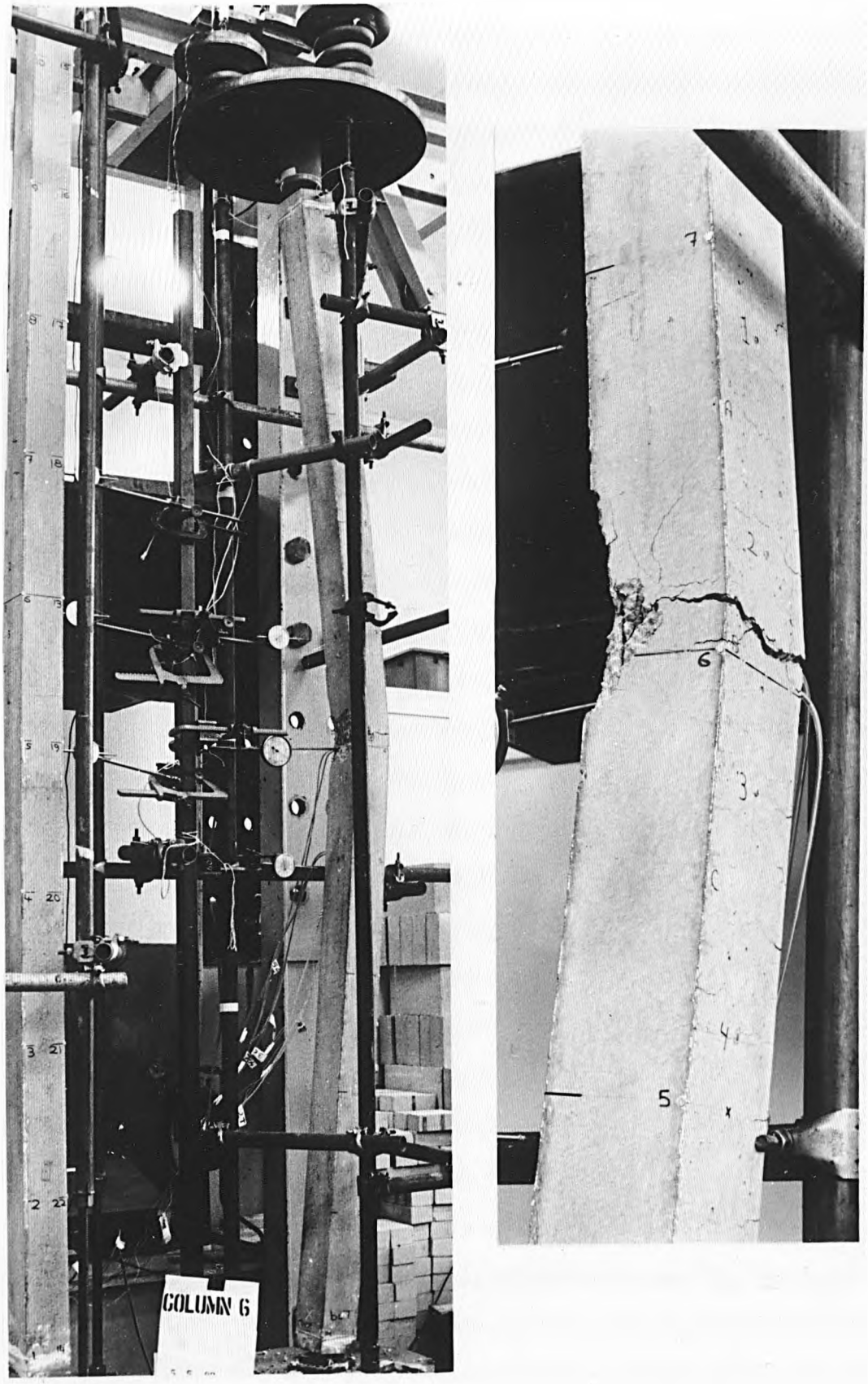

Fig.6.8 Material failure of C6 after passing the point of instability.

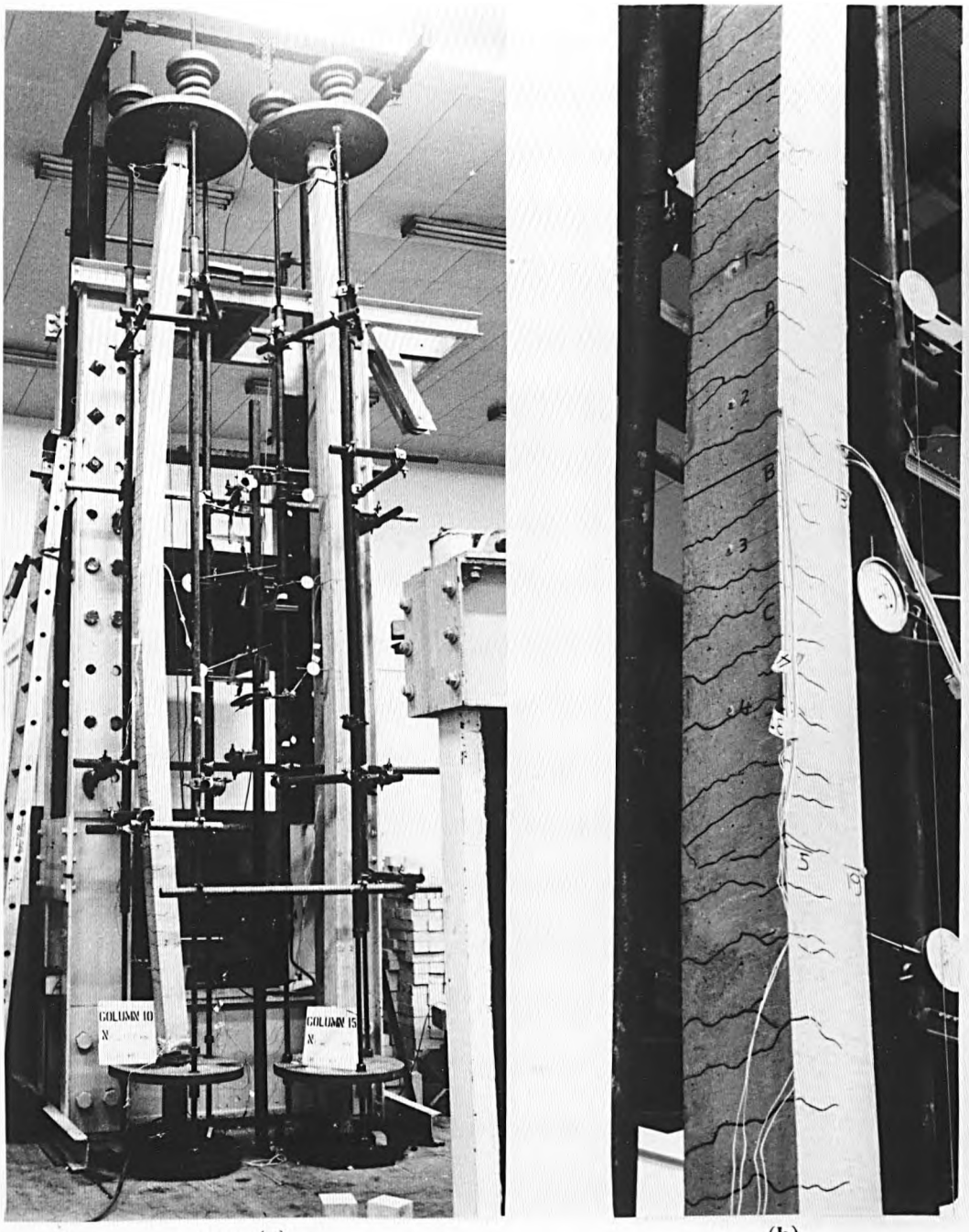

(a) (b)

Fig.6.9 (a) Bending profile of C10 after instability failure, (to the right C15 under load).

(b) Close-up of C10.

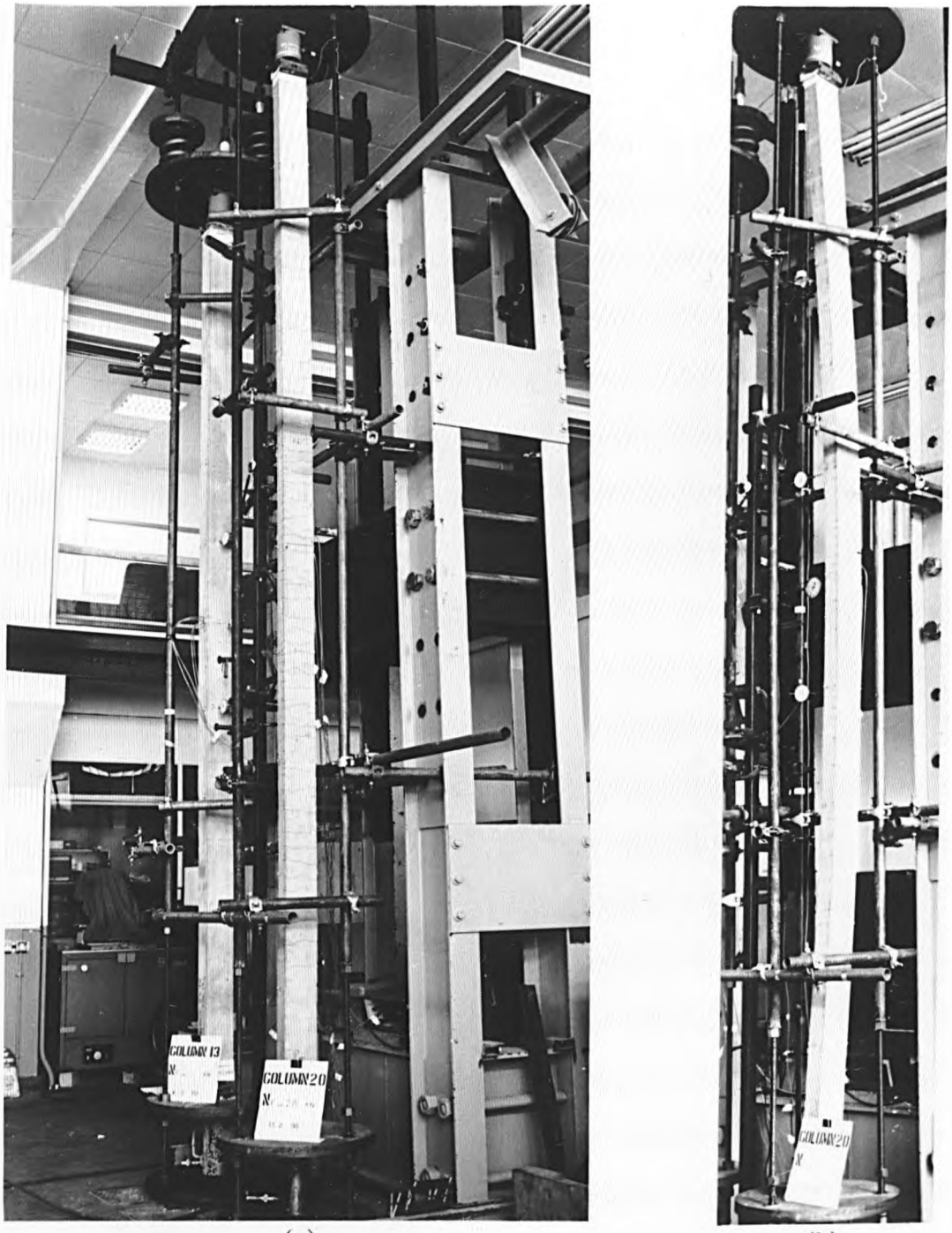

(a) (b)

Fig.6.10 (a) Crack pattern on the tension face of C20.

(b) Bending profile of C20.

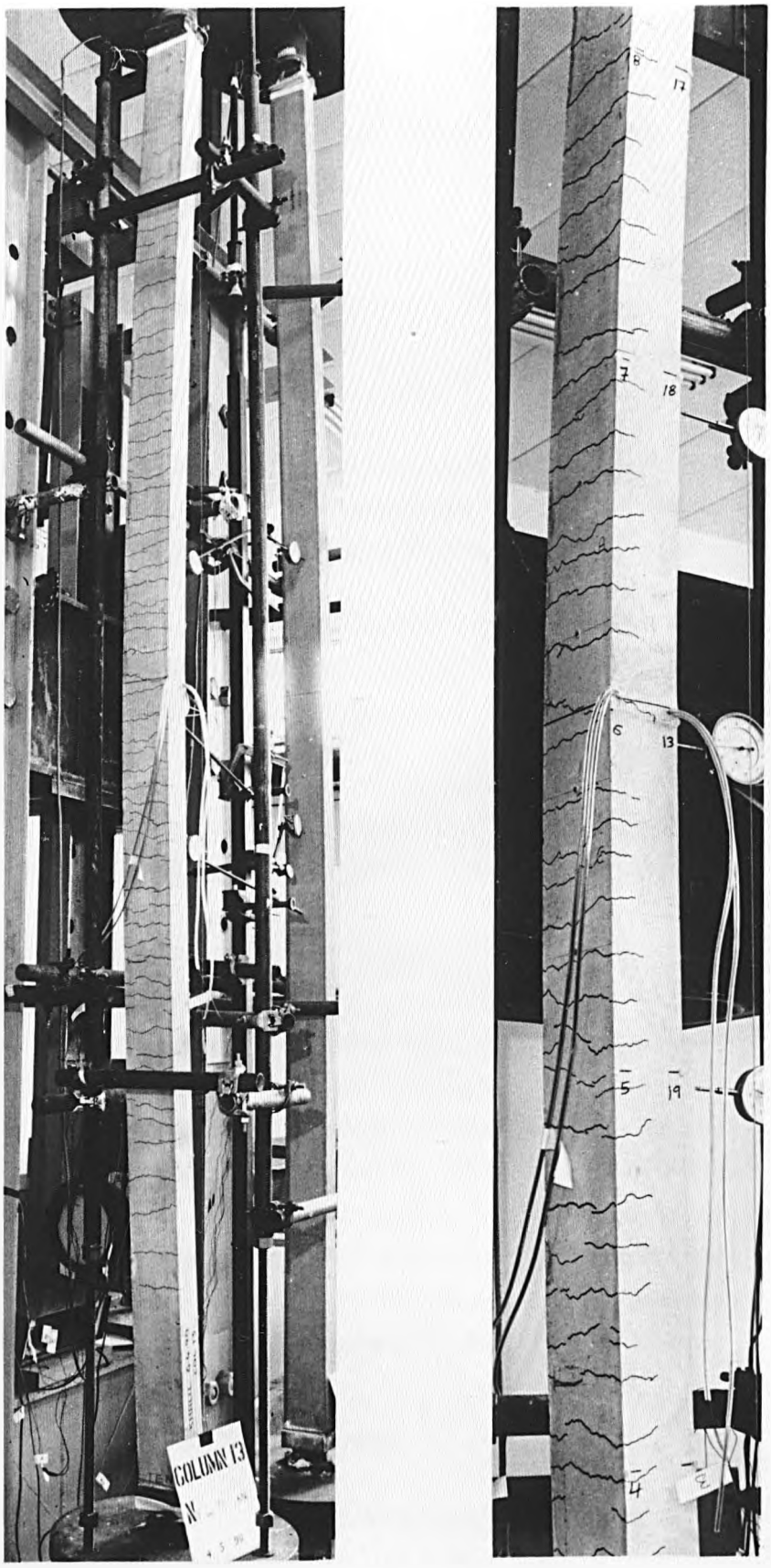

Fig.6.11 Typical crack pattern (C13).

CHAPTER SEVEN

ANALYSIS AND DISCUSSION OF RESULTS

7.1 Introduction

The applicability of the proposed analysis is checked by extensive comparisons with test results reported by various investigators. In total 118 tests are considered, of which 65 are short-term tests and 53 are long-term tests.

The theories adopted in the two Codes of Practice BS8110 and ACI318 are used to predict the experimental failure loads for columns tested in this work and they are compared against the theory proposed in Chapter 3.

These comparisons are made to examine the general validity of the approach over a wide range. This Chapter provides coverage of all the assumptions made to perform these comparisons. The results obtained are evaluated and discussed.

7.2 Comparison with codes of practice

Two Codes of Practice are selected for the comparison with the experimental work, BS8110 and ACI318-89. Eurocode No.2 is excluded; as explained in Chapter 2 (see 2.2.3) the final version is not available yet. However, the resemblance is obvious between the method recommended for slender columns in the final draft and BS8110. Hence, it is expected that it would give similar results to the BS8110 approach. The Japanese Code, covered in section 2.2.4.1, is disregarded because it does not specify any particular method for slender columns; the Australian Code described in section 2.2.4.2 is not considered because of its close similarity to the ACI318-89 procedure.

7.2.1 British standard BS8110: 1985

BS8110 approach [6] is based on the additional moment concept, fully described in Chapter 2. The method as presented in the Code is a design tool; in order to predict experimental failure loads, interaction diagrams giving the characteristic failure conditions were necessary. The following assumptions were used in producing Figs.7.1, 7.2 and 7.3:

(a) In the assessment of the strength of sections, the stress-strain curves for concrete and steel as given in Figs.3.1 and 3.2 were used to produce Figs.7.1 and 7.2 (the difference is negligible between the two figures, see 7.2.1.2). Figure 3.1 was modified to allow for long-term effects by multiplying the strains by $(1+\phi)$, and then it was used with Fig.3.2 to produce Fig.7.3. Factors of safety were omitted and actual material properties were used.

(b) The depth of the simplified rectangular stress block for concrete and the centroid of the concrete compressive force (see Fig.B.2 in Appendix B) were calculated according to the cube strength appropriate to the time when the column actually collapsed. Average values for the constants k_1 and k_2 were then used. The effective depth ratio d/h was taken as 0.8.

(c) The interaction diagrams were produced in terms of $\rho f_y/f_{cu}$; and their values were chosen to cover the range of the experimental variables.

(d) The vertical axis of the interaction diagrams gives the values of P_0/bhf_{cu} (i.e when $M/bh^2f_{cu}=0$). In the preparation of these charts, the gross area of the concrete has been used at all times, no reduction has been made for the area occupied by the reinforcement.

In finding P_{BS} for short and long term tests, the design method as presented in BS8110 was employed in its entirety (specifically Clauses 3.8.3.1 to 3.8.3.5). With regard to the assessment of effective length, this has been taken as equal to the actual column height. After examining Clauses 3.8.3.3 to 3.8.3.5, all columns were analysed as uniaxially bent about their minor axis. The steps followed in the analysis are summarised below:

1- Calculate the additional eccentricity e_u assuming the reduction factor K=1:

$$e_u = \frac{1}{2000}\left(\frac{l_e}{h}\right)^2 K\, h \qquad \text{(Eq.2.2)} \qquad (7.1)$$

2- Calculate the total eccentricity e_t at the mid-height of the column:

$$e_t = e_0 + e_i + e_u \qquad (7.2)$$

This is the maximum eccentricity which was found to govern the design, where

e_0 = initial imperfection = $5.68\times10^{-4}L$

e_i = initial load eccentricity = 10 mm

3- Plot the line e_t/h on the chart; at the intersection point of this line with the relevant $\rho f_y/f_{cu}$ curve for the column under analysis, read the value of P/bhf_{cu}. P is the load at which section failure will occur.

4- Knowing the values of P_0,P_{bal} and P, K can be calculated from the equation:

$$K = \frac{(P_0 - P)}{(P_0 - P_{bal})} \leq 1.0 \qquad \text{(Eq.2.4)} \qquad (7.3)$$

P_0 is as given in Eq.(3.8)

5- Use K to calculate amended additional eccentricity

6- Repeat stages (2) to (4)

7- If new K is within ± 1% of the initial value, the process is finished and the last value of P is the failure load P_{BS}.

8- If new K is substantially different, go to stage (5), bearing in mind that it is the basic additional eccentricity which will be modified.

9- Repeat the process until the condition in stage (7) is reached.

7.2.1.1 Comparison with the short-term tests

For comparisons with the short-term tests, the interaction diagram given in Fig.7.1 was used to assess section strength. The constants k_1 and k_2 were found to be 0.84 and 0.43 respectively. The design method, implementing the iteration procedure outlined above, was then used to predict the experimental failure loads and values are given in Table 7.1. Also to be found in the table are the values of P_{BS}, if K was set as unity in the analysis.

7.2.1.2 Comparison with the long-term tests

Due to the fact that BS8110 does not allow for long-term effects, Figs.3.1 and 3.2 were used in the assessment of section strength to produce the interaction diagram given in Fig.7.2. The only variations were in the constants k_1 and k_2 of the simplified concrete stress block which varied due to age effects represented by the f_{cu} value. These were taken as 0.82 and 0.42 respectively. However, the differences between Figs.7.1 and 7.2 due to this were found to be negligible.

The design method was applied to obtain P_{BS} and the values determined are provided in Table 7.2. The values of P_{BS}, calculated when K=1, are also in the same table.

The interaction diagram in Fig.7.2 was modified to take account of creep effects in the same manner as in the proposed theory in order to compare the results. The concrete stress-strain curve of Fig.3.1, modified as explained in 7.2.1(a), was used in assessing the strength of the section. The resulting interaction chart is illustrated in Fig.7.3. The creep coefficient ϕ was taken as 2.0, as used in the proposed theory and as found by the experimental creep study. To calculate failure loads, the design method presented in 7.2.1 was employed without any modification. Results obtained are provided in Table 7.2.

7.2.2 American standard ACI318-89

The theory adopted in the recent American Code ACI318-89 [7] is based on the moment magnification method described in Chapter 2, which relates slender column design to strength calculation. This method is allowed only for columns with $kL/r \leq 100$ ($l_e/h=30$); for columns with $kL/r>100$ second order analysis has to be made. However, as explained in the Commentary to the Code [7], such analysis is more relevant for frames as it gives the moments only at the ends of the column. For a slender column, the maximum moment may occur between its ends, depending on the deflected shape of the column. In such a situation it is necessary to compute a magnified moment. The Commentary to the Code provides a formula to check whether the maximum moment is at one of the column ends or between them.

The slenderness ratio in terms of kL/r (taking r=0.3h) was found to range between 60 and 96 for columns C1 to C6 and between 112 and 208 for columns C7 to C20. However, all columns were pin-ended, bent in single curvature and therefore the maximum moment occurs at mid-height and the moment magnification method is applicable for analysing all the columns.

To make valid comparison with the experiments, the interaction diagrams needed to be produced without applying the strength reduction factors and using actual material properties. The stress-strain relationships for concrete and steel as described in section 10.2 in the Code were used to assess the strength of the section. The cylinder strength was taken as 0.8 of the cube strength. The depth of the simplified rectangular stress block was calculated according to the equivalent cylinder strength relevant to the time of testing the column, accordingly the factor k_1 (referred to as β_1 in the ACI Code) was found to be 0.746 for short-term tests and 0.704 for long-term tests; the factor k_2 was taken as $k_1/2$.

The fact that the presence of the reinforcement has occupied a corresponding amount of concrete area is neglected here as for the BS8110 calculations.

The interaction diagrams given in terms of $\rho f_y/f'_c$ are shown in Figures 7.4 and 7.5 for short and long-term tests respectively. The differences between the two figures are due to the variation in the k_1 value.

To calculate the theoretical failure loads P_{ACI} using Figs.7.4 and 7.5, the design method presented in the Code in section 10.11.5 was employed as follows:

1- Calculate the actual eccentricity acting on the column: $e_i + e_0$

2- Calculate the critical load P_c:

$$P_c = \frac{\pi^2 EI}{(kL)^2} \qquad \text{(Eq.2.14)} \qquad (7.4)$$

Taking the effective length factor k=1, L = actual length of the column.

$$EI = \frac{(E_c I_g / 5 + E_s I_{se})}{1 + \beta_d} \qquad \text{(Eq.2.16)} \qquad (7.5)$$

$E_c = w_c^{1.5}\, 0.043\sqrt{f'_c}$ (N/mm^2), where w_c is the density of concrete (kg/m^3) and f'_c is the cylinder strength at the time of testing the column (N/mm^2).

$\beta_d = 0.0$ for short-term tests

$\beta_d = 1.0$ for long-term tests

3- Compute the moment magnification factor δ_b from the following equation assuming a value for P less than P_c:

$$\delta_b = \frac{C_m}{1 - \dfrac{P}{\phi_1 P_c}} \geq 1.0 \qquad \text{(Eq.2.12)} \qquad (7.6)$$

where C_m=1.0 because of equal end eccentricities and ϕ_1=1.0

4- Calculate the magnified eccentricity: $e_m = \delta_b (e_i + e_0)$

5- Plot the line e_m/h on the chart (either Fig.7.4 for the short-term tests or Fig.7.5 for the long-term tests), at the intersection point of this line with the relevant $\rho f_y/f'_c$ curve for column under consideration, read the value of P/bhf'_c, then calculate P.

6- If the new P is the same as the one assumed, the process is over and P defines the failure load P_{ACI}.

7- If the new P is substantially different, go to stage (3) bearing in mind that it is the basic eccentricity which will be modified.

Results are provided in Table 7.1 for short-term tests and in Table 7.2 for the long-term tests.

7.3 Discussion

All the statistical values for the ratios P_{test}/P_{BS} and P_{test}/P_{ACI} are to be found in Table 7.3. Both methods adopted in BS8110 and ACI318 have the advantages that they are easy to use and are based on established concepts of analysis known to the designer. However, neither provides a rational basis for instability failure because both are based on the material failure mode. Instability as proved by tests occurs at relatively low strains of the order 0.001-0.002 well below the ultimate strain capacity 0.0035 in BS8110 and 0.003 in ACI318.

The section curvature at failure in BS8110 is calculated from strains 0.0035 at the extreme concrete compression fibre and 0.002 tensile strain in the steel. If a sinusoidal deflected shape is assumed then the mid-height eccentricity will be given by the formula:

$$e_u = \frac{1}{1631}\left(\frac{l_e}{h}\right)^2 K\, h \qquad \text{(taking h=1.1d [91])} \qquad (7.7)$$

This is rounded to

$$e_u = \frac{1}{2000}\left(\frac{l_e}{h}\right)^2 K\, h \qquad \text{(Eq.7.1)}$$

The Code reduces the value of the deflection to allow for the conservatism implicit in the derivation, because using the balanced conditions overestimates the deflection as the stiffness away from the critical section is considerably higher than implied by the balanced curvature [52]. Furthermore, for a section with greater axial load than the balanced value, the strain in the steel near the least compressed face will be less than the yield strain [91]. This leads to the ultimate curvature being less than that for a balanced section. This is allowed for by introducing an empirical reduction factor K, where as stated in the Code "it will always be conservative to assume that K=1.0".

It can be seen from Table 7.1 that the BS8110 approach can give results as high as 32% above the experimental failure load; more acceptable answers are obtained if K is always set as unity, rather than being reduced by iteration. Similar results were found by *Beal* [52] who argues that, at high load eccentricities, the yield strain 0.002 in the steel

can be easily exceeded at failure resulting in an increase in the curvature beyond the value assumed. In fact the balanced conditions used in producing Figs.7.1 and 7.2 based on 0.00265 yield strain in the steel and 0.0035 maximum compressive strain in the concrete will give the following additional eccentricity:

$$e_u = \frac{1}{1284}\left(\frac{l_e}{h}\right)^2 K\,h \qquad \text{(based on d=0.8h)} \qquad (7.8)$$

This formula will give results 56% higher than the formula applied by the design method Eq.(7.1).

Turning now to Table 7.2 for long-term results, the overall impression is that BS8110 is extremely unsafe giving results higher than the test failure loads by up to 56%. Little improvement is achieved by setting K=1.0 and the results are still unconservative. The reason for this is that BS8110 does not allow for long-term effects and recommends a short-term failure strain in concrete of 0.0035, but due to creep the long-term failure strain in concrete could reach a magnitude of 0.008-0.009. This was proved experimentally by *Rüsch* [96] who found that creep affects strain at failure in the same way as other values of strain. It has also been proved by *Ferguson and Breen* [83] who measured concrete compressive strains of 0.0082, 0.0088 and 0.0091 under sustained load without any real observable distress. This indicates the magnitude of the strains attainable under sustained load. *Beal*, in the discussion to his paper [52], raised this matter as a serious error in BS8110; he pointed out that a failure strain of 0.008 rather than 0.0035 would approximately double the curvature and consequently double the additional moment.

Including the effect of creep in the same manner as in the proposed theory to produce the modified BS8110 interaction diagrams shown in Fig.7.3, did not improve the results. On the contrary, the mean value of the ratio P_{test}/P_{BS} (refer to Table 7.3) decreased from 0.82 to 0.79 and the minimum value from 0.64 to 0.61. The increase in strains due to creep results in higher stresses in the reinforcement, which increases the values of P/bhf_{cu} and M/bh^2f_{cu} (compare Fig.7.2 and 7.3). Consequently higher values are obtained for P_{BS}. In addition the balanced conditions used in this modified interaction diagram are based on 0.00265 yield strain in steel and 0.0105 maximum concrete compressive strain due to creep (ϕ taken as 2.0). Such conditions yield the following formula for the additional eccentricity:

$$e_u = \frac{1}{600}\left(\frac{l_e}{h}\right)^2 K\,h \qquad (7.9)$$

compared again with $e_u = \frac{1}{2000}\left(\frac{l_e}{h}\right)^2 K\,h$ quoted for design in BS8110 and used to obtain P_{BS} from Fig.7.3. This value appears to be only 30% of the value the theory requires for

long-term loads. Bearing in mind that usually most of the load on concrete columns in real structures is permanent, the long-term strain capacity is therefore very relevant to design.

Maisel and Beeby in their discussion to *Beal's* paper [52], analysed a number of pin-ended columns under short-term and sustained loads, using a computer program initially developed by *Cranston*. The program is effectively a specialized non-linear finite element program which gives a rigorous mathematical solution to the state of a reinforced concrete column under a defined loading with defined material properties. The BS8110 parabolic-rectangular curve has been used for the concrete and a bilinear stress-strain curve for the steel. The results are compared with those obtained using the graphical method as originally proposed by *Beal* [52] and those obtained using the BS8110 approach. In all cases there was remarkable agreement between the program and the graphical method in predicting the maximum loads. However, the BS8110 solution, which gives the load under which the ultimate capacity of the section will be reached, seems to underestimate the strength of the columns considered. This comparison confirmed the accuracy of the graphical method in column capacity prediction and its improvement over the BS8110 approach.

BS8110 does not account for initial imperfections; the arbitrary figure 0.05h for the minimum eccentricity, which is essentially for construction tolerances, is considered separately, i.e it is not added to the additional eccentricity.

In conclusion the BS8110 approach compares favourably with the short-term tests, but it greatly overestimates the long-term failure loads, indicating that this method is inadequate for dealing with cases of structural instability.

ACI318-89 allows two procedures to evaluate slenderness effects in compression members. Wherever possible the ACI building Code encourages the use of second-order frame analysis which includes the effects of sway deflections on axial loads and moments in frames. Generally, the moments from a second-order analysis are a better estimation of the real moments, than those obtained by the moment magnification method which is given as an alternative design procedure for columns with $kL/r \leq 100$. Though this method is based on strength calculation like BS8110, it was found to be conservative because it allows for stiffness effects upon the strength, which is the case for slender columns.

The average P_{test}/P_{ACI} for short-term tests (refer to Table 7.3) is 1.46 with a standard deviation of 20%. The stiffness parameter E_cI_g included in EI expression to define the critical load was reduced by 5 to apparently account for stiffness variations due to cracking and the non-linearity of the concrete stress-strain curve. However, this factor appears to be high. The factor β_d has been taken as zero. *Mirza and MacGregor* in a discussion to their paper [60], confirmed that in the case of slender columns with low end

eccentricities, ACI gives conservative answers, while it is unconservative for the case of slender columns with high end eccentricities. Their work was concerned with the determination of the variability of short-term ultimate strength of slender reinforced concrete columns of rectangular shape.

The comparison of ACI theory to long-term tests are given in Table 7.2. Despite the fact that ACI recommends 0.003 as a maximum usable compressive strain for concrete, it gives more conservative results than those for short-term tests because of the further reduction in the stiffness parameter EI, which is reduced by $(1+\beta_d)$, where β_d is the ratio of the maximum factored axial dead load to the maximum total factored axial load. This factor has been taken as unity to perform the comparison with the long-term tests. The average P_{test}/P_{ACI} was 2.26 with a standard deviation of 0.23 (Table 7.3). *Ferguson and Breen* [83] according to their findings (see page 156) pointed out the inadequacy of the ACI Code procedure based on a maximum strain of 0.003 to predict the effect of sustained load. *Rangan* [2,62], when he compared ACI theory with his analytical study of the strength of reinforced concrete slender columns under sustained loads, stated that the ACI method is significantly conservative for columns with larger slenderness ratio and smaller eccentricity.

MacGregor et al [65] compared the moment magnification method for 65 hinged and restrained concrete columns and 36 hinged prestressed concrete columns, under short-term and sustained loads. They concluded that the approximate design method is more conservative but less accurate for columns with kL/r greater than 100.

The expression: $w_c^{1.5}\ 0.043\sqrt{f'_c}$ used to calculate the modulus of elasticity E_c (for concrete having w_c value between 90-155 Ib per cu.ft) in the ACI method, was found to give better correlation with experimental values than the corresponding BS8110 expression. As can be seen in Table 7.4, the values of E_c given by BS8110 expression $5.5\ \sqrt{f_{cu}}$ are higher than the experimental values by up to about 30%. The effect of adopting the BS8110 expression for E_c in the proposed theory is examined and discussed in Chapter 5 (see 5.5). For normal weight concrete ACI318 offers another formula for E_c as $4700\ \sqrt{f'_c}$ which also agrees better with the experiments than the BS8110 formula. The ACI318 expression for $E_c=w_c^{1.5}\ 0.043\sqrt{f'_c}$ was also found by *Goyal* [33] to give reasonable agreement with the initial tangent modulus measured on the specimens.

7.4 Comparison with other researchers

To provide a general indication of the validity and accuracy of the proposed theory, comparisons with other researchers' tests have been carried out. There is now considerable test data available, especially on full-scale columns having high slenderness ratios up to 80. A number of short and long-term tests have been selected. The results are

presented in Tables 7.5 to 7.9. Summary of the statistical parameters obtained for the ratio P_{test}/P_{theory} is given in Table 7.10.

The major task in performing these comparisons was in preparing the load eccentricity-curvature graphs which suit each individual author's tests. The **COLUMNBS PASCAL** program prepared for short-term loads and **COLMNBSL PASCAL** program for long-term loads (described in Chapter 3) were used to produce the data required to plot the graphs.

Where individual authors have reported cylinder strengths, the cube strength has been assumed to be 1.25 times these strengths. For long-term tests if authors did not report any information about creep, the 1970 CEB method [97] was used to predict the creep coefficient.

In preparing buckling deflection-curvature graphs, the **BUCKDEF PASCAL** program (described in Chapter 3) was used to produce data relevant to the range of slenderness ratios used by each author, considering the initial imperfections wherever they are reported.

7.4.1 Comparison with *Pancholi's* tests

Pancholi [29] tested axially loaded pin-ended reinforced concrete columns having slenderness ratios between 30 and 79, under short and long-term loading conditions. Details of these columns are given in Table 7.5. Thirty seven columns were cast for the short-term programme, columns numbered 2, 3 and 7 were discarded because of unsatisfactory casting, column 21 for test 17 was damaged during test, therefore it was also discarded. Columns numbered 1, 4, 5 and 6 were pilot tests.

In preparing load eccentricity-curvature graphs, the actual materials' properties were used i.e f_y equals 300 and 278 N/mm^2, $\%A_s$ 5.44 and 4.52. Values of f_{cu} were chosen to cover the range of experimental figures. A value of d/h equal to 0.75 was used in the analysis. Taking account of these variables seven graphs were required. The initial imperfections were reported not to exceed 2 mm; this was converted to an eccentricity e_0 with relation to the column length. An average value for e_0 of 4.437×10^{-4}L was included in the buckling deflection-curvature graph. Results of the comparisons are provided in Tables 7.5(a) to 7.5(c).

The values of P_{test}/P_{theory} varied between 0.72 and 1.20 with a mean value of 0.89 and standard deviation of 0.13. In obtaining these values the pilot tests were excluded because the values of failure load are suspect. *Pancholi* in calculating his statistical parameters, in addition to excluding the pilot tests, also discarded columns 11, 13 and 25. It was noticed from the table that column 14, which was similar to column 13,

actually failed at a lower load, though it had higher concrete strength than column 13. No explanation was offered by the author. The same thing was noticed for columns 15 and 17, columns 22, 24 and 25 and columns 40 and 42.

With regard to E_c values, those which are given by the BS8110 expression adopted in the theory, were compared by the author with the experimental values obtained by *Pancholi* using 150×300 mm cylinders. Again the BS8110 expression gave higher results by up to 40%. This might justify the low P_{test}/P_{theory} ratios in Table 7.5.

To compare with *Pancholi's* long-term tests, eight load eccentricity-curvature graphs were required. Nine columns were tested under long-term loading conditions. Columns 5, 6 and 8 were excluded because they have been used previously for short-term tests. The creep coefficients used in the analysis of the remaining columns, as estimated using the 1970 CEB method [97], were 1.4 for columns 10 and 12, and 2 for columns 16, 23, 31 and 39. A value of 0.75 was used for d/h.

The loads reported for columns 16 and 39 for tests number 12C and 35C are the sustained loads; therefore they cannot be considered in the comparison. Column 16 was taken out of the rig to allow for further tests without failing it, while column 39 was tested at the end of the programme and was still under load by the time the work was completed. The failure load of column 31 (test 34C) is doubtful, as there is a discrepancy in the thesis between the values reported in a table and those shown in a figure for the load and its duration. P_{test}/P_{theory} for the remaining columns 10, 12 and 23 were found to be 1.12, 1.33 and 0.71 respectively. No reason is apparent why the last value does not follow the same pattern, particularly as the proposed theory was found to be generally conservative for long-term analysis.

These uncertainties make the likelihood of experimental error quite high and *Pancholi's* long-term work was not considered reliable enough to merit further consideration.

7.4.2 Comparison with *Dracos's* tests

A total of thirty six eccentrically pin-ended slender reinforced concrete columns were reported [5] as tested under short-term loading conditions. Details of these are to be found in Table 7.6. To generate load eccentricity-curvature graphs the actual materials' properties were used. A value of 0.75 was used for d/h in the analysis.

In order to minimise the number of graphs required the average values of f_y given by the author were used; these were 289 N/mm^2 for the range 273-315 N/mm^2 and 407 N/mm^2 for the range 395-410 N/mm^2. The reinforcement used throughout the investigation was mild steel bars having average value of E_s equal to 200 kN/mm^2. To

provide coverage for all the experimental values, seven graphs were required. Out-of-straightness, reported by the author not to exceed 2 mm, was expressed in terms of column length as $e_0=4.74\times10^{-4}L$, this eccentricity was then used in producing the buckling deflection-curvature graph.

Remarkable correlation between the proposed theory and the experiments can be seen from Table 7.6. The mean value of P_{test}/P_{theory} was 0.98 with a standard deviation of 0.09. These figures agree closely with the author's values. The minimum P_{test}/P_{theory} was 0.83 compared with *Dracos's* value of 0.78. It is of interest to note that the *Dracos* theory involves an iterative computer process for the solution of curvature, deflection and position of neutral axis along the full length of a column. When the speed and simplicity of the proposed theory based on graphical analysis is considered, this suggests its potential is significant.

The assumption of using only two values for f_y (289 and 407 N/mm^2) in the analysis, results in overestimation of the carrying capacity of columns having an actual value of f_y less than the one assumed. Consequently the ratio P_{test}/P_{theory} for these columns will decrease. Good agreement was noticed, when the values of static modulus of elasticity obtained experimentally by *Dracos* using 150×300 mm cylinders, were compared by the author with those employed in the proposed theory using the BS8110 expression.

Dracos tested four columns under variable sustained stress levels, for periods ranging between 509 and 625 days. No information was reported about the creep during these loading periods; therefore the 1970 CEB method [97] was employed to estimate the creep coefficient from the data available. Table 7.7 provides details of these columns. Columns C3 and C4 failed upon the application of the last incremental load, while columns C1 and C2 did not fail by the end of the investigation and as such the sustained load was instantaneously increased to failure.

An average value for the creep coefficient of 1.4 was used in the analysis of columns C1, C3 and C4 and a value of 1.0 was used for column C2. Considering the number of variables involved, six load eccentricity-curvature graphs were prepared.

Values of P_{test}/P_{theory} are to be found in Table 7.7. In general these values are less than one, which may be attributed to the approximate estimation of the creep coefficient. It is likely that this has affected the theoretical prediction, as shown in Chapter 6 (refer to Table 6.7). At such low values of creep coefficient (within the range 1 to 2.5) the influence of ϕ is more considerable on P_{theory} than at higher values (greater than 2.5). P_{test}/P_{theory} for column C3 does not follow the trend; the author mentioned that this column failed at an unusually high load. He believed that the loading plates slipped during

one of the increments; as a consequence the original applied load eccentricity may have been reduced.

7.4.3 Comparison with the *Ramu et al* tests

Ramu et al [32] tested thirty one eccentrically loaded pin-ended columns under sustained loads. For twelve columns the sustained load was increased stepwise in a final short-term test at the end of the loading period, while nineteen columns were left under load until failure occurred. These tests were performed in four groups; the variables studied were the eccentricity of load, the percentage of reinforcement, the age at first loading and the slenderness of the columns. Details of these groups are provided in Table 7.8. A value of 2.0 was chosen for the creep coefficient, as measured by the authors, in producing load eccentricity-curvature graphs. Ten graphs were required to cover the variables involved. The initial imperfection was taken as zero when producing the buckling deflection-curvature graph.

Two columns numbered 55 and 56 were excluded from the comparison because of an unsymmetrical distribution of reinforcement. As explained in Chapter 3 the program available applies to equal steel areas at both faces of the section. This leaves twenty nine columns for comparison. Columns 81, 44, 15, 16, 55, 65 and 66 were excluded by the authors without giving any reasons, therefore they are considered here. According to the BS8110 classification, column 74 is a short column (l_e/h=14.4); however, the proposed theory is capable of predicting the capacity of the column of any slenderness ratio.

The results are shown in Table 7.8. In general the theory appears to be conservative in predicting the long-term failure loads; the mean value of P_{test}/P_{theory} is 1.17 with a standard deviation of 0.14.

7.4.4 Comparison with *Goyal's* tests

As mentioned in Chapter 6 (see 6.6), *Goyal* [33] investigated the behaviour of twenty pin-ended eccentrically loaded columns subjected to sustained load for a period of six months and then to an increasing load, under short-term loading conditions, until failure occurred. Details of these columns are provided in Table 7.9.

Five load eccentricity-curvature graphs were required to carry out the comparison. A creep coefficient of 2.4 was used in the analysis as measured experimentally. The initial imperfections were not measured and a zero value was assumed in producing the buckling deflection-curvature graph. Results of the comparison are given in Table 7.9.

Reasonable agreement can be seen from the table between the predicted failure loads using the proposed theory and the experimental results. The average value for the ratio P_{test}/P_{theory} is 1.15 with a standard deviation of 0.07.

Columns O, P and Q were reported by the author to have been inadvertently sprinkled with water a few times during laboratory cleaning while stored in the laboratory. Therefore, *Goyal* believes that it is quite likely the concrete strength of these columns had increased. The control specimens which were not sprinkled with water showed no significant change in concrete strength. Column D which was under sustained load of 40 percent of the ultimate short-term capacity, failed at a lower load than the corresponding column C which was under 60% of the ultimate short-term capacity. The author justifies this by the possibility of a slight increase in the end eccentricity of column D over that intended, though he could not detect this by direct measurement.

The comparison with the *Goyal* tests was repeated assuming two different values for the initial imperfection: 5.68×10^{-4}L and 1.136×10^{-3}L. The mean value for the ratio P_{test}/P_{theory} in the first case was 1.18 with a standard deviation of 0.075, while in the second case the mean was 1.21 and the standard deviation 0.08. It appears that the influence of the initial imperfection is insignificant mainly because the slenderness ratios were not very high and the load was applied at relatively high eccentricities.

7.5 Conclusions

1- The proposed analytical theory closely estimates the failure loads obtained from the tests carried out under the present investigation on nineteen eccentrically loaded hinged reinforced concrete columns having slenderness ratios between 18 and 63, under both short-term and sustained loads (Tables 7.1 and 7.2), with reasonable safety margins in predicting the long-term capacity giving a mean of 1.26 for the ratio P_{test}/P_{theory} compared with 0.82 and 2.26 given by BS8110 and ACI318 respectively (Table 7.3).

2- The additional moment approach adopted in BS8110 gives a reasonable estimate of the short-term ultimate capacity of a slender column (Table 7.1), while it provides an upper bound solution to the long-term instability problem (Table 7.2). The design method is based on strength calculation, while the maximum load depends on stiffness upon which creep has a major influence. No allowance has been made for such effects in BS8110 resulting in an overestimation of the slender column long-term capacity. Hence, revisions to the British standard method regarding slender column design should be made.

3- The design method in the ACI318 Code based on the moment magnification approach gives a lower bound estimate of the slender column carrying capacity because of the nature of the EI expression (Tables 7.1, 7.2 and 7.3).

4- Through a series of comparisons covering a wide range of experiments on columns with different slenderness ratios under both short and long-term loads, the accuracy of the proposed theory based on graphical analysis has been further established. Investigating the statistical figures given in Tables 7.5 to 7.9 and summarized in Table 7.10, it is possible to see the potential usefulness in this accurate and simple prediction of column capacity without involving complicated numerical calculations. Individual short-term and long-term ratios (P_{test}/P_{theory}) deviated from 1.0. Discrepancies are attributed to uncertainties over test details, especially those related to the properties of the materials used and to the assumptions made in the theory in the process of performing the comparisons (i.e values assumed for f_y, d/h, E_c, ϕ and e_0).

Table 7.1 : Comparison of experimental and theoretical short-term buckling loads with Code recommendations.

Col.	P_{test} (kN)	P_{theory} (kN)	$\frac{P_{test}}{P_{theory}}$	P_{BS} (kN)	$\frac{P_{test}}{P_{BS}}$	P_{BS} K=1	$\frac{P_{test}}{P_{BS}}$ K=1	P_{ACI} (kN)	$\frac{P_{test}}{P_{ACI}}$
C1	450	439	1.03	521	0.86	409	1.10	379	1.19
C2	400	445	0.90	526	0.76	415	0.96	384	1.04
C3	210	172	1.22	201	1.04	180	1.17	121	1.74
C4	180	154	1.17	188	0.96	164	1.10	114	1.58
C5	360	386	0.93	419	0.86	357	1.01	244	1.48
C7	250	291	0.86	297	0.84	273	0.92	180	1.39
C9	205	237	0.87	227	0.90	221	0.93	141	1.45
C11	102	111	0.92	94	1.09	94	1.09	68	1.50
C14	85	97	0.87	75	1.13	75	1.13	58	1.47
C17	65	62	1.05	60	1.08	60	1.08	42	1.55
C19	45	41	1.10	37	1.22	37	1.22	27	1.67

Table 7.2 : Comparison of experimental and theoretical long-term buckling loads with Code recommendations.

Col.	P_{test} (kN)	P_{theory} (kN)	$\frac{P_{test}}{P_{theory}}$	P_{BS} (kN)	$\frac{P_{test}}{P_{BS}}$	P_{BS} K=1	$\frac{P_{test}}{P_{BS}}$ K=1	P_{BS} modified (kN)	$\frac{P_{test}}{P_{BS}}$ modified	P_{ACI} (kN)	$\frac{P_{test}}{P_{ACI}}$
C6	269	255	1.05	422	0.64	368	0.73	442	0.61	133	2.02
C8	225	194	1.16	313	0.72	297	0.76	333	0.68	100	2.25
C10	157	150	1.05	238	0.66	238	0.66	253	0.62	77	2.04
C12	88	65	1.35	94	0.94	94	0.94	100	0.88	36	2.44
C13	93	64	1.45	95	0.98	95	0.98	99	0.94	36	2.58
C15	73	55	1.33	81	0.90	81	0.90	82	0.89	32	2.28
C18	52	34	1.53	60	0.87	60	0.87	60	0.87	21	2.48
C20	28	24	1.17	32	0.88	32	0.88	34	0.82	14	2.00

Table 7.3 : Summary of Tables 7.1 and 7.2.

Tests ref.	Statistical parameter	$\frac{P_{test}}{P_{theory}}$	$\frac{P_{test}}{P_{BS}}$	$\frac{P_{test}}{P_{BS}}$ K=1	$\frac{P_{test}}{P_{BS}}$ modified	$\frac{P_{test}}{P_{ACI}}$
Short-term tests	Min. ratio	0.86	0.76	0.92	-	1.04
	Max. ratio	1.22	1.22	1.22	-	1.74
	Mean	0.99	0.98	1.07	-	1.46
	Standard deviation	0.13	0.14	0.10	-	0.20
	Coefficient of variation	13.1%	14.3%	9.35%	-	13.7%
	Number of tests	11				
Long-term tests	Min. ratio	1.05	0.64	0.66	0.61	2.00
	Max. ratio	1.53	0.98	0.98	0.94	2.58
	Mean	1.26	0.82	0.84	0.79	2.26
	Standard deviation	0.18	0.13	0.11	0.13	0.23
	Coefficient of variation	14.3%	15.9%	13.1%	16.5%	10.2%
	Number of tests	8				

Table 7.4 : Modulus of elasticity of concrete *.

Col. ref.	$E_{c\text{-}exp}$ (kN/mm^2)	$E_{c\text{-}BS}$ $5.5\sqrt{f_{cu}}$ (kN/mm^2)	$E_{c\text{-}ACI}$ (kN/mm^2)		$\frac{E_{c\text{-}exp}}{E_{c\text{-}BS}}$	$\frac{E_{c\text{-}exp}}{E_{c\text{-}ACI}}$ (1)	$\frac{E_{c\text{-}exp}}{E_{c\text{-}ACI}}$ (2)
			$w_c^{1.5}\ 0.043\sqrt{f'_c}$ (1)	$4700\sqrt{f'_c}$ (2)			
C1	30.6	39.7	32.6	30.4	0.77	0.94	1.01
C2	35.3	40.1	33.3	30.7	0.88	1.06	1.15
C3	32.8	41.6	34.1	31.8	0.79	0.96	1.03
C4	-	38.4	31.8	29.3	-	-	-
C5	34.4	41.3	34.2	31.6	0.83	1.01	1.09
C7	30.0	39.6	31.9	30.2	0.76	0.94	0.99
C9	32.5	39.7	31.8	30.3	0.82	1.02	1.07
C11	29.7	37.9	30.8	28.9	0.78	0.96	0.97
C14	30.8	40.0	32.8	30.6	0.77	0.94	1.01
C17	35.9	40.7	33.9	31.1	0.88	1.06	1.15
C19	34.6	38.9	31.9	29.8	0.89	1.08	1.16
C6	35.1	43.7	35.4	33.4	0.80	0.99	1.05
C8	36.2	43.4	35.9	33.2	0.83	1.01	1.09
C10	34.8	43.2	35.5	33.0	0.81	0.98	1.05
C12	35.4	40.1	32.5	30.7	0.88	1.09	1.15
C13	33.2	39.6	32.4	30.3	0.84	1.02	1.10
C15	36.1	45.0	37.0	34.4	0.80	0.98	1.05
C18	33.2	40.9	33.2	31.2	0.81	1.00	1.06
C20	34.2	40.9	33.4	31.2	0.84	1.02	1.10
			Minimum ratio		0.76	0.94	0.97
			Maximum ratio		0.89	1.09	1.16
			Mean		0.82	1.00	1.07
			Standard deviation		0.04	0.05	0.06
			Coefficient of variation		4.88%	5.00%	5.61%
			Number of tests		19		

* E_c values correspond to the time of testing the column.

Table 7.5(a) : Comparison with *Pancholi's* short-term tests.

Col. No.	Test No.	b (mm)	h (mm)	d/h	$\%A_s$	f_y (N/mm^2)	f_{cu} (N/mm^2)	e_i/h	l_e/h	P_{test} (kN)	$\frac{P_{test}}{P_{theory}}$ Pancholi	P_{theory} (kN)	$\frac{P_{test}}{P_{theory}}$
1	1	76	76	0.77	5.44	300	57.3	0	79	41.9	Pilot-test	29.2	1.43
2	-						Unsatisfactory cast - discarded						
3	-						Unsatisfactory cast - discarded						
4	2						34.8	0	79	15.0	Pilot-test	23.6	0.64
5	3	100	100	0.74	4.52	278	36.1	0	60.04	64.6	Pilot-test	71.0	0.91
6	4						49.3	0	60.04	48.8	Pilot-test	79.6	0.61
7	-						Unsatisfactory cast - discarded						
8	5						44.3	0	60.04	72.7	1.18	77.3	0.94
9	6						44.9	0	60.04	72.2	1.20	78.0	0.93
10	6C						43.1	0	60.04	44.8	Creep test		
11*	7	76	76	0.77	5.44	300	44.4	0	79	29.9	1.35	26.8	1.12
12	9C						47.2	0	79	18.9	Creep test		
13*	8						44.8	0	79	31.9	1.46	26.9	1.19
14	10						51.6	0	79	21.9	0.98	28.8	0.76
15	11	76	76	0.77	5.44	300	52.0	0	60.13	35.9	0.93	49.5	0.73

Table 7.5(b) : Comparison with *Pancholi's* short-term tests.

Col. No.	Test No.	b (mm)	h (mm)	d/h	%A_s	f_y (N/mm^2)	f_{cu} (N/mm^2)	e_i/h	l_e/h	P_{test} (kN)	$\frac{P_{test}}{P_{theory}}$ Pancholi	P_{theory} (kN)	$\frac{P_{test}}{P_{theory}}$
16	12C						57.0	0	60.13	Creep test			
17	13	76	76	0.77	5.44	300	45.2	0	60.13	39.9	1.04	46.0	0.87
18	14						51.1	0	60.13	39.9	0.99	49.2	0.81
19	15						47.7	0	65	31.9	0.92	39.6	0.81
20	16	76	76	0.77	5.44	300	51.2	0	65	37.9	1.13	40.5	0.94
21	-						Damaged during test - discarded						
43	17						32.3	0	65	31.9	0.99	33.7	0.95
22	18						43.6	0	70.09	33.9	1.17	33.2	1.02
23	22C	76	76	0.77	5.44	300	46.6	0	70.09	Creep test			
24	19						44.0	0	70.09	25.9	0.90	33.2	0.78
25*	20						38.3	0	70.09	37.9	1.42	31.7	1.20
26	21						41.3	0	75	19.9	0.86	27.7	0.72
27	23	76	76	0.77	5.44	300	42.6	0	75	21.9	0.96	28.1	0.78
28	24						40.3	0	75	21.9	0.92	27.5	0.80
29	25						39.8	0	50.13	53.8	1.02	60.7	0.89
30	26	76	76	0.77	5.44	300	37.3	0	50.13	51.8	1.00	59.0	0.88
31	34C						38.0	0	50.13	Creep test			

Table 7.5(c) : Comparison with *Pancholi's* short-term tests.

Col. No.	Test No.	b (mm)	h (mm)	d/h	$\%A_s$	f_y (N/mm^2)	f_{cu} (N/mm^2)	e_i/h	l_e/h	P_{test} (kN)	$\frac{P_{test}}{P_{theory}}$ Pancholi	P_{theory} (kN)	$\frac{P_{test}}{P_{theory}}$
32	27	76	76	0.77	5.44	300	42.6	0	50.13	59.8	1.13	62.6	0.96
33	28	100	100	0.74	4.52	278	40.2	0	50	89.7	1.13	100	0.90
34	29						35.3	0	50	71.7	0.92	93.8	0.76
35	30						39.0	0	50	85.7	1.06	98.7	0.87
36	31	100	100	0.74	4.52	278	41.5	0	40	115	0.97	150	0.77
37	32						46.7	0	40	120	0.93	160	0.75
38	33						42.8	0	40	120	0.97	152	0.79
39	35C						-	0	40	Creep test			
40	36	100	100	0.74	4.52	278	41.0	0	30	189	0.84	224	0.84
41	37						45.8	0	30	219	0.94	239	0.92
42	37						38.8	0	30	219	0.99	216	1.01

* Tests excluded by the author

Minimum ratio	0.84	0.72
Maximum ratio	1.20	1.20
Mean	1.00	0.89
Standard deviation	0.10	0.13
Coefficient of variation	10.0%	14.6%
Number of tests	26	29

Table 7.6(a) : Comparison with *Dracos's* short-term tests.

Test No.	b (mm)	h (mm)	d/h	$\%A_s$	f_y (N/mm^2)	f_{cu} (N/mm^2)	e_i/h	l_e/h	P_{test} (kN)	$\frac{P_{test}}{P_{theory}}$ Dracos	P_{theory} (kN)	$\frac{P_{test}}{P_{theory}}$
S1					313	44.6	0.096	28.9	160	0.99	163	0.98
S2					315	45.9	0.144	28.9	128	0.99	131	0.98
S3	104	104	0.73	4.20	277	40.4	0.096	28.9	155	1.02	156	0.99
S4					282	41.2	0.144	28.9	128	1.03	124	1.03
S5					278	40.1	0.096	28.9	174	1.10	156	1.12
S6					280	43.0	0.144	28.9	118	0.91	127	0.93
S7					280	40.6	0.144	38.5	68	0.87	79	0.86
S8					280	42.3	0.096	38.5	98	0.98	101	0.97
S9	104	104	0.73	4.20	280	44.9	0.144	38.5	78	0.98	82	0.95
S10					293	37.2	0.096	38.5	84	0.82	94.9	0.89
S11					293	38.7	0.144	38.5	82	1.03	77.4	1.06
S12					292	44.5	0.096	38.5	107	0.97	103	1.04
S13					283	36.7	0.144	48.1	45	0.90	50.8	0.89
S14					315	39.7	0.096	48.1	54	0.82	64.7	0.83
S15	104	104	0.73	4.20	300	33.5	0.096	48.1	66	0.97	59.7	1.11
S16					293	36.1	0.144	48.1	52	1.00	50.5	1.03
S17					300	43.0	0.096	48.1	56	0.85	67.4	0.83

Table 7.6(b) : Comparison with *Dracos's* short-term tests.

Test No.	b (mm)	h (mm)	d/h	$\%A_s$	f_y (N/mm^2)	f_{cu} (N/mm^2)	e_i/h	l_e/h	P_{test} (kN)	$\frac{P_{test}}{P_{theory}}$ Dracos	P_{theory} (kN)	$\frac{P_{test}}{P_{theory}}$
S18	104	104	0.73	4.20	300	40.8	0.144	48.1	52	0.96	53.2	0.98
S19	104	104	0.73	4.20	280	40.4	0.096	57.7	44	0.88	46.5	0.95
S20					282	41.3	0.144	57.7	36	0.95	36.5	0.99
S21					275	40.1	0.096	57.7	42	0.88	46.2	0.91
S22					275	40.3	0.144	57.7	30	0.83	36.1	0.83
S23					278	42.2	0.096	57.7	39	0.78	47.2	0.83
S24					280	40.1	0.144	57.7	34	0.90	35.9	0.95
S25					282	26.9	0.144	57.7	36	1.13	32.5	1.11
S26					273	25.8	0.144	57.7	30	1.00	32.2	0.93
S27					297	24.6	0.144	57.7	30	1.00	31.9	0.94
S28	104	104	0.73	4.20	304	25.3	0.144	48.1	44	1.00	43.8	1.00
S29					290	27.3	0.144	48.1	40	0.95	45.2	0.88
S30					300	29.6	0.144	48.1	48	1.04	46.7	1.03
S31	102	102	0.74	4.34	405	28.0	0.147	39.2	67	1.08	62.8	1.07
S32					410	26.8	0.147	39.2	60	0.97	61.5	0.98
S33					410	29.3	0.147	39.2	60	0.94	64.0	0.94
S34	102	102	0.74	4.34	410	31.5	0.147	29.4	115	1.11	101	1.14

Table 7.6(c) : Comparison with *Dracos's* short-term tests.

Test No.	b (mm)	h (mm)	d/h	%A_s	f_y (N/mm^2)	f_{cu} (N/mm^2)	e_i/h	l_e/h	P_{test} (kN)	$\frac{P_{test}}{P_{theory}}$ Dracos	P_{theory} (kN)	$\frac{P_{test}}{P_{theory}}$
S35	102	102	0.74	4.34	395	34.2	0.147	29.4	106	0.98	106	1.00
S36					410	27.5	0.147	29.4	108	1.13	94.6	1.14

Minimum ratio	0.78	0.83
Maximum ratio	1.13	1.14
Mean	0.97	0.98
Standard deviation	0.09	0.09
Coefficient of variation	9.28%	9.18%
Number of tests	36	36

Table 7.7 : Comparison with *Dracos's* long-term tests.

Test No.	b (mm)	h (mm)	d/h	%A_s	f_y (N/mm^2)	f_{cu} (N/mm^2)	e_i/h	l_e/h	P_{test} (kN)	$\frac{P_{test}}{P_{theory}}$ Dracos	P_{theory} (kN)	$\frac{P_{test}}{P_{theory}}$
C1	104	104	0.73	4.20	300	38.9	0.096	38.5	54.7	1.05	62.6	0.87
C2					414	36.4	0.144	38.5	58.6	1.27	59.5	0.98
C3					355	34.6	0.096	48.1	51.1	1.55	38.9	1.31
C4					278	37.2	0.144	48.1	34.4	1.07	35.9	0.96

Table 7.8(a) : Comparison with *Ramu's* long-term tests.

Gr.	Col. No.	Loading†	b (mm)	h (mm)	d/h	%A_s	l_e/h	f_y (N/mm^2)	f_{cu} (N/mm^2)	e_i/h	t_0 ** (days)	Sustained load (kN)	P_{test} (kN)	P_{theory} (kN)	$\frac{P_{test}}{P_{theory}}$
	61	L							42.7	0.00	28	659	659	520	1.27
	81*	L							38.5	0.00	28	612	612	489	1.25
	42	L							31.3	0.033	28	416	416	359	1.16
	43	L							32.4	0.033	28	435	435	364	1.20
	44*	L							26.8	0.033	28	436	436	334	1.31
	51	L-S							54.4	0.033	28	438	500	463	1.08
	11	L-S							38.2	0.100	28	151	389	278	1.40
1	12	L-S	250	150	0.83	1.68	28.9	452	41.7	0.100	28	234	295	287	1.03
	13	L							34.2	0.100	28	311	311	268	1.16
	15*	L							36.0	0.100	28	349	349	273	1.28
	16*	L							27.3	0.100	28	330	330	247	1.34
	21	L-S							34.8	0.100	28	266	308	270	1.14
	22	L							35.9	0.250	28	189	189	191	0.99
	23	L-S							36.6	0.250	28	140	185	192	0.96
	25	L-S							29.3	0.250	28	164	194	178	1.09

Table 7.8(b) : Comparison with *Ramu's* long-term tests.

Gr.	Col. No.	Loading†	b (mm)	h (mm)	d/h	%A_s	l_e/h	f_y (N/mm^2)	f_{cu} (N/mm^2)	e_i/h	t_0 ** (days)	Sustained load (kN)	P_{test} (kN)	P_{theory} (kN)	$\frac{P_{test}}{P_{theory}}$
1	52	L-S	250	150	0.83	1.68	28.9	452	54.4	0.25	28	189	224	178	1.26
	32	L-S							35.8	1.00	28	70	78	85.5	0.91
	33	L-S							34.6	1.00	28	64 73	83	85.1	0.98
2	55*	L	250	150	0.83	4.30	28.9	518	39.5	0.033	28	435	435	Unsymmetrical steel	
	56	L							45.5	0.250	28	187	187	Unsymmetrical steel	
	83	L							39.1	0.00	28	775	775	692	1.12
	64	L							33.0	0.033	27	444 643	643	538	1.20
	63	L-S							49.4	0.250	28	192 351	362	373	0.97
3	54	L	250	150	0.83	1.68	28.9	452	42.0	0.033	16	440	440	404	1.09
	62	L							45.0	0.033	56	437 496	496	420	1.18
4	65*	L	250	100	0.80	1.70	43.3	452	30.5	0.05	28	159	159	109	1.46
	71	L							40.0	0.05	28	140	140	120	1.16
	82	L-S							45.0	0.05	28	103	178	125	1.42
	66*	L							31.0	0.375	28	67	67	52.4	1.28

Table 7.8(c) : Comparison with *Ramu's* long-term tests.

Gr.	Col. No.	Loading†	b (mm)	h (mm)	d/h	%A_s	l_e/h	f_y (N/mm^2)	f_{cu} (N/mm^2)	e_i/h	t_0 ** (days)	Sustained load (kN)	P_{test} (kN)	P_{theory} (kN)	$\frac{P_{test}}{P_{theory}}$
4	72	L	250	100	0.80	1.70	43.3	452	39.8	0.375	28	62	62	54.9	1.13
	74	L-S		150	0.83	1.68	14.4		40.6	0.033	28	651	922	877	1.05

† The load classifications are as follows:

L = Long-term load maintained to failure.

L-S = Long-term load followed by short-term test to failure.

* Tests excluded by the authors.

** t_0 = age at first loading.

Minimum ratio	0.91
Maximum ratio	1.46
Mean	1.17
Standard deviation	0.14
Coefficient of variation	12.0%
Number of tests	29

Table 7.9(a) : Comparison with *Goyal's* long-term tests.

Col.	b=h (mm)	d/h	$\%A_s$	f_y (N/mm^2)	f_{cu} (N/mm^2)	e_i/h	l_e/h	Sustained load (kN)	% of ult. short-term	P_{test} (kN)	$\frac{P_{test}}{P_{theory}}$ Goyal	P_{theory} (kN)	$\frac{P_{test}}{P_{theory}}$
A	76.2	0.83	2.44	352	33.6	0.50	24	19.9	60	32.0	0.99	29.2	1.09
B					33.6	0.50	24	13.3	40	32.3	0.97	29.2	1.11
C					36.6	0.333	24	26.7	60	42.9	0.96	38.2	1.12
D					36.6	0.333	24	17.8	40	40.4	0.88	38.2	1.06
E					38.4	0.167	24	40.0	60	59.4	1.01	52.5	1.13
F					38.4	0.167	24	26.7	40	59.3	0.91	52.5	1.13
G					39.1	0.250	24	33.4	60	50.0	1.01	44.8	1.12
H					39.1	0.250	24	22.2	40	49.8	0.95	44.8	1.11
I			1.70	310	39.7	0.167	24	36.0	60	44.3	0.98	44.2	1.00
J					39.7	0.167	24	24.0	40	58.2	1.05	44.2	1.32
K					40.5	0.250	24	27.9	60	40.9	1.04	36.4	1.12
L					40.5	0.250	24	18.6	40	43.8	1.01	36.4	1.20
M					40.1	0.333	24	22.2	60	36.4	1.08	30.5	1.19
N					40.1	0.333	24	14.8	40	36.0	1.00	30.5	1.18
O	76.2	0.83	1.70	310	41.3	0.167	16	49.4	60	89.2	1.26	70.0	1.27

Table 7.9(b) : Comparison with *Goyal's* long-term tests.

Col.	b=h (mm)	d/h	$\%A_s$	f_y (N/mm^2)	f_{cu} (N/mm^2)	e_i/h	l_e/h	Sustained load (kN)	% of ult. short-term	P_{test} (kN)	$\frac{P_{test}}{P_{theory}}$ Goyal	P_{theory} (kN)	$\frac{P_{test}}{P_{theory}}$
P	76.2	0.83	1.70	310	41.3	0.250	16	38.7	60	67.1	1.15	56.2	1.19
Q					33.6	0.333	16	30.7	60	50.2	1.13	42.5	1.18
R					37.5	0.167	36	20.0	60	24.1	0.94	22.1	1.09
S					36.5	0.250	36	14.0	60	21.6	0.94	19.0	1.14
T					36.2	0.333	36	11.7	60	19.7	0.99	16.5	1.19

Minimum ratio	0.88	1.00
Maximum ratio	1.26	1.32
Mean	1.01	1.15
Standard deviation	0.089	0.07
Coefficient of variation	8.81%	6.09%
Number of tests	20	20

Table 7.10 : Summary of Tables 7.5 to 7.9 for P_{test}/P_{theory}*.

Statistical parameter	Short-term tests	Long-term tests
Minimum ratio	0.72	0.87
Maximum ratio	1.20	1.46
Mean	0.94	1.15
Standard deviation	0.12	0.13
Coefficient of variation	12.8%	11.3%
Number of tests	65	53

* P_{test} = experimental buckling load obtained by other researchers.

P_{theory} = theoretical buckling load obtained by the proposed theory.

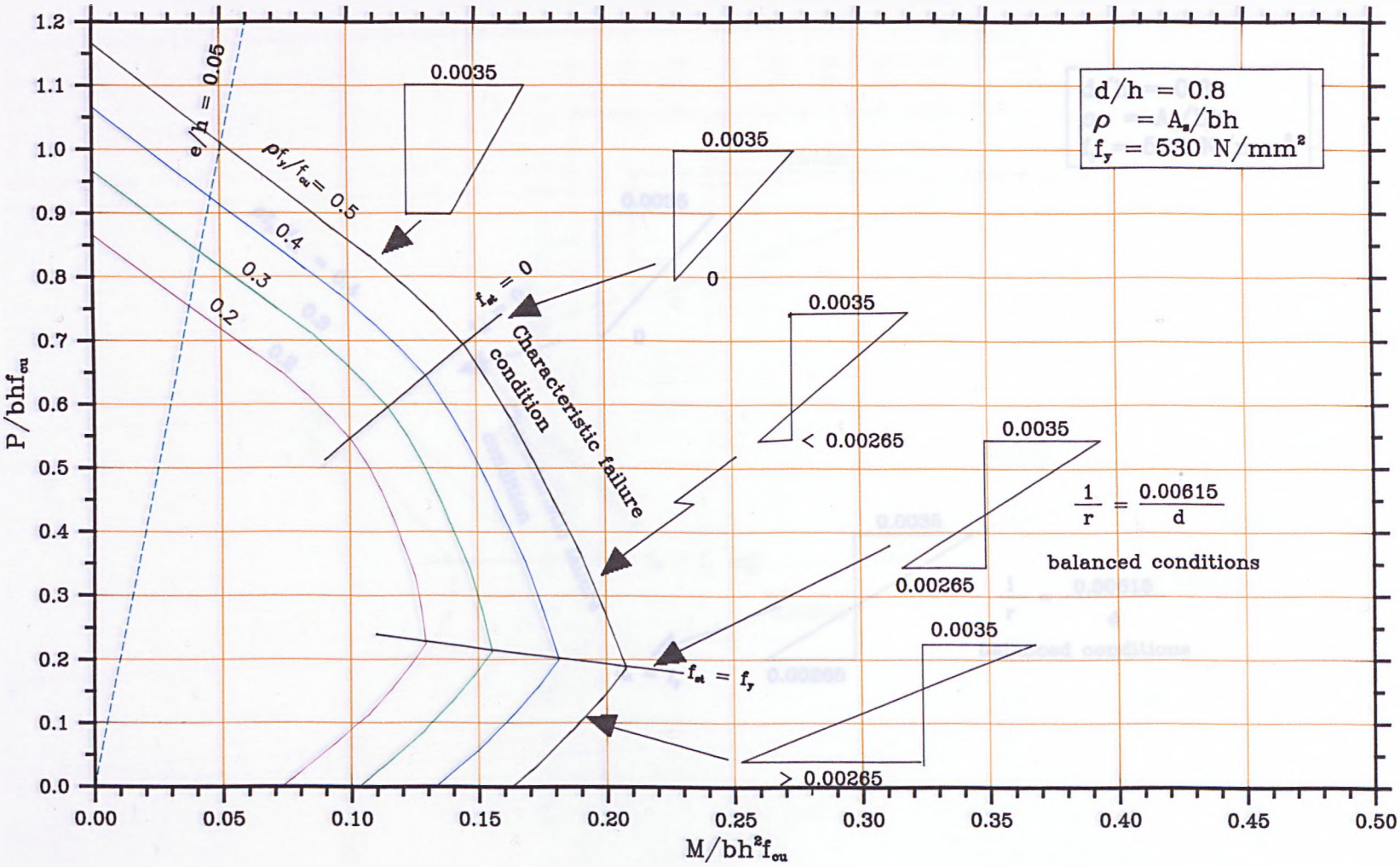

Fig.7.1 BS8110 interaction diagram for comparison with the short-term tests.

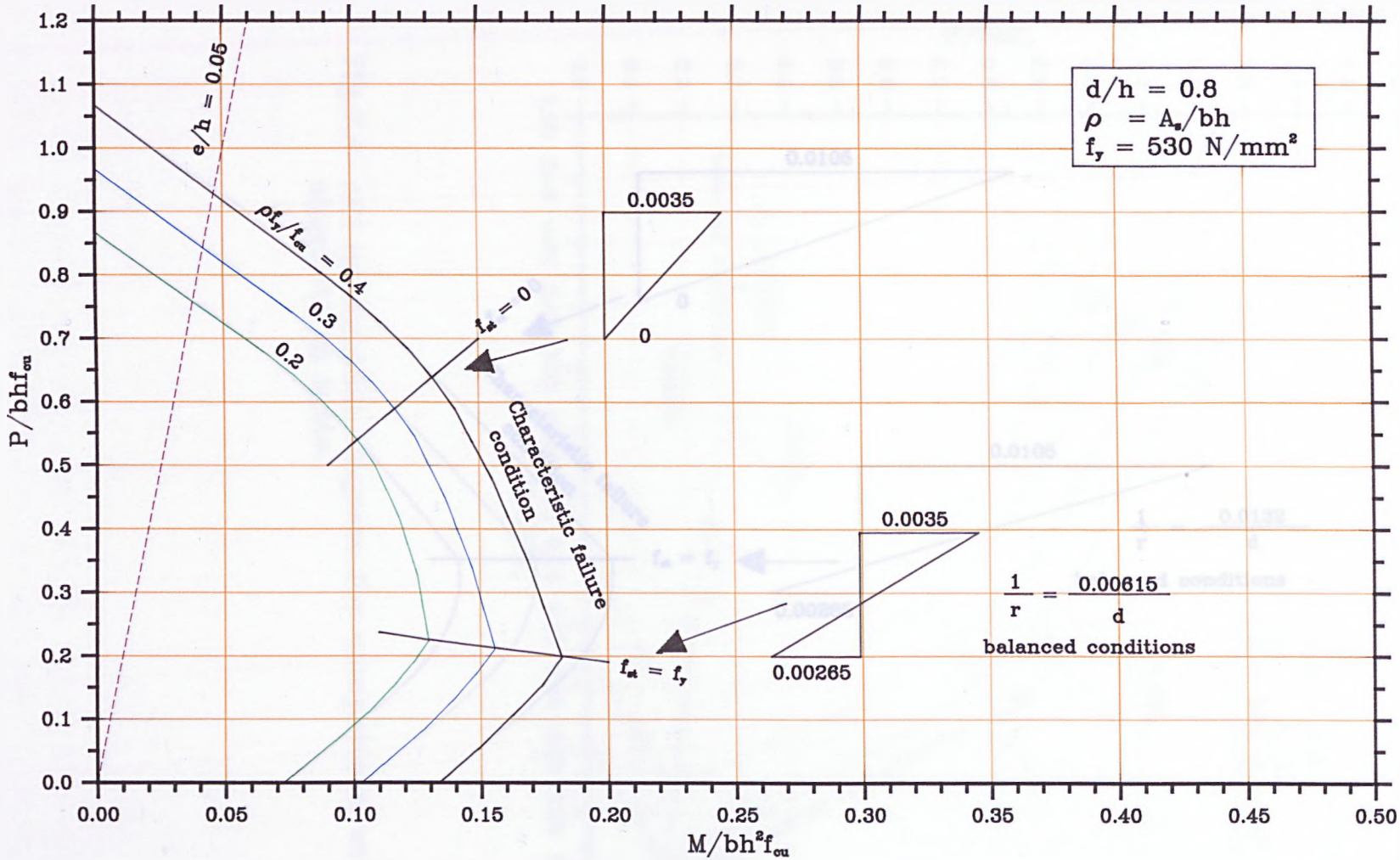

Fig.7.2 BS8110 interaction diagram for comparison with the long-term tests.

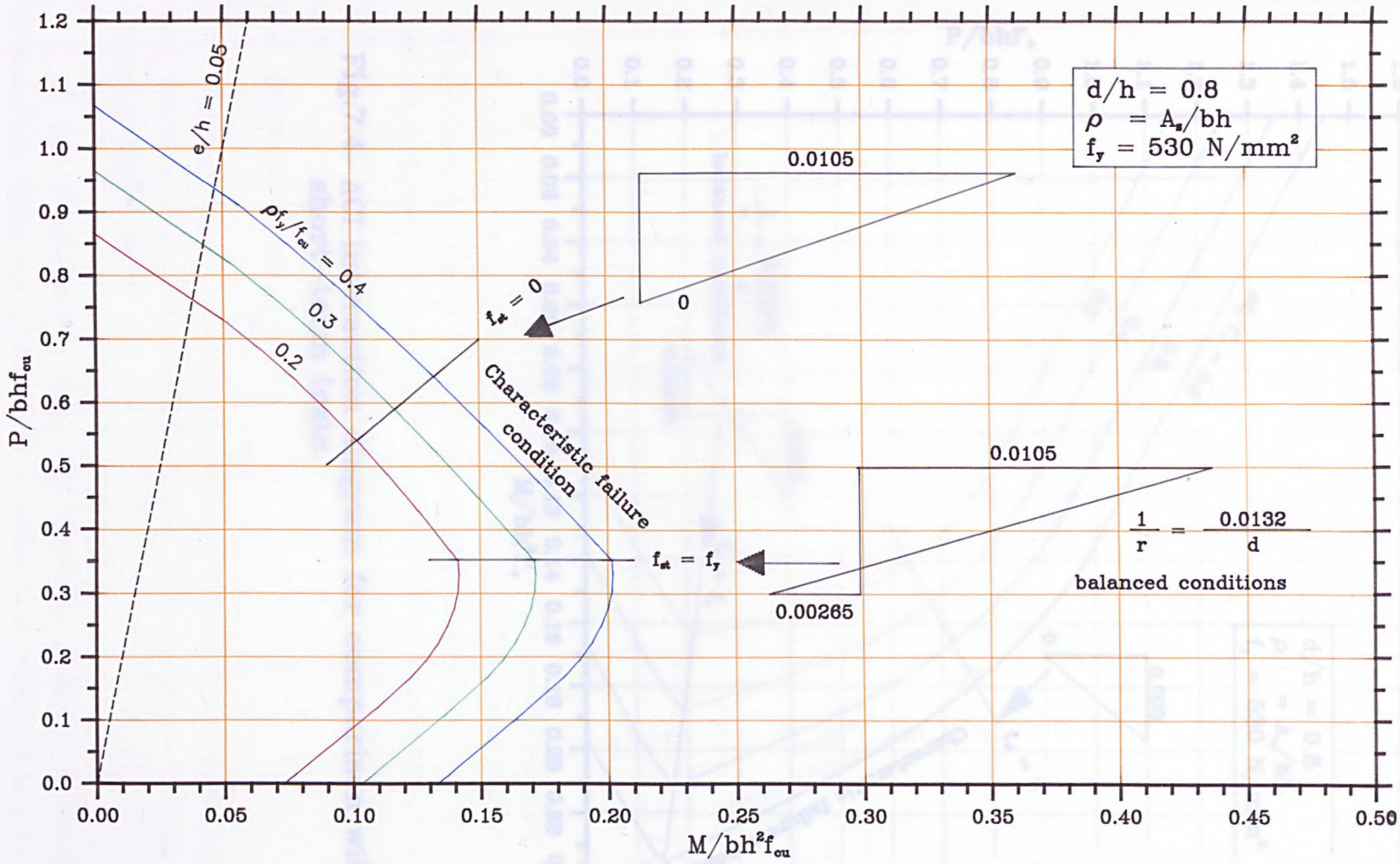

Fig.7.3 Modified BS8110 interaction diagram for comparison with the long-term tests.

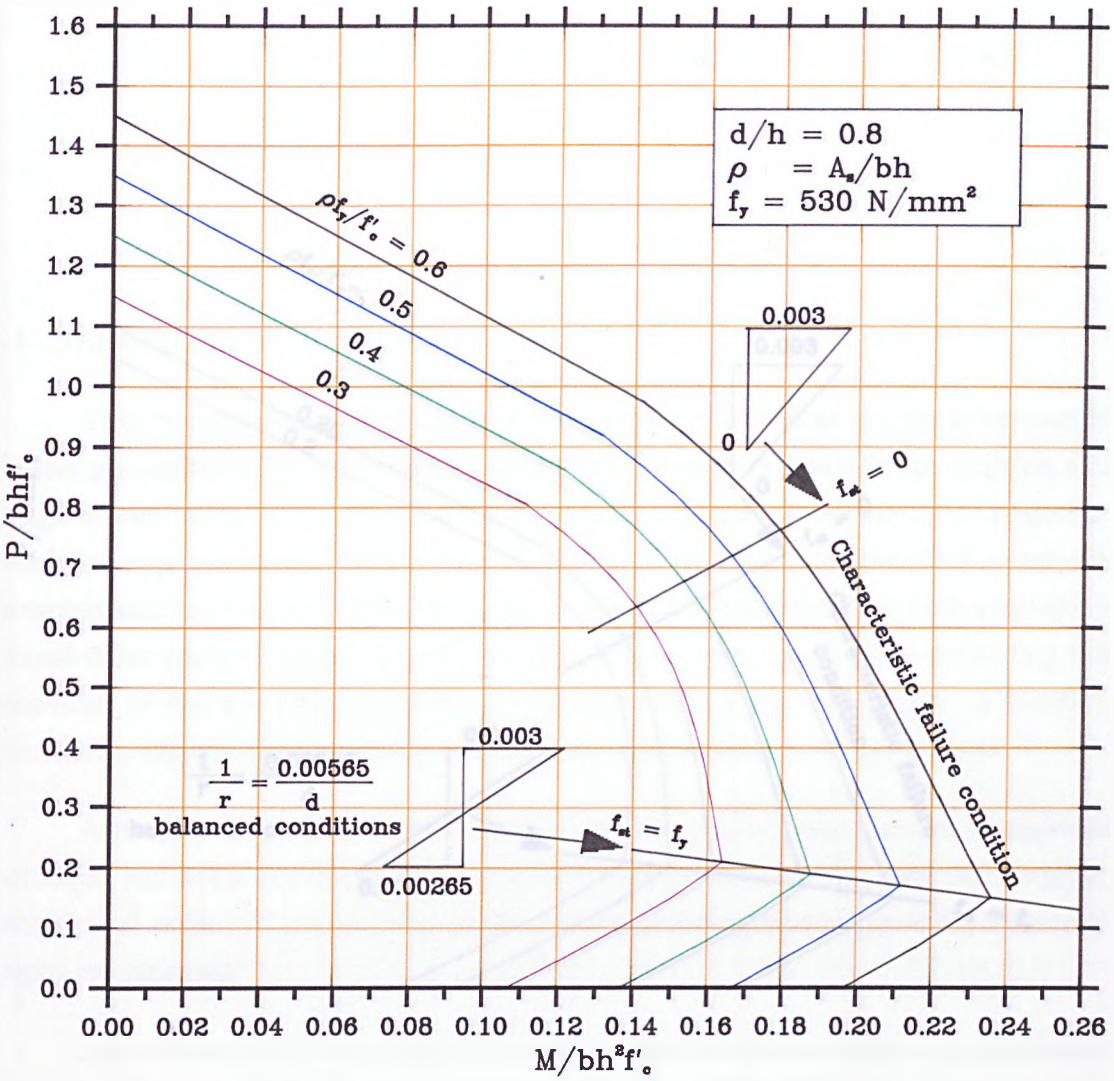

Fig.7.4 ACI interaction diagram for comparison with the short-term tests.

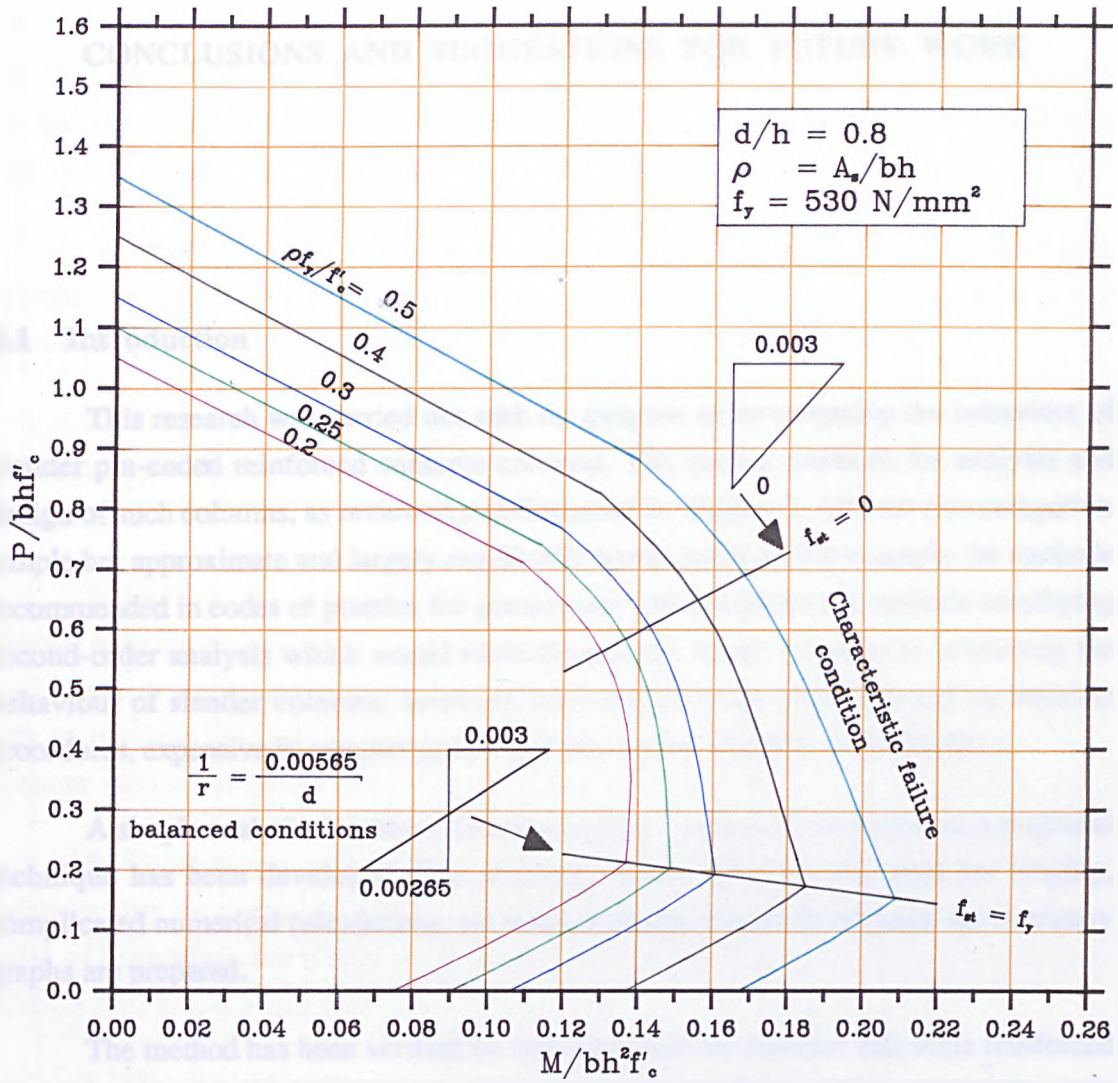

Fig.7.5 ACI interaction diagram for comparison with the long-term tests.

CHAPTER EIGHT

CONCLUSIONS AND SUGGESTIONS FOR FUTURE WORK

8.1 Introduction

This research was carried out with the purpose of investigating the behaviour of slender pin-ended reinforced concrete columns. The current methods for analysis and design of such columns, as reviewed and discussed in Chapter 2, fall into two categories: simple but approximate and largely empirically-based methods (for example the methods recommended in codes of practice for general use) and computerized methods employing second-order analysis which would normally provide better accuracy in predicting the behaviour of slender columns; however, such methods are usually based on iterative procedures, expensive in computing time and not readily available to the designer.

A simple analytical method, founded on *Beal's* approach and based on a graphical technique has been developed. The proposed theory removes the need for lengthy, complicated numerical calculations, yet is accurate and simple to use once the necessary graphs are prepared.

The method has been verified by intensive tests on nineteen full-scale reinforced concrete columns with slenderness ratios between 18 and 63, loaded eccentrically under short and long-term conditions. The method compares reasonably well with the results of these tests and other data covering a wide range of columns. It also shows a significant improvement over the design methods adopted in BS8110: 1985 and ACI318-89.

8.2 Summary of conclusions

Detailed discussions and full coverage of the theoretical and experimental results were presented in previous Chapters. A brief summary of the investigation and conclusions is given below:

1- The proposed method enables rapid, accurate analysis of slender pin-ended reinforced concrete columns, concentrically or eccentrically loaded. It takes account of the non-linear properties of concrete and allows prediction of the column capacity without iteration or resort to simplification of section behaviour.

2- The theory involves the transformation of standard graphs of moment against curvature into graphs of load eccentricity versus curvature in terms of the capacity ratio (P/P_0). A second set of graphs is required to relate section curvature to load eccentricity in terms of the slenderness ratio (l_e/h). Once these graphs are prepared, it is straightforward to determine section capacity. At the point of instability, the total eccentricity at mid-height can also be easily determined (refer to Chapter 3).

3- Programs of wide application have been developed for use in a main-frame computer to generate the data and plot the graphs. These are given in Appendix A and present no computational difficulties in terms of run time or storage space.

4- The stress-strain curve for concrete was modified to account for creep effects under sustained load; thus the reduction in column capacity due to long-term loading can be predicted.

5- Casting, handling and testing very slender reinforced concrete columns require special techniques and skills and present several difficulties. During the course of the experimental work, this resulted in the design and construction of a special mould and rigs to perform the tests as originally planned. Precautions were taken to ensure an accurate standard in taking measurements and tests utilized novel techniques (Chapter 4).

6- Comparisons with test results showed that the theoretical approach closely estimated the short-term buckling loads and the value of mid-height eccentricity at the point of instability; but tended to be conservative in predicting the long-term capacity (Tables 5.3, 5.4, 6.3 and 6.4).

7- The experimental results substantiated the fact that instability is the primary failure criterion for slender columns. Material failure then follows, which for slenderness ratios of 33.6 and above requires considerable bending to occur.

8- Instability failures occurred at relatively low concrete compressive strains of the order of 0.001-0.002 (Figures 5.2, 5.3 and 6.1).

9- The experimental results substantiated the following assumptions made in the proposed theory:

- Linear strain distribution across the section (Figs.5.4 and 6.3)
- The deflected shape of a pin-ended column follows a sine curve as it buckles (Figs.5.6 and 6.6)
- Single curvature bending in X direction is valid, as bending in Y direction was found to be negligible up to the point of instability.

Since the theory predicts the mid-height eccentricity at the point of instability, using the sine curve formula enables the profile of the column to be obtained.

10- Initial imperfections are inevitable during column construction; this was allowed for in the theory, in the form of an additional eccentricity at the column mid-height and was expressed in terms of column length. The results obtained (Table 5.7) suggest that the value of the initial imperfections, however small, should be considered particularly in the case of low end moments and high slenderness ratios.

11- A comparative study of the effects of the static modulus of elasticity of concrete (Table 5.6) and the creep coefficient (Table 6.7) on the theoretical results, emphasised their influence. It confirmed that the reduction in E_c value due to creep should be allowed for in long-term analysis.

12- For sustained loads equal to 60% of the short-term ultimate capacity, a considerable reduction in column short-term strength may occur, which can be as high as 40% (Table 6.5).

13- For sustained loads equal to 60% of the short-term ultimate capacity, the lateral deflection at the column mid-height, can typically reach a magnitude of about 4 times the value on initial loading (Figures 6.4(a), 6.5(a) and 6.6(a)); thus reflecting the size of secondary moments attainable in slender columns due to creep.

14- The design method adopted in BS8110, employing the additional moment concept, was found to be unsafe in predicting the long-term buckling loads of the columns tested (Tables 7.2 and 7.3). This is due to the fact that the BS8110 approach is based on strength calculations, which are almost irrelevant for slender columns (see 7 and 8 above), and does not allow for the reduction in column stiffness due to creep.

15- The conservative nature of the ACI318 recommendations for columns with small end eccentricities was demonstrated when compared with the experimental buckling loads obtained in this investigation, for short and long term tests (Tables 7.1, 7.2 and 7.3). However, as concluded by other investigators [60], the ACI318 procedure produces unconservative results for slender columns subjected to high end eccentricities.

16- There is no distinction in the graphical analysis between short and slender columns. For all slenderness ratios, capacity reduction factors can be obtained, which are sensible and realistic. This is in contrast to Codes of Practice, where a clear demarcation is specified between the two types of column, giving a sharp decrease in strength at the boundary value for slenderness.

17- The accuracy of the proposed approach is further confirmed when applied to a wide range of columns tested by other investigators (Table 7.10).

8.3 Suggestions for future work

In terms of the objective of developing a viable design tool for slender reinforced concrete columns, the basic steps have been established and their accuracy and validity are confirmed analytically and experimentally. The following areas of work are recommended for future investigation to fully achieve this aim:

1- The variability of the capacity reduction factor (P/P_0) due to the following parameters: f_{cu}, f_y, $\%A_s$, e_0, e_i and ϕ.

2- The behaviour of reinforced concrete columns with different reinforcement layouts, need to be analysed to see how this affects the reduction in capacity.

3- Different loading patterns (i.e size and sign of end eccentricities) need to be considered in the extended analysis.

4- The behaviour of reinforced concrete columns with different cross-section shapes, in particular, circular columns.

5- The method so far deals with bending about one axis, which is the normal design situation, however, the case of biaxial bending requires investigation.

6- Computerizing the graph overlay process for capacity prediction of slender columns.

7- The scope of the method could be further widened to deal with various types of compression members such as slender concrete deep beams, plain and lightly reinforced concrete walls, brickwork walls and structures with solid steel sections.

8- In view of the capacity reduction due to sustained loads and the limited number of tests carried out to date, particularly on full-scale columns under long-term loading conditions, further tests are essential to provide data on the role of creep in reducing the long-term capacity.

9- The behaviour of slender reinforced concrete columns as frame members with attention to moment redistribution at column ends. Experimental work on this type of column would be of considerable importance.

10- The adequacy of a proposed cross-section can be directly checked against failure using the present analytical method. Future work is expected to yield capacity

reduction factors for general design purposes, perhaps as a function of f_{cu}, l_e/h, $\%A_s$ and e_i. As a guideline for the design of slender reinforced pin-ended columns, these reduction factors can be applied to the load and moment obtained from first order elastic analysis to determine the required area of reinforcement using interaction diagrams.

11- More information is required on:

- Creep under tension and in bending.

- Effect of reinforcement on time-dependent deformations.

- Size of initial imperfections which occur in practice.

REFERENCES

[1]. **Mirsa, S.A.,** "Flexural stiffness of rectangular reinforced concrete columns", *ACI Structural Journal,* Vol.87, No.4, July-August 1990, pp.425-435.

[2]. **Rangan, B.V.,** "Strength of reinforced concrete slender columns", *ACI Structural Journal,* Vol.87, No.1, January-February 1990, pp.32-38.

[3]. **MacGregor, J.G. Oelhafen, U.H. and Hage, S.E.,** "A re-examination of the EI value for slender columns", *ACI SP-50,* 1975, pp.1-40.

[4]. **Jackson, P.A.,** "Slender concrete bridge piers to BS5400", *The Journal of the Institution of Highways and Transportation,* January 1988, pp.21-25.

[5]. **Dracos, A.,** *"Long slender reinforced concrete columns"*, Ph.D. Thesis, University of Bradford, August.1982.

[6]. **British Standards Institution,** *"BS8110 Structural use of concrete"*, Part 1: Code of Practice for design and construction, BSI, London, 1985.

[7]. **ACI committee 318,** *"Building Code Requirements for Reinforced Concrete (ACI318-89) and Commentary-ACI318R-89"*, American Concrete Institute, Detroit, 1989.

[8]. **Todhunter, I. and Pearson, K.,** *"A history of the theory of elasticity and of the strength of materials"*, Cambridge University Press, Cambridge, 1886-1893. (republished by Dover Publications, New York, 1960).

[9]. **Timoshenko, S.P.,** *"History of strength of materials"*, McGraw-Hill, New York, 1953.

[10]. **Love, A.E.H.,** *"A treatise on the mathematical theory of elasticity"*, 4th edition, Cambridge University Press, Cambridge, 1927. (republished by Dover Press, New York, 1944).

[11]. **Salmon, E.H.,** *"Columns"* Oxford Technical Publications, Frowde, London, 1921.

[12]. **Osgood, W.R.,** *"Double-modulus theory of column action"*, Civil Engineering, Vol.5, No.3, March 1935, pp.173-175.

[13]. **Timoshenko, S.P.,** *"Theory of elastic stability"*, 2nd edition, McGraw-Hill, New York & London, 1961.

[14]. **Bleich, F.,** *"Buckling strength of metal structures"*, McGraw-Hill, New York, 1952.

[15]. **Johnston, B.G.,** "Column buckling theory: Historic highlights", *Journal of Structural Engineering ASCE,* Vol.109, No.9, September 1983, pp.2086-2096.

[16]. **Baumann, O.,** *"Die Knickung der Eisenbeton-Säulen"*, (Buckling of reinforced concrete columns), Zürich, Eidgenossische Materialsprüfungsanstalt an der Eidgenossiche Technischen Hochschule, Zürich, 1934, Bericht No.89.

[17]. **Thomas, F.G.,** *"The strength of long reinforced concrete columns in short period tests to destruction"*, Building Research Station Technical Paper No.24, Studies in reinforced concrete No.7, London, HMSO, 1939, pp.29.

[18]. **Hognestad, E.,** *"A study of combined bending and axial load in the reinforced concrete members"*, Engineering Experiment Station, Bulletin No.399, University of Illinois, Urbana, 1951.

[19]. **Ernst, G.C. Hromadik, J.J. and Riveland, A.R.,** *"Inelastic buckling of plain and reinforced concrete columns, plates and shells"*, Engineering Experiment Station, Bulletin No.3, University of Nebraska, Lincoln, 1953, pp.66.

[20]. **Broms, B. and Viest, I.M.,** "Ultimate strength analysis of long hinged reinforced concrete columns", *Journal of the Structural Division, Proceedings ASCE,* Vol.84, No.ST1, January 1958, pp.1510-1, 1510-38.

[21]. **Pfrang, E.O. and Siess, C.P.,** "Predicting structural behaviour analytically", *Journal of the Structural Division, Proceedings ASCE,* Vol.90, No.ST5, October 1964, pp.99-111.

[22]. **Pfrang, E.O. Siess, C.P. and Sozen, M.A.,** "Load-moment-curvature characteristics of reinforced concrete cross-sections", *ACI Journal, Proceedings* Vol.61, No.7, July 1964, pp.763-777.

[23]. **Breen, J.E.,** *"Computer use in studies of frames with long columns"*, in Proceedings of the International symposium on Flexural mechanics of reinforced concrete, ACI SP-12, Miami, Florida, November 1964, pp.535-556.

[24]. **Cranston, W.B.,** "A computer method for the analysis of restrained columns", *Cement and Concrete Association.* Technical Report TRA 402, April 1967.

[25]. Chang, W.F. and Ferguson, P.M., "Long hinged reinforced concrete columns", *ACI Journal, Proceedings* Vol.60, No.1, January 1963, pp.1-25.

[26]. Sáenz, L.P. and Martin, I., "Test of reinforced concrete columns with high slenderness ratios", *ACI Journal, Proceedings* Vol.60, No.5, May 1963, pp.589-616.

[27]. Breen, J.E. and Ferguson, P.M., "The restrained long concrete column as a part of a rectangular frame", *ACI Journal, Proceedings* Vol.61, No.5, May 1964, pp.563-587.

[28]. Pannell, F.N. and Robinson, J.L., "Slender reinforced concrete columns with biaxial eccentricity of loading", *Magazine of Concrete Research,* Vol.20, No.65, December 1968, pp.195-204.

[29]. Pancholi, V.R., *"The instability of slender reinforced concrete columns"*, Ph.D. Thesis, University of Bradford, September 1977.

[30]. Schofield, D., *"Slender reinforced concrete columns under load and moment"*, Ph.D. Thesis, University of Bradford, August 1983.

[31]. Green, R. and Breen, J.E., "Eccentrically loaded concrete columns under sustained load", *ACI Journal, Proceedings* Vol.66, No.11, November 1969, pp.866-874.

[32]. Ramu, P. Grenacher, M. Baumann, M. and Thürlimann, B., *"Versuche an gelenkig gelagerten stahlbetonstützen unter dauerlast"*, (Long-term tests on pin-ended reinforced concrete columns), Zürich, Institut für Baustatik Eidgenössische Technische Hochschule, May 1969, Bericht No.6418-1.

[33]. Goyal, B.B., *"Ultimate strength of reinforced concrete columns under sustained load"*, Ph.D. Thesis, University of Dundee, 1970.

[34]. Hellesland, J. and Green, R., "Sustained and cyclic loading of concrete columns", *Journal of the Structural Division, Proceedings ASCE,* Vol.97, No.ST4, April 1971, PP.1113-1128.

[35]. Drysdale, R.G. and Huggins, M.W., "Sustained biaxial load on slender concrete columns", *Journal of the Structural Division, Proceedings ASCE,* Vol.97, No.ST5, May 1971, PP.1423-1443.

[36]. Cranston, W.B. and Sturrock, R.D., *"Lateral instability of slender reinforced concrete columns"*, Experimental analysis of instability problems on reduced and full-scale models. RILEM International Symposium, Buenos Aires, 1971, Theme 1, pp.117-141.

[37]. Cranston, W.B., "Analysis and design of reinforced concrete columns", *Cement and Concrete Association,* Research Report 20, 1972.

[38]. British Standards Institution, *"CP110 The structural use of concrete"*, Part 1: Design, materials and workmanship, BSI, London, 1972.

[39]. Green, R. and Hellesland, J., "Repeated loading tests of reinforced concrete columns", *ACI SP50-3,* 1975, pp.67-91.

[40]. Blomeier, G.A. and Breen, J.E., "Effect of yielding of restraint on slender concrete columns with sidesway prevented", *ACI SP50-2,* 1975, pp.41-65.

[41]. MacGregor, J.G. and Hage, S.E., "Stability analysis and design of concrete frames", *Journal of the Structural Division, Proceedings ASCE,* Vol.103, No.ST10, October 1977, PP.1953-1970.

[42]. Behan, J.E., "Slender reinforced concrete columns: Creep buckling", *Proceedings, Sixth Australasian Conference on the Mechanics of Structures and Materials,* Christchurch, New Zealand, August 1977, pp.238-245.

[43]. Wu, H. and Huggins, M.W., "Size and sustained load effects in concrete columns", *Journal of the Structural Division, Proceedings ASCE,* Vol.103, No.ST3, March 1977, pp 493-506.

[44]. Wood, B.R. Beaulieu, D. and Adams, P.F., "Column design by P-Delta method", *Journal of the Structural Division, Proceedings ASCE,* Vol.102, No.ST2, February 1976, PP.411-427.

[45]. Wood, B.R. Beaulieu, D. and Adams, P.F., "Further aspects of design by P-Delta method", *Journal of the Structural Division, Proceedings ASCE,* Vol.102, No.ST3, March 1976, PP.487-500.

[46]. Behan, J.E. and O'Connor, C., "Creep buckling of reinforced concrete columns", *Journal of the Structural Division, Proceedings ASCE,* Vol.108, No.ST12, December 1982, PP.2799-2818.

[47]. Sakai, .K. Kakuta, Y. and Nomachi, S., "Design of slender reinforced concrete columns", *Transactions of JSCE,* Vol.15, 1983, pp.514-517.

[48]. Sakai, .K. Kakuta, Y. and Nomachi, S., "Design of slender reinforced concrete columns", *Concrete Library of JSCE,* No.4, December 1984, pp.297-313.

[49]. Kwan, K.H. and Liauw, T.C., "Computer-aided design of reinforced concrete members subjected to axial compression and biaxial bending", *The Structural Engineer,* Vol.63B, No.2, June 1985, pp.34-40.

[50]. Davister, M.D., "Analysis of reinforced concrete columns of arbitrary geometry subjected to axial load and biaxial bending: A computer program for exact analysis", *Concrete International,* Vol.8, No.7, July 1986, pp.56-61.

[51]. Iwai, S. Minami, K. and Wakabayashi, M., "Stability of slender reinforced concrete columns subjected to biaxially eccentric loads", *Bulletin of the Disaster Prevention Research Institute,* Vol.36, Parts 3-4, No.321, Kyoto University, December 1986, pp.137-157.

[52]. Beal, A.N., "The design of slender columns", *Proceedings Inst. Civ. Engrs.,* Part 2, Vol.81, September 1986, pp.397-414. Discussion, *Proceedings Inst. Civ. Engrs.,* Part 2, Vol. 83, June 1987, pp.483-496.

[53]. Kong, F.K. Paine, J.M. and Wong, H.H.A., "Computer-aided analysis and design of slender concrete columns", Conference on Computer Applications in Concrete. *Singapore Concrete Institute and Nanyang Technological Institute,* Singapore, March 1986, pp.C68-C98.

[54]. Kong, F.K. and Wong, H.H.A., "Buckling failure of slender concrete columns -a computer method of prediction", International Conference on Structural Failure. *Singapore Concrete Institute and Nanyang Technological Institute,* Singapore, March 1987, pp.J15-J51.

[55]. Cauvin, A. and Macchi, G., "New definition of slenderness of reinforced concrete columns", *IABSE Proceedings* P-110/87, May 1987, pp.45-68.

[56]. Dinku, A., *"Design of pin-ended slender columns"*, M.Sc. Dissertation, University of Leeds, October 1987.

[57]. Towfighi, S., "Design aids for reinforced concrete columns", *Concrete International,* Vol.10, No.3, March 1988, pp.49-54.

[58]. El-Metwally, S.E. El-Shahhat, A.M. and Chen, W.F., "3-D nonlinear analysis of R/C slender columns", *Computers and Structures,* Vol.37, No.5, 1990, pp.863-872.

[59]. Cranston, W.B., "Analysis of slender biaxially loaded restrained columns", *Cement and Concrete Association,* prepared for CEB Commission 3, Buckling and Instability, Munich, October 1982.

[60]. Mirza, S.A. and MacGregor, J.G., "Slenderness and strength reliability of reinforced concrete columns", *ACI Structural Journal,* Vol.86, No.4, July-August 1989, pp.428-438. Discussion, *ACI Structural Journal,* Vol.87, No.3, May-June 1990, pp.366.

[61]. Gilbert, R.I., "A procedure for the analysis of slender concrete columns under sustained eccentric loading", *Inst. Eng. Aust. Civ., Eng. Trans.,* Vol.CE31, No.1, May 1989, pp.39-46.

[62]. Rangan, B.V., "Lateral deflection of slender reinforced concrete columns under sustained load", *ACI Structural Journal,* Vol.86, No.6, November-December 1989, pp.660-663.

[63]. British Standards Institution, *"CP114 The structural use of reinforced concrete in buildings"*, BSI, London, 1969.

[64]. Australian Standard 3600-1988, *"Concrete Structures"*, Standards Association of Australia, 1988.

[65]. MacGregor, J.G. Breen, J.E. and Pfrang, E.O., "Design of slender concrete columns", *ACI Journal, Proceedings* Vol.67, No.1, January 1970, pp.6-28.

[66]. Commission of the European Communities, Eurocode No.2: Common unified rules for concrete structures, 1984.

[67]. Mirza, S.A. and MacGregor, J.G., "Limit states design of concrete slender columns", *Can. J. Civ. Eng.,* Vol.14, No.4, August 1987, pp.439-446.

[68]. Mirza, S.A. Lee, P.M. and Morgan, D.L., "ACI stability resistance factor for RC columns", *Journal of Structural Engineering, Proceedings ASCE,* Vol.113, No.9, September 1987, pp.1963-1976.

[69]. Mirza, S.A., "Probability-based strength criterion for reinforced concrete slender columns", *ACI Structural Journal,* Vol.84, No.6, November-December 1987, pp.459-466.

[70]. Commission of the European Communities, *"Design of concrete structures"*, Draft Eurocode No.2: part 1: General rules and rules for buildings, October 1990.

[71]. Standard Specification for Design and Construction of Concrete Structures, Japan Society of Civil Engineers, 1986.

[72]. **Mirza, S.A.,** "Flexural stiffness of rectangular reinforced concrete columns", *ACI Structural Journal,* Vol.87, No.4, July-August 1990, pp.425-435.

[73]. **Wilby, C.B. and Pancholi, V.R.,** "Design of very slender reinforced concrete columns", *Civil Engineering* (UK), November 1978, pp.70-71.

[74]. **Rambøll, B.J.,** *"Reinforced concrete columns concentrically and eccentrically loaded"*, Copenhagen, Teknisk Førlag, 1951.

[75]. **Gehler, W. and Hütter, A.,** *"Knickversuche mit stahlbetonsäulen"*, (Buckling tests on reinforced concrete columns). Deutscher Ausschuss für Stahlbeton. Berlin, Wilhelm Ernst und Sohn, Heft 113, 1954, pp.1-56.

[76]. **Gaede, K.,** *"Knicken von stahlbetonstäben unter kurz-und langzeitbelastung"*, (Buckling tests on reinforced concrete columns under short and long-term loading), Deutscher Ausschuss für Stahlbeton. Berlin, Wilhelm Ernst und Sohn, Heft 129, 1958, pp.80.

[77]. **Kordina, K.,** Unpublished. Cited in reference [37].

[78]. **Aas-Jakobsen, A.,** Unpublished. Cited in reference [37].

[79]. **Ramamurthy, L.N.,** "Investigation of the ultimate strength of square and rectangular columns under biaxially eccentric loads", Symposium on reinforced concrete columns, *ACI SP-13,* Detroit, 1966, pp.263-298.

[80]. **Martin, I. and Olivieri, E.,** "Test of slender reinforced concrete columns bent in double curvature", Symposium on reinforced concrete columns, *ACI SP-13,* Detroit, 1966, pp.121-138.

[81]. **MacGregor, J.G. and Barter, S.L.,** "Long eccentrically loaded concrete columns bent in double curvature", Symposium on reinforced concrete columns, *ACI SP-13,* Detroit, 1966, pp.139-156.

[82]. **Furlong, R.W. and Ferguson, P.M.,** "Tests of frames with columns in single curvature", Symposium on reinforced concrete columns, *ACI SP-13,* Detroit, 1966, pp.55-73.

[83]. Ferguson, P.M. and Breen, J.E., "Investigation of the long concrete column in a frame subject to lateral loads", Symposium on reinforced concrete columns, *ACI SP-13,* Detroit, 1966, pp.75-114.

[84]. Green, R., *"Behaviour of unrestrained reinforced concrete columns under sustained load"*, Ph.D. Thesis, University of Texas, Austin, 1966.

[85]. Mehmel, A. Schwarz, H. Kasparek, K.H. and Makovi, J., *"Tragverhalten ausmitting beanspruchter stahlbetondruckglieder"*, (Load-carrying capacity of eccentrically loaded reinforced concrete compression members), Deutscher Ausschuss für Stahlbeton, Berlin, Wilhelm Ernst und Sohn, Heft 204, 1969, pp.54.

[86]. Breen, J.E. and Ferguson, P.M., "Long cantilever columns subject to lateral forces", *ACI Journal, Proceedings* Vol.66, No.11, November 1969, pp.884-893.

[87]. Hirasawa, M., *"Behaviour of biaxially loaded reinforced concrete columns"*, Ph.D. Thesis, Kyoto University, Kyoto, Japan, 1974.

[88]. Kordina, K., *"Langzeitversuche an stahlbetonstützen"*, Deutscher Ausschuss für Stahlbeton, Berlin, Wilhelm Ernst und Sohn, Heft 250, 1975, p.36.

[89]. Gruber, L. and Menn, C., *"Berechnung und bemessung schlanker stahlbetonstützen"*, Bericht No.84, Institut für Baustatik ETH Zürich, 1978, p.23.

[90]. Bate, S.C.C. et al, *"Handbook on the Unified Code for Structural Concrete (CP110: 1972)"*, Cement and Concrete Association, London, 1972.

[91]. Rowe, R.E. et al, *"Handbook to British Standard (BS8110: 1985: Structural use of concrete)"*, Palladian Publications LTD, London, 1987.

[92]. British Standards Institution, *"BS1726 Coil springs"*, Part 1: Guide for the design of helical compression springs, BSI, London, 1987.

[93]. Megson, T.H.G., *"Strength of materials for civil engineers"*, 2nd edition, Edward Arnold (UK), 1987.

[94]. Kong, F.K. and Evans, R.H., *"Reinforced and prestressed concrete"*, 3rd edition, Van Nostrand Reinhold (UK), 1987.

[95]. Neville, A.M. and Brooks, J.J., *"Concrete technology"* Longman Group (UK), 1987.

[96]. Rüsch, H., "Researches toward a general flexural theory for structural concrete", *ACI Journal,* Vol.57, No.1, July 1960, pp.1-28.

[97]. **CEB-FIP,** International Recommendations for the Design and Construction of Concrete Structures -Principles and Recommendations, Comité Européen du Béton-Fédération Internationale de la Précontrainte, FIP Sixth Congress, Prague, June 1970; Published by Cement and Concrete Association, 1970, pp.80.

[98]. **CEB-FIP,** Model Code for Concrete Structures, Comité Euro-International du Béton-Fédération Internationale de la Précontrainte, Paris, 1978, pp.348.

[99]. **ACI Committe 209,** Prediction of Creep, Shrinkage and Temperature Effects in Concrete Structures, 2nd Draft, *American Concrete Institute,* Detroit, Oct. 1978, pp.98.

[100]. **Bazant, Z.P. and Panula, L.,** *"Simplified prediction of concrete creep and shrinkage from strength and mix"*, Structural Engineering Report No.78-10/6405, Department of Civil Engineering, Northwestern University, Illinois, Oct. 1978, pp.24.

[101]. **Concrete Society,** "A simplified method for estimating the elastic modulus and creep of normal weight concrete", *Cement and Concrete Association,* Training Centre Publication, No.TDH-7376, London, June 1978, p.1.

[102]. **Neville, A.M. Dilger, W.H. and Brooks, J.J.,** *"Creep of plain and structural concrete"*, Construction Press, London, 1983.

APPENDIX A

COMPUTER PROGRAMS

[1]. COLUMNBS PASCAL

```
PROGRAM COLUMNBS(PRT1, PRT2, DATAFILE, INFILE, OUTPUT);
LABEL 1000 ;
TYPE
  DATAARRAY = ARRAY[1..35,1..41] OF REAL ;
  VECTOR = ARRAY[1..35] OF REAL ;

  SINGLECASE = RECORD
       EPSILON  : DATAARRAY ;
       SIGMA    : DATAARRAY ;
       EPSILONS : DATAARRAY ;
       SFORCE   : DATAARRAY ;
       MCONC    : VECTOR ;

  WRITELN(PRT2,'CONCSTRENGTH = ',CONCSTRENGTH:5:1,' MIN NEUTRAL AXIS = ',
NEUTRALAXIS:3,' YIELD STRESS = ',YIELDSTRESS:6:1) ;
 WRITELN(PRT2,
      ' PERCENTAGE  STEEL AREA = ',STEELAREA:4:1,' FACTOR OF SAFETY'
     ,' OF CONCRETE = ',GAMMAMC:5:2,' FACTOR OF SAFETY OF STEEL =',
      GAMMAMS:5:2,' EFFECTIVE DEPTH RATIO =',DRATIO:5:3);
 WRITELN(DATAFILE,CONCSTRENGTH:5:2,' ',NEUTRALAXIS:3,' ',
            YIELDSTRESS:6:1,' ',STEELAREA:5:3,' ',DRATIO:5:3,' ',
           GAMMAMC:5:2,' ',GAMMAMS:5:2);
END ;

PROCEDURE STRAIN(VAR STRAIN: DATAARRAY; NEUTRALAXIS:
                                        INTEGER);
VAR
 STRAIN41,INTERVALS,I : INTEGER ;
```

```
  MAXSTRAIN : REAL ;
 BEGIN
  INTERVALS:=41-NEUTRALAXIS ;
  FOR STRAIN41:=1 TO 35 DO
  BEGIN
   MAXSTRAIN:=STRAIN41/10 ;
   FOR I:=1 TO 41 DO
   BEGIN
    IF I<=NEUTRALAXIS THEN
     STRAIN[STRAIN41,I]:=0
    ELSE
     STRAIN[STRAIN41,I] :=(MAXSTRAIN/INTERVALS)*(I-NEUTRALAXIS) ;
   END ;
  END ;
END ;

PROCEDURE STRESS(VAR STRESS: DATAARRAY; STRAIN: DATAARRAY;
                                        GAMMAMC: REAL);
VAR
 I,J:INTEGER;
 MAXSIGMA,MAXEPSILON: REAL ;
BEGIN
 MAXSIGMA :=(FCU*(2/3))/GAMMAMC;
 MAXEPSILON :=0.24 * SQRT(FCU/GAMMAMC);
 FOR I:=1 TO 35 DO
  FOR J:=1 TO 41 DO
  BEGIN
   IF STRAIN[I,J]=0 THEN STRESS[I,J]:=0   ELSE
    STRESS[I,J] := 5.5*STRAIN[I,J]*(SQRT(FCU/GAMMAMC) - 2.08334*STRAIN[I,J]);
   IF (STRESS[I,J]>MAXSIGMA)  OR (STRAIN[I,J]>MAXEPSILON) THEN
    STRESS[I,J]:=MAXSIGMA;
  END;
END;

PROCEDURE CONCRETEMOMENT(VAR MOMENT:VECTOR; STRESS:
                                                DATAARRAY);
VAR
 I,J:INTEGER ;
 M :REAL ;
BEGIN
```

```
  FOR I:=1 TO 35 DO
  BEGIN
   M := 0.00417*STRESS[I,1]+0.49583*STRESS[I,41] ;
   FOR J:=2 TO 40 DO
    M := M + ((J-1)/40)*STRESS[I,J] ;
   MOMENT[I]:= M/40 ;
  END ;
 END ;

 PROCEDURE CONCRETEFORCE(VAR FORCE: VECTOR; STRESS:
                                              DATAARRAY);
 VAR
  I,J:INTEGER ;
  SUMAREA : REAL;
 BEGIN
  FOR I:=1 TO 35 DO
  BEGIN
   SUMAREA := STRESS[I,1] + STRESS[I,41] ;
   FOR J:=2 TO 40 DO
    SUMAREA := SUMAREA + 2*STRESS[I,J] ;
   FORCE[I] := SUMAREA/80 ;
  END ;
 END ;

 PROCEDURE CONCRETECURVITURE(VAR RRADIUS: VECTOR;
                                          STRAIN: DATAARRAY);
 VAR
  I:INTEGER ;
 BEGIN
  FOR I:=1 TO 35 DO
   RRADIUS[I]:=(STRAIN[I,41]-STRAIN[I,40])*40 ;
 END ;

 PROCEDURE STEELSTRAIN(VAR STRAIN: DATAARRAY;
                          NEUTRALAXIS,POS1,POS2: INTEGER);
 VAR
  INTERVALS,STRAIN41,I : INTEGER ;
  MAXSTRAIN, STEP : REAL;
 BEGIN
  INTERVALS := 41-NEUTRALAXIS ;
```

```
  FOR STRAIN41 := 1 TO 35 DO
   FOR I:= 1 TO 41 DO STRAIN[STRAIN41,I] := 0 ;
  FOR STRAIN41 := 1 TO 35 DO
  BEGIN
   MAXSTRAIN := STRAIN41/10 ;
   STEP := MAXSTRAIN/INTERVALS ;
   STRAIN[STRAIN41,POS1]:=(POS1-NEUTRALAXIS)*STEP ;
   STRAIN[STRAIN41,POS2] := (POS2-NEUTRALAXIS)*STEP ;
  END ;
END ;

PROCEDURE STEELFORCE(VAR FORCE: DATAARRAY; STRAIN:
                     DATAARRAY; POS1,POS2: INTEGER; GAMMAMS: REAL);
VAR
 I,J : INTEGER ;
 BAND1,SLOPE1,EPSILONVAL : REAL ;
BEGIN
 SLOPE1 := 200 ;
 BAND1 := (FY/GAMMAMS)/200;
 FOR I:= 1 TO 35 DO
  FOR J:= 1 TO 41 DO
  IF (J=POS2) OR (J=POS1) THEN
  BEGIN
   EPSILONVAL := STRAIN[I,J] ;
    IF ABS(EPSILONVAL)<BAND1 THEN FORCE[I,J]:= EPSILONVAL*SLOPE1
     ELSE
      IF EPSILONVAL>= BAND1 THEN
       FORCE[I,J] := FY/GAMMAMS
      ELSE FORCE[I,J] := -1*FY/GAMMAMS ;
    END
  ELSE FORCE[I,J] := 0.0 ;
  FOR I:= 1 TO 35 DO
   FOR J:= 1 TO 41 DO FORCE[I,J]:= FORCE[I,J]*(STEELAREA/2)*(1/100) ;
END ;

PROCEDURE CONCRETEPRATIO(VAR FORCERATIO: VECTOR; FORCE:
                                          VECTOR; GAMMAMC: REAL);
VAR
 I : INTEGER ;
 AREA,PO : REAL ;
```

```
BEGIN
 AREA := 1.0 ;
 PO:=AREA*(2/3)*(FCU/GAMMAMC) ;
 FOR I:=1 TO 35 DO
  FORCERATIO[I] := FORCE[I]/PO ;
END ;

PROCEDURE SUMSTEELFORCE(VAR SUMFORCE: VECTOR; FORCE:
                                    DATAARRAY; POS1, POS2: INTEGER);
VAR
 I : INTEGER ;
BEGIN
 FOR I:=1 TO 35 DO
  SUMFORCE[I]:=FORCE[I,POS2] + FORCE[I,POS1];
END ;

PROCEDURE STEELMOMENT(VAR MOMENT: VECTOR; FORCE:
                        DATAARRAY; POS1,POS2: INTEGER; A1,A2: REAL);
VAR
 I : INTEGER ;
BEGIN
 FOR I:=1 TO 35 DO
  MOMENT[I] := FORCE[I,POS2]*A2 + FORCE[I,POS1]*A1 ;
END ;

PROCEDURE REINFFORCE(VAR REINFFORCE: VECTOR;
                                    CONCFORCE, STEELFORCE: VECTOR);
VAR
 I : INTEGER ;
BEGIN
 FOR I:=1 TO 35 DO
  REINFFORCE[I] := CONCFORCE[I]+STEELFORCE[I] ;
END ;

PROCEDURE REINFMOMENT(VAR REINFMOMENT: VECTOR;
                                    MOMCONCRETE, MOMSTEEL: VECTOR);
VAR
 I : INTEGER ;
BEGIN
 FOR I:=1 TO 35 DO
```

```
    REINFMOMENT[I] := MOMCONCRETE[I] + MOMSTEEL[I] ;
  END ;

  PROCEDURE EXCENTRICITY(VAR EXCE: VECTOR; MOMENT, FORCE:
                                                    VECTOR);
  VAR
   I:INTEGER ;
  BEGIN
   FOR I:=1 TO 35 DO
    EXCE[I] := MOMENT[I]/FORCE[I] - 0.5 ;
  END ;

  PROCEDURE RFFORCERATIO(VAR RATIO: VECTOR; FORCE: VECTOR;
                                        GAMMAMC, GAMMAMS: REAL);
  VAR
   I:INTEGER ;
   AREA,PO : REAL ;
  BEGIN
   AREA:=1 ;
   PO :=(2/3)*(FCU/GAMMAMC)*AREA + (FY/GAMMAMS)*(STEELAREA/100);
   FOR I:= 1 TO 35 DO
    RATIO[I] := FORCE[I]/PO
  END ;

  PROCEDURE INTERPOLER (COLUMN: CASEARRAY);
  VAR
   N,I,J,COUNT : INTEGER ;
   PRATIO,FRACTION : REAL ;
   ESTEXCEN,ESTCURV : ARRAY[-41..40] OF REAL ;
   RATIO : ARRAY[1..10] OF REAL ;
  BEGIN
   FOR I:= -41 TO 40 DO
   BEGIN
    ESTEXCEN[I]:= -1 ;
    ESTCURV[I] := -1 ;
   END ;
   FOR I:=1 TO 10 DO RATIO[I] := (I-1)/10 ;
   RATIO[1] := 0.05 ;
   FOR I:= 1 TO 10 DO
  BEGIN
```

```
    PRATIO:= RATIO[I] ;
    FOR N:= MINNEUTRALAXIS TO 40 DO
    BEGIN
     ESTEXCEN[N] := -1 ;
     ESTCURV[N]  := -1 ;
    END ;
    FOR N:= MINNEUTRALAXIS TO 40 DO
    WITH COLUMN[N] DO
    IF (PRATIO>=RCPRATIO[1]) AND (PRATIO<=RCPRATIO[35]) THEN
    BEGIN
     J:=0 ;
     REPEAT
      J:=J+1 ;
    UNTIL (PRATIO>=RCPRATIO[J]) AND (PRATIO<=RCPRATIO[J+1]) ;
    IF (RCPRATIO[J]>=0 ) THEN
    BEGIN
     FRACTION := (PRATIO - RCPRATIO[J])/(RCPRATIO[J+1] - RCPRATIO[J]) ;
     ESTEXCEN[N] := ((RCEXCEN[J+1]-RCEXCEN[J])*FRACTION)+RCEXCEN[J] ;
     ESTCURV[N] := ((RCONC[J+1]-RCONC[J])*FRACTION)+RCONC[J] ;
     WRITELN(PRT2,'NEUTRALAXIS = ',N:3,' P RATIO      = ',PRATIO:7:4,
          ' EST EXCEN= ',ESTEXCEN[N]:7:4,' 1/R = ',ESTCURV[N]:7:4) ;
    END;
   END ;
   WRITELN(PRT2) ;
   COUNT := 0 ;
   FOR N:=MINNEUTRALAXIS TO 40 DO
    IF ((ESTEXCEN[N]>=0.0) AND  (ESTCURV[N]>=0.0))THEN COUNT := COUNT+1 ;
   WRITELN(DATAFILE,COUNT:3) ;
   FOR N:=MINNEUTRALAXIS TO 40 DO
    IF ((ESTEXCEN[N]>=0.0)AND (ESTCURV[N]>=0.0) ) THEN
     WRITELN(DATAFILE,PRATIO:7:4,' ',ESTEXCEN[N]:7:4,'
',ESTCURV[N]:7:4);
  END;
END ;
PROCEDURE TERMINALP(COLUMN: CASEARRAY);
VAR
 I,J : INTEGER ;
 RATIO : ARRAY [1..10] OF REAL ;
 PRATIO,FRACTION,ESTEXCEN,ESTCURV : REAL ;
BEGIN
```

```
  FOR I:=1 TO 10 DO RATIO[I]:= (I-1)/10 ;
  RATIO[1] := 0.05 ;
  FOR I:=1 TO 10 DO
  BEGIN
   PRATIO:= RATIO[I] ;
   IF (PRATIO<=COLUMN[MINNEUTRALAXIS].RCPRATIO[35]) AND
                    (PRATIO>=COLUMN[40].RCPRATIO[35] )
     THEN
   BEGIN
    J:=MINNEUTRALAXIS-1 ;
    REPEAT J:=J+1
    UNTIL
    (PRATIO<=COLUMN[J].RCPRATIO[35])AND(PRATIO>=COLUMN[J+1].RCPRATIO[35]);
   IF ((COLUMN[J+1].RCPRATIO[35]>=0)AND(COLUMN[J].RCPRATIO[35]>=0)) THEN
    BEGIN
     FRACTION :=  (COLUMN[J].RCPRATIO[35]-PRATIO )/
              (COLUMN[J].RCPRATIO[35]-COLUMN[J+1].RCPRATIO[35]) ;
     ESTEXCEN := COLUMN[J].RCEXCEN[35] +
 ((COLUMN[J+1].RCEXCEN[35]-COLUMN[J].RCEXCEN[35])*FRACTION);
     ESTCURV := COLUMN[J].RCONC[35] +
          ((COLUMN[J+1].RCONC[35]-COLUMN[J].RCONC[35])*FRACTION);
     WRITELN(PRT2,'P/PO = ',PRATIO:7:4,' EST EXCENTRICITY = ',ESTEXCEN:7:4,
          ' CURVATURE = ',ESTCURV:7:4);
     WRITELN(DATAFILE,PRATIO:7:4,' ',ESTEXCEN:7:4,' ',ESTCURV:7:4) ;
    END
   ELSE WRITELN(DATAFILE,PRATIO:7:4,' -1.0000 -1.0000 ') ;
   END
 ELSE WRITELN(DATAFILE,PRATIO:7:4,' -1.0000 -1.0000 ');

 END ;
WRITELN(PRT2) ;
WRITELN(PRT2) ;
END ;

PROCEDURE TERMINALE(COLUMN: CASEARRAY; POS1: INTEGER);
VAR
 I,J : INTEGER ;
 RATIO : ARRAY [1..10] OF REAL ;
 ERATIO,FRACTION,ESTPRATIO,ESTCURV : REAL ;
BEGIN
```

```
  FOR I:=1 TO 8 DO RATIO[I]:= I/20 ;
  FOR I:=1 TO 8 DO
  BEGIN
   ERATIO:= RATIO[I] ;
   FOR J:=MINNEUTRALAXIS TO POS1 DO
   IF ((ERATIO>=COLUMN[J].RCEXCEN[35])AND(ERATIO<=COLUMN[J+1].RCEXCEN[35]))
AND((COLUMN[J].RCPRATIO[35]>=0)AND(COLUMN[J+1].RCPRATIO[35]>=0))THEN
     BEGIN
      FRACTION :=  (ERATIO-COLUMN[J].RCEXCEN[35])/
                (COLUMN[J+1].RCEXCEN[35]-COLUMN[J].RCEXCEN[35]) ;
      ESTPRATIO := COLUMN[J].RCPRATIO[35] -
           ((COLUMN[J].RCPRATIO[35]-COLUMN[J+1].RCPRATIO[35])*FRACTION);
     ESTCURV := COLUMN[J].RCONC[35] +
              ((COLUMN[J+1].RCONC[35]-COLUMN[J].RCONC[35])*FRACTION);
    WRITELN(PRT2,'EXCENTRICITY = ',ERATIO:7:4,' EST P/PO =
 ',ESTPRATIO:7:4, '  CURVATURE = ',ESTCURV:7:4);
    END ;
  END ;
 WRITELN(PRT2) ;
 WRITELN(PRT2) ;
 END ;

 PROCEDURE INTERPOLPR(COLUMN: CASEARRAY);
 VAR
  N,I,J : INTEGER ;
  ERATIO,FRACTION,ESTPRATIO,ESTCURV : REAL ;
  RATIO : ARRAY[1..8] OF REAL ;
 BEGIN
  FOR I:=1 TO 8 DO RATIO[I] := I/20 ;
  FOR I:= 1 TO 8 DO
  BEGIN
   ERATIO:= RATIO[I] ;
   FOR N:= MINNEUTRALAXIS TO 40 DO
   WITH COLUMN[N] DO
   BEGIN
    FOR J:=1 TO 34 DO
    IF((ERATIO>=RCEXCEN[J])AND(ERATIO<=RCEXCEN[J+1])) OR
     ((ERATIO<=RCEXCEN[J]) AND(ERATIO>=RCEXCEN[J+1])) THEN
     BEGIN
     IF (ERATIO>=RCEXCEN[J]) THEN
```

```
        FRACTION := (ERATIO - RCEXCEN[J])/(RCEXCEN[J+1] - RCEXCEN[J])
      ELSE
        FRACTION := 1-((ERATIO-RCEXCEN[J+1])/(RCEXCEN[J]-RCEXCEN[J+1])) ;
        ESTPRATIO := ((RCPRATIO[J+1]-RCPRATIO[J])*FRACTION)+RCPRATIO[J] ;
        ESTCURV := ((RCONC[J+1]-RCONC[J])*FRACTION)+RCONC[J] ;
        WRITELN(PRT2,'NEUTRALAXIS = ',N:3,' EXCENTRICITY = ',ERATIO:5:2,
                EST P/PO = ',ESTPRATIO:7:4,' 1/R = ',ESTCURV:7:4,
                RCEXCEN[J]:7:4,RCEXCEN[J+1]:7:4 ) ;
      END ;
    END ;

  END;
END ;

BEGIN
 REWRITE(PRT1) ;
 REWRITE(PRT2) ;
 REWRITE(DATAFILE) ;
 INPUT(FCU,FY,STEELAREA,DRATIO,GAMMAMC,GAMMAMS,
MINNEUTRALAXIS);
 A1:= DRATIO ;
 A2:= 1-DRATIO ;
 XA1:=(A1/0.025) + 1 ;
 XA2:=(A2/0.025) + 1 ;
 POS1:= ROUND(XA1);
 POS2:= ROUND(XA2);
 IF ((XA1-POS1 ) > 0.5 )  THEN  POS1 := POS1 + 1   ;
 IF ((XA1-POS1 ) < -0.5)  THEN  POS1 := POS1 - 1   ;
 IF ((XA2-POS2 ) > 0.5 )  THEN  POS2 := POS2 + 1   ;
 IF ((XA2-POS2 ) < -0.5)  THEN  POS2 := POS2 - 1   ;
 WRITELN('POS1 = ',POS1:4,'      POS2 =',POS2:4);
 FOR NAXIS:= 40 DOWNTO MINNEUTRALAXIS DO
WITH COLUMNDATA DO

 BEGIN
 STRAIN(EPSILON,NAXIS);
 STRESS(SIGMA,EPSILON,GAMMAMC) ;
 CONCRETEMOMENT(MCONC,SIGMA) ;
 CONCRETEFORCE(PCONC,SIGMA) ;
 CONCRETEPRATIO(CPRATIO,PCONC,GAMMAMC) ;
```

```
  CONCRETECURVITURE(INTERDATA[NAXIS].RCONC,EPSILON) ;
  STEELSTRAIN(EPSILONS,NAXIS,POS1,POS2) ;
  STEELFORCE(SFORCE,EPSILONS,POS1,POS2,GAMMAMS) ;
  SUMSTEELFORCE(PSTEEL,SFORCE,POS1,POS2) ;
  STEELMOMENT(MSTEEL,SFORCE,POS1,POS2,A1,A2) ;
  REINFFORCE(PRC,PCONC,PSTEEL) ;
  REINFMOMENT(MRC,MCONC,MSTEEL) ;
  EXCENTRICITY(INTERDATA[NAXIS].RCEXCEN,MRC,PRC) ;
  RFFORCERATIO(INTERDATA[NAXIS].RCPRATIO,PRC,GAMMAMC ,GAMMAMS) ;
 WRITELN(PRT1) ;
 WRITELN( ' NEUTRAL AXIS IS AT POSITION ',NAXIS);
 WRITELN(PRT1, ' NEUTRAL AXIS IS AT POSITION ',NAXIS);
 WRITELN(PRT1) ;
 FOR I:=1 TO 35 DO
 BEGIN
  J:=1;
  WHILE J<= 41  DO
  BEGIN
  WRITE(PRT1,EPSILON[I,J]:6:3);
  J:=J+2 ;
  END ;
  WRITELN(PRT1);
  J:=1 ;
  WHILE J <= 41  DO
  BEGIN
  WRITE(PRT1,SIGMA[I,J]:6:3);
  J:=J+2 ;
  END ;
  WRITELN(PRT1);
  J:=1;
  WHILE  J<= 41   DO
  BEGIN
  WRITE(PRT1,EPSILONS[I,J]:6:3) ;
  J:= J+2 ;
  END ;
  WRITELN(PRT1);
  J:=1 ;
  WHILE J <= 41  DO
 BEGIN
 WRITE(PRT1,SFORCE[I,J]:6:3);
```

```
 J:=J+2 ;
 END;
 WRITELN(PRT1);
 WRITELN(PRT1,'          P      M    E     P/PO    1/R ');
 WRITELN(PRT1,'  CONC  ',PCONC[I]:7:3,MCONC[I]:7:3,'       ',
       CPRATIO[I]:7:3,INTERDATA[NAXIS].RCONC[I]:7:3 ) ;
 WRITELN(PRT1,'  ST    ',PSTEEL[I]:7:3,MSTEEL[I]:7:3 ) ;
 WRITELN(PRT1, '  RC    ',PRC[I]:7:3,MRC[I]:7:3,
 INTERDATA[NAXIS].RCEXCEN[I]:7:3,INTERDATA[NAXIS].RCPRATIO[I]:8:4) ;
 WRITELN(PRT1) ;
 END ;
END ;
TERMINALP(INTERDATA) ;
INTERPOLER(INTERDATA) ;
TERMINALP(INTERDATA) ;
TERMINALE(INTERDATA,POS1) ;
INTERPOLPR(INTERDATA) ;
WRITELN(PRT2) ;
WRITELN(PRT2,' N    P/PO   E     1/R ') ;
FOR I:=MINNEUTRALAXIS TO 40 DO
  WRITELN(PRT2,I:3, INTERDATA[I].RCPRATIO[35]:7:4,
       INTERDATA[I].RCEXCEN[35]:7:4,INTERDATA[I].RCONC[35]:7:4);
1000:
END.
```

[21. COLMNBSL PASCAL

```
PROGRAM COLMNBSL(PRT1,PRT2,DATAFILE,INFILE,OUTPUT);
LABEL 1000;
CONST PHI = 2.0 ;
      SIZE = 53 ;
{The value of PHI may vary between (0.5 & 4) then SIZE must change accordingly }
{SIZE=ROUND((1+PHI)*35) i.e it should be an integer. Two procedures will }
{change slightly: }
{PROCEDURE STRAIN and.PROCEDURE STEELSTRAIN}
TYPE
  DATAARRAY = ARRAY[1..SIZE,1..41] OF REAL ;
  VECTOR = ARRAY[1..SIZE] OF REAL ;

  SINGLECASE = RECORD
        EPSILON : DATAARRAY ;
        SIGMA   : DATAARRAY ;
        EPSILONS : DATAARRAY ;
        SFORCE  : DATAARRAY ;
        MCONC   : VECTOR ;
        PCONC   : VECTOR ;
        CPRATIO : VECTOR ;
        MSTEEL  : VECTOR ;
        PSTEEL  : VECTOR ;
        PRC     : VECTOR ;
        MRC     : VECTOR ;
  END ;
TESTCASE = RECORD
        RCONC   : VECTOR ;
        RCEXCEN : VECTOR ;
        RCPRATIO : VECTOR ;
  END ;
 CASEARRAY = ARRAY[-41..40] OF TESTCASE  ;

VAR
  INFILE,PRT1,PRT2,DATAFILE : TEXT ;
  NAXIS,MINNEUTRALAXIS,POS1,POS2,I,J : INTEGER ;
  FCU,FY, STEELAREA,DRATIO,A1,A2,XA1,XA2, GAMMAMC, GAMMAMS : REAL;
```

```
  COLUMNDATA : SINGLECASE;
  INTERDATA  : CASEARRAY ;

PROCEDURE INPUT(VAR CONCSTRENGTH, YIELDSTRESS, STEELAREA,
DRATIO, GAMMAMC, GAMMAMS: REAL; VAR NEUTRALAXIS: INTEGER);
BEGIN
 WRITELN('INPUT CONCSTRENGTH ') ;
 RESET(INFILE) ;
 READ(INFILE,CONCSTRENGTH) ;
 REPEAT
  WRITELN('INPUT MIN POSITION OF THE NEUTRAL AXIS  (-41 TO 40) ');
  READ(INFILE,NEUTRALAXIS ) ;
 UNTIL (NEUTRALAXIS<41) AND (NEUTRALAXIS> -42) ;
 WRITELN('INPUT YIELDSTRESS ');
 READ(INFILE,YIELDSTRESS);
 WRITELN('INPUT PERCENTAGE STEEL REINFORCEMENT AREA ');
 READ(INFILE,STEELAREA);
 WRITELN('INPUT EFFECTIVE DEPTH RATIO  D/H  (BY INCREMENT OF 0.025)');
 READ(INFILE,DRATIO);
 WRITELN('INPUT FACTOR OF SAFETY OF CONC. AND STEEL');
 READ(INFILE,GAMMAMC,GAMMAMS);
  WRITELN(PRT1,'CONCSTRENGTH =', CONCSTRENGTH:5:1,' MIN NEUTRAL AXIS = ',
NEUTRALAXIS:3,' YIELD STRESS = ',YIELDSTRESS:6:1) ;
 WRITELN(PRT1,
   'PERCENTAGE  STEEL AREA = ',STEELAREA:5:3,' FACTOR OF SAFETY'
  ,' OF CONCRETE = ',GAMMAMC:5:2,' FACTOR OF SAFETY OF STEEL =',
     GAMMAMS:5:2,'  CREEP COEFFICIENT =', PHI:4:1);
 WRITELN(PRT1,'EFFECTIVE DEPTH RATIO =',DRATIO:5:3);
  WRITELN(PRT2,'CONCSTRENGTH = ',CONCSTRENGTH:5:1,' MIN NEUTRAL AXIS = ',
NEUTRALAXIS:3,' YIELD STRESS = ',YIELDSTRESS:6:1) ;
 WRITELN(PRT2,
    ' PERCENTAGE  STEEL AREA = ',STEELAREA:4:1,' FACTOR OF SAFETY'
    ,' OF CONCRETE = ',GAMMAMC:5:2,' FACTOR OF SAFETY OF STEEL =',
      GAMMAMS:5:2,' CREEP COEFFICIENT =', PHI:4:1);
 WRITELN(PRT2,'EFFECTIVE DEPTH RATIO =',DRATIO:5:3);
 WRITELN(DATAFILE,CONCSTRENGTH:5:1,' ',NEUTRALAXIS:3,' ',
        YIELDSTRESS:6:1,' ',STEELAREA:5:3,' ',DRATIO:5:3,' ',
          GAMMAMC:5:2,' ',GAMMAMS:5:2,' ',PHI:4:1);
END ;
```

```
PROCEDURE STRAIN(VAR STRAIN: DATAARRAY;
                                    NEUTRALAXIS:INTEGER);
VAR
 STRAIN41,INTERVALS,I : INTEGER ;
 MAXSTRAIN : REAL ;
BEGIN
 INTERVALS:=41-NEUTRALAXIS ;
 FOR STRAIN41:=1 TO SIZE DO
 BEGIN
  IF STRAIN41< ((1+PHI)*35)/2 THEN   MAXSTRAIN := STRAIN41/5
    ELSE MAXSTRAIN := ((1+PHI)*35)/10 ;
  FOR I:=1 TO 41 DO
  BEGIN
   IF I<=NEUTRALAXIS THEN
     STRAIN[STRAIN41,I]:=0
   ELSE
     STRAIN[STRAIN41,I] :=(MAXSTRAIN/INTERVALS)*(I-NEUTRALAXIS) ;
  END ;
 END ;
END ;

PROCEDURE STRESS(VAR STRESS: DATAARRAY; STRAIN:DATAARRAY;
                                    GAMMAMC:REAL);
VAR
 I,J:INTEGER ;
 MAXSIGMA,MAXEPSILON : REAL ;
BEGIN
 MAXSIGMA :=(FCU*(2/3))/GAMMAMC ;
 MAXEPSILON :=0.24*(1+PHI)* SQRT(FCU/GAMMAMC);
 FOR I:=1 TO SIZE DO
  FOR J:=1 TO 41 DO
  BEGIN
   IF STRAIN[I,J]=0 THEN STRESS[I,J]:=0   ELSE
     STRESS[I,J] := 5.5*(1/(1+PHI))*STRAIN[I,J]*(SQRT(FCU/GAMMAMC) -
                    2.08334 *(1/(1+PHI))*STRAIN[I,J]);
   IF (STRESS[I,J]>MAXSIGMA)  OR (STRAIN[I,J]>MAXEPSILON) THEN
     STRESS[I,J]:=MAXSIGMA;
  END;
END;
```

```
PROCEDURE CONCRETEMOMENT(VAR MOMENT:VECTOR;
                                    STRESS:DATAARRAY);
 VAR
  I,J:INTEGER ;
  M :REAL ;
 BEGIN
  FOR I:=1 TO SIZE DO
  BEGIN
    M := 0.00417*STRESS[I,1]+0.49583*STRESS[I,41] ;
   FOR J:=2 TO 40 DO
    M := M + ((J-1)/40)*STRESS[I,J] ;
   MOMENT[I]:= M/40 ;
  END ;
 END ;

 PROCEDURE CONCRETEFORCE(VAR FORCE: VECTOR;
                                    STRESS:DATAARRAY);
 VAR
  I,J:INTEGER ;
  SUMAREA : REAL;
 BEGIN
  FOR I:=1 TO SIZE DO
  BEGIN
   SUMAREA := STRESS[I,1] + STRESS[I,41] ;
   FOR J:=2 TO 40 DO
    SUMAREA := SUMAREA + 2*STRESS[I,J] ;
   FORCE[I] := SUMAREA/80 ;
  END ;
 END ;

PROCEDURE CONCRETECURVITURE(VAR RRADIUS: VECTOR;
                                    STRAIN: DATAARRAY);
VAR
 I:INTEGER ;
BEGIN
 FOR I:=1 TO SIZE DO
  RRADIUS[I]:=(STRAIN[I,41]-STRAIN[I,40])*40 ;
END ;
```

```
PROCEDURE STEELSTRAIN(VAR STRAIN: DATAARRAY;
                                    NEUTRALAXIS, POS1, POS2: INTEGER);
VAR
 INTERVALS,STRAIN41,I : INTEGER ;
 MAXSTRAIN, STEP : REAL;
BEGIN
 INTERVALS := 41-NEUTRALAXIS ;
 FOR STRAIN41 := 1 TO SIZE DO
  FOR I:= 1 TO 41 DO STRAIN[STRAIN41,I] := 0 ;
 FOR STRAIN41 := 1 TO SIZE DO
 BEGIN
  IF STRAIN41 < ((1+PHI)*35)/2 THEN  MAXSTRAIN := STRAIN41/5
   ELSE MAXSTRAIN := ((1+PHI)*35)/10 ;
  STEP := MAXSTRAIN/INTERVALS ;
  STRAIN[STRAIN41,POS1]:=(POS1-NEUTRALAXIS)*STEP ;
  STRAIN[STRAIN41,POS2] := (POS2-NEUTRALAXIS)*STEP ;
 END ;
END ;

PROCEDURE STEELFORCE(VAR FORCE: DATAARRAY; STRAIN:
          DATAARRAY POS1,POS2: INTEGER; GAMMAMS: REAL);
VAR
 I,J : INTEGER ;
 BAND1,SLOPE1,EPSILONVAL : REAL ;
BEGIN
 SLOPE1 := 200 ;
 BAND1 := (FY/GAMMAMS)/200;
 FOR I:= 1 TO SIZE DO
  FOR J:= 1 TO 41 DO
  IF (J=POS2) OR (J=POS1) THEN
  BEGIN
   EPSILONVAL := STRAIN[I,J] ;
    IF ABS(EPSILONVAL)<BAND1 THEN FORCE[I,J]:= EPSILONVAL*SLOPE1
     ELSE
      IF EPSILONVAL>= BAND1  THEN
       FORCE[I,J] := FY/GAMMAMS
      ELSE FORCE[I,J] := -1*FY/GAMMAMS ;
    END
  ELSE FORCE[I,J] := 0.0 ;
  FOR I:= 1 TO SIZE DO
```

```
    FOR J:= 1 TO 41 DO FORCE[I,J]:= FORCE[I,J]*(STEELAREA/2)*(1/100) ;
   END ;

 PROCEDURE CONCRETEPRATIO(VAR FORCERATIO: VECTOR; FORCE:
                          VECTOR; GAMMAMC:REAL);
 VAR
  I : INTEGER ;
  AREA,PO : REAL ;
 BEGIN
  AREA := 1.0 ;
  PO:=AREA*(2/3)*(FCU/GAMMAMC) ;
  FOR I:=1 TO SIZE DO
   FORCERATIO[I] := FORCE[I]/PO ;
 END ;

 PROCEDURE SUMSTEELFORCE(VAR SUMFORCE: VECTOR; FORCE:
                         DATAARRAY; POS1,POS2: INTEGER);
 VAR
  I : INTEGER ;
 BEGIN
  FOR I:=1 TO SIZE DO
   SUMFORCE[I]:=FORCE[I,POS2] + FORCE[I,POS1];
 END ;

 PROCEDURE STEELMOMENT(VAR MOMENT: VECTOR; FORCE:
                       DATAARRAY; POS1,POS2: INTEGER; A1,A2: REAL);
 VAR
  I : INTEGER ;
 BEGIN
  FOR I:=1 TO SIZE DO
   MOMENT[I] := FORCE[I,POS2]*A2 + FORCE[I,POS1]*A1 ;
 END ;

 PROCEDURE REINFFORCE(VAR REINFFORCE: VECTOR;
                      CONCFORCE,STEELFORCE: VECTOR);
 VAR
  I : INTEGER ;
 BEGIN
  FOR I:=1 TO SIZE DO
   REINFFORCE[I] := CONCFORCE[I]+STEELFORCE[I] ;
```

```
 END ;

 PROCEDURE REINFMOMENT(VAR REINFMOMENT: VECTOR;
                       MOMCONCRETE,MOMSTEEL: VECTOR);
 VAR
  I : INTEGER ;
 BEGIN
  FOR I:=1 TO SIZE DO
   REINFMOMENT[I] := MOMCONCRETE[I] + MOMSTEEL[I] ;
 END ;

 PROCEDURE EXCENTRICITY(VAR EXCE:VECTOR; MOMENT,FORCE: VECTOR) ;
 VAR
  I:INTEGER ;
 BEGIN
  FOR I:=1 TO SIZE DO
   EXCE[I] := MOMENT[I]/FORCE[I] - 0.5 ;
 END ;

 PROCEDURE RFFORCERATIO(VAR RATIO: VECTOR; FORCE:VECTOR;
                        VAR GAMMAMC, GAMMAMS: REAL);
 VAR
  I:INTEGER ;
  AREA,PO : REAL ;
 BEGIN
  AREA:=1 ;
  PO :=(2/3)*(FCU/GAMMAMC)*AREA + (FY/GAMMAMS)*(STEELAREA/100);
  FOR I:= 1 TO SIZE DO
   RATIO[I] := FORCE[I]/PO
 END ;

 PROCEDURE INTERPOLER(COLUMN: CASEARRAY);
 VAR
  N,I,J,COUNT : INTEGER ;
  PRATIO,FRACTION : REAL ;
  ESTEXCEN,ESTCURV : ARRAY[-41..40] OF REAL ;
  RATIO : ARRAY[1..10] OF REAL ;
 BEGIN
  FOR I:= -41 TO 40 DO
  BEGIN
```

```
    ESTEXCEN[I]:= -1 ;
    ESTCURV[I] := -1 ;
   END ;
   FOR I:=1 TO 10 DO RATIO[I] := (I-1)/10 ;
   RATIO[1] := 0.02 ;
   FOR I:= 1 TO 10 DO
  BEGIN
   PRATIO:= RATIO[I] ;
   FOR N:= MINNEUTRALAXIS TO 40 DO
   BEGIN
    ESTEXCEN[N] := -1 ;
    ESTCURV[N]  := -1 ;
   END ;
   FOR N:= MINNEUTRALAXIS TO 40 DO
   WITH COLUMN[N] DO
   IF (PRATIO>=RCPRATIO[1]) AND (PRATIO<=RCPRATIO[SIZE]) THEN
   BEGIN
    J:=0 ;
    REPEAT
     J:=J+1 ;
    UNTIL (PRATIO>=RCPRATIO[J]) AND (PRATIO<=RCPRATIO[J+1]) ;
    IF (RCPRATIO[J]>=0 ) THEN
    BEGIN
     FRACTION := (PRATIO - RCPRATIO[J])/(RCPRATIO[J+1] - RCPRATIO[J]) ;
  ESTEXCEN[N] := ((RCEXCEN[J+1]-RCEXCEN[J])*FRACTION)+ RCEXCEN[J] ;
     ESTCURV[N] := ((RCONC[J+1]-RCONC[J])*FRACTION)+RCONC[J] ;
     WRITELN(PRT2,'NEUTRALAXIS = ',N:3,' P RATIO     = ',PRATIO:7:4,
       ' EST EXCEN= ',ESTEXCEN[N]:7:4,' 1/R = ',ESTCURV[N]:7:4) ;
    END;
   END ;
   WRITELN(PRT2) ;
   COUNT := 0 ;
   FOR N:=MINNEUTRALAXIS TO 40 DO
    IF ((ESTEXCEN[N]>=0.0) AND  (ESTCURV[N]>=0.0))THEN COUNT := COUNT+1 ;
   WRITELN(DATAFILE,COUNT:3) ;
   FOR N:=MINNEUTRALAXIS TO 40 DO
    IF ((ESTEXCEN[N]>=0.0)AND (ESTCURV[N]>=0.0) ) THEN
   WRITELN(DATAFILE,PRATIO:7:4,' ',ESTEXCEN[N]:7:4,' ',ESTCURV[N]:7:4);
  END;
END ;
```

```
PROCEDURE TERMINALP(COLUMN: CASEARRAY);
VAR
 I,J : INTEGER ;
 RATIO : ARRAY [1..10] OF REAL ;
 PRATIO,FRACTION,ESTEXCEN,ESTCURV : REAL ;
BEGIN
 FOR I:=1 TO 10 DO RATIO[I]:= (I-1)/10 ;
 RATIO[1] := 0.02 ;
 FOR I:=1 TO 10 DO
 BEGIN
  PRATIO:= RATIO[I] ;
  IF (PRATIO<=COLUMN[MINNEUTRALAXIS].RCPRATIO[SIZE]) AND
                    (PRATIO>=COLUMN[40].RCPRATIO[SIZE] )
    THEN
  BEGIN
   J:=MINNEUTRALAXIS-1 ;
   REPEAT J:=J+1
   UNTIL
   (PRATIO<=COLUMN[J].RCPRATIO[SIZE])AND(PRATIO>=COLUMN[J+1].RCPRATIO
        [SIZE]);
   IF ((COLUMN[J+1].RCPRATIO[SIZE]>=0)AND(COLUMN[J].RCPRATIO[SIZE]>=0)) THEN
   BEGIN
    FRACTION :=  (COLUMN[J].RCPRATIO[SIZE]-PRATIO )/
            (COLUMN[J].RCPRATIO[SIZE]-COLUMN[J+1].RCPRATIO[SIZE]) ;
    ESTEXCEN := COLUMN[J].RCEXCEN[SIZE] +
((COLUMN[J+1].RCEXCEN[SIZE]-COLUMN[J].RCEXCEN[SIZE])*FRACTION);
    ESTCURV := COLUMN[J].RCONC[SIZE] +
          ((COLUMN[J+1].RCONC[SIZE]-COLUMN[J].RCONC[SIZE])*FRACTION);
 WRITELN(PRT2,'P/PO = ',PRATIO:7:4,' EST EXCENTRICITY =
',ESTEXCEN:7:4,'  CURVATURE = ',ESTCURV:7:4);
    WRITELN(DATAFILE,PRATIO:7:4,' ',ESTEXCEN:7:4,' ',ESTCURV:7:4) ;
   END
  ELSE WRITELN(DATAFILE,PRATIO:7:4,' -1.0000 -1.0000 ') ;
  END
 ELSE WRITELN(DATAFILE,PRATIO:7:4,' -1.0000 -1.0000 ');

 END ;
WRITELN(PRT2) ;
WRITELN(PRT2) ;
```

```
  END ;

  PROCEDURE TERMINALE(COLUMN: CASEARRAY; POS1: INTEGER);
  VAR
   I,J : INTEGER ;
   RATIO : ARRAY [1..10] OF REAL ;
   ERATIO,FRACTION,ESTPRATIO,ESTCURV : REAL ;
  BEGIN
   FOR I:=1 TO 8 DO RATIO[I]:= I/20 ;
   FOR I:=1 TO 8 DO
   BEGIN
    ERATIO:= RATIO[I] ;
    FOR J:=MINNEUTRALAXIS TO POS1 DO
    IF ((ERATIO>=COLUMN[J].RCEXCEN[SIZE])AND(ERATIO<=COLUMN[J+1].
         RCEXCEN [SIZE]))
     AND((COLUMN[J].RCPRATIO[SIZE]>=0)AND(COLUMN[J+1].RCPRATIO[SIZE]>=0)) THEN
     BEGIN
      FRACTION :=  (ERATIO-COLUMN[J].RCEXCEN[SIZE])/
                  (COLUMN[J+1].RCEXCEN[SIZE]-COLUMN[J].RCEXCEN[SIZE]) ;
  ESTPRATIO := COLUMN[J].RCPRATIO[SIZE] -
((COLUMN[J]. RCPRATIO[SIZE]-COLUMN[J+1].RCPRATIO[SIZE])*FRACTION);
      ESTCURV := COLUMN[J].RCONC[SIZE] +
           ((COLUMN[J+1].RCONC[SIZE]-COLUMN[J].RCONC[SIZE])*FRACTION);
     WRITELN(PRT2,'EXCENTRICITY = ',ERATIO:7:4,' EST
P/PO = ',ESTPRATIO:7:4,'  CURVATURE = ',ESTCURV:7:4);
    END ;
  END ;
WRITELN(PRT2) ;
WRITELN(PRT2) ;
END ;

PROCEDURE INTERPOLPR( COLUMN: CASEARRAY);
VAR
 N,I,J : INTEGER ;
 ERATIO,FRACTION,ESTPRATIO,ESTCURV : REAL ;
 RATIO : ARRAY[1..8] OF REAL ;
BEGIN
 FOR I:=1 TO 8 DO RATIO[I] := I/20 ;
 FOR I:= 1 TO 8 DO
 BEGIN
```

```
    ERATIO:= RATIO[I] ;
    FOR N:= MINNEUTRALAXIS TO 40 DO
    WITH COLUMN[N] DO
    BEGIN
     FOR J:=1 TO (SIZE-1)  DO
      IF((ERATIO>=RCEXCEN[J])AND(ERATIO<=RCEXCEN[J+1])) OR
          ((ERATIO<=RCEXCEN[J]) AND(ERATIO>=RCEXCEN[J+1])) THEN
       BEGIN
       IF (ERATIO>=RCEXCEN[J]) THEN
        FRACTION := (ERATIO - RCEXCEN[J])/(RCEXCEN[J+1] - RCEXCEN[J])
       ELSE
        FRACTION := 1-((ERATIO-RCEXCEN[J+1])/(RCEXCEN[J]-RCEXCEN[J+1])) ;
        ESTPRATIO := ((RCPRATIO[J+1]-RCPRATIO[J])*FRACTION)+ RCPRATIO[J] ;
        ESTCURV := ((RCONC[J+1]-RCONC[J])*FRACTION)+RCONC[J] ;
        WRITELN(PRT2,'NEUTRALAXIS = ',N:3,' EXCENTRICITY = ',ERATIO:5:2,
    ' EST P/PO = ',ESTPRATIO:7:4,' 1/R = ',ESTCURV:7:4,RCEXCEN[J]:7:4,RCEXCEN[J+1]:7:4 ) ;
       END ;
     END ;

    END;
  END ;

  BEGIN
   REWRITE(PRT1) ;
   REWRITE(PRT2) ;
   REWRITE(DATAFILE) ;
   INPUT(FCU,FY,STEELAREA,DRATIO,GAMMAMC,GAMMAMS,MINNEUTRALAXIS);
   A1 := DRATIO ;
   A2 := 1 - DRATIO ;
   XA1 := (A1/0.025) + 1 ;
   XA2 := (A2/0.025) + 1 ;
   POS1:= ROUND(XA1) ;
   POS2:= ROUND(XA2) ;
   IF ((XA1 - POS1) >  0.5 )    THEN   POS1 := POS1 + 1  ;
   IF ((XA1 - POS1) < -0.5 )    THEN   POS1 := POS1 - 1  ;
   IF ((XA2 - POS2) >  0.5 )    THEN   POS2 := POS2 + 1  ;
   IF ((XA2 - POS2) < -0.5 )    THEN   POS2 := POS2 - 1  ;
   WRITELN('POS1 = ',POS1 :4,'       POS2 = ',POS2 :4);
  FOR NAXIS:= 40 DOWNTO MINNEUTRALAXIS DO
  WITH COLUMNDATA  DO
```

```
  BEGIN
  STRAIN(EPSILON,NAXIS);
  STRESS(SIGMA,EPSILON,GAMMAMC) ;
  CONCRETEMOMENT(MCONC,SIGMA) ;
  CONCRETEFORCE(PCONC,SIGMA) ;
  CONCRETEPRATIO(CPRATIO,PCONC,GAMMAMC) ;
  CONCRETECURVITURE(INTERDATA[NAXIS].RCONC,EPSILON) ;
  STEELSTRAIN(EPSILONS,NAXIS,POS1,POS2) ;
  STEELFORCE(SFORCE,EPSILONS,POS1,POS2,GAMMAMS) ;
  SUMSTEELFORCE(PSTEEL,SFORCE,POS1,POS2) ;
  STEELMOMENT(MSTEEL,SFORCE,POS1,POS2,A1,A2) ;
  REINFFORCE(PRC,PCONC,PSTEEL) ;
  REINFMOMENT(MRC,MCONC,MSTEEL) ;
  EXCENTRICITY(INTERDATA[NAXIS].RCEXCEN,MRC,PRC) ;
  RFFORCERATIO(INTERDATA[NAXIS].RCPRATIO,PRC,GAMMAMC ,GAMMAMS) ;
 WRITELN(PRT1);
 WRITELN( ' NEUTRAL AXIS IS AT POSITION ',NAXIS);
WRITELN(PRT1, ' NEUTRAL AXIS IS AT POSITION ',NAXIS);
 WRITELN(PRT1) ;
 FOR I:=1 TO SIZE DO
 BEGIN
 J:=1;
 WHILE J<= 41  DO
 BEGIN
 WRITE(PRT1,EPSILON[I,J]:6:3);
 J:= J+2;
 END;
 WRITELN(PRT1);
 J:=1;
 WHILE J<= 41 DO
BEGIN
 WRITE(PRT1,SIGMA[I,J]:6:3);
 J:=J+2;
 END;
 WRITELN(PRT1);
 J:=1;
 WHILE J<= 41  DO
BEGIN
WRITE(PRT1,EPSILONS[I,J]:6:3);
```

```
  J:=J+2;
  END;
  WRITELN(PRT1);
  J:=1;
  WHILE J<= 41 DO
  BEGIN
  WRITE(PRT1,SFORCE[I,J]:6:3);
  J:=J+2
  END;
  WRITELN(PRT1);
  WRITELN(PRT1,'          P     M    E     P/PO   1/R ');
  WRITELN(PRT1,' CONC  ',PCONC[I]:7:3,MCONC[I]:7:3,'       ',
    CPRATIO[I]:7:3,INTERDATA[NAXIS].RCONC[I]:7:3 ) ;
  WRITELN(PRT1,' ST    ',PSTEEL[I]:7:3,MSTEEL[I]:7:3 ) ;
  WRITELN(PRT1, ' RC    ',PRC[I]:7:3,MRC[I]:7:3,
 INTERDATA[NAXIS].RCEXCEN[I]:7:3,INTERDATA[NAXIS].RCPRATIO[I]:8:4) ;
  WRITELN(PRT1) ;
  END ;
 END ;
 TERMINALP(INTERDATA) ;
 INTERPOLER(INTERDATA) ;
 TERMINALP(INTERDATA) ;
 TERMINALE(INTERDATA,POS1) ;
 INTERPOLPR(INTERDATA) ;
 WRITELN(PRT2) ;
 WRITELN(PRT2,' N   P/PO  E    1/R ') ;
 FOR I:=MINNEUTRALAXIS TO 40 DO
   WRITELN(PRT2,I:3, INTERDATA[I].RCPRATIO[SIZE]:7:4,
         INTERDATA[I].RCEXCEN[SIZE]:7:4,INTERDATA[I].RCONC[SIZE]:7:4);


1000:
END.
```

[3]. BUCKDEF PASCAL

```
PROGRAM BUCKDEF(DATA,INFILE,OUTPUT);
  {This program gives the relationship between Buckling deflection and Curvature with}
  {various values of the initial imperfection.}
  {SR = Slenderness Ratio = L/H and the Initial Imperfection = X*L}
CONST  PI = 3.141593  ;
       H  = 1.0  ;
VAR
  DATA,INFILE : TEXT ;
  X  ,  EXEN ,SR : REAL ;
  CURV  : INTEGER ;
BEGIN
  WRITELN('INPUT X ');
  RESET(INFILE);
  READ(INFILE , X);
  REWRITE(DATA) ;
  WRITELN(DATA,' INITIAL IMPERFECTION = ',X:8:6,' L ');
WRITELN(DATA,'═══════════════════════════════════════');
  WRITELN;
  WRITELN(DATA,'  L/H          E/H          H/R*0.001  ');
 WRITELN(DATA,'---------------------------------------');
 SR := 28.85 ;
    REPEAT
     BEGIN
      WRITELN;
     WRITELN(DATA,'14');
     FOR  CURV := 0  TO 13   DO
     BEGIN
       EXEN :=(((1/SQR(PI))*H*CURV*0.001* SQR(SR)) + (X* SR))*H  ;
       WRITELN(DATA,SR:4:2, EXEN:16:4  ,  CURV :11);
       WRITELN(SR:4:2 ,EXEN:16:4 ,CURV:11 );
     END;
     IF (SR >= 20.0) THEN   SR :=  SR +9.61
       ELSE   SR :=SR+5.0 ;
       END;
    UNTIL   SR> 60.0 ;
END.
```

[4]. UGHOST44 FORTRAN

```
      PARAMETER(IDI=100)                                                UGH00010
      COMMON /BLK1/ XMIN,XMAX,YMIN,YMAX                                 UGH00020
      DIMENSION X(IDI),X1(IDI),Y1(IDI),Y(IDI),ISIMB(10),                UGH00030
     +SET1(15),SET2(15),SET3(15),IDASH(4),SS1(15),SS2(15),SS3(15)       UGH00040
      CHARACTER FIGNUM*5                                                UGH00050
C     CHARACTER*20 LEGEND(15),FIGNUM*4                                  UGH00060
      DATA ISIMB /12,1,2,3,4,18,21,22,5,11/                             UGH00070
C     DATA IFCU,IFY,AS,DH/20,460,0.8,0.8/                               UGH00080
      data idash/3,8,3,8/                                               UGH00090
C     DATA LEGEND /LEGEND          $','BELOW MID-HEIGHT  $',            UGH00100
C     +          'ABOVE MID-HEIGHT  $','AT MID-HEIGHT     $'/         UGH00110
      PRINT*,' ENTER FCU, FY,AS,D/H'                                    UGH00120
      READ*,FCU,IFY,AS,DH                                               UGH00130
      PRINT*,' ENTER XMIN,XMAX,YMIN,YMAX FOR THIS PLOT'                 UGH00140
      READ*,XMIN,XMAX,YMIN,YMAX                                         UGH00150
      PRINT*,'  '                                                       UGH00160
      PRINT*,'  ENTER THE NUMBER OF DATA SETS TO BE PLOTTED'
                                                                        UGH00170
      READ(5,*)NSET                                                     UGH00180
      PRINT*,'  ENTER THE FIGURE  NUMBER '                              UGH00190
      READ(*,'(A5)')FIGNUM                                              UGH00200
      PRINT*,'  ENTER THE SEGMENT NUMBER '                              UGH00210
      READ*,NSEG                                                        UGH00220
      PRINT*,' ENTER THE PAGE NUMBER'                                   UGH00230
      READ*, PAGE                                                       UGH00240
      CALL GROUTE('LIST      ')                                         UGH00250
      CALL GOPEN                                                        UGH00260
C     CALL GSEGWK(0)                                                    UGH00270
      CALL GSEGCR(1   )                                                 UGH00280
                                                                        UGH00290
                                                                        UGH00300
      READ(1,*) FCU, NAXIS,FY,STAREA                                    UGH00310
C     READ END POINTS AND STOR THEM IN SET1,SET2,SET3                   UGH00320
C                                                                       UGH00330
      DO 300 I=1,NSET                                                   UGH00340
      READ(1,*)SET1(I),SET2(I),SET3(I)                                  UGH00350
```

```
300   CONTINUE                                                    UGH00360
      CALL GLIMIT (XMIN,XMAX,YMIN,YMAX,0.,0.)                     UGH00370
      CALL GVPORT (40.,115.,130.,120.)                            UGH00380
      CALL BGRAF(40.,115.,130.,120.)                              UGH00390
      CALL GCHARF('COMP')                                         UGH00400
      CALL BAXLAB(3.,2.,999,999)                                  UGH00410
      CALL BAXIS(1,XMIN,1.,XMAX,'Curvature h/r (*0.001)$')        UGH00420
      CALL BAXLAB(3.,2.,1,0 )                                     UGH00430
      CALL BAXIS(2,YMIN,0.1,YMAX,'Eccentricity e/h $')            UGH00440
      CALL BFRAME(0.2)                                            UGH00460
      CALL GCLIP                                                  UGH00480
      DO 310 K=1,NSET                                             UGH00490
C     READ IN THE NUMBER OF POINTS FOR SET NUMBER K               UGH00500
      READ(1,*)NPT                                                UGH00510
C     READ THE PRATIO,X,Y OF DATA SET K                           UGH00520
      DO 180 I=1,NPT                                              UGH00530
      READ(1,*)PRATIO,Y(I),X(I)                                   UGH00540
C     PRINT*, PRATIO,Y(I),X(I)                                    UGH00550
180   CONTINUE                                                    UGH00560
      IF((SET3(K).LT.0.).OR.(SET2(K).LT.0.))THEN                  UGH00570
      SET3(K)=XMAX                                                UGH00580
      SET2(K)=Y(NPT)                                              UGH00590
      ENDIF                                                       UGH00600
310   CONTINUE                                                    UGH00610
      CALL BMARKH(2.0)                                            UGH00620
      CALL BMARKC(K)                                              UGH00630
      CALL BMARK(ISIMB(K),0)                                      UGH00640
      CALL BLICOL (K)                                             UGH00650
      CALL BLIWDH (0.1)                                           UGH00660
C     DRAW THE END POINTS LINE DASHED                             UGH00670
      CALL BLICOL(1)                                              UGH00680
      CALL BDASH(7)                                               UGH00690
      CALL BLINE(SET3,SET2,NSET)                                  UGH00700
                                                                  UGH00710
C                                                                 UGH00720
      REWIND 1                                                    UGH00730
      READ(1,*) FCU, NAXIS,FY,STAREA                              UGH00740
C     READ END POINTS AND STOR THEM IN SET1,SET2,SET3             UGH00750
C                                                                 UGH00760
      DO 330 I=1,NSET                                             UGH00770
```

```
      READ(1,*)S1,S2,S3                                                  UGH00780
330   CONTINUE                                                           UGH00790
      DO 320 K=1,NSET                                                    UGH00800
C     READ IN THE NUMBER OF POINTS FOR SET NUMBER K                      UGH00810
      READ(1,*)NPT                                                       UGH00820
C     READ THE PRATIO,X,Y OF DATA SET K                                  UGH00830
      DO 185 I=1,NPT                                                     UGH00840
      READ(1,*)PRATIO,Y(I),X(I)                                          UGH00850
185   CONTINUE                                                           UGH00860
      X(NPT+1)=SET3(K)                                                   UGH00870
      Y(NPT+1)=SET2(K)                                                   UGH00880
      IF(K.GT.7)THEN                                                     UGH00890
         KO=K-7                                                          UGH00900
       ELSE                                                              UGH00910
         KO=K                                                            UGH00920
       ENDIF                                                             UGH00930
      CALL GWICOL (-1.,KO)                                               UGH00940
      CALL BBLINE(X,Y,NPT+1,0.1)                                         UGH00950
320   CONTINUE                                                           UGH00960
C                                                                        UGH00970
      CALL GNCLIP                                                        UGH00980
      CALL GRESET                                                        UGH00990
      CALL GVPORT(30.,55.,130.,30.)                                      UGH01000
      CALL GCHARF('COMP')                                                UGH01010
      CALL GCHAR('F<C<U$',117.,76.,3.0)                                  UGH01020
      CALL GCHAR('= $',130.,76.,3.0)                                     UGH01030
      CALL GNUMB(      FCU ,9999.,9999.,3.0,0)                           UGH01040
      CALL GCHAR(' N/mm>2$',9999.,9999.,3.0)                             UGH01050
                                                                         UGH01060
      CALL GCHAR('F<Y$',117.,70.,3.0)                                    UGH01070
      CALL GCHAR('= $',130.,70.,3.0)                                     UGH01080
      CALL GNUMB(FLOAT(IFY),9999.,9999.,3.0,0)                           UGH01090
      CALL GCHAR(' N/mm>2$',9999.,9999.,3.0)                             UGH01100
                                                                         UGH01110
      CALL GCHAR('%A<S$',117.,64.,3.0)                                   UGH01120
      CALL GCHAR('= $',130.,64.,3.0)                                     UGH01130
      CALL GNUMB(     AS ,9999.,9999.,3.0,1)                             UGH01140
                                                                         UGH01150
      CALL GCHAR('d/h$',117.,58.,3.0)                                    UGH01160
      CALL GCHAR('= $',130.,58.,3.0)                                     UGH01170
```

```
      CALL GNUMB( dh ,9999.,9999.,3.0,2)                                UGH01180
      CALL GVPORT(25.,25.,140.,20.)                                     UGH01190
      CALL GCHAR (' Fig.$',35.,40.,3.)                                  UGH01200
      CALL GCHAR (FIGNUM,9999.,9999.,3.)                                UGH01210
      CALL GCHAR (' Eccentricity vs Curvature relationship for$         UGH01220
     +',9999.,9999.,3.)                                                 UGH01230
      CALL GCHAR ('          Long-Term loading.$',35.,34.,3.)           UGH01240
      CALL GLIMIT (XMIN,XMAX,YMIN,YMAX,0.,0.)                           UGH01250
      CALL GVPORT(40.,115.,130.,120.)                                   UGH01260
      CALL GWBOX(130./120.,1.,0.)                                       UGH01270
      CALL GSCALE                                                       UGH01280
C     END POINTS AND STOR THEM IN SET1,SET2,SET3                        UGH01290
C                                                                       UGH01300
      DO 350 I=1,NSET                                                   UGH01310
      IF(SET3(I)+1..GE.XMAX)THEN                                        UGH01320
          SS3(I)=XMAX-1.0                                               UGH01330
       ELSE                                                             UGH01340
        SS3(I)=SET3(I)+0.3                                              UGH01350
       ENDIF                                                            UGH01360
       IF(SET2(I).GE.YMAX)THEN                                          UGH01370
        SS2(I)=YMAX-0.03                                                UGH01380
        SS3(I)= 7.0                                                     UGH01390
       ELSE                                                             UGH01400
        SS2(I)=SET2(I)                                                  UGH01410
       ENDIF                                                            UGH01420
350   CONTINUE                                                          UGH01430
      CALL GCHARJ(2)                                                    UGH01440
      CALL GCHAR('P/P<0 = $',2.4,SS2(1)-0.02,2.)                        UGH01450
      CALL GNUMB(SET1(1),9999.,9999.,2.,2)                              UGH01460
      CALL GCHARJ(0)                                                    UGH01470
C     next line change the second number                                UGH01480
C     CALL GNUMB(number, x-cord,ycord,hight, decimal)                   UGH01490
      CALL GNUMB(SET1(2),SS3(2)+0.1,SS2(2)-0.02,2.,2)                   UGH01500
C     this for data set 3  to nset                                      UGH01510
      DO 181 LL=3,NSET                                                  UGH01520
      CALL GNUMB(SET1(LL),SS3(LL)+0.1,SS2(LL),2.,2)                     UGH01530
181   CONTINUE                                                          UGH01540
      CALL GVPORT (40.,235.,130.,20.)                                   UGH01550
      CALL GSCAMM                                                       UGH01560
      CALL GNUMB(PAGE,100.,255.,2.,0)                                   UGH01570
```

```
CALL GSEGCL(1)                                                    UGH01580
CALL GCLOSE                                                       UGH01590
STOP                                                              UGH01600
END                                                               UGH01610
```

[5]. UGHOST99 FORTRAN

```
      PARAMETER(IDI=100)                                                UGH00010
      COMMON /BLK1/ XMIN,XMAX,YMIN,YMAX                                 UGH00020
      REAL IPAGE                                                        UGH00030
      DIMENSION X(IDI),X1(IDI),Y1(IDI),Y(IDI),ISIMB(10),                UGH00040
     +SET1(15),SET2(15),SET3(15),IDASH(4),SET4(15)                      UGH00050
      CHARACTER FIGNUM*5,DUM*80                                         UGH00060
C     CHARACTER*20 LEGEND(15),FIGNUM*4                                  UGH00070
      DATA ISIMB /12,1,2,3,4,18,21,22,5,11/                             UGH00080
      data idash/3,8,3,8/                                               UGH00090
C     DATA LEGEND /LEGEND          $','BELOW MID-HEIGHT                 UGH00100
C     +          'ABOVE MID-HEIGHT  $','AT MID-HEIGHT     $'/          UGH00110
      PRINT*,' ENTER XMIN,XMAX,YMIN,YMAX FOR THIS PLOT'                 UGH00120
      READ*,XMIN,XMAX,YMIN,YMAX                                         UGH00130
      PRINT*,'  '                                                       UGH00140
      PRINT*,' ENTER THE NUMBER OF DATA SETS TO BE PLOTTED'
                                                                        UGH00150
      READ(5,*)NSET                                                     UGH00160
      PRINT*,' ENTER THE FIGURE  NUMBER '                               UGH00170
      READ(*,'(A5)')FIGNUM                                              UGH00180
      PRINT*,' ENTER THE SEGMENT NUMBER '                               UGH00190
      READ*,NSEG                                                        UGH00200
      PRINT*,' ENTER THE PAGE NUMBER'                                   UGH00210
      READ*, PAGE                                                       UGH00220
      CALL GROUTE('LIST      ')                                         UGH00230
      CALL GOPEN                                                        UGH00240
C     CALL GSEGWK(0)                                                    UGH00250
      CALL GSEGCR(1   )                                                 UGH00260
                                                                        UGH00270
                                                                        UGH00280
      CALL GLIMIT (XMIN,XMAX,YMIN,YMAX,0.,0.)                           UGH00290
      CALL GVPORT (40.,115.,130.,120.)                                  UGH00300
      CALL BGRAF(40.,115.,130.,120.)                                    UGH00310
      CALL GCHARF('COMP')                                               UGH00320
      CALL BAXLAB(3.,2.,999,999)                                        UGH00330
      CALL BAXIS(1,XMIN,1.,XMAX,'Curvature h/r (*0.001)$')              UGH00340
      CALL BAXLAB(3.,2.,1,0 )                                           UGH00350
```

```
      CALL BAXIS(2,YMIN,0.1,YMAX,'Eccentricity e/h$')                    UGH00360
                                                                         UGH00370
      CALL BFRAME(0.2)                                                   UGH00380
                                                                         UGH00390
C     CALL GCLIP                                                         UGH00400
C                                                                        UGH00410
      DO 1991 I=1,4                                                      UGH00420
1991     READ(1,1990)DUM                                                 UGH00430
1990     FORMAT(80A1)                                                    UGH00440
      DO 320 K=1,NSET                                                    UGH00450
C     READ IN THE NUMBER OF POINTS FOR SET NUMBER K                      UGH00460
      READ(1,*)NPTT                                                      UGH00470
C     READ THE PRATIO,X,Y OF DATA SET K                                  UGH00480
      DO 185 I=1,NPTT                                                    UGH00490
      READ(1,*)SET1(K),Y(I),X(I)                                         UGH00500
185   CONTINUE                                                           UGH00510
      SET2(K)=(Y(NPTT)-Y(1))/(X(NPTT)-X(1))                              UGH00520
      DO 187 I=1,NPTT                                                    UGH00530
      IF((Y(I).GT.YMAX).OR.(X(I).GT.XMAX))THEN                           UGH00540
        IF((Y(I).GT.YMAX).AND.(X(I).LE.XMAX))THEN                        UGH00550
          SET3(K)= YMAX                                                  UGH00560
          YY=Y(I)-YMAX                                                   UGH00570
          XX=YY/SET2(K)                                                  UGH00580
          X(I)=X(I)-XX                                                   UGH00590
          Y(I)=YMAX                                                      UGH00600
      ELSEIF((X(I).GT.XMAX).AND.(Y(I).LE.YMAX))THEN                      UGH00610
          SET4(K)=XMAX                                                   UGH00620
          XX=XMAX                                                        UGH00630
          YY=XX*SET2(K)                                                  UGH00640
          Y(I)=YY                                                        UGH00650
          X(I)=XMAX                                                      UGH00660
       ELSE                                                              UGH00670
          SET4(K)=XMAX                                                   UGH00680
          SET3(K)=YMAX                                                   UGH00690
       ENDIF                                                             UGH00700
       NPT=I                                                             UGH00710
       GO TO 186                                                         UGH00720
     ELSE                                                                UGH00730
       NPT=I                                                             UGH00740
       SET3(K)=Y(I)                                                      UGH00750
```

```
      SET4(K)=X(I)                                                    UGH00760
      ENDIF                                                           UGH00770
187   CONTINUE                                                        UGH00780
186   CONTINUE                                                        UGH00790
C     PRINT*,SET2(K)                                                  UGH00800
      IF(K.GT.6)THEN                                                  UGH00810
        KO=K-6                                                        UGH00820
      ELSE                                                            UGH00830
        KO=K                                                          UGH00840
      ENDIF                                                           UGH00850
      CALL GWICOL (-1.,KO)                                            UGH00860
      CALL  BLINE(X,Y,NPT )                                           UGH00870
320   CONTINUE                                                        UGH00880
C                                                                     UGH00890
C     CALL GNCLIP                                                     UGH00900
      CALL GRESET                                                     UGH00910
      CALL GVPORT(30.,55.,140.,30.)                                   UGH00920
      CALL GCHARF('COMP')                                             UGH00930
                                                                      UGH00940
C     CALL GVPORT(25.,25.,140.,20.)                                   UGH00950
      CALL GCHAR ('Fig.$',35.,75.,3.)                                 UGH00960
      CALL GCHAR (FIGNUM ,9999.,9999.,3.)                             UGH00970
      CALL GCHAR (' Buckling deflection vs curvature relationship$    UGH00980
      +',9999.,9999.,3.)                                              UGH00990
      CALL GCHAR ('        with initial imperfection of 0.000568L.$   UGH01000
      +',35.,69.,3.)                                                  UGH01010
      CALL GLIMIT (XMIN,XMAX,YMIN,YMAX,0.,0.)                         UGH01020
      CALL GVPORT(40.,115.,130.,120.)                                 UGH01030
      CALL GWBOX(130./120.,1.,0.)                                     UGH01040
      CALL GSCALE                                                     UGH01050
C     END POINTS AND STOR THEM IN SET1,SET2,SET3                      UGH01060
C                                                                     UGH01070
      PPI=180./3.141592654                                            UGH01080
      DO 350 I=1,NSET                                                 UGH01090
      ANGL=PPI*SET2(I)                                                UGH01100
      IANGL=NINT(ANGL)                                                UGH01110
      CALL GCHARJ(2)                                                  UGH01120
      CALL GCHARA(IANGL)                                              UGH01130
C     PRINT*,IANGL                                                    UGH01140
C     CALL GCHAR('L/H = $',SET4(I)-1.,SET3(I)+0.01,2.)                UGH01150
```

```
C     CALL GCHARJ(0)                                          UGH01160
C     CALL GNUMB(SET1(I),9999.,9999.,2.,0)                    UGH01170
350   CONTINUE                                                UGH01180
      CALL GVPORT(40.,235.,130.,20.)                          UGH01190
      CALL GSCAMM                                             UGH01200
      CALL GNUMB (PAGE,100.,255.,2.,0)                        UGH01210
      CALL GSEGCL(1)                                          UGH01220
      CALL GCLOSE                                             UGH01230
      STOP                                                    UGH01240
      END                                                     UGH01250
```

APPENDIX B

METHODS TO FIND END-POINTS OF LOAD ECCENTRICITY-CURVATURE GRAPHS

[1]. Alternative method for the trapezoidal rule (See section 3.4.2)

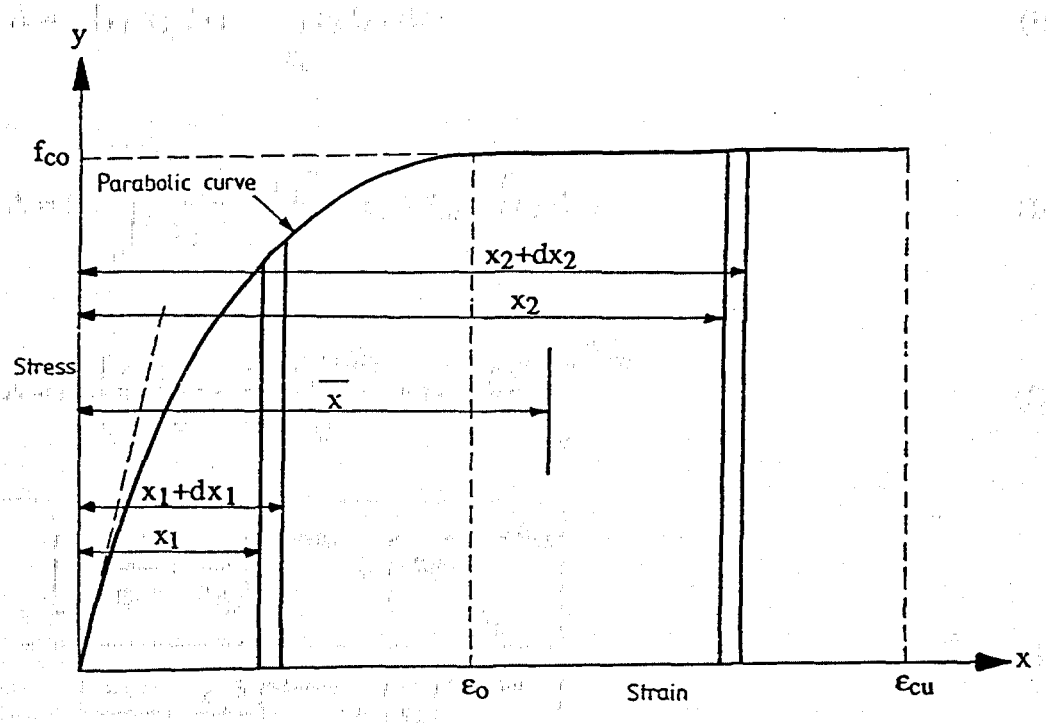

Fig.B.1 : Stress-strain curve for normal weight concrete.

The equation for the parabola is given as:

$$y_1 = a_1x_1 - b_1x_1^2 + c_1 \qquad (B.1)$$

Using the boundary conditions to define the constants, the following equation results:

$$y_1 = f_{co}\left(\frac{2x_1}{\varepsilon_o} - \frac{x_1^2}{\varepsilon_o^2}\right) \qquad (B.2)$$

The total area of the stress-strain block:

$$A = \int_0^{x_1 \le \varepsilon_o} y_1 \, dx_1 + \int_{\varepsilon_o}^{x_2 \le \varepsilon_{cu}} f_{co} \, dx_2 \tag{B.3}$$

$$\boxed{A = f_{co}\left[\left(\frac{x_1^2}{\varepsilon_o} - \frac{x_1^3}{3\varepsilon_o^2}\right)\right]_0^{x_1 \le \varepsilon_o} + f_{co}\left[x_2\right]_{\varepsilon_o}^{x_2 \le \varepsilon_{cu}}} \tag{B.4}$$

And the centroid is given by:

$$\bar{x}\, A = \int_0^{x_1 \le \varepsilon_o} y_1 \, x_1 \, dx_1 + \int_{\varepsilon_o}^{x_2 \le \varepsilon_{cu}} x_2 \, f_{co} \, dx_2 \tag{B.5}$$

$$\bar{x}\, A = f_{co} \int_0^{x_1 \le \varepsilon_o} \left(\frac{2x_1^2}{\varepsilon_o} - \frac{x_1^3}{\varepsilon_o^2}\right) dx_1 + f_{co} \int_{\varepsilon_o}^{x_2 \le \varepsilon_{cu}} x_2 \, dx_2 \tag{B.6}$$

$$\bar{x}\, A = f_{co}\left[\frac{2}{3}\frac{x_1^3}{\varepsilon_o} - \frac{x_1^4}{4\varepsilon_o^2}\right]_0^{x_1 \le \varepsilon_o} + f_{co}\left[\frac{x_2^2}{2}\right]_{\varepsilon_o}^{x_2 \le \varepsilon_{cu}} \tag{B.7}$$

$$\boxed{\bar{x} = \frac{\left[\frac{2}{3}\frac{x_1^3}{\varepsilon_o} - \frac{x_1^4}{4\varepsilon_o^2}\right]_0^{x_1 \le \varepsilon_o} + \left[\frac{x_2^2}{2}\right]_{\varepsilon_o}^{x_2 \le \varepsilon_{cu}}}{\left[\frac{x_1^2}{\varepsilon_o} - \frac{x_1^3}{3\varepsilon_o^2}\right]_0^{x_1 \le \varepsilon_o} + \left[x_2\right]_{\varepsilon_o}^{x_2 \le \varepsilon_{cu}}}} \tag{B.8}$$

Examples:

(a) When $x = \varepsilon_o$:

$$A = f_{co}\left[\varepsilon_o - \frac{\varepsilon_o}{3}\right] = \frac{2}{3}\varepsilon_o f_{co}$$

$$\bar{x} = \frac{5}{8}\varepsilon_o$$

(b) When $x = \varepsilon_{cu}$:

$$A = \frac{2}{3}\varepsilon_o f_{co} + f_{co}(\varepsilon_{cu} - \varepsilon_o)$$

$$\bar{x} = \frac{1}{4}\varepsilon_{cu}\frac{(6-\varepsilon_o^2/\varepsilon_{cu}^2)}{(3-\varepsilon_o/\varepsilon_{cu})}$$

[2]. Exact solution for the end points (see section 3.4.2)

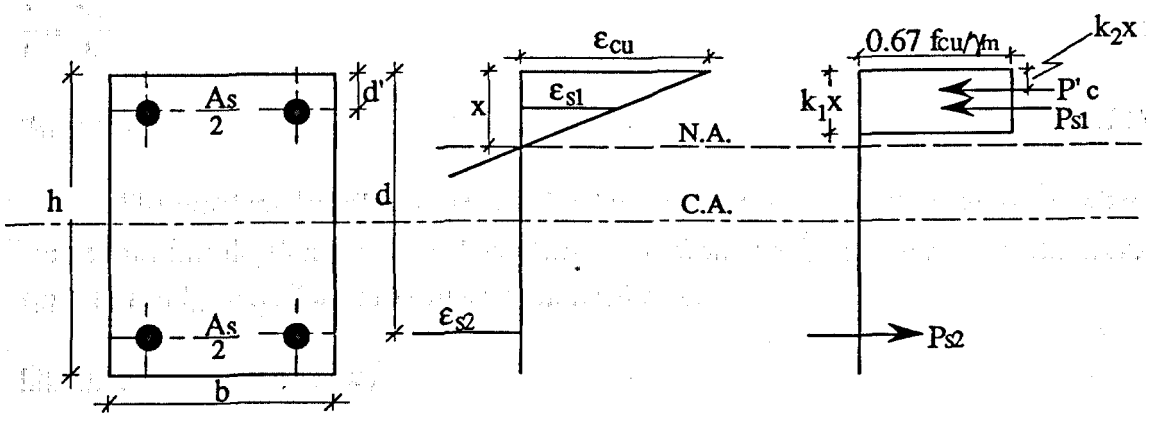

Fig.B.2 : Simplified stress block for concrete at ultimate limit state.

$$\varepsilon_{s1} = \frac{x-d'}{x}\varepsilon_{cu} \qquad (B.9)$$

$$\varepsilon_{s2} = \frac{d-x}{x}\varepsilon_{cu} \qquad (B.10)$$

$$k_1 = 1-\frac{\eta}{3} \qquad (x \le h) \qquad (B.11)$$

$$k_2 = \frac{1}{k_1}\left[\frac{1}{2} - \frac{1}{3}\eta + \frac{1}{12}\eta^2\right] \qquad (B.12)$$

where: $\eta = \dfrac{\varepsilon_o}{\varepsilon_{cu}}$ (see Fig.B.1)

$$P'_c = 0.67\,\frac{f_{cu}}{\gamma_m}\,k_1\,x\,b \qquad (B.13)$$

$$M'_c = P_c\,(0.5h - k_2\,x) \qquad \text{about C.A} \qquad (B.14)$$

$$P_s = P_{s1} - P_{s2} = f_{s1}\frac{A_s}{2} - f_{s2}\frac{A_s}{2} \qquad (B.15)$$

$$M_s = P_{s1}\,(0.5h - d') + P_{s2}\,(d - 0.5h) \qquad \text{about C.A} \qquad (B.16)$$

$$P_{RC} = P'_c + P_s = P \qquad (B.17)$$

$$M_{RC} = M'_c + M_s = M \qquad (B.18)$$

$$e = \frac{M}{P} \tag{B.19}$$

$$\frac{1}{r} = \frac{\varepsilon_{cu}}{x} \tag{B.20}$$

$$\gamma_m = 1.0 \tag{B.21}$$

The problem described in section 3.4.2 regarding the trapezoidal rule, arises when the neutral axis depth x is within about 0.2h or less from the top of the section, therefore $\varepsilon_{s2} \geq \varepsilon_y$ and $f_{s2} = f_y$. Two cases to be considered here:

Case (1) When $\varepsilon_{s1} < \varepsilon_y$

Equation (B.17) becomes:

$$P = 0.67 f_{cu} k_1 x b + \varepsilon_{s1} E_s \frac{A_s}{2} - f_y \frac{A_s}{2} \tag{B.22}$$

$$P = 0.67 f_{cu} k_1 x b + \left(\frac{x-d'}{x}\right) \varepsilon_{cu} E_s \frac{A_s}{2} - f_y \frac{A_s}{2} \tag{B.23}$$

$$\boxed{0.67 f_{cu} k_1 b x^2 + \left(\varepsilon_{cu} E_s \frac{A_s}{2} - f_y \frac{A_s}{2} - P\right) x - \varepsilon_{cu} E_s \frac{A_s}{2} d' = 0} \tag{B.24}$$

Case (2) When $\varepsilon_{s1} \geq \varepsilon_y$ this gives $f_{s1} = f_y$

Equation (B.17) becomes:

$$\boxed{P = 0.67 f_{cu} k_1 x b} \tag{B.25}$$

The ratio P/P_0 is known for each curve, P_0 can be determined from Eq.(3.8), therefore P is known. The only unknown left in either Eq.(B.24) or Eq.(B.25) is the neutral axis depth x, which then can be evaluated. Hence, the eccentricity and curvature can now be determined from Eqs.(B.19) and (B.20) respectively and the end point is precisely calculated.